

JOHN MADEY: A SHORT HISTORY OF MY FRIEND AND COLLEAGUE

Luis Elias, University of Hawaii, Manoa (R), Hawaii, USA



Figure 1: John Madey (1943-2016) in his Hawaii Laboratory.

BRIEF HISTORY AT STANFORD UNIVERSITY

I thank the organizing committee for inviting me to share with you some stories of my friend and colleague John Madey, who passed away on July 2016 in Honolulu, Hawaii.

I will first summarize to you the early history of John Madey's FEL at Stanford University. Then, I will try to briefly relate to you about our joint work at the University of Hawaii. Lastly, I will share with you some final thoughts on John's achievements.

I met John Madey in 1973 at Stanford University right after he and I received our respective Ph. D degrees in Physics. He from Stanford University and I from the University of Wisconsin in Madison. It was through a connection between Professors Alan Schwettman and Arthur Schawlow of Stanford University with my major professor William Yen, from the University of Wisconsin, that I was hired to assist John Madey in the demonstration of his SBR laser. Perhaps my experience with experimental vacuum synchrotron radiation spectroscopy contributed to their hiring decision.

Before arriving at SU, John's proposal goal to show "Stimulated Bremsstrahlung Radiation" had been already funded by the US Air Force Office for Scientific Research

(AFSOR). Instead of SBR, J. Madey later coined the acronym FEL (Free Electron Laser) to describe the device.

After meeting him in 1973, it did not take long for me to recognize the genius character of John Madey. During an early visit to his house in Palo Alto, I discovered that most of his house was filled with old radio electronic equipment. I then learned that John and his brother Jules had been actively involved in ham radio communications since 1956. As is well known now, when John was 13 and Jules was 16, they began relaying communications from the south pole to families and friends in the United States. I then realized that before his interest in the FEL came about, John had already accumulated a vast experience in the field of electronic devices, including his latest electronics accomplishment. It was digital communication equipment that allowed John, in Palo Alto, to communicate with his older brother Jules, in Marin County, by means of two very old teletype machines. It was a major achievement because at that time internet communication was not invented.

I remember that in 1973 there were not many scientists, including some professors at Stanford who believed that John's FEL would work. As described in his original publication [1], his physical interpretation of EM field amplification occurred because during electron radiation inside the static undulator field, the electron energy recoil can favor photon emission process over photon absorption. His quantum calculation of FEL gain was made in terms of photon energy $\hbar\omega$. I recall clearly how in one of John's presentations of his theory of the FEL to the Physics department, professors Felix Bloch and Arthur Schawlow pointed out the fact that in John's gain formula calculation \hbar mysteriously disappeared from the equation. Despite of their objection, I was quite impressed with John's valiant and intelligent defense of his theory, considering that the objections were made by Nobel Laureates in physics.

As it turned out, John's gain equation was correct and his objectors were also correct because, as we know now, quantum electrodynamics is not totally needed to explain the gain result. The theory of FEL can be satisfactorily explained in terms of classical electrodynamics.

Because of Stanford University rules professor Alan Schwettman became the principal investigator of the FEL program and consequently our boss. As director of the Superconducting Acceleration (SCA) program, he allowed us the use of the SCA in the FEL program. After my arrival at Stanford University, Alan hired Todd Smith to run the SCA. Consequently, the three of us (John, Todd and I) were charged with the responsibility of implementing the FEL program in 1973.

The Stanford FEL program was divided into three major experimental subprograms that included: (1) the electron beam system, (2) the magnetic undulator and the (3) the optics system. Todd was responsible for the electron beam,

COHERENCE LIMITS OF X-RAY FEL RADIATION

E.A. Schneidmiller, M.V. Yurkov, DESY, Hamburg, Germany

Abstract

The radiation from SASE FELs has always limited value of the degree of transverse coherence. When transverse size of the electron beam significantly exceeds diffraction limit, the mode competition effect does not provide the selection of the ground mode, and spatial coherence degrades due to contribution of the higher order transverse modes. It is important that the most strong higher modes are azimuthally non-symmetric which leads to fluctuations of the spot size and of the pointing stability of the photon beam. These fluctuations are fundamental and originate from the shot noise in the electron beam. The effect of the pointing instability becomes more pronouncing for shorter wavelengths. We analyze in detail the case of optimized SASE FELs and derive universal dependencies applicable to all operating and planned x-ray FELs. It is shown that x-ray FELs driven by low energy electron beams will exhibit poor spatial coherence and bad pointing stability.

INTRODUCTION

Coherence properties of the radiation from SASE FELs strongly evolve during the amplification process [1–5]. At the initial stage of amplification the spatial coherence is poor, and the radiation consists of a large number of transverse modes [5–13]. In the exponential stage of amplification the transverse modes with higher gain dominate over modes with lower gain when the undulator length progresses. The mode selection process stops at the onset of the nonlinear regime, and the maximum values of the degree of the transverse coherence is reached at this point.

Gain separation of the FEL radiation modes is mainly defined by the value of the diffraction parameter B [10] describing diffraction expansion of the radiation with respect to the electron beam size. For FELs with diffraction limited beams the value of the diffraction parameter is less than or about unity, and spatial coherence at saturation reaches values of about 90%. Large values of the diffraction parameter ($B \gtrsim 10 \dots 100$) are typical for SASE FELs operating in the hard x-ray range [14–18]. Increase of the diffraction parameter results in a decrease of diffraction expansion and of relative separation of the gain of the modes. In this case we deal with the mode degeneration effect [7, 10]. Since the number of gain lengths to saturation is limited (about 10 for x-ray FELs), the contribution of the higher spatial modes to the total power grows with the value of the diffraction parameter, and the transverse coherence degrades.

The main competitor of the ground TEM_{00} mode is the first azimuthal TEM_{10} mode. When contribution of TEM_{10} mode to the total power exceeds a few per cent level, a fundamental effect of bad pointing stability becomes to be pronouncing. For optimized SASE FEL the power of the effect grows with the parameter $\hat{\epsilon} = 2\pi\epsilon/\lambda$. SASE FELs operating

at short wavelengths and low electron beam energy with the value of $\hat{\epsilon} \gtrsim 1$ suffer from the mode degeneration effect resulting in significant degradation of the spatial coherence and pointing stability of the photon beam. The effect of the photon beam pointing jitter is a fundamental one, and can not be eliminated by elimination of the jitters of machine parameters (orbit, phase, etc.).

FEL RADIATION MODES AND MODE DEGENERATION EFFECT

We consider the axisymmetric model of the electron beam. It is assumed that the transverse distribution function of the electron beam is Gaussian, so rms transverse size of matched beam is $\sigma = \sqrt{\epsilon\beta}$, where $\epsilon = \epsilon_n/\gamma$ is rms beam emittance and β is the beta-function. In the framework of the three-dimensional theory the operation of a short-wavelength FEL amplifier is described by the following parameters: the diffraction parameter B , the energy spread parameter $\hat{\Lambda}_T^2$, the betatron motion parameter \hat{k}_β and detuning parameter \hat{C} [9, 10]:

$$\begin{aligned} B &= 2\bar{\Gamma}\sigma^2\omega/c, & \hat{C} &= C/\bar{\Gamma}, \\ \hat{k}_\beta &= 1/(\beta\bar{\Gamma}), & \hat{\Lambda}_T^2 &= (\sigma_E/E)^2/\bar{\rho}^2, \end{aligned} \quad (1)$$

The gain parameter $\bar{\Gamma}$ and efficiency parameter $\bar{\rho}$ are given by:

$$\bar{\Gamma} = \left[\frac{I}{I_A} \frac{8\pi^2 K^2 A_{JJ}^2}{\lambda\lambda_w\gamma^3} \right]^{1/2}, \quad \bar{\rho} = \frac{\lambda_w\bar{\Gamma}}{4\pi}. \quad (2)$$

Here $E = \gamma mc^2$ is the energy of electron, γ is relativistic factor, and $C = 2\pi/\lambda_w - \omega/(2c\gamma_z^2)$ is the detuning of the electron with the nominal energy \mathcal{E}_0 . Note that the efficiency parameter $\bar{\rho}$ entering equations of the three dimensional theory relates to the one-dimensional parameter ρ

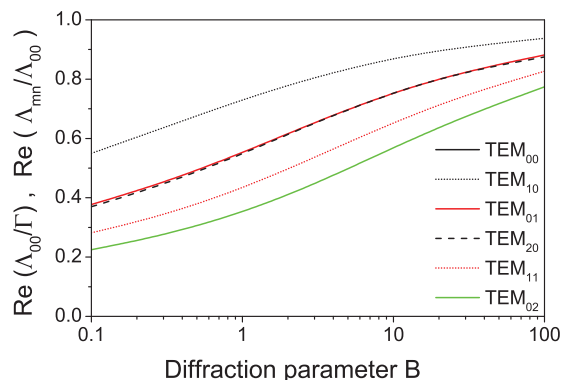


Figure 1: The ratio of the maximum gain of the higher modes to the maximum gain of the fundamental mode $\text{Re}(\Lambda_{mn})/\text{Re}(\Lambda_{00})$ versus diffraction parameter B for the case of the “cold” electron beam. Calculations have been performed with the code FAST [20].

COMMISSIONING AND FIRST LASING OF THE EUROPEAN XFEL*

H. Weise[†], W. Decking, Deutsches Elektronen-Synchrotron DESY, Hamburg, Germany
on behalf of the European XFEL Accelerator Consortium and the Commissioning Team

Abstract

The European X-ray Free-Electron Laser (XFEL) in Hamburg, Northern Germany, aims at producing X-rays in the range from 0.25 up to 25 keV out of three undulators that can be operated simultaneously with up to 27,000 pulses per second. The XFEL is driven by a 17.5-GeV superconducting linac. This linac is the world-wide largest installation based on superconducting radio-frequency acceleration. The design is using the so-called TESLA technology which was developed for the superconducting version of an international electron positron linear collider. After eight years of construction the facility is now brought into operation. First lasing was demonstrated in May 2017. Experience with the superconducting accelerator as well as beam commissioning results will be presented. The path to the first user experiments will be laid down.

INTRODUCTION

The European XFEL aims at delivering X-rays from 0.25 to up to 25 keV out of three SASE undulators [1, 2]. The radiators are driven by a superconducting linear accelerator based on TESLA technology [3]. The linac operates in 10 Hz pulsed mode and can deliver up to 2,700 bunches per pulse. Electron beams will be distributed to three different beamlines, this within a pulse. Three experiments can be operated in parallel.

The European XFEL is being realized as a joint effort by 11 European countries (Denmark, France, Germany, Hungary, Italy, Poland, Russia, Slovakia, Spain, Sweden, and Switzerland). The accelerator of the European XFEL and major parts of the infrastructure are contributed by the accelerator construction consortium, coordinated by DESY. The consortium consists of CEA/IRFU (Saclay, France), CNRS/IN2P3 (Orsay, France), DESY (Hamburg, Germany), INFN-LASA (Milano, Italy), NCBJ (Świerk, Poland), WUT (Wrocław, Poland), IFJ-PAN (Kraków, Poland), IHEP (Protvino, Russia), NIIIEFA (St. Petersburg, Russia), BINP (Novosibirsk, Russia), INR (Moscow, Russia), CIEMAT (Madrid, Spain), UPM (Madrid, Spain), SU (Stockholm, Sweden), UU (Uppsala, Sweden), and PSI (Villigen, Switzerland). DESY will also be responsible for the operation, maintenance and upgrade of the accelerator.

Construction of the European XFEL started in early 2009. The commissioning of the linear accelerator began end of 2015 with the injector, and end of 2016 with the cool-down of the main accelerator.

* Work supported by the respective funding agencies of the contributing institutes; for details please see <http://www.xfel.eu>

[†] hans.weise@desy.de

FACILITY LAYOUT

The complete facility is constructed underground, in a 5.2 m diameter tunnel about 25 to 6 m below the surface level and fully immersed in the ground water. The 50 m long injector is installed at the lowest level of a 7 stories underground building whose downstream end also serves as the entry shaft to the main linac tunnel. Next access to the tunnel is only about 2 km downstream, at the bifurcation point into the beam distribution lines. The beam distribution provides space for in total 5 undulators – 3 being initially installed. Each undulator is feeding a separate beamline so that a fan of 5 almost parallel tunnels, separated each by about 17 m, enters the experimental hall located 3.3 km away from the electron source.

The accelerator of the European XFEL starts with a photo-injector based on a normal-conducting 1.3 GHz 1.6 cell accelerating cavity [4]. A Cs₂Te-cathode, illuminated by a Nd:YLF laser operating at 1047 nm and converted to UV wavelength, produces 600 μs long bunch trains of 2,700 bunches. The photo-injector is followed by a standard XFEL superconducting (s.c.) 1.3 GHz accelerating module, and a 3rd harmonic (3.9 GHz) linearizer, also housing eight 9-cell s.c. cavities. A laser-heater, a diagnostic section and a high-power dump complete the injector.



Figure 1: First bunch compression chicane.

The European XFEL uses a three stage bunch compression scheme. All magnetic chicanes are tuneable within a wide range of R_{56} to allow for flexible compression scenarios, for instance balancing peak current and arrival time stability with LLRF performance. The tuning is achieved by means of large pole width dipole magnets and accordingly wide (400 mm) vacuum chambers (see Fig. 1). Special care was taken in the design of the vacuum chambers. There are no moving parts in order to min-

STATUS OF THE FLASH FEL USER FACILITY AT DESY

K. Honkavaara*, DESY, Hamburg, Germany[†]

Abstract

The FLASH facility at DESY (Hamburg, Germany) provides high brilliance FEL radiation at XUV and soft X-ray wavelengths for user experiments. Since April 2016, the second undulator beamline, FLASH2, is in user operation. We summarize the performance of the FLASH facility during the last two years including our experience to deliver FEL radiation to two user experiments simultaneously.

INTRODUCTION

FLASH [1–7], the free-electron laser (FEL) user facility at DESY (Hamburg), delivers high brilliance XUV and soft X-ray FEL radiation for photon experiments.

FLASH, originally called the VUV-FEL at TTF2, was constructed in the early 2000s based on the experience gathered from the TTF-FEL operation [8]. The user operation of the FLASH facility started in summer 2005 with one undulator beamline, which is still in use with its original fixed gap undulators (FLASH1). In order to fulfill the continuously increasing demands on beam time and on photon beam properties, a second beamline with variable gap undulators (FLASH2) has been constructed. The first lasing of FLASH2 was achieved in August 2014 [9], and since April 2016 FLASH2 is in regular user operation.

Figure 1 shows an aerial view of the north side of DESY in summer 2016. The FLASH facility with its two experimental halls is in the middle of the picture: the FLASH1 hall ("Albert Einstein") is on the right, the FLASH2 hall ("Kai Siegbahn") on the left.



Figure 1: Aerial view of the north side of DESY. The FLASH facility is in the middle of the picture: the FLASH1 experimental hall is on the right, the FLASH2 hall on the left. Next to FLASH are two experimental halls of the PETRA III synchrotron light source.

This paper reports on the status of the FLASH facility and its performance in 2016/17. Part of this material has been presented in previous conferences, most recently in [7].

THE FLASH FACILITY

Figure 2 shows a schematic layout of the FLASH facility. The seeding experiment sFLASH [10] located upstream of the FLASH1 undulators, and the FLASHForward plasma wakefield acceleration experiment [11], under construction at the FLASH3 beamline, are indicated as well.

The generation of high quality electron bunches is realized by an RF-gun based photoinjector. An exchangeable Cs₂Te photocathode is installed on the back-plane of the normal conducting RF-gun. The presently installed photocathode is in use already more than two years without any significant degradation of the quantum efficiency: the QE is still at an 8% level [12]. The photocathode laser system has three independent lasers [13], allowing a flexible operation and production of electron bunch trains with different parameters (number of bunches, bunch spacing, bunch charge).

The FLASH linac has seven TESLA type 1.3 GHz accelerating modules providing a maximum electron beam energy of 1.25 GeV. The use of superconducting RF cavities allows operation with long RF-pulses, i.e. with long electron bunch trains. The maximum length of the bunch train is defined by the RF flat top of the acceleration modules (800 μs) and of the RF-gun (presently 650 μs). The bunch train repetition rate is 10 Hz, and different discrete bunch spacings between 1 μs (1 MHz) and 25 μs (40 kHz) are possible. The train is shared between two undulator beamlines, allowing to serve simultaneously two photon experiments, one at FLASH1 and the other one at FLASH2, both at 10 Hz pulse train repetition rate.

The RF-gun and the accelerator modules are regulated by an outstanding MTCA.4 based low level RF (LLRF) system [14, 15], which allows, within certain limits, different RF amplitudes and phases for the FLASH1 and FLASH2 bunch trains. The arrival time stability down to a few tens of femtoseconds level is realized by a state of the art optical synchronization system [16].

The production of FEL radiation, both at FLASH1 and FLASH2, is based on the SASE (Self Amplified Spontaneous Emission) process. The electron beam peak current required for SASE process is achieved by compressing the electron bunches in two magnetic chicane bunch compressors at beam energies of 150 MeV and 450 MeV, respectively.

FLASH1 has six 4.5 m long fixed gap (12 mm) undulator modules, FLASH2 twelve 2.5 m long variable gap undulators. A planar electromagnetic undulator, installed downstream of the FLASH1 SASE undulators, provides, on request, THz radiation for user experiments.

* katja.honkavaara@desy.de

[†] for the FLASH team

STATUS AND PERSPECTIVES OF THE FERMI FEL FACILITY

L. Giannessi[†], E. Allaria, L. Badano, F. Bencivenga, C. Callegari, F. Capotondi, F. Cilento, P. Cinquegrana, M. Coreno, I. Cudin, M. B. Danailov, G. D'Auria, R. De Monte, G. De Ninno, P. Delgiusto, A. Demidovich, M. Di Fraia, S. Di Mitri, B. Diviaco, A. Fabris, R. Fabris, W. M. Fawley, M. Ferianis, P. Furlan Radivo, G. Gaio, D. Gauthier, F. Gelmetti, F. Iazzourene, S. Krecic, M. Lonza, N. Mahne, M. Malvestuto, C. Masciovecchio, M. Milloch, N. Mirian, F. Parmigiani, G. Penco, A. Perucchi, L. Pivetta, O. Plekan, M. Predonzani, E. Principi, L. Raimondi, P. Rebernik Ribič, F. Rossi, E. Roussel, L. Rumiz, C. Scafuri, C. Serpico, P. Sigalotti, S. Spampinati, C. Spezzani, M. Svandrlik, M. Trovò, A. Vascotto, M. Veronese, R. Visintini, D. Zangrando, M. Zangrando, Elettra Sincrotrone Trieste S.C.p.A., 34149 Basovizza, Italy

Abstract

FERMI is a seeded Free Electron Laser (FEL) user facility at the Elettra laboratory in Trieste, operating in the VUV to EUV and soft X-rays spectral range; the radiation produced by the seeded FEL is characterized by a number of desirable properties, such as wavelength stability, low temporal jitter and longitudinal coherence. In this paper, after an overview of the FELs performances, we will present the development plans under consideration for the next 3 to 5 years. These include an upgrade of the linac and of the existing FEL lines, the possibility to perform multi-pulse experiments in different configurations and an Echo Enabled Harmonic Generation (EEHG) experiment on FEL-2, the FEL line extending to 4 nm (310 eV).

INTRODUCTION

FERMI is located at the Elettra laboratory in Trieste. The FEL facility covers the VUV to soft X-ray photon energy range with two FELs, FEL-1 and FEL-2, both based on the High Gain Harmonic Generation seeded mode (HG HG) [1,2]. The HG HG scheme consists in preparing the electron beam phase space in a modulator where the interaction with an external laser induces a controlled and periodic modulation in the electron beam longitudinal energy distribution. The beam propagates through a dispersive section which converts the energy modulation into a density modulation. The density modulated beam is then injected in an amplifier where the amplification process is initially enhanced by the presence of the modulation. This HG HG scheme is implemented in FERMI FEL-1, to generate fully coherent radiation pulses in the VUV spectral range [3]. The seed signal, continuously tuneable typically in the range of 230-260 nm, is obtained from a sequence of nonlinear harmonic generation and mixing conversion processes from an optical parametric amplifier. The radiation resulting from conversion in the FEL up to the 13-15th harmonics is routinely delivered to user experiments [4]. The amplitude of the energy modulation necessary to initiate the HG HG process grows with the order of the harmonic conversion and the induced energy dispersion has a detrimental effect on

the high gain amplification in the final radiator. During the past few years of operations, we have demonstrated the ability to operate the FEL at even higher harmonic orders with reduced performances, e.g., up to the 20th harmonic, but substantially higher orders can be reached with a double stage HG HG cascade, where the harmonic conversion is repeated twice. The double conversion is done with the fresh bunch injection technique [5] on FERMI FEL-2. The FEL is composed by a first stage, analogous to FEL-1, followed by a delay line, a magnetic chicane slowing down the electron beam with respect to the light pulse generated in the first stage. The light pulse from the first stage is shifted to a longitudinal portion of the beam unperturbed by the seed in the first stage. The light from the first stage functions as a short wavelength seed for the second stage. This scheme was implemented for the first time on FERMI FEL-2 [6] and was used to demonstrate the seeded FEL coherent emission in the soft-X rays, up to harmonic orders of 65, and more [7].

A first upgrade program of FERMI was completed beginning of 2016, with the installation of two new linac structures, an additional undulator segment for the radiator of the first stage of FEL-2, and a second regenerative amplifier for the seed laser system of FEL-2 [8]. After these upgrades the maximum attainable energy is 1.55 GeV for a “compressed” and “linearized” electron beam. The higher beam energy improved the performances of both the FELs, particularly for FEL-2 in the high end of the photon energy spectral range. FEL-2 has reached stable operation, with harmonic conversion factor 13 in the first stage and 5 in the second stage, at the shortest wavelength of the operating range of 4 nm. Since June 2016 the repetition rate of the source can be selected between 10 and 50 Hz. Two operation modes are foreseen: low and medium energy (electron beam energy up to 1350 MeV), at 50 Hz rep rate; high energy (1550 MeV) at 10 Hz rep rate. Harmonics of FEL-2 were measured down to 1.33 nm, as the third harmonic of the FEL tuned with the fundamental at 4 nm (this corresponds to harmonic 195 of the seed, see Fig. 2 below). In November 2016, it was possible to use at the DIPROI end-station, the 3rd harmonic of the FEL at the Cobalt L-edge, $\lambda = 1.6$ nm (778 eV).

[†] luca.giannessi@elettra.eu

MATTER-RADIATION INTERACTIONS IN EXTREMES (MARIE) PROJECT OVERVIEW

R. L. Sheffield,[†] C. W. Barnes,^{*} and J. P. Tapia,[‡]
Los Alamos National Laboratory, Los Alamos, NM 87544, USA

Abstract

The National Nuclear Security Administration (NNSA) has a mission need to understand and test how material structures, defects and interfaces determine performance in extreme environments. The MaRIE Project will provide the science ability for control of materials and their production for vital national security missions. To meet the mission requirements, MaRIE must be a high-brilliance, short-pulse, coherent x-ray source with a very flexible pulse train to observe phenomena at time scales relevant to advanced manufacturing processes and dynamic events, with high enough energy to study high-Z materials. This paper will cover the rationale for the machine requirements, a pre-conceptual reference design that can meet those requirements, and preliminary research needed to address the critical high risk technologies.

MARIE MISSION

MaRIE will provide critical data to advance the state-of-art in understanding materials performance in dynamic environments and to guide advanced manufacturing. Providing this capability requires two coupled key elements: state-of-art computing platforms and advanced models, and experimental facilities which can inform these models and validate the resulting calculations. These experimental facilities must be able to perform across an extremely wide range of environmental conditions, time scales, and physical resolutions. MaRIE complements the planned National Strategic Computing Initiative by providing the data to allow resolved calculations of component manufacturing processes and system response and performance in both normal and abnormal environments. Together, MaRIE and Exascale computing will enable rapid and confident development of new materials and systems through more cost-effective and more rigorous science-based approaches.

As stated in the Basic Energy Science (BES) report on Opportunities for Mesoscale Science [1], in many important areas the functionality critical to macroscopic behaviour begins to manifest itself not at the atomic or nanoscale but at the mesoscale, where defects, interfaces, and non-equilibrium structures dominate behaviour. Microstructure is important because it determines the material's macroscopic engineering properties, such as strength, elasticity, stability under heat and pressure, and how those properties evolve with time and use. The MaRIE effort will deliver the ability to study, and thus control, time-dependent processes, structures, and properties during the manufacturing process. Experimental characterization will be complemented by capabilities in synthesis and fabrication and will be integrated with advanced

theory, modelling, and computation.

MaRIE will address this capability gap, which derives from our inability to see into and through optically opaque objects at the mesoscale, by using a coherent, brilliant x-ray source that has the required photon energy and repetition rate characteristics.

PROJECT STATUS

The MaRIE project has been in development since the late 2000s. In reviewing possible laboratory futures during the last contract transition, LANL determined that a National Security mission gap existed and a new science capability was needed. The Department of Energy has a formal process for the submission of major capabilities enhancements. The first step in this process is Critical-Decision 0, CD-0, that confirms a mission gap of national importance exists. However, CD-0 explicitly does not specify how the gap will be filled, such as what type of facilities or approaches are required. MaRIE had formal approval of Mission Need, CD-0, in March, 2016.

To understand the possible future budgetary impacts on DOE, a required part of the CD-0 submission is a schedule and budget estimate. A "plausible alternative" that will address most of the foreseen science gaps must be developed to define the required estimate of the project. The pre-conceptual reference design given later in this paper formed the basis of a schedule and budget estimate.

Following CD-0, the first step towards CD-1 is confirmation of Scientific Functional Requirements (SFRs) intended to address the mission gaps identified in CD-0. The Technical Functional Requirements (TFRs) follow from the SFRs and guide the Analysis of Alternatives (AoA). An independent review of the SFRs and TFRs by an external peer review committee was conducted in September, 2016. The AoA evaluates possible practical approaches to resolving the TFRs and does not assume the previously mentioned reference design will be the correct solution. The result of the AoA is a delineation of the facility requirements that will be addressed in a Conceptual Design. Presently, the DOE is convening a panel to conduct an independent AoA, which will be followed by the start of Conceptual Design. The remaining major Critical Decision gates after CD-1 are: Preliminary Design (CD-2), Final Design (CD-3), and Approval for Operations (CD-4).

SCIENTIFIC REQUIREMENTS

Careful assessment and analysis, based on the efforts of many working groups and the results of workshops [2], resulted in a set of Scientific Functional Requirements [3] that, if met, will provide the necessary measurements of

email addresses: [†]sheff@lanl.gov, ^{*}cbarnes@lanl.gov, [‡]john_t@lanl.gov

DIAMOND DOUBLE-CRYSTAL SYSTEM FOR A FORWARD BRAGG DIFFRACTION X-RAY MONOCHROMATOR OF THE SELF-SEEDED PAL XFEL

Yu. Shvyd'ko*, S. Kearney, K.-J. Kim, T. Kolodziej, D. Shu
 Argonne National Laboratory, Lemont, IL 60439, USA

V. D. Blank, S. Terentyev

Technological Institute for Superhard and Novel Carbon Materials, Troitsk, Russian Federation

H.-S. Kang, C.-K. Min, B. Oh

Pohang Accelerator Laboratory, Gyeongbuk, Republic of Korea

P. Vodnala, Northern Illinois University, DeKalb, IL 60115, USA

J. Anton, University of Illinois at Chicago, Chicago, IL 60607, USA

Abstract

PAL XFEL (Republic of Korea) is being planned to be operated in the self-seeded mode in a 3-keV to 10-keV photon spectral range. Monochromatization of x-rays in the self-seeding system will be achieved by forward Bragg diffraction (FBD) from two diamond single crystals in the [100] and [110] orientations (one at a time). We present results on the optical and engineering designs, on the manufacturing, and on the x-ray diffraction topography characterization of the diamond double-crystal systems for the FBD monochromator.

PHYSICAL REQUIREMENTS AND OPTICAL DESIGN

Seeded x-ray free-electron lasers (XFELs) [1, 2] generate fully coherent x-rays with a well-defined spectrum and high spectral flux. A hard x-ray self-seeding scheme uses x-rays from the first half of the FEL system (electron beam in a magnetic undulator system) to generate radiation by the self-amplified spontaneous emission process and seed the electron bunch in the second half of the FEL system via an x-ray monochromator [3, 4]. PAL XFEL [5] plans the hard x-ray self-seeding system operating in the spectral range from 3 keV to 10 keV, to be installed and commissioned in 2018. The concept of the system is based on the LCLS design [1], which utilizes the one-crystal forward Bragg diffraction (FBD) x-ray monochromator proposed at DESY [4].

X-rays in Bragg diffraction from a crystal, see Fig. 1, are emitted with a time delayed t upon excitation with an x-ray pulse and subsequent multiple scattering in the crystal either at a Bragg angle θ to the reflecting atomic planes (indicated in blue) or in the forward direction (in red). The FBD time response of an x-ray-transparent crystal, such as diamond, can be presented by the analytical expression [6, 7]

$$|G_{00}(t)|^2 \propto \left[\frac{1}{2\mathcal{T}_0} \frac{J_1 \left[\sqrt{\frac{t}{\mathcal{T}_0} \left(1 + \frac{t}{\mathcal{T}_d} \right)} \right]}{\sqrt{\frac{t}{\mathcal{T}_0} \left(1 + \frac{t}{\mathcal{T}_d} \right)}} \right]^2 \quad (1)$$

with the characteristic time parameters

$$\mathcal{T}_0 = \frac{2[\bar{\Lambda}_H^{(s)}]^2 \sin(\theta + \eta)}{cd}, \quad \mathcal{T}_d = \frac{2d \sin^2 \theta}{c|\sin(\theta - \eta)|}. \quad (2)$$

where \mathcal{T}_0 is the FBD time constant, see Fig. 1(c), $\bar{\Lambda}_H^{(s)}$ is the extinction length (a Bragg reflection invariant), $\mathbf{H} = (hkl)$ is the Bragg diffraction vector, d is the crystal thickness, η is the asymmetry angle between the crystal surface and the reflecting atomic planes, c is the speed of light, and J_1 is the Bessel function of the first kind. The FBD time response is shown by the red line in Fig. 1(c) for a particular case. The FBD photons are concentrated within a spectral bandwidth,

$$\Delta E_0 = \frac{\hbar}{\pi\mathcal{T}_0}, \quad (3)$$

see Fig. 1(b), which is typically larger than $\Delta E_H = \Delta E_0 (2\pi\bar{\Lambda}_H^{(s)}/d)$, the spectral width of BD, see Fig. 1(a).

The first trailing maximum of the FBD time response appears at time delay $t_s = 26\mathcal{T}_0$, see Fig. 1(c), and its duration is $\Delta t_s = 16\mathcal{T}_0$ (assuming $t \ll \mathcal{T}_d$). The intensity, delay, duration, and monochromaticity of the x-ray photons are defined by the single parameter \mathcal{T}_0 . For efficient seeding, we require that the peak of the electron bunch is delayed by t_s , to overlap with the first trailing maximum. The optimal delay is $t_s = 20 - 25$ fs. As a result, the FBD monochromator crystal parameters d , $\bar{\Lambda}_H^{(s)}$, θ , and η should be chosen such that $\mathcal{T}_0 \approx 0.75 - 1$ fs.

An x-ray pulse emanating from the crystal in FBD is not only delayed, it experiences also a lateral shift [6, 7]

$$x = tc \cot \theta, \quad (4)$$

proportional to the time delay t schematically shown in the left graph of Fig. 1. To ensure efficient seeding, the lateral shift x_s at the time delay t_s should be much smaller than the electron beam size, which is $\approx 25 \mu\text{m}$ (rms) for PAL XFEL.

A practically important question for the fabrication of the FBD monochromator crystals is an admissible angular spread $\Delta\theta_A$ of the crystal lattice deformation due to crystal defects or mounting strain. From Bragg's law $E = E_H \sin \theta$ ($E_H = hc/2d$ is a backreflection photon energy) the variation δE of the peak reflectivity in BD and of the FBD spectral function with angle is $\delta E = E_H \delta\theta \cos \theta$. If we require that

* shvydko@aps.anl.gov

CONCEPT FOR A SEEDED FEL AT FLASH2*

C. Lechner[†], R. W. Assmann, J. Bödewadt, M. Dohlus, N. Ekanayake[‡], G. Feng, I. Hartl, T. Laarmann, T. Lang, L. Winkelmann, I. Zagorodnov, DESY, 22607 Hamburg, Germany
 S. Khan, DELTA, TU Dortmund University, 44227 Dortmund, Germany
 A. Azima, M. Drescher, Th. Maltezopoulos[§], T. Plath[¶],
 J. Rossbach, W. Wurth, University of Hamburg, 22671 Hamburg, Germany

Abstract

The free-electron laser (FEL) FLASH is a user facility delivering photon pulses down to 4 nm wavelength. Recently, the second FEL undulator beamline 'FLASH2' was added to the facility. Operating in self-amplified spontaneous emission (SASE) mode, the exponential amplification process is initiated by shot noise of the electron bunch resulting in photon pulses of limited temporal coherence. In seeded FELs, the FEL process is initiated by coherent seed radiation, improving the longitudinal coherence of the generated photon pulses. The conceptual design of a possible seeding option for the FLASH2 beamline envisages the installation of the hardware needed for high-gain harmonic generation (HG) seeding upstream of the already existing undulator system. In this contribution, we present the beamline design and numerical simulations of the seeded FEL.

INTRODUCTION

High-gain free-electron lasers (FELs) [1–4] generate ultrashort photon pulses of unparalleled intensities, enabling the study of fundamental processes with unprecedented temporal and spatial resolution. In a self-amplified spontaneous emission (SASE) FEL, the exponential amplification process is initiated by the shot-noise of the electron bunch, resulting in poor longitudinal coherence of the FEL radiation. Seeding techniques using external light pulses can be applied to transform the FEL into a fully coherent light source. High-gain harmonic generation (HG) [5] uses an external, longitudinally coherent, light pulse that manipulates the electron beam in a short undulator (the modulator) generating a sinusoidal energy modulation. The following chicane converts the energy modulation into a periodic pattern of microbunches. The harmonic content of this density modulation initiates longitudinally coherent FEL emission in the radiator at the desired harmonic. As the seeding process increases the energy spread of the electron beam, the achievable harmonic number is limited [6]. Single-stage HG seeding up to the 15th harmonic was demonstrated at the seeded FEL user facility FERMI [7].

Table 1: Parameters for HG seeding at FLASH2 (for operation at the 14th harmonic)

Parameter	Value
electron beam energy	1000 MeV
rms slice energy spread	150 keV
seed laser wavelength	267 nm
seed pulse energy	50 μ J
seed pulse duration	50 fs
harmonic number	14
FEL wavelength	19.0 nm
repetition rate:	
initial	10 Hz
after upgrade	(up to) 800 Hz

The FEL user facility FLASH [8] at DESY in Hamburg (see Fig. 1) has been in operation since 2005 [9], delivering high-brilliance SASE FEL radiation at wavelengths down to 4.2 nm. The superconducting linear accelerator is operated with 10 long radio-frequency pulses per second, during which trains with up to 800 high-brightness electron bunches (at a repetition rate of 1 MHz) can be accelerated to energies of up to 1.25 GeV. These bunch trains are distributed over two undulator beamlines using flat-top kickers. This enables operation at the 10-Hz bunch train repetition rate in both beamlines, the FLASH1 beamline with a fixed-gap undulator, where also the seeding experiment sFLASH [10] is installed, and the recently added FLASH2 beamline. Simultaneous SASE FEL delivery to photon user experiments at both FLASH1 and FLASH2 is now routinely achieved [11, 12] and simultaneous three-beamline SASE lasing (FLASH1, FLASH2, and sFLASH) was demonstrated [13] during machine studies.

Cascaded HG seeding was studied [14] in the conceptual planning phase of the FLASH2 undulator beamline. However, this scheme was not implemented. In the present paper, the proposed implementation of single-stage HG seeding at FLASH2 up to a maximum harmonic number of 14, corresponding to a shortest wavelength of 19 nm, is described. Table 1 lists the key parameters for HG-seeded operation at 19 nm. The initial implementation Phase 1A would provide seeding at a repetition rate of 10 Hz. Implementation Phase 1B is entered by upgrading the seed laser system to high-repetition-rate operation at a 100-kHz burst rate, matching the bunch pattern delivered by the superconducting linac. Thanks to this combination of superconducting linear accelerator and high-repetition-rate

* Work supported by Federal Ministry of Education and Research of Germany under contract No. 05K13GU4, 05K13PE3, and 05K16PEA.

[†] christoph.lechner@desy.de

[‡] present address: Michigan State University, East Lansing, MI 48824, USA

[§] present address: European XFEL GmbH, 22869 Schenefeld, Germany

[¶] present address: DELTA, TU Dortmund University, 44227 Dortmund, Germany

Content from this work may be used under the terms of the CC BY 3.0 licence (© 2018). Any distribution of this work must maintain attribution to the author(s), title of the work, publisher, and DOI.

FEL PULSE SHORTENING BY SUPERRADIANCE AT FERMI

N. S. Mirian¹, S. Spampinati¹, L. Giannessi^{1,2}

¹Elettra-Sincrotrone Trieste, 34149 Trieste, Italy

²ENEA, CR Frascati, Via E. Fermi 45, 00044 Frascati (Rome), Italy

Abstract

Explorations of saturated superradiant regime is one of the methods that could be used to reduce the duration of the pulses delivered by FERMI. Here we present simulation studies that show the possible application of a superradiant cascade leading to a minimum pulse duration below 8 fs and to a peak power exceeding the GW level in both FEL lines FEL-1 and FEL-2.

INTRODUCTION

FERMI is an externally seeded free electron laser (FEL) user facility producing photons in extreme-ultraviolet and soft x-ray spectral region, with a high degree of coherence and spectral stability [1]. FERMI hosts two FEL lines, FEL-1, which covers the wavelength range between 100 and 17 nm and FEL-2 in the range between 17 and 4 nm. The shortest pulses delivered by the FELs are expected to be in the ranges 40-90 fs on FEL-1 [2] and 20-40 fs on FEL-2, according to the seed duration and the final wavelength [1,3]. The FERMI FELs have already been exploited in fast time resolution studies, however a shorter-duration pulse, in the few femtoseconds regime, would allow resolving very fast processes as electronic rearrangements, and would increase the number of targeted experiments. One of the remarks about the implementation of ultrashort-ultraintense pulses in structural studies is that it should be possible to outrun radiation damage while collecting single-shot diffraction images with high spatial resolution [4–7].

Several techniques were proposed to obtain shorter FEL pulses at FERMI, as the chirped pulse amplification (CPA) method [8] or the manipulation of electron beam energy spread at the laser heater to longitudinally reduce the lasing portion of the beam itself [9, 10]. The method we investigate in this contribution relies on the exploration of superradiant regime in a cascaded FEL [11–16] to reduce the pulse length below the cooperation length, while preserving or even enhancing the FEL peak power beyond the saturation level ($P_{\text{sat}} \approx \rho P_{\text{beam}}$).

According to the theory [16–18], when the seed duration L_{seed} is comparable or shorter than slippage distance over a synchrotron period, slippage itself, combined with the saturation process, can shorten the pulse pushing it forward into fresh, unmodulated electrons. In this regime the pulse energy continues to grow at the expense of the electron energy and the peak power increases as $P \propto z^2$; the pulse duration δs is related to the peak power and scales as the slippage distance in half synchrotron oscillation period $2\pi/\omega_s$, i.e. proportionally to the root of the optical field amplitude, $\delta s \propto z^{-1/2}$.



Figure 1: Layout of FERMI FEL-1. The modulator (period length of $\lambda_m = 10$ cm) is tuned to the seed wavelength ($\lambda_s = 232$ nm). The amplifier is composed of two parts. Two undulators are resonant with the 5th harmonic of the seed ($\lambda_1 = 46$ nm) and the last four undulators are tuned to the 10th ($\lambda_f = 23.2$ nm) or 15th ($\lambda_f = 15.6$ nm) harmonics of the seed.

The FEL pulse is therefore temporally compressed and may become significantly shorter than the input seed.

The initial pulse formation may be induced by an external seed or may be the result of an equivalent density modulation of the electron current. In a cascaded undulator configuration, the power growth is indeed proportional to the profile of the bunching ($G(z, s) \propto b(z, s)$) at the resonant frequency in each stage of the cascade. This configuration, based on a sequence of FEL amplifiers, allows to seed an undulator at optical frequencies while inducing the growth of a superradiant pulse in the VUV range of the spectrum [16]. The scheme was investigated at SPARC, where the transition in a two stages cascade with frequency doubling at optical frequencies was studied [13]. A similar setup in the frame of the FERMI FEL-1 or FEL-2 allowing an undulator cascade made by three or four stages should enable reaching with the final wavelength the VUV or even the soft X-ray spectral range.

In this contribution we have studied via Genesis simulations [20], the applications of superradiance at FERMI FEL-1 and FEL-2 as a method to achieve extremely short pulses.

FERMI FEL-1

The superradiant cascade may be configured at FERMI by tuning the variable gap undulators defining different undulator segments resonant at the different wavelengths. The undulator line of FERMI FEL-1 is composed by a modulator resonant with the UV seed laser and a sequence of six radiators amplifying the desired harmonic order in the VUV, with harmonics typically in the range of 3-15. A superradiant cascade may be configured by tuning the undulator resonances of FEL-1 as shown in Fig. 1.

The electron beam energy at FERMI can be adjusted in the range 0.9 to 1.5 GeV. Table 1 summarizes typical electron beam parameters from the FERMI LINAC, which were used in the simulation. The electron beam profiles were retrieved

STATUS OF THE HARD X-RAY SELF-SEEDING PROJECT AT THE EUROPEAN XFEL

X. Dong, G. Geloni*, S. Karabekyan, L. Samoylova, S. Serkez, H. Sinn,
European XFEL, Schenefeld, Germany
W. Decking, C. Engling, N. Golubeva, V. Kocharyan,
B. Krause, S. Lederer, S. Liu, A. Petrov, E. Saldin, T. Wohlenberg,
DESY, Hamburg, Germany
D. Shu, ANL, Argonne, USA
V. D. Blank, S. Terentiev, TISNCM, Troitsk, Russian Federation

Abstract

A Hard X-ray Self-Seeding setup is currently under realization at the European XFEL, and will be ready for installation in 2018. The setup consists of two single-crystal monochromators that will be installed at the SASE2 undulator line. In this contribution, after a short summary of the physical principles and of the design, we will discuss the present status of the project including both electron beam and X-ray optics hardware. We will also briefly discuss the expected performance of the setup, which should produce nearly Fourier-limited pulses of X-ray radiation with increased brightness compared to the baseline of the European XFEL, as well as possible complementary uses of the two electron chicanes.

THE HARD X-RAY SELF-SEEDING PROJECT AT THE EUROPEAN XFEL

Hard X-ray Self-Seeding (HXRSS) setups based on single-crystal monochromators [1] are active filtering systems allowing for the production of nearly Fourier-limited Hard X-ray radiation pulses at XFELs. They take advantage of the specific impulse response function of single thin crystals in transmission geometry, usually diamond crystals with a thickness around 100 μm , which is constituted by a first response similar to a Dirac δ -function followed by a long tail. The principle was first demonstrated at the LCLS [2].

A Hard X-ray Self-Seeding setup is currently under realization at the European XFEL, and will be ready for installation in 2018.

Double-Chicane Design and Performance

The specific characteristics of the European XFEL, compared to other XFELs, are the high-repetition rate and the availability of long, variable-gap undulators [3]. The latter allows for efficient tapering of the self-seeded signal, and the former for an increase of the average signal brightness, compared to low repetition-rate machines.

In order to increase the signal-to-noise ratio between seed signal and competing SASE (which constitutes, in this case, noise) we rely on a double magnetic chicane design, as sketched in Fig. 1.

We illustrate the advantages of the double-chicane design in Fig. 2, in which we show the filtering stages, Stage 2 and Stage 4, where the C004 reflection from a 100 μm -thick diamond crystal, symmetrically cut, is used. The two undulator parts in Stage 1 and Stage 3 have the same magnetic length. As it can be seen, Stage 4 suffers from poor signal-to-noise ratio. If one proceed with amplification, the seed signal would be lost due to a rapidly growing SASE signal. However, at the filtering position the signal is still almost Fourier limited and therefore the spectral density is higher than that at Stage 2. As a result, the seed signal in the time-domain is larger in Stage 4, compared to Stage 2 of a factor about equal to the ratio between the SASE and the seeded signal bandwidths. The scheme will therefore be highly beneficial in the increase of the signal-to-noise ratio of the seed.

Crystal reflections are available starting from about 3 keV, and although heat loading will likely limit the repetition rate at these very low seed energies, the double-chicane setup will help to improve the situation (see the next subsection). Simulations show that reaching to 14.4 keV should be possible on the high-energy side of the spectrum. The long undulators available at the European XFEL allow for increasing the final output power via tapering. The energy-range around 9 keV is expected to yield optimal performance. Previous studies [4] show that, for a nominal 250 pC electron beam (calculated by s2e simulations [5]) at 17.5 GeV electron energy, combining seeding and tapering one could obtain TW class beams with about 1eV bandwidth, with $7 \cdot 10^{12}$ photons per pulse. Owing to the high-repetition rate of the European XFEL, an average spectral flux of about $2 \cdot 10^{14}$ ph/s/meV can be expected.

Heat Loading Issues

The high-repetition rate of the European XFEL is also related with an increase of heat-loading of the crystals because of impinging X-rays due both to spontaneous emission and SASE/seeded radiation pulses. For both cases, the burst pattern of the European XFEL will lead to a steady temperature increase during a given bunch train, followed by a temperature decrease between one train and the next. If the temperature increase is associated to a shift of the seed frequency of the crystal well beyond a Darwin width, an overall deterioration of the bandwidth is to be expected.

* gianluca.geloni@xfel.eu

CONSTRAINTS ON PULSE DURATION PRODUCED BY ECHO-ENABLED HARMONIC GENERATION*

G. Penn[†], LBNL, Berkeley, USA

B. Garcia, E. Hemsing, G. Marcus, SNL, Menlo Park, USA

Abstract

Echo-enabled harmonic generation (EEHG) is well-suited for producing long, coherent pulses at high harmonics of seeding lasers. There have also been schemes proposed to adapt EEHG to output extremely short, sub-fs pulses by beam manipulations or through extremely short seed lasers, but the photon flux is generally lower than that produced by other schemes. For the standard EEHG layout, it is still interesting to consider different parameter regimes and evaluate how short a pulse can be generated. EEHG at high harmonics uses a large dispersive chicane which can change the relative distance of electrons substantially, even longer than a typical FEL coherence length. We evaluate the ability to produce short pulses (in the femtosecond to 10 fs range) using a combination of theory and simulations.

INTRODUCTION

The radiation produced by free electron lasers (FELs) can be enhanced in many ways through seeding techniques. Echo-enabled harmonic generation (EEHG) [1] uses two energy modulations from external lasers to generate a much shorter output wavelength. A schematic of an EEHG beamline is shown in Fig. 1. It has several advantages over seeding schemes with a single seed laser, such as high-gain harmonic generation (HG) [2]. EEHG allows for a very large jump in photon energy in a single stage, without requiring the fresh-bunch technique. It is capable of producing narrow bandwidths by having long output pulses and it can also be less sensitive to distortions in the current or energy profile. However, short pulses with a corresponding large bandwidth are also of interest for many scientific applications. Therefore, it is worth exploring how to produce pulses shorter than 10 fs using the EEHG technique. Here, we only examine initial seeding to produce microbunches at the desired wavelength, which then radiate and amplify in a conventional FEL system. Attosecond schemes are not considered.

CONSTRAINTS ON ELECTRON BUNCH DURATION

We first consider using a very short electron bunch to limit the duration of the output radiation. In this case, the main limitation is that the EEHG scheme produces bunching over a multiple of frequency intervals. The frequency components of the electron current profile can interact with these other microbunching components to yield a combination that will

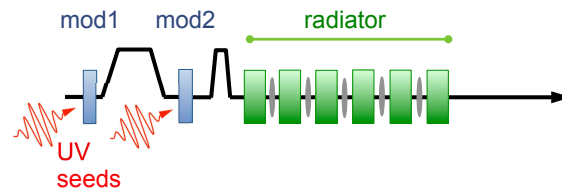


Figure 1: Schematic of an EEHG beamline, showing chicanes, modulating undulators, lasers, and radiating undulators.

either disrupt the FEL gain or introduce a large number of modes. This concern leads to an approximate constraint on the final pulse duration σ_z :

$$\sigma_z \geq \frac{\lambda_1 \lambda_2 E_{M1}}{\lambda_{\text{echo}} E_{M2}} \frac{1}{\sqrt{2} \pi (|n|^{4/3} + |n|^{2/3})}. \quad (1)$$

Here $\lambda_{1,2}$ are the wavelengths of the two incident lasers which modulation, λ_{echo} is the desired output wavelength, $E_{M1,2}$ are the amplitudes of the two energy modulations, and n is one of the mode numbers for the wave mixing. Typically, $n = -1$.

This constraint can also be viewed in terms of time. To obtain a given harmonic, the product of E_{M2} and the strength of the dispersive element after the first modulation are tightly constrained. If the second energy modulation is decreased, the dispersion, which can be quite large, has to be increased. Because the dispersion follows the first energy modulation, electrons will be displaced by an amount proportional to the amplitude of the first energy modulation. Thus, even if a very short initial bunch is used, by the time the EEHG manipulations are finished the bunch could be significantly longer, and the output pulse will match this new bunch length. For a short bunch, the induced bunching tends to reach a minimum in the center, and double-peaked pulses are the first sign that the bunch length is becoming too short for a particular EEHG configuration.

CONSTRAINTS ON DURATION OF SEEDING LASERS

Another way to produce short bunches is to use short lasers to only generate bunching over a fraction of the electron bunch. One constraint here is over the duration of the first energy modulation. If it is very short, the chicane will again spread these particles out, leaving a localized low-current hole in the electron bunch. This is the same effect used for laser slicing techniques in storage rings [4]. To

* This work was supported by the Director, Office of Science, Office of Basic Energy Sciences, U.S. Department of Energy under Contract Nos. DE-AC02-05CH11231 and DE-AC02-76SF00515.

[†] gepenn@lbl.gov

STRONGLY TAPERED UNDULATOR DESIGN FOR HIGH EFFICIENCY AND HIGH GAIN AMPLIFICATION AT 266 nm

Youna Park, Nick Sudar, Pietro Musumeci, UCLA, Los Angeles, CA 90095, USA
 Yine Sun, Alexander Zholents, ANL, Argonne, IL 60439, USA
 Alex Murokh, RadiaBeam, Los Angeles, CA 90404, USA
 David Bruhwiler, Chris Hall, Stephen Webb, RadiaSoft, Boulder, CO 80301, USA

Abstract

Tapering Enhanced Stimulated Superradiant Amplification (TESSA) is a scheme developed at UCLA to increase efficiency of Free Electron Laser (FEL) light to above 10% using intense seed pulses, strongly tapered undulators and prebunched electron beams. Initial results validating this method have already been obtained at 10- μm wavelength at Brookhaven National Laboratory. In this paper we will discuss the design of an experiment to demonstrate the TESSA scheme at high gain and shorter wavelength (266 nm) using the Linac Extension Area (LEA) beamline at the Advanced Photon Source of Argonne National Laboratory (ANL) to obtain conversion efficiencies around 10% depending on the length of the tapered undulator (up to 4m).

INTRODUCTION

X-ray Free Electron Lasers (FEL) have revolutionized the trajectory of science opening the door to the direct study at atomic spatial and temporal scales of fundamental systems such as chemical bond formation, motion of electrons through materials, 3D images of proteins and many more [1]. In high gain FELs the efficiency of electron beam energy conversion into radiation is typically limited to less than 1% due to the saturation effect [2]. Tapering the undulator parameters offers an opportunity to extend the interaction beyond initial saturation [3], and has been shown to provide a boost in efficiency. The Tapering Enhanced Stimulated Superradiant Amplification (TESSA) [4] method using a strongly tapered undulator an intense input seed laser and prebunched electron beams to greatly increase the conversion efficiency has been validated at Brookhaven National Laboratory (BNL) for 10 μm wavelength and 50 cm strongly tapered undulator demonstrating efficiency greater than 35% [5].

In this paper we discuss the design of an experiment where we will demonstrate TESSA at shorter wavelength (266 nm) using the higher energy electron beam at APS linac. This experiment, which we will refer to as TESSA-266, will start with GW-level seed power and demonstrate 30 MeV/m energy exchange rates leading to a final gain of a factor of 10 in laser power. For this experiment we will use the APS injector linac at Argonne National Laboratory (ANL) which has been recently upgraded with an LCLS style photoinjector and can deliver high brightness beams to an experimental beamline where we will install the tapered undulator.

In an FEL, resonant wavelength of interaction is defined as $\lambda = (\lambda_w/2\gamma^2)(1 + K^2)$, where γ is particle energy, K undulator vector potential, and λ_w undulator period.

Table 1: Simulation Parameters of APS Linac

Electron beam energy	375 MeV
Peak current	1 kA
Seed power	< 1 GW
Normalized emittance	2 μm

The particle energy evolution can be written as $d\gamma^2/dz = -2kK_l K \sin(\Psi_r)$ where $K_l = eE_0/km_e c^2$ laser vector potential and E_0 electric field of radiation, K undulator vector potential, and Ψ_r resonant phase. By taking the derivative of the resonance condition and using energy evolution equation we obtain the tapering equation for the normalized magnetic field amplitude along the helical undulator:

$$\frac{dK}{dz} = \frac{(1 + K^2)(dk_w/dz)}{2Kk_w} - k_w K_l \sin \Psi_r. \quad (1)$$

While period tapering is a possibility, we will limit this initial discussion to a constant period case (i.e. $dk_w/dz = 0$) and allow the gap inside the undulator to change to modify the magnetic field amplitude.

MAGNETIC SIMULATION OF UNDULATOR

Undulator Period vs. Beam Clearance

We used Radia to find the peak magnetic field for different undulator periods and gap at the center of the undulator. Figure 1 shows how the undulator vector potential K would vary as we change the undulator period. Where the resonance

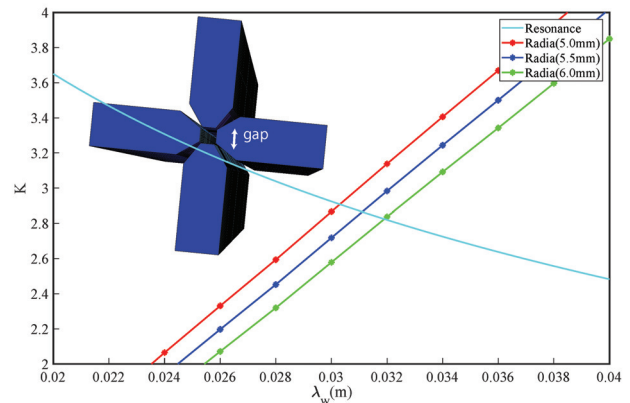


Figure 1: Undulator vector potential vs. undulator period for different gaps plotted with resonance condition.

HUNDRED-GIGAWATT X-RAY SELF-SEEDED HIGH-GAIN HARMONIC GENERATION

L. Zeng[#], S. Zhao, W. Qin, S. Huang, K. Liu

Institute of Heavy Ion Physics, School of Physics, Peking University, Beijing 100871, China

Y. Ding, Z. Huang

SLAC National Accelerator Laboratory, Menlo Park, CA 94025, USA

Abstract

Self-seeded high-gain harmonic generation is a possible way to extend the wavelength of a soft x-ray free-electron laser (FEL). We have carried out simulation study on harmonic generation within the photon energy range from 2 keV to 4.5 keV, which is difficult to be achieved due to a lack of monochromator materials. In this work we demonstrate the third harmonic FEL with the fundamental wavelength at 1.52 nm. Our result shows that, by using undulator tapering technique, hundred-gigawatt narrow-bandwidth FEL output can be obtained.

*INTRODUCTION

Free-electron lasers, the so called fourth generation of light source, allow one to carry out completely new experiments in atomic and molecular physics, chemistry and many other areas. Self-amplified spontaneous emission (SASE) [1,2] is the baseline FEL operation mode in X-ray region, which has good transverse coherence. However, it starts from the shot noise of the electron beam, which leads to the poor properties in terms of a spectral bandwidth.

Several external seeding FEL schemes are proposed to obtain good longitudinal coherence. For example, directly HHG[3], HGHG[4,5], cascade HGHG[6], EEHG[7,8] and so on. Because of lacking external seeds with short wavelength, these external seeding FEL schemes have difficulty in demonstrating at hard X-ray region.

Self-seeding [9] is a way to narrow the SASE bandwidth of XFELs significantly in order to produce nearly transform-limited pulses. Last several years, self-seeding scheme has been demonstrated in both soft and hard x-ray FELs [10,11]. The monochromator for soft x-ray self-seeding FEL (the photon energy below 2 keV) is a grating-based optic system[10], while the hard x-ray self-seeding FEL (the photon energy above 4.5 keV) usually uses diamond-based monochromator[11]. However, the self-seeded FEL has not been demonstrated in the energy region between 2 to 4.5 keV. Previous study in self-seeded HGHG FEL scheme [12] can not only fill the above energy gap, but also extend the wavelength in hard X-ray self-seeding FEL. Ultra-high power FELs are more attractive for the science application like nonlinear Compton scattering[13]. In this paper, the self-seeded HGHG FEL scheme is further studied to obtain ultra-high peak power.

THE SCHEME

The schematic of the self-seeded HGHG FEL is shown in Fig. 1. At first, the electron beam goes through the undulator U_S , generating SASE radiation in the linear regime. At the exit of U_S , the SASE radiation passes through the grating-based X-ray monochromator so as to obtain a narrow-band seed for the following undulator while the electron beam goes through a bypass chicane C_{B1} . The bypass chicane C_{B1} can not only provides a proper delay to make the electron beam and the seed recombine at the entrance of undulator U_A but also help to wash out the microbunching of the electron beam built up in the SASE undulator. Then, we should notice that this seed is different to external seed of regular HGHG FEL[6]. This seed radiation from the monochromator has a much lower power, limited to a few hundred kilowatts herein because of avoiding damaging the state-of-the-art X-ray monochromator optics. As a result, we need to amplify the seed radiation. At the same time, we have to eliminate the impact of electron energy spread degradation in the seed amplification process. Consequently, an electron beam with longer bunch length is used to generate double-spike seed after monochromator. The head spike of the seed is then aligned with the tail part of the electron bunch at the entrance of the amplifying undulator U_A . Therefore only the tail part of the electron bunch is used to amplify the seed while the head part is kept undisturbed and “fresh”. After the U_A undulator, the electron bunch is delayed by a small chicane (C_{B2}), and consequently the head part is aligned with the seed radiation in the modulation undulator (U_{M2}) and gets energy-modulated. The energy modulated electron beam then goes through the dispersion chicane with proper R_{56} , getting density modulated, and radiates at the harmonic wavelength of the seed.

Compared to previous work in 2016[12], we have finished further study in this paper. (1) Further optimization in the amplifier (U_A), modulator (U_{M2}) and dispersion section (C_D), (2) Tapered radiator (U_R) study for higher output harmonic radiation FEL power. The details in both two parts will be shown in the following section.

[#]zengling@pku.edu.cn

HARMONIC LASING TOWARDS SHORTER WAVELENGTHS IN SOFT X-RAY SELF-SEEDING FELS

L. Zeng[#], S. Zhao, W. Qin, S. Huang, K. Liu

Institute of Heavy Ion Physics, School of Physics, Peking University, Beijing, China

Y. Ding, Z. Huang

SLAC National Accelerator Laboratory, Menlo Park, USA

Abstract

In this paper, we study a simple harmonic lasing scheme to extend the wavelength of X-ray self-seeding FELs. The self-seeding amplifier comprises two stages. In the first stage, the fundamental radiation is amplified but well restricted below saturation, and meanwhile harmonic radiation is generated. In the second stage, the fundamental radiation is suppressed and the harmonic radiation is amplified to saturation. We performed start-to-end simulation to demonstrate third harmonic lasing in a soft x-ray self-seeding FEL at the fundamental wavelength of 1.52 nm. Our simulations show that a stable narrow-band FEL at GW level can be obtained.

INTRODUCTION

X-ray free electron lasers (XFELs) are tunable light sources with high power, coherent radiation over a broad spectral range. Self-amplified spontaneous emission (SASE) [1,2] is a usual operation mode in single pass XFEL which has excellent transverse coherence. However, because of starting from shot noise of electron beams, SASE has poor temporal coherence.

Self-seeding [3] is a way to improve the temporal coherence of SASE which consists of two undulators and an X-ray monochromator between them. The monochromator selects a narrow band of radiation from the SASE in the first undulator as the seed. Then the seed is amplified to saturation in the second undulator. This self-seeding scheme works both for soft and hard x-rays and has been demonstrated recently [4,5]. Generally, the main material for monochromator grating when the photon energy is below 2 keV [4]. While the diamond is used for the monochromator when the photon energy is above 4.5 keV [5]. However, because of lacking proper materials, the energy gap between 2 keV to 4.5 keV for self-seeding FEL has not been achieved now.

A possible way to extend the operating range of a soft X-ray self-seeding FEL is to use nonlinear harmonic generation [6]. The odd harmonics can be radiated in the same undulator [7]. However, the intensity of harmonics is rather small because of the dominance of the interaction at the fundamental radiation [7-9]. In this paper, we study the harmonic lasing in soft X-ray self-seeding FEL which could fill the energy gap not easily achieved by regular self-seeding schemes. By suppressing the fundamental frequency, we can obtain the odd harmonic radiations with higher intensity.

HARMONIC ANALYSIS FOR THE SELF-SEEDED FEL

In a planar undulator, the resonance condition for the radiation is written as

$$\lambda_h = \frac{\lambda_u(1+K^2/2)}{2h\gamma^2} \quad (1)$$

Here h is the harmonic number, λ_h is the harmonic wavelength, λ_u is the undulator period, γ is relativistic factor, and K is the undulator parameter.

In a high-gain FEL, odd linear and nonlinear harmonics can be radiated on axis [7]. The linear amplification of harmonics is always smaller than the fundamental. The nonlinear harmonic generation occurs when a beam is strongly bunched by the fundamental frequency and the bunch spectrum develops rich harmonic contents. Especially, the growth rate of the nonlinear harmonics is h times higher than that of the fundamental. However, the dominance of the interaction at the fundamental radiation will limit the nonlinear harmonic interaction. So the intensity of harmonics is rather small. Typically, the third harmonic is at the level of a percent of the fundamental.

We study the third harmonic radiation in the soft X-ray self-seeding FEL and our simulation study is based on the LCLS parameters, which are shown in Table 1. Time-dependent simulation result by GENESIS [10] code of the soft X-ray self-seeding is shown in Fig. 1 and Fig. 2. It is clear that after the monochromator, the seed power of radiation is about 200 kW. Fig. 2 shows the evolution of the power of the fundamental and 3rd harmonic in the undulator U_2 . It's clear that the linear gain process is at $z < 15m$ and the linear harmonic grows much more slowly than the fundamental.

Table 1: Parameters Used for Soft X-ray Self-seeding FEL Simulation at LCLS

Parameter	Value	Unit
Electron beam energy	4.3	GeV
Peak current	3	kA
Energy spread	1	MeV
Emittance	0.5	mm-mmrad
Mono. central wavelength	1.52	nm
Mono. resolving power	5000	
Mono. power efficiency	0.02	
Undulator period	0.03	m
U_1 length	19.8	m
U_1 parameter K (rms)	2.4749	

COMPARING FEL CODES FOR ADVANCED CONFIGURATIONS

B. Garcia*, G. Marcus, SLAC, Menlo Park, California, USA
S. Reiche, Paul Scherrer Institut (PSI), Villigen, Switzerland
L. T. Campbell^{1,2}, B. W. McNeil¹, SUPA, Department of Physics,
University of Strathclyde, Glasgow, UK
¹also at Cockcroft Institute, Warrington, UK
²also at ASTeC, STFC Daresbury Laboratory, Warrington, UK

Abstract

Various FEL codes employ different approximations and strategies to model the FEL radiation generation process. Many codes perform averaging procedures over various length scales in order to simplify the underlying dynamics. As FELs are developed in more advanced configurations beyond simple SASE, the assumptions of some codes may be called into question. We compare the unaveraged code Puffin to averaged FEL codes including a new version of GENESIS in a variety of situations. In particular, we study a harmonic lasing setup, a High-Gain Harmonic Generation (HGHG) configuration modeled after the FERMI setup, and a potential Echo-Enabled Harmonic Generation (EEHG) configuration also at FERMI. We find the codes are in good agreement, although small discrepancies do exist.

INTRODUCTION

Numerical simulation is an important tool in assessing the performance of any X-ray FEL. While there has been significant work benchmarking numerical codes to SASE studies [1, 2], comparatively little has been done on other operation modes. In this study, we consider advanced schemes designed to extend the maximum attainable photon energy (harmonic lasing [3]) and improve the temporal coherence (beam-based seeding [4]).

The first harmonic lasing of a self-seeded X-ray FEL has recently been achieved [5], and there is considerable interest in employing this technique to XFELs. In these harmonic lasing setups, the fundamental radiation is disrupted while the higher harmonic emission is allowed to grow unfettered.

We also consider both the High-Gain Harmonic Generation (HGHG) [6, 7] and Echo-Enabled Harmonic Generation (EEHG) [8, 9] seeding schemes. This type of seeding potentially allows the full longitudinal coherence of conventional lasers to be transferred to an X-ray FEL.

Previous work has compared the harmonic generation capabilities of some codes for a seeded beam [10]. This was extended by work which compared the results of FAST, GENESIS, and GINGER in the cases of both artificial and phase-shifted harmonic lasing [11] starting from noise. We extend this result by adding additional simulation results from the un-averaged code PUFFIN. We then provide benchmarks for FERMI inspired HGHG [12] and EEHG configurations between both PUFFIN and GENESIS.

* bryantg@stanford.edu

CODE DESCRIPTIONS

The FEL simulation codes used in this study are PUFFIN [13] and GENESIS [14]. While for the harmonic lasing studies results from the codes FAST and GINGER are presented, no new simulations are performed with these codes and a description of these previous results is found in [11]. Although PUFFIN and GENESIS are both high gain FEL simulation codes, they contain some important differences so we briefly describe each in turn.

GENESIS

GENESIS is a time-dependent, 3D FEL simulation code in which both the radiation field and electron macroparticles are distributed on a Cartesian mesh. GENESIS averages over the motion of an individual undulator period, and therefore computes harmonic emission by employing an effective coupling factor [15]. Furthermore, GENESIS employs the so-called Slowly Varying Envelope Approximation (SVEA) [16] which allows one to average the radiation envelope over a radiation wavelength. While these approximations offer a large computational speedup, advanced FEL configurations may violate one or more of them.

Recent updates to GENESIS, referred to here as GENESIS V4, have made it possible to model each individual electron [17]. These so-called one4one simulations (one electron is one macroparticle) have noise statistics that are automatically correct at any wavelength. This allows for the electron beam to be re-sliced at any harmonic where the dynamics between current spikes, which result from HGHG or EEHG processes, can be modeled consistently. The HGHG and EEHG simulations shown below use this new version while the harmonic lasing simulations from 2014 use the nominal Fortran version.

PUFFIN

In contrast to GENESIS, PUFFIN does not employ the SVEA or average the electron motion. The electric field is instead discretized on a sub-wavelength scale with frequency resolution limited only by the Nyquist frequency. Similarly, the detailed electron motion resolution is limited only by the number of integration steps performed per undulator period. The cost of this is an orders of magnitude increase in computational complexity and memory requirements. While the physics captured is ostensibly more accurate as a result, one would like to benchmark the two codes in only a few

ECHO-ENABLED HARMONIC GENERATION RESULTS WITH ENERGY CHIRP

B. Garcia*, M.P. Dunning, C. Hast, E. Hemsing, T.O. Raubenheimer, SLAC, Menlo Park, USA
 D. Xiang, Shanghai Jiao Tong University, Shanghai, China

Abstract

We report here on several experimental results from the NLCTA at SLAC involving chirped Echo-Enabled Harmonic Generation (EEHG) beams. We directly observe the sensitivity of the different n EEHG modes to a linear beam chirp. This differential sensitivity results in a multi-color EEHG signal which can be fine tuned through the EEHG parameters and beam chirp. We also generate a beam which, due to a timing delay between the two seed lasers, contains both regions of EEHG and High-Gain Harmonic Generation (HGHG) bunching. The two regions are clearly separated on the resulting radiation spectrum due to a linear energy chirp, and one can simultaneously monitor their sensitivities.

INTRODUCTION

There has long been an interest in producing fully coherent X-ray pulses in free electron laser facilities. One promising direction is to seed the electron beam with microbunching structure at the desired wavelength. Two popular methods to do this use either a single modulator-chicane combination, as in High-Gain Harmonic Generation (HGHG) [1] [2], or a dual modulator-chicane setup as in Echo-Enabled Harmonic Generation (EEHG) [3] [4].

We report here the results from a chirped electron beam with simultaneous regions of HGHG and EEHG bunching. The two regions are clearly distinguished by their central wavelength shift [5] and sensitivity to the chirp on the electron beam.

We also directly observe the sensitivity of the different $|n|$ EEHG modes to the linear chirp. By establishing an EEHG configuration with non-negligible and simultaneous bunching at multiple $|n|$ modes, we measure the sensitivity of these modes by observing their wavelength shift as a function of electron beam chirp.

Both of these setups generate a tunable, multi-color EEHG-seeded beam. These experiments were performed in 2015 at SLAC's NLCTA facility, concurrent with work towards producing an EEHG beam capable of radiating at the 75th harmonic of a 2400 nm seed laser [6].

THE NLCTA FACILITY

The electron beam at NLCTA is generated from a 1.6 cell BNL/ANL/UCLA/SLAC S-band ($f = 2.856$ GHz) photocathode gun and is boosted by two subsequent X-band ($f = 11.424$ GHz) accelerating structures to 120 MeV. At this point, the beam has a FWHM duration of ≈ 1 ps, a

bunch charge of approximately 50 pC, and a small slice energy spread $\sigma_E \approx 1$ keV.

The beam then enters a modulating undulator (10 periods, $\lambda_u = 3.3$ cm, $K = 1.82$) where it interacts with an 800 nm (≈ 1 ps FWHM) laser. It then encounters a tunable four-dipole chicane before reaching a second modulating undulator (10 periods, $\lambda_u = 5.5$ cm, $K = 2.76$) where it interacts again with either a 800 nm or 2400 nm laser. The beam traverses a final magnetic chicane before being accelerated by a third X-band cavity which takes the energy to 160 – 192 MeV depending on the experiment. The beam finally enters a two-meter section of the VISA undulator [7] (100 periods, $\lambda_u = 1.8$ cm, $K = 1.26$) where any bunching produced by the upstream transformations is radiated as coherent radiation. This radiation is then diagnosed by a downstream EUV or VUV photon spectrometer [8].

SIMULTANEOUS EEHG AND HGHG SIGNALS

One difference between EEHG and HGHG signals is their response to a linear energy chirp. It has been shown that for the $n = -1$ EEHG mode and an HGHG configuration at the same target harmonic, the central wavelength of the HGHG setup is more sensitive to electron beam chirp than EEHG [5] [9]. This provides a powerful way of discriminating between EEHG and HGHG signals should both be present on the same electron beam.

In HGHG a single modulator produces a sinusoidal energy modulation of magnitude ΔE and at wavenumber k_1 which is converted into a density modulation by a chicane with longitudinal dispersion R_{56} . The resulting bunching is significant at integer harmonics of the laser wavenumber $k = ak_1$ and is [2],

$$b_a^{\text{HGHG}} = \left| e^{-\frac{1}{2}(B_1^2 a^2)} J_n(-aA_1 B_1) \right|, \quad (1)$$

where $A_1 = \Delta E_1 / \sigma_E$, $B_1 = R_{56}^{(1)} k_1 \sigma_E / E_0$. Notably, in order to increase the bunching at a higher harmonic, one must increase the modulation amplitude A_1 and hence the induced energy spread.

In EEHG, there are two chicanes and two separate laser modulators with possibly different laser wavenumbers and the relation $\kappa = k_2 / k_1$. This process produces bunching at wavenumbers $k_{n,m} = nk_1 + mk_2$ which is given by [3],

$$b_{n,m} = \left| e^{-\frac{1}{2}(nB_1 + aB_2)^2} J_n(nB_1 + aB_2) J_m(-aA_2 B_2) \right|, \quad (2)$$

where $a = n + m\kappa$. Analysis of this bunching spectrum reveals that the $n = -1$ harmonics can achieve the most significant bunching. The finely-spaced energy bands created

* bryantg@stanford.edu

DISTRIBUTED SELF-SEEDING SCHEME FOR LCLS-II*Chuan Yang^{1,2†}, Juhao Wu^{1‡}, Guanqun Zhou^{1,3}, Bo Yang⁴,
Cheng-Ying Tsai¹, Moohyun Yoon^{1,5}, Yiping Feng¹, Tor Raubenheimer¹¹SLAC National Accelerator Laboratory, Menlo Park, California, USA²NSRL, University of Science and Technology of China, Hefei, Anhui, China³Institute of High Energy Physics, and UCAS, Chinese Academy of Sciences, Beijing, China⁴University of Texas at Arlington, Arlington, Texas, USA⁵Department of Physics, Pohang University of Science and Technology, Pohang, Korea**Abstract**

Self-seeding is a successful approach for generating high-brightness X-ray free electron laser (XFEL). A single-crystal monochromator in-between the undulator sections to generate a coherent seed is adopted in LCLS. However, for a high-repetition rate machine like LCLS-II, the crystal monochromator in current setup cannot sustain the high average power; hence a distributed self-seeding scheme utilizing multi-stages is necessary. Based on the criteria set on the crystal, the maximum allowed X-ray energy deposited in the crystal will determine the machine configuration for such a distributed self-seeding scheme. In this paper, a distributed self-seeding configuration is discussed for LCLS-II type projects in the hard X-ray FEL energy regime. The study is carried out based on numerical simulation.

INTRODUCTION

Linac Coherent Light Source (LCLS), the world's first hard X-ray FEL has been successfully operated in SASE mode [1]. Conventional SASE FEL has full transverse coherence, but the longitudinal coherence is limited [1,2]. In order to improve the longitudinal coherence, self-seeding scheme has been proposed [3]. A self-seeding X-ray FEL consists of two undulator sections separated in a drift section by a monochromator and an electron by-pass chicane. A grating monochromator was adopted for the soft X-ray [3], while a single crystal monochromator oriented in Bragg transmission geometry can be used for the hard X-ray [4]. The radiation generated by the first undulator section and the electron beam are separated in the drift section between the two undulator sections. The radiation passes through the monochromator, which can filter the radiation spectrum. The electron beam passes through the chicane, which washes out the micro-bunching induced by the first undulator section and delays the electron beam relative to the radiation pulse. The purified radiation and the electron beam are recombined at the entrance of the second undulator section, through which the radiation is amplified up to saturation.

The operation of self-seeding has been successfully achieved at LCLS, in which the repetition rate is 120 Hz.

However, LCLS-II FEL project is designed to operate at a higher repetition rates of 0.93MHz. In this case, the heat load on the monochromator will become an issue and limit the maximal seed power. The multi-stages self-seeding scheme can generate higher spectral purity, which can reduce the heat load of the monochromator.

For the LCLS-II hard X-ray self-seeding (HXRSS) baseline undulator system, there will be two 'missing segments' after segment 7 and 14, which are reserved for self-seeding station shown in Fig. 1. This two-stages self-seeding configuration was considered for the photon energy range of (4 keV~8 keV). In this paper, we study the two-stage self-seeding configuration for LCLS-II project with GENESIS simulation code [5] for 4 keV and 8.3 keV hard X-ray with LCLS-II parameters. All the data refer to single shot realization.

Table 1: The Relevant Parameters used in 4keV and 8.3keV Simulation.

Parameters	Value	Unit
Electron beam energy	4.0/8.0	GeV
Energy spread	0.5	MeV
Peak current	1/3	kA
Normalized emittance	0.45	mm-mrad
FEL photon energy	4/8.3	keV
Charge	100/300	pC
Undulator parameter K	0.96/1.91	-
Undulator period	2.6	cm
Number of period per undulator section	130	-
Total number of sections	32	-
Drift length	1.17	m

NUMERICAL SIMULATION*4-keV Self-Seeding Simulation*

Here we focus on 4keV self-seeding simulation to study LCLS-II HXRSS project in the low photon energy range. The baseline undulator system is shown in Fig. 1. Relevant simulation parameters are presented in Table 1. We assume that the average betatron function is 17.0 m. In the two monochromators, we choose symmetric diamond C(111) crystal to generate the wake seed, and the crystal thickness is 30 μm . The two crystal monochroma-

*The work was supported by the US Department of Energy (DOE) under contract DE-AC02-76SF00515 and the US DOE Office of Science Early Career Research Program grant FWP-2013-SLAC-100164.

†chuany@SLAC.Stanford.EDU

‡jhwu@SLAC.Stanford.EDU

TRANSIENT THERMAL STRESS WAVE ANALYSIS OF A THIN DIAMOND CRYSTAL UNDER LASER HEAT LOAD*

Bo Yang[†], Department of Mechanical & Aerospace Engineering, University of Texas at Arlington, Arlington, TX 76019, USA

Juhao Wu[‡], SLAC National Accelerator Laboratory, Menlo Park, California, 94025, USA

Abstract

When a laser pulse impinges on a thin crystal, energy is deposited resulting in an instantaneous temperature surge in the local volume and emission of stress waves. In the present work, we perform a transient thermal stress wave analysis of a diamond layer 200 μm thick in the low energy deposition per pulse regime. The layer thickness and laser spot size are comparable. The analysis reveals the characteristic non-planar stress wave propagation. The stress wave emission lasts by hundreds of nanoseconds, at a time scale relevant to the high-repetition-rate FELs at the megahertz range. The kinetic energy converted from the thermal strain energy is calculated, which may be important to estimate the vibrational amplitude of the thin crystal when excited under repeated heat loads. The transient heat transfer plays an important role in draining the mechanical energy during the dynamic wave emission process.

INTRODUCTION

Thin crystals play an important role in enabling X-ray FELs of high peak-brightness, Angstrom wavelengths, and femtosecond/sub-femtosecond pulse durations [1]. They are used as monochromator for self-seeding [2,3] and one-shot spectrometer [4-6], for example. To function properly, they must be able to sustain the ever-increasing heat load, especially from multiple pulses at high repetition rates. When a high-intensity light pulse strikes a crystal, energy is deposited through photon-electron interaction. The energy is further passed on to the lattice. It results in a temperature surge over the volume on its way of passage. It is speculated that the deposited thermal strain energy would trigger stress waves. The dynamic strain field may directly affect the optics performance. The stress wave emission may also convert a part of the deformation energy into kinetic energy. When cumulated near a resonant frequency, it may lead to severe vibration impairing the device steadiness.

In the present work, we perform a transient thermal stress wave analysis to elucidate the dynamics of stress wave emission in a thin diamond crystal under heat load of an X-ray FEL pulse. The equation of motion and the equation of energy conservation are solved together for both transient stress wave propagation and transient heat transfer. Although the mechanical deformation process does not affect much the heat transfer process, their coupling is im-

portant to reveal how the initial thermal strain energy is relaxed, i.e., partially to the kinetic energy, and partially back to the thermal energy. The case from Ref. 7 is (re-)examined. The diamond crystal thickness is 200 μm . The laser spot size is about twice the thickness. The absorption rate is adjusted such that the initial temperature rise is less than 2 K at the center of the Gaussian beam, in the low energy deposition regime. The problem is numerically solved by applying a finite volume method. The analysis reveals the characteristic non-planar stress wave propagation. While the deformation energy stored in the radial normal strain component is released in part through radial longitudinal and surface stress waves, that stored in the through-thickness normal strain component is depleted by emitting radial longitudinal stress waves due to Poisson's effect. This latter emission process lasts by hundreds of nanoseconds, at a time scale relevant to the high-repetition-rate FELs at the megahertz range. The resulting kinetic energy is calculated, which may be important to estimate the vibrational amplitude of the thin crystal when excited under repeated heat loads. The transient heat transfer plays an important role in draining the mechanical energy during the dynamic thermal stress wave emission process.

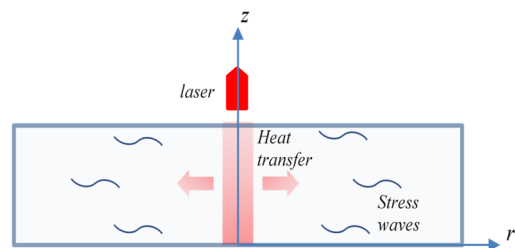


Figure 1: Schematic showing instantaneous heating and subsequent stress wave emission and heat transfer upon laser energy deposition in a thin crystal layer. The cylindrical coordinate system with axisymmetry is established.

PROBLEM FORMULATION

Consider an X-ray FEL impinging on a thin crystal, as schematically shown in Fig. 1. It interacts with the electrons and deposits a part of its energy first onto the electrons [8]. Later the energy is transferred to the lattice raising the local temperature. Then, the thermalized lattice expands dynamically emitting stress waves. The thermal diffusion begins at the same time. We aim to analyse the process of transient thermal stress wave emission. A cylindrical coordinate system (r, θ, z) is established with z -axis normal to the crystal surface. Only a laser beam perpendicular to the crystal surface is considered.

* Work supported by the US Department of Energy (DOE) under contract DE-AC02-76SF00515 and the US DOE Office of Science Early Career Research Program grant FWP-2013-SLAC-100164.

[†] boyang@uta.edu

[‡] jhwu@slac.stanford.edu

SIDEBAND INSTABILITY IN A TAPERED FREE ELECTRON LASER*

Cheng-Ying Tsai^{1†}, Juhao Wu^{1‡}, Chuan Yang^{1,2}, Moohyun Yoon^{1,3}, and Guanqun Zhou^{1,4}

¹SLAC National Accelerator Laboratory, Menlo Park, USA

²NSRL, University of Science and Technology of China, Hefei, Anhui, China

³Department of Physics, Pohang University of Science and Technology, Pohang, Korea

⁴Institute of High Energy Physics, and UCAS, Chinese Academy of Sciences, Beijing, China

Abstract

For a high-gain tapered free electron laser (FEL), it is known that there is a so-called second saturation point where the FEL power growth stops. Sideband instability is one of the major reasons leading to this second-saturation and thus prevents from reaching hundreds of gigawatt (GW) or even terawatt (TW) level power output in an x-ray FEL. It was believed that a strong taper can effectively suppress the sideband instability and further improves the efficiency and peak power. In this paper, we give quantitative analysis of the dependence of taper gradient on the sideband growth. The study is carried out semi-analytically together with numerical simulation. The numerical parameters are taken from LCLS-like electron bunch and undulator system. The results confirm the effectiveness of strong undulator tapering on sideband suppression.

INTRODUCTION

Free electron laser (FEL) is known to be capable of generating coherent high-power radiation over a broad range of spectrum. In the x-ray FEL regime, the power efficiency is about 10^{-3} , indicating that the first saturated power can be ~ 50 GW for electron beam with peak current ~ 5 kA and energy ~ 10 GeV operating in the self-amplified spontaneous emission (SASE) mode in a ~ 100 -m-long untapered undulator. With undulator tapering, the efficiency can be improved and the power can be further increased in the post-saturation regime but eventually will reach a so-called second saturation and the radiation then approaches another equilibrium. Although numerical simulations show that the TW level of temporally integrated FEL power can be possible when the undulator tapering (of helical type) is optimized and the self-seeded scheme is employed [1], in the post-saturation regime it is the sideband instability that still limits the growth of the main signal [2–6]. Enhancing the FEL peak power can be envisioned once the sideband instability is effectively suppressed. Such instability in FELs is caused by the interaction of the electromagnetic field with the electron synchrotron motion in the ponderomotive potential well. The potential well, formed by the undulator field and the main signal, will trap electrons and result in oscillation with a synchrotron frequency (and its multiples) away from the resonance or

main-signal frequency. Once the interaction creates a positive feedback, the electron beam energy will transfer and contribute to the electromagnetic field with the synchrotron sideband frequency. Then the sideband signal will grow and usually bring about undesirable consequences. In this paper we will focus on the sideband instability in a single-pass high-gain tapered FEL in the post-saturation regime based on single-particle description in a one-dimensional (1-D) model. The validity of 1-D analysis assumes that the transverse size of the electron beam is large compared with that of the radiation field, thus ignoring the effects of diffraction and gradient of transverse electron beam density. Using a single-particle approach, we can obtain the corresponding dispersion equation, which accounts for sideband-related dynamical quantities. Then, by quantifying the so-called sideband field gain, we compare the theoretical predictions with the results from a 1-D FEL simulation and they show good agreement. We particularly focus on the effect of undulator tapering on the sideband growth and study both the gentle and strong undulator tapering, compared with the untapered case. Our numerical simulations are based on similar parameters to those of the Linac Coherent Light Source (LCLS), the LCLS-like parameters.

THEORETICAL FORMULATION

In 1-D FEL, the main signal is governed by the resonance condition, $\lambda_R = \frac{\lambda_u}{2\gamma_R^2(z)} \left(1 + \frac{K^2(z)}{2}\right)$, where λ_u is the undulator period, λ_R is the radiation wavelength of the main signal, γ_R is the electron reference energy in unit of its rest mass energy, $K \approx 0.934B_0[\text{Tesla}]\lambda_u[\text{cm}]$ is the (peak) undulator parameter, and B_0 the peak undulator magnetic field. Here λ_u is assumed constant, and K is in general a function of the undulator axis z with $B(z) = B_0 f_B(z)$ and $f_B(z)$ is the tapering profile. The 1-D FEL process can be formulated based on the following electron dynamics and wave equations [7, 8]:

$$\frac{d\theta}{dz} = \frac{\partial \mathcal{H}}{\partial \eta} = \frac{\eta - \eta_R}{f_R}, \quad (1)$$

$$\frac{d\eta}{dz} = -\frac{\partial \mathcal{H}}{\partial \theta} = -\frac{f_B}{f_R} \left(\mathcal{E} e^{i\theta} + \mathcal{E}^* e^{-i\theta} \right), \quad (2)$$

and

$$\frac{d\mathcal{E}}{dz} = \left(\frac{\partial}{\partial z} + \frac{\partial}{\partial \hat{u}} \right) \mathcal{E} = \frac{f_B}{f_R} \langle e^{-i\theta} \rangle. \quad (3)$$

In the equations, $\theta = (k_R + k_u)z - \omega_R t$ is the electron phase with respect to the radiation, and $\eta \equiv (\gamma - \gamma_R(0))/\rho\gamma_R(0)$

* The work was supported by the US Department of Energy (DOE) under contract DE-AC02-76SF00515 and the US DOE Office of Science Early Career Research Program grant FWP-2013-SLAC-100164.

† jcytsai@SLAC.Stanford.EDU

‡ jhwu@SLAC.Stanford.EDU

SIDEBAND SUPPRESSION IN TAPERED FREE ELECTRON LASERS*

Cheng-Ying Tsai^{1†}, Juhao Wu^{1‡}, Chuan Yang^{1,2}, Moohyun Yoon^{1,3}, and Guanqun Zhou^{1,4}

¹SLAC National Accelerator Laboratory, Menlo Park, California, USA

²NSRL, University of Science and Technology of China, Hefei, Anhui, China

³Department of Physics, Pohang University of Science and Technology, Pohang, Korea

⁴Institute of High Energy Physics, and UCAS, Chinese Academy of Sciences, Beijing, China

Abstract

It is known that in a high-gain tapered free electron laser (FEL) there is the so-called second saturation point where the FEL power ceases to grow. Sideband instability is one of the major reasons causing this second saturation. Electron synchrotron oscillation coupling to the sideband SASE radiation leads to the appearance of sidebands in the FEL spectrum, and is believed to prevent a self-seeding tapered FEL from reaching very high peak power or improved spectral purity without resorting to external monochromators. In this paper, we propose a simple method of using phase shifters to suppress the undesired sideband signal. This method requires no external optical device and so is applicable at any wavelength. The phase-shift method is implemented in the post-saturation regime where the main signal shall have reached its available power level. Numerical simulations based on Pohang Accelerator Laboratory x-ray FEL beam and undulator system confirm the effectiveness of this method. The results show that the sideband signals are clearly suppressed while the main signal remains a comparable level to that without employing such a method.

INTRODUCTION

Generating an intense high-power x-ray free electron laser (FEL) can be of great interest, e.g. the pulse power at the level of ~50 GW, since such power level of output radiation has stimulated numerous experiments in various scientific areas [1–3]. The output characteristics of FEL are determined by its operation modes (see, for example, Ref. [4] for introduction of short-wavelength FEL basics). In the x-ray wavelength regime a single-pass high-gain FEL can work either in the Self-Amplified Spontaneous Emission (SASE) or seeded mode, despite the lack of direct seeding source. In the SASE mode [5], the initial seeding originates from shot noise of the electron beam. Therefore the output characteristics of SASE can be chaotic in both temporal and spectral profile, although the transverse coherence can be excellent. Acting as an amplifier, the seeded mode indeed requires an input source. It has been known that utilizing higher harmonics generation, e.g. high-gain harmonics generation (HG) [6, 7] or echo-enabled harmonic generation (EEHG) [8, 9], can be an option. Another option is the so-

called self-seeding [10–12]. In the self-seeding option the FEL system starts with the first section of undulators based on SASE mode and is followed by a crystal monochromator or mirrors to select/purify the output spectrum, serving as the subsequent input signal. Then a second section of undulators proceeds, acting as an amplifier, and will amplify the (purified) signal, i.e. the main signal, up to saturation. Compared with SASE, the output characteristics of seeded FEL are in general with much narrower spectral bandwidth and better wavelength stability.

In some applications when an even higher pulse power can be desired, e.g. the femtosecond x-ray protein nanocrystallography, single molecule imaging and so on, dedicated undulator taperings are typically employed [13–16]. Recently the efficiency enhancement based on phase jump method is also proposed [17]. In other situations when the temporal coherence or spectral brightness may be benefited or even required, e.g. the resonant scattering experiment, mixing-wave experiment or those which rely on spectroscopic techniques, the seeded mode shall be considered. However, the higher spectral purity may be prevented by the so-called FEL sideband instability (see, for example, [13, 18–20]). Such instability in FEL is caused by the interaction of the radiation field with the electron synchrotron motion in the ponderomotive potential well after the first saturation of FEL. Such a potential well, formed by the undulator magnetic field and the main signal, will trap electrons and result in the oscillation with a synchrotron frequency (and its multiples) away from the resonance frequency (i.e. the frequency of the main signal). Once the interaction creates a positive feedback, the electron beam energy will continuously transfer and contribute to the electromagnetic field with the specific synchrotron sideband frequency. Then the sideband signal will grow and the output radiation spectrum will feature a main-signal peak with surrounding sideband peaks or a pedestal-like structure. This usually brings about undesirable consequences; the sideband effect can not only degrade the spectral purity but also limit the level of the saturation power of FEL. Employing a post-undulator monochromator may help clean the sideband structure. A dedicated monochromator however depends on specific wavelength range or photon energy and may limit the tunability. The method introduced here requires no external optical device and so is applicable at any wavelength.

In this paper we propose a simple method of using a set of phase shifters to suppress the undesired sideband signal. As mentioned above, because the phase shifters used for

* The work was supported by the US Department of Energy (DOE) under contract DE-AC02-76SF00515 and the US DOE Office of Science Early Career Research Program grant FWP-2013-SLAC-100164.

† jcytsai@SLAC.Stanford.EDU

‡ jhwu@SLAC.Stanford.EDU

TWO-COLOR SOFT X-RAY GENERATION AT THE SXFEL USER FACILITY BASED ON THE EEHG SCHEME

Zheng Qi^{1,2}, Chao Feng¹, Wenyang Zhang¹, Bo Liu¹, Zhentang Zhao*¹

¹Shanghai Institute of Applied Physics, Chinese Academy of Sciences, Shanghai, China

²University of Chinese Academy of Sciences, Beijing, China

Abstract

We study the two-color soft x-ray generation at the Shanghai soft X-ray Free Electron Laser (SXFEL) user facility based on the echo-enabled harmonic generation (EEHG) scheme. Using the twin-pulse seed laser with different central wavelengths, an preliminary simulation result indicates that two-color soft x-ray FEL radiation with wavelengths at 8.890 nm and 8.917 nm can be obtained from the ultraviolet seed laser. The radiation power is about 600 MW and the time delay is adjustable.

INTRODUCTION

The free electron laser (FEL) has served as a prominent tool for the state-of-the-art research in many scientific frontiers ranging from physics, to chemistry and biology [1, 2]. Through the well-known pump-probe technique [3], the ultrahigh intensity, ultrashort, FEL radiation pulses can be applied to measure ultrafast phenomena inside matter. Typically, the pump-probe technique will use two laser pulses with adjustable time delay and different central wavelengths. The pump laser will give the system a perturbation to excite some reactions within the sample. The probe laser will then reach and interact within the sample after a certain time. By observing the modulation of the probe laser, one can retrieve the state of the system. Changing the time delay between the pump and probe laser pulses, the evolution of the reaction can be “filmed” as a movie while it decays back to the equilibrium state.

The FEL based pump-probe technique extends the photo energy coverage up to vacuum ultraviolet (VUV) or x-ray range, which enables the stimulation and investigation of the inner-shell electronic energy level transition [4]. Therefore it can be used to study the material structure and the ultrafast process in the atomic and molecular scale. The most important FEL based pump-probe scheme termed as the two-color FEL is based on the novel achievements developed recently in the high gain FEL research area. Basically, the two-color FEL is aiming to provide two ultrashort FEL radiation pulses with the time delay and the central wavelength could being adjusted continuously and separately.

The two-color FEL is of great interests in the scientific communities. Several schemes have been proposed and demonstrated experimentally in LCLS, SACLA and FERMI [5–8]. These schemes are generally based the self-

amplified spontaneous emission (SASE) or the high gain harmonic generation (HG) [9]. However, the SASE FEL has poor temporal coherence and power stability as the radiation initiates from the shot noise. And the HG FEL can hardly reach the x-ray wavelength range due to the limitation of the frequency up-conversion efficiency. In this paper, we study the two-color soft x-ray generation at the Shanghai soft X-ray Free Electron Laser (SXFEL) user facility based on the echo-enabled harmonic generation (EEHG) [10, 11].

LAYOUT AND MAIN PARAMETERS

The schematic layout of our design is shown in Fig. 1. It is basically a conventional EEHG configuration, consisting of a two stage energy modulation section, M1 and M2, two dispersion sections, DS1 and DS2, and a long undulator section, R. The electron bunch obtained from the LINAC upstream will interact with Seed1 in M1 to get an energy modulation with an amplitude $A1 = 2.78$. Then the electron beam is sent through the strong dispersion section DS1 with $R56 = 10$ mm to stretch the longitudinal phase space of the electron beam to form periodic structures. Seed2 will imprint another energy modulation into the electron bunch with the amplitude $A2 = 1.39$. And the second dispersion section DS2 with $R56 = 0.34$ mm will convert the energy modulation into harmonic density modulation. The bunched electron beam will then go through the radiator R to generate FEL radiation.

Seed1 is a long pulse seed laser so that it can cover the whole electron bunch during the first energy modulation process in M1. Seed2 is a twin-pulse seed laser with the two pulses of different central wavelengths and a certain time interval. Due to the principle that the FEL radiation generated in the EEHG is at the high harmonics of the seed laser, the two-color FEL radiation can be eventually obtained. The wavelength of Seed1 is 266.7 nm. The wavelengths of the two pulses in Seed2 are respectively 266.7 nm and 267.5 nm. The EEHG FEL is tuned at the 30th harmonic of the seed laser. Therefore the intended two-color soft x-ray FEL radiation is at 8.890 nm and 8.917 nm. The time delay of the two-color soft x-ray FEL can be adjusted through the time intervals between the two pulses in Seed2. According to our design of the optical system, the wavelength tunable range of the two pulses in Seed2 is $266.7 \text{ nm} \pm 2 \text{ nm}$. And the time delay can be adjusted between 0 and 1 ps. The main parameters of our design are shown in Table 1.

* zhaozhentang@sinap.ac.cn

SIMULATION AND OPTIMIZATION FOR SOFT X-RAY SELF-SEEDING AT SXFEL USER FACILITY

Kaiqing Zhang, Chao Feng, Dong Wang, Zhentang Zhao
Shanghai Institute of Applied Physics, Chinese Academy of Sciences, Shanghai 201800, China
University of Chinese Academy of Sciences, Beijing 100049, China

Abstract

The simulation and optimization studies for the soft x-ray self-seeding experiment at SXFEL have been presented in this paper. Some critical physical problems have been intensively studied to help us obtain a more stable output and a clearer spectrum. The monochromator is optimized considering various unideal conditions such as the reflection rate, diffraction rate and the roughness of the grating and the mirrors. An integrated self-seeding simulation is also presented. The calculation and simulation results show that the properties of the self-seeding can be significantly improved by using the optimized design of the whole system and the evaluation of grating monochromator shows that the presented design is reliable for soft x-ray self-seeding experiment at SXFEL.

INTRODUCTION

The successful achievement of SASE FEL [1-3] opens a new chapter to high-brightness photon source with tunable wavelength and it provides a reliable instrument to research scientific frontier within the material, biological and chemical sciences. However, SASE FEL suffers from shot noise, poor longitudinal coherence and poor spectral bandwidth. A harmonic lasing scheme with external seeding, such as HGHG [4-5] and EEHG [6-8], can be used to generate relative short wavelength radiation with longitudinal coherence. However, it is unable to probe photon energy beyond a few hundred of eV. To improve the longitudinal coherence of SASE FEL, self-seeding [9] is proposed at DESY in 1997, after that, soft and hard X-ray self-seeding are demonstrated at LCLS separately in 2014 [10] and 2012 [11] separately. Since then, self-seeding schemes are regarded as a reliable method to obtain high brightness, longitudinal coherence and short-wavelength FEL radiation.

The self-seeding scheme separates the long radiation undulator into two parts by inserting a monochromator and a four-dipole chicane. The first undulator works on the SASE mode, the radiation and electron bunch are extracted before saturation. After that, the radiation is passed through a monochromator to purify the spectrum and the electron bunch is passed through the chicane to eliminate the beam microbunching. After that, the monochromatic radiation and the fresh electron beam are sent to the radiation undulator. In the seed undulator, the monochromatic radiation is used as a seed to interact with the electron beam. Finally, the output will be longitudinal coherent when saturation. In the previous system design, we have given preliminary design and simulation for SXFEL user facility [12]. In this paper, some critical

physical problems have been intensively studied to help us obtain a more stable output and a clearer spectrum. We give the simulation method to optimize the undulator length. The reflection and diffraction rate are calculated to get the transfer efficiency and the simulation process is more reliable considering the transfer efficiency. The monochromator is optimized considering various unideal conditions such as the roughness of the grating and the mirrors. In the previous optical simulation, we use shadow to simulate the power resolution of designed grating monochromator and the parameters of light source are not considered. In this paper, we use the calculated parameters of radiation pulse to simulate the power resolution of grating monochromator and we also give a detail simulation for designed simulation.

THE GRATING MONOCHROMATOR DESIGN

The layout of self-seeding scheme is shown in Fig. 1. The grating monochromator has five elements: a VLS toroidal grating monochromator disperses the light pulse to different transverse position as well as focuses the light pulse, a plane mirror reflects the light to horizontal direction, a slit selects out the light pulse wavelength, a spherical mirror focus the sagittal direction of pulse and another plane mirror reflects the light to the entrance of the undulator. In the previous optical system design, the layout and the parameters of optical elements have been described. Recently, some detail studies about grating monochromator have been carried out. In soft X-ray regime, the gold is generally chosen as the material of optical elemental. Based on the element material and the designed parameters, we calculate the reflection and diffraction rate of the grating monochromator. For a grating, the diffraction efficiency can be expressed as follows:

$$E_0 = \frac{R}{4} \left(1 + 2(1 - P) \cos \left(\frac{4\pi \cos(\alpha)}{\lambda} \right) + (1 - P)^2 \right),$$

where α is the incidence angle, h is the depth of the grating groove, P can be expressed as: $P = (4h \tan \alpha) / d_0$, where d_0 is the line width of adjacent grating groove and R can be expressed as: $R = \sqrt{\alpha_G \beta_G}$, where $\alpha_G = \pi/2 - \alpha$, $\beta_G = \pi/2 - \beta$, α, β is the incidence and diffraction angle separately, and the diffraction angle is related with diffraction order, here we only consider the first diffraction order. Based on the designed parameters, the diffraction efficiency can be calculated as 0.039 with gold substrate. For optical elements, the reflection efficiency can be expressed as

STUDY OF AN ECHO-ENABLED HARMONIC GENERATION SCHEME FOR THE FRENCH FEL PROJECT LUNEX5

E. Roussel*, M. E. Couprie, A. Ghaith, A. Loulergue
Synchrotron SOLEIL, Gif-sur-Yvette, France
C. Evain, PhLAM/CERLA, Villeneuve d'Ascq, France
D. Garzella, CEA, Gif-sur-Yvette, France
on behalf of the LUNEX5 team

Abstract

In the French LUNEX5 projet (free electron Laser Using a New accelerator for the Exploitation of X-ray radiation of 5th generation), a compact advanced Free-Electron Laser (FEL) is driven by either a superconducting linac or a laser-plasma accelerator that can deliver a 400 MeV electron beam. LUNEX5 aims to produce FEL radiation in the ultraviolet and extreme ultraviolet (EUV) range. To improve the longitudinal coherence of the FEL pulses and reduce the gain length, it will operate in Echo-Enabled Harmonic Generation (EEHG) seeding configuration [1]. EEHG is a strongly nonlinear harmonic up-conversion process based on a two seed laser interaction that enables to reach very high harmonics of the seed laser. Recent experimental demonstration of ECHO75, starting from an infrared seed laser, was recently achieved at SLAC [2] and opened the way for EEHG scheme in the EUV and soft x-ray range. Furthermore, FELs are promising candidates for the next generation lithography technology using EUV light. In this work, we report a preliminary study of EEHG scheme for LUNEX5 in order to reach the target wavelength of 13.5 nm, currently expected for application to lithography.

INTRODUCTION

More than fifty years after the discovery of the laser [3], the Free-Electron Lasers (FELs) are nowadays the brightest sources in the extreme ultraviolet (EUV) and x-ray domains [4]. Thanks to the remarkable properties of the FEL pulses, like the spatial coherence, the high peak brightness, the narrow bandwidth spectrum and the ultra short duration in the sub-100 fs range, the operational FEL facilities [5–9] have opened the way to new possibilities in ultrafast dynamic of excited systems and in imaging. Besides the unprecedented capabilities of FEL light sources, new researches are going towards the generation of even shorter FEL pulses and Fourier limits over a wide spectral range. An other trend is investigating the possibility to reduce the size of the FEL facilities by means of seeding schemes, like the echo-enabled harmonic generation (EEHG) scheme [1, 10] that enables to reach very high harmonic of the seed laser, or by replacing one of the components by an alternative, e.g. the use of cryogenic permanent magnet-based undulator (CPMU) [11, 12] or the use of new accelerator concepts like the laser-plasma acceleration (LWFA: Laser WakeField Acceleration) [13].

* eleonore.roussel@synchrotron-soleil.fr

LUNEX5 PROJECT

The LUNEX5 [14, 15] is an advanced and compact FEL demonstrator project (shown in Fig. 1) that aims at producing ultra short, coherent and intense pulses in the EUV domain. A 400-MeV electron beam will be delivered by two XFEL-type cryomodules (Fig. 1, yellow) for high repetition rate operation (see Table 1 for electron beam parameters), to a FEL line (Fig. 1, purple) composed of two modulators and four radiators based on the cryogenic permanent magnet technology for compactness. Two pilot user experiments (Fig. 1, green) in gas phase and condensed matter will qualify the FEL performance in the different cases. Measuring and controlling the temporal properties of the radiation emitted by LUNEX5 is essential for users application. A new method called MIX-FROG, based on the FROG (Frequency Resolved Optical Gating) technique, enabling to characterize these properties even in the presence of partial longitudinal coherence has been proposed and developed [16].

Table 1: Electron Beam Parameters

Beam energy	400	MeV
Bunch charge	1	nC
Bunch length	1	ps (RMS)
Peak current	400	A
Normalized slice emittance	1.5	mm.mrad
Energy spread	80	keV

The construction is not launched yet, but Research and Development programs are underway. The LUCRECE project aims at developing elementary RF cell with a 20-kW solid state amplifier. The operation at high repetition rate will also present challenges from the diagnostics point of view. This is particularly true for shot-by-shot electron bunch shape characterization. For that purpose, an original single-shot detection has been developed based on the electro-optic sampling that consists in encoding the electron bunch shape in the spectrum of a laser pulse, coupled to a photonic-time stretch strategy that slows down the signal to be detected. The feasibility of the method has been verified and applied on the detection of coherent THz pulses in synchrotron light sources [17, 18].

An alternative accelerator line is also considered (Fig. 1) that will explore the qualification of a laser plasma acceleration process by a FEL application, using the same FEL line components and a specific transport line for handling the

SEEDING OF ELECTRON BUNCHES IN STORAGE RINGS*

S. Khan[†], B. Büsing, N. M. Lockmann, C. Mai, A. Meyer auf der Heide,
 R. Niemczyk[‡], B. Riemann, B. Sawadski, M. Suski, P. Ungelenk[§],
 Zentrum für Synchrotronstrahlung (DELTA), TU Dortmund, 44227 Dortmund, Germany

Abstract

Seeding schemes for free-electron lasers (FELs) can be adopted to generate ultrashort radiation pulses in storage rings. Creating laser-induced microbunches within a short slice of a long electron bunch gives rise to coherent emission at harmonics of the seed wavelength. In addition, THz radiation is produced over many turns. Even without FEL gain, a storage ring is an excellent testbed to study many aspects of seeding schemes and short-pulse diagnostics, given the high repetition rate and stability of the electron bunches. At DELTA, a 1.5-GeV electron storage ring operated by the TU Dortmund University in Germany, coherent harmonic generation (CHG) with single and double 40-fs seed pulses is performed at wavelengths of 800 nm or 400 nm. As a preparation for echo-enabled harmonic generation (EEHG), simultaneous seeding with 800 and 400 nm pulses in two different undulators is performed and several techniques are employed to ensure optimum timing between the seed pulses.

INTRODUCTION

Seeding of high-gain free-electron lasers (FELs) with external radiation pulses allows to control and improve spectrottemporal properties of FEL pulses at short wavelengths [1]. In electron storage rings, seeding methods can be adopted to generate femtosecond radiation pulses emitted by a short “slice” within a several 10 ps long electron bunch [2]. For pump-probe applications, another advantage of external seeding is the natural synchronization between two pulses, i.e., the seed pulse, from which a fraction is used to pump a sample, and the probe pulse resulting from the seeding process. The basic seeding mechanism is a periodic modulation of the electron energy induced by the electric field of a laser pulse co-propagating with the electrons in an undulator (the “modulator”).

In an FEL seeding scheme known as “high-gain harmonic generation” (HG) [3], a magnetic chicane converts the energy modulation into a periodic density modulation (“microbunching”) which gives rise to FEL gain at harmonics of the seed pulse wavelength in a second undulator (the “radiator”). Presently, FERMI (Trieste, Italy) is the only HG-seeded FEL in user operation [4]. The bunching factor and thus the efficiency of the seeding process decreases exponentially with increasing harmonic order. One method to reach shorter wavelengths is to use the resulting FEL pulse

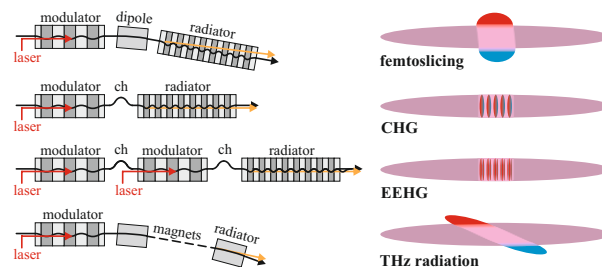


Figure 1: Applications of laser-induced energy modulation in storage rings. Left: Magnetic layout with undulators and chicanes (ch). Right: Resulting electron bunch structure (red and blue: electrons with energy gain and loss).

as seed for a second modulator. This two-stage (or cascaded) HG process has been demonstrated at FERMI [5]. Another method to obtain FEL gain at shorter wavelengths is “echo-enabled harmonic generation” (EEHG) involving a twofold laser-induced energy modulation to generate a density pattern with high harmonic content [6]. EEHG has been studied at NLCTA (SLAC, Menlo Park, USA) [7, 8] and at SDUV-FEL (SINAP, Shanghai, China) [9].

SEEDING IN STORAGE RINGS

In storage rings, the energy modulation induced by a femtosecond laser pulse applies to $\approx 1/1000$ of the bunch length and can be employed in several ways (see Fig. 1).

After passing a dipole magnet, the off-energy electrons are transversely displaced and emit a short off-axis pulse of synchrotron radiation in an undulator tuned to any wavelength [10]. Since the electrons are not microbunched, the pulse energy is proportional to the number of electrons and about 10^{-4} times lower than the energy emitted from the whole bunch. This scheme, known as “femtosing”, has been demonstrated at ALS (LBNL, Berkeley, USA) [11] and is employed in user operation at BESSY (Berlin, Germany) [12], SLS (PSI, Villigen, Switzerland) [13], and SOLEIL (Saint-Auban, France) [14].

Similar to HG, microbunching with a chicane causes coherent emission of radiation at harmonics of the seed wavelength. Without FEL gain, this process is called “coherent harmonic generation” (CHG) and was first demonstrated with ps laser pulses at ACO (Orsay, France) [15]. Short-pulse generation via CHG was performed at UVSOR (Okasaki, Japan) [16], ELETTRA (Trieste, Italy) [17], and DELTA (Dortmund, Germany) [18]. Due to coherent emission, the pulse energy is proportional to the number of electrons squared. Even for $1/1000$ of the electrons in the bunch, the CHG pulse energy exceeds that of incoherent

* Work supported by BMBF (05K15PEA, 05K15PEB), MERCUR (Pr-2014-0047), DFG (INST 212/236-1 FUGG) and the Land NRW.

[†] shaukat.khan@tu-dortmund.de

[‡] now at: DESY, 15738 Zeuthen, Germany

[§] now at: GRS gGmbH, 50667 Köln, Germany

EXTRACTION OF THE LONGITUDINAL PROFILE OF THE TRANSVERSE EMITTANCE FROM SINGLE-SHOT RF DEFLECTOR MEASUREMENTS AT sFLASH*

T. Plath[†], S. Khan, Technische Universität Dortmund, Dortmund, Germany
Ph. Amstutz, L. L. Lazzarino, V. Miltchev, J. Roßbach, Universität Hamburg, Hamburg, Germany
Th. Maltezopoulos, European XFEL GmbH, Schenefeld, Germany
J. Bödewadt, T. Laarmann, C. Lechner, Deutsches Elektronen-Synchrotron DESY, Hamburg, Germany
N. Ekanayake, Michigan State University, East Lansing, MI, USA

Abstract

The gain length of the free-electron laser (FEL) process strongly depends on the slice energy spread, slice emittance, and current of the electron bunch. At an FEL with only moderately compressed electron bunches, the slice energy spread is mainly determined by the compression process. In this regime, single-shot measurements using a transverse deflecting rf cavity enable the extraction of the longitudinal profile of the transverse emittance. At the free-electron laser FLASH at DESY, this technique was used to determine the slice properties of the electron bunch set up for seeded operation in the sFLASH experiment. Thereby, the performance of the seeded FEL process as a function of seed laser-electron timing can be predicted from these slice properties with the semi-analytical Ming-Xie model. The prediction is well in line with the FEL peak power observed during an experimental laser-electron timing scan. The power profiles of the FEL pulses were reconstructed from the longitudinal phase-space measurements of the seeded electron bunches that were measured with the transverse deflecting cavity.

For an HGHG-seeded FEL, it is essential to maintain the longitudinal and transverse overlap between the seed laser pulse and electron bunch. In the transverse plane, the laser pulse is usually larger than the electron bunch. This way, all electrons in a longitudinal slice of the electron bunch experience a similar amplitude of the electric field and a similar modulation amplitude. Longitudinally, however, the laser pulse is usually shorter than the electron bunch and the question arises which relative timing between them has to be chosen for optimum lasing performance.

While a straightforward method to optimize the longitudinal overlap is a scan of the relative timing between laser pulse and electron bunch, the optimum timing can also be determined from an analysis of single-shot measurements of the longitudinal phase-space distribution. This analysis reveals the longitudinal profile of the transverse emittance and reveals the longitudinal fraction of the electron bunch that supports best FEL performance. Here, profile refers to the physical quantity being a function that changes its value with the longitudinal coordinate in the electron bunch.

INTRODUCTION

When starting a high-gain free-electron laser (FEL) from noise, properties of the generated photon pulses such as central wavelength and spectral shape are subject to fluctuations. Additionally, the longitudinal coherence of a SASE pulse is limited due to several longitudinal modes lasing independently from each other. One option to overcome these limitations is an FEL seeded by high-gain harmonic generation (HG). In this seeding scheme, an energy modulation is induced in the electron bunch by the interaction with an external seed laser. This sinusoidal modulation is then transferred to a density modulation when the electron bunch traverses a subsequent dispersive chicane. The electron density distribution shows micro-bunching with the periodicity of the seed laser and can efficiently start the FEL process in a downstream undulator on the seed laser wavelength and its harmonics [1].

To measure the longitudinal phase-space distribution of the electron bunches, a transverse deflecting structure (TDS) is used in combination with a subsequent dispersive dipole spectrometer. While fields in the cavity kick electrons dependent on their arrival time in the vertical plane, the spectrometer deflects horizontally. On a screen downstream of the dipole, the longitudinal phase-space distribution can be measured with a time resolution below 10 fs.

At the seeding experiment sFLASH at FLASH in Hamburg the TDS is located downstream of the radiating undulator [2–4]. Here, the longitudinal phase-space distribution of seeded electron bunches can be measured. The energy drop of the seeded portion of the bunch can be used to extract seeded FEL pulse power profiles. While this method has been used before on an FEL process started from noise [5], this contribution shows its applicability to HGHG-seeded FEL pulses. Thus, when extracting the seeded power profiles, the seeding process can serve as a local probe to verify the emittance profile extracted from the TDS measurements and the derived performance prediction.

* Work supported by the Federal Ministry of Education and Research of Germany under contract No. 05K16PEA, 05K16GU4, 05K13PE3, and the German Research Foundation program graduate school 1355.

[†] tim.plath@desy.de

FIRST OPERATION OF A HARMONIC LASING SELF-SEEDED FEL

E.A. Schneidmiller, B. Faatz, M. Kuhlmann, J. Roensch-Schulenburg,
S. Schreiber, M. Tischer, M.V. Yurkov, DESY, Hamburg, Germany

Abstract

Harmonic lasing is a perspective mode of operation of X-ray FEL user facilities that provide brilliant beams of higher energy photons for user experiments. Another useful application of harmonic lasing is so called Harmonic Lasing Self-Seeded Free Electron Laser (HLSS FEL) that improves spectral brightness of these facilities. In the past, harmonic lasing has been demonstrated in the FEL oscillators in infrared and visible wavelength ranges, but not in high-gain FELs, and not at short wavelengths. In this paper we report on the first evidence of the harmonic lasing and the first operation of the HLSS FEL at the soft X-ray FEL user facility FLASH in the wavelength range between 4.5 nm and 15 nm. Spectral brightness was improved in comparison with Self-Amplified Spontaneous emission (SASE) FEL by a factor of six in the exponential gain regime. A better performance of HLSS FEL with respect to SASE FEL in the post-saturation regime with a tapered undulator was observed as well. The first demonstration of harmonic lasing in a high-gain FEL and at short wavelengths paves the way for a variety of applications of this new operation mode in X-ray FELs.

INTRODUCTION

Successful operation of X-ray free electron lasers (FELs) down to the Ångström regime opens up new horizons for photon science. Even shorter wavelengths are requested by the scientific community.

One of the most promising ways to extend the photon energy range of high-gain X-ray FELs is to use harmonic lasing which is the FEL instability at an odd harmonic of the planar undulator [1–5] developing independently from the lasing at the fundamental. Contrary to the nonlinear harmonic generation (which is driven by the fundamental in the vicinity of saturation), harmonic lasing can provide much more intense, stable, and narrow-band radiation if the fundamental is suppressed. The most attractive feature of saturated harmonic lasing is that the spectral brightness of a harmonic is comparable to that of the fundamental [5].

Another interesting option, proposed in [5], is the possibility to improve spectral brightness of an X-ray FEL by the combined lasing on a harmonic in the first part of the undulator (with an increased undulator parameter K) and on the fundamental in the second part of the undulator. Later this concept was named Harmonic Lasing Self-Seeded FEL (HLSS FEL) [6]. Even though this scheme is not expected to provide an ultimate monochromatization of the FEL radiation as do self-seeding schemes using optical elements [7, 8], it has other advantages that we briefly discuss below in the paper.

Harmonic lasing was initially proposed for FEL oscillators [9] and was tested experimentally in infrared and visible wavelength ranges. It was, however, never demonstrated in high-gain FELs and at a short wavelength. In this paper we present the first successful demonstration of this effect at the second branch of the soft X-ray FEL user facility FLASH [10, 11] where we managed to run HLSS FEL in the wavelength range between 4.5 nm and 15 nm.

HARMONIC LASING

Harmonic lasing in single-pass high-gain FELs [1–5] is the amplification process in a planar undulator of higher odd harmonics developing independently of each other (and of the fundamental) in the exponential gain regime. The most attractive feature of the saturated harmonic lasing is that the spectral brightness (or brilliance) of harmonics is comparable to that of the fundamental [5]. Indeed, a good estimate for the saturation efficiency is $\lambda_w / (hL_{\text{sat},h})$, where λ_w is the undulator period, h is harmonic number, and $L_{\text{sat},h}$ is the saturation length of a harmonic. At the same time, the relative rms bandwidth has the same scaling. In other words, reduction of power is compensated by the bandwidth reduction and the spectral power remains the same.

Although known theoretically for a long time [1–4], harmonic lasing in high-gain FELs was never demonstrated experimentally. Moreover, it was never considered for practical applications in X-ray FELs. The situation was changed after publication of ref. [5] where it was concluded that the harmonic lasing in X-ray FELs is much more robust than usually thought, and can be effectively used in both existing and future X-ray FELs. In particular, the European XFEL [12] can greatly outperform the specifications in terms of the highest possible photon energy: it can reach the 60–100 keV range for the third harmonic lasing. It was also shown in [13] that one can keep sub-Ångström range of operation of the European XFEL after CW upgrade of the accelerator with a reduction of electron energy from 17.5 GeV to 7 GeV. Another application of harmonic lasing is a possible upgrade of FLASH with the aim to increase the photon energy up to 1 keV with the present energy 1.25 GeV of the accelerator. To achieve this goal, one should install a specially designed undulator optimized for the third harmonic lasing as suggested in [14].

HARMONIC LASING SELF-SEEDED FEL

A poor longitudinal coherence of SASE FELs has stimulated efforts for its improvement. Since an external seeding seems to be difficult to realize in the X-ray regime, a so called self-seeding has been proposed in [7, 8]. There are alternative approaches for reducing bandwidth and increasing spectral brightness of X-ray FELs without using optical

REVERSE UNDULATOR TAPERING FOR POLARIZATION CONTROL AND BACKGROUND-FREE HARMONIC PRODUCTION IN XFELS: RESULTS FROM FLASH

E.A. Schneidmiller and M.V. Yurkov, DESY, Hamburg, Germany

Abstract

Nonlinear harmonics in X-ray FELs can be parasitically produced as soon as the FEL reaches saturation, or can be radiated in dedicated afterburners. In both cases there is a strong background at the fundamental since it is much stronger than the harmonics. One can get around this problem applying the recently proposed reverse undulator tapering. In this contribution we present recent results from FLASH where the second and the third harmonics were efficiently generated with a low background at the fundamental. We also present the results for a high-contrast operation when the afterburner is tuned to the fundamental.

INTRODUCTION

Successful operation of X-ray free electron lasers (FELs) [1–3] based on the self-amplified spontaneous emission (SASE) principle [4], opens up new horizons for photon science. One of the important requirements of FEL users in the near future will be polarization control of X-ray radiation. Baseline design of a typical X-ray FEL undulator assumes a planar configuration which results in a linear polarization of the FEL radiation. However, many experiments at X-ray FEL user facilities would profit from using a circularly polarized radiation. There are different ideas for possible upgrades of the existing (or planned) planar undulator beamlines.

As a cheap upgrade one can consider an installation of a short helical afterburner as it was done at LCLS where a so called DELTA undulator was installed behind the main undulator [5]. However, to obtain high degree of circular polarization one needs to suppress powerful linearly polarized radiation from the main undulator. A method for suppression of the linearly polarized background from the main undulator was proposed in [6] is an application of the reverse undulator taper. It was shown that in some range of the taper strength the bunching factor at saturation is practically the same as in the reference case of the non-tapered undulator, the saturation length increases moderately while the saturation power is suppressed by orders of magnitude. Therefore, the proposed scheme is conceptually very simple (see Fig. 1): in a tapered main (planar) undulator the saturation is achieved with a strong microbunching and suppressed radiation power, then the modulated beam radiates at full power in a helical afterburner tuned to resonance. This method (in combination with the spatial separation) was used at LCLS to obtain a high degree of circular polarization [7] and is routinely used now in user operation.

Obviously, the afterburner (helical or planar) can be tuned to a harmonic of the main undulator. In this case the har-



Figure 1: Conceptual scheme for obtaining circular polarization at X-ray FELs.

monics can be efficiently generated with a low background at the fundamental.

In this paper we present experimental results from FLASH [1, 8, 9] where a high contrast between the radiation from the "afterburner" (the last two undulator sections) and from the reverse-tapered undulator was demonstrated recently. Also, the results on an efficient background-free production of high harmonics from the afterburner are presented.

POTENTIAL APPLICATIONS OF REVERSE TAPER IN HIGH-GAIN FELS

Polarization Control

Undulators of X-ray FEL user facilities are usually planar, and the FEL radiation is linearly polarized. However, there is a strong interest from users in obtaining circularly polarized radiation, or, more generally, to have full polarization control. To achieve this goal one can install a short variable-polarization afterburner, and to suppress a strong linearly polarized background from the main undulator. Reverse tapering seems to be an ideal solution to this problem since it does not require any additional installations. Moreover, not only FEL power is suppressed, but also the energy modulations are strongly reduced in comparison with on-resonance operation [6]. Thus, fully bunched electron beam with small energy modulations can more efficiently radiate in the afterburner.

Efficient Background-Free Generation of High Harmonics

The afterburner can also be tuned to a harmonic of the main undulator. In this case a powerful background-free generation of this harmonic can be expected. Indeed, the modulated electron beam at saturation contains harmonics of density, and the energy modulation is small. Therefore, these density harmonics exist longer in the radiator (planar or helical), and a significant intensity can be produced at a selected harmonic. At the same time, the radiation at the fundamental and at harmonics of the main undulator is strongly suppressed (a suppression is much stronger for harmonics than for the fundamental), i.e. the background is small. In particular, if a helical afterburner is tuned to the

BASELINE PARAMETERS OF THE EUROPEAN XFEL

E.A. Schneidmiller, M.V. Yurkov, DESY, Hamburg, Germany

Abstract

We present the latest update of the baseline parameters of the European XFEL. It is planned that the electron linac will operate at four fixed electron energies of 8.5, 12, 14, and 17.5 GeV. Tunable gap undulators provide the possibility to change the radiation wavelength in a wide range. Operation with different bunch charges (0.02, 0.1, 0.25, 0.5 and 1 nC) provides the possibility to operate XFEL with different radiation pulse duration. We also discuss potential extension of the parameter space which does not require new hardware and can be realized at a very early stage of the European XFEL operation.

BASELINE PARAMETERS

The European XFEL is driven by a superconducting accelerator with a maximum energy of electrons of 17.5 GeV [1, 2]. It operates in the burst mode with 10 Hz repetition rate of 0.6 ms pulse duration. Each pulse brings train of up to 2700 electron bunches (up to 4.5 MHz repetition rate). Three undulators are installed in the first stage of the project: SASE1, SASE2, and SASE3 (see Table 1). SASE3 undulator is placed sequentially after SASE1 undulator in the same electron beamline. All undulators

have similar mechanical design. The length of the undulator module is equal to 5 meters. The length of the undulator intersection is equal to 1.1 m. The undulators of SASE1 and SASE2 are identical: period length is 40 mm, number of modules is 35, the range of the gap variation is 10 to 20 mm. SASE3 undulator consists of 21 modules, the period is 68 mm, the gap tunability range is 10 to 25 mm [3]. Tunability range of the undulators has been corrected on the base of magnetic measurements [3], and in terms of undulator parameter is 1.65 - 4 and 4 - 9 for SASE1/SASE2 and SASE3, respectively. The tunability range in terms of $\lambda_{\max}/\lambda_{\min}$ is 3.5 for SASE1/2 and 4.6 for SASE3.

Requirements of users are summarized and analyzed in a proper way to provide maximum opportunities for every instrument and experiment simultaneously [4–7]. The tunability ranges of the undulators are not sufficient to cover the required wavelength ranges at one fixed electron beam energy, and four electron beam energies have been defined: 8.5 GeV, 12 GeV, 14 GeV, and 17.5 GeV [4, 5]. Five operating points for the bunch charge has been fixed: 20 pC, 100 pC, 250 pC, 500 pC, and 1 nC (see Table 3). The beam formation system is designed to produce peak beam current of 5 kA with nearly Gaussian shape. Electron bunches with different bunch charges will generate radiation pulses with different radiation pulse duration. Figure 1 shows an overview of the main photon beam properties of the European XFEL for the bunch charge 1 nC. The left and right columns in these plots correspond to the SASE1/SASE2 and SASE3 undulators, and allow visual tracing of the operating wavelength bands, pulse energy, and brilliance as function of the electron energy. The general tendency is that operation with higher charges provides higher pulse energy and higher average brilliance, nearly proportional to the bunch charge.

Properties of the radiation from SASE3 are presented in Fig. 1, we assume that the electron beam is not disturbed by FEL interaction in the SASE1 undulator. Decoupling of SASE3 and SASE1 operation can be performed with an application of the betatron switcher [7, 9]. Feedback kickers can be used to test and operate this option at the initial stage. In case of positive results dedicated kickers need to be installed [6]. Operation of SASE3 as an afterburner of SASE1 is also possible, but with reduced range of accessible wavelengths and reduced power [7]. General problem is that tuning of SASE1 to higher pulse energies leads to higher induced energy spread in the electron beam, and to degradation of the SASE3 performance. For instance, operation of SASE3 at the energy of 17.5 GeV is impossible at any wavelength if wavelength of SASE1 is longer than 0.1 nm, and radiation power of

Table 1: Undulators at the European XFEL [3]

	Units	SASE1/2	SASE3
Period length	cm	4	6.8
Maximum field	T	1.11	1.66
Gap range	cm	1 – 2	1 – 2.5
K range	#	3.9 – 1.65	9.0 – 4.08
Length of module	m		5
Length of intersection	m		1.1
Number of modules	#	35	21
Total magnetic length	m	175	105

Table 2: Working Points and Tunability Ranges of the European XFEL

	SASE1/2	SASE3
Tunability, $\lambda_{\max}/\lambda_{\min}$	3.64	4.45
El. energy, GeV	Photon energy range, keV	
8.5	1.99 – 7.27	0.24 – 1.08
12.0	3.97 – 14.48	0.48 – 2.16
14.0	5.41 – 19.71	0.66 – 2.94
17.5	8.45 – 30.80	1.03 – 4.59
	Photon wavelength range, nm	
8.5	0.171 – 0.622	1.15 – 5.10
12.0	0.086 – 0.312	0.57 – 2.56
14.0	0.063 – 0.229	0.42 – 1.88
17.5	0.040 – 0.147	0.27 – 1.20

OPTIMUM UNDULATOR TAPERING OF SASE FEL: THEORY AND EXPERIMENTAL RESULTS FROM FLASH2

E.A. Schneidmiller and M.V. Yurkov, DESY, Hamburg, Germany

Abstract

In this report we present recent results of the experimental studies at FLASH2 free electron laser on application of undulator tapering for efficiency increase. Optimization of the amplification process in FEL amplifier with diffraction effects taken into account results in a specific law of the undulator tapering [1–3]. It is a smooth function with quadratic behavior in the beginning of the tapering section which transforms to a linear behavior for a long undulator. Obtained experimental results are in reasonable agreement with theoretical predictions.

UNIVERSAL TAPERING LAW

Effective energy exchange between the electron beam moving in an undulator and electromagnetic wave happens when resonance condition takes place. When amplification process enters nonlinear stage, the energy losses by electrons become to be pronouncing which leads to the violation of the resonance condition and to the saturation of the amplification process. Application of the undulator tapering [4] allows to a further increase of the conversion efficiency. An idea is to adjust undulator parameters (field or period) according to the electron energy loss such that the resonance condition is preserved. Undulator tapering has been successfully demonstrated at long wavelength FEL amplifiers [5,6], and is routinely used at x-ray FEL facilities LCLS and SACLA [7,8]. In the framework of the one-dimensional theory an optimum law of the undulator tapering is quadratic [9–15]. Similar physical situation occurs in the FEL amplifier with a waveguide [5]. Parameters of FEL amplifiers operating in the infrared, visible, and x-ray wavelength ranges are such that diffraction of radiation is an essential physical effect influencing optimization of the tapering process. In the limit of thin electron beam (small value of the diffraction parameter) linear undulator tapering works well from almost the very beginning [12]. It has been shown in [10] that: i) tapering law should be linear for the case of thin electron beam, ii) optimum tapering at the initial stage should follow quadratic dependence, iii) tapering should start approximately two field gain length before saturation.

Comprehensive analysis of the problem of the undulator tapering in the presence of diffraction effects has been performed in [1–3]. It has been shown that the key element for understanding the physics of the undulator tapering is given by the model of the modulated electron beam which provides relevant interdependence of the problem parameters. Finally, application of similarity techniques to the results of numerical simulations led to the universal law of the undulator tapering:

$$\hat{C} = \alpha_{tap}(\hat{z} - \hat{z}_0) \left[\arctan\left(\frac{1}{2N}\right) + N \ln\left(\frac{4N^2}{4N^2 + 1}\right) \right], \quad (1)$$

with Fresnel number N fitted by $N = \beta_{tap}/(\hat{z} - \hat{z}_0)$. Undulator tapering starts by two field gain length $2 \times L_g$ before the saturation point at $z_0 = z_{sat} - 2 \times L_g$. Parameter β_{tap} is rather well approximated with the linear dependency on diffraction parameter, $\beta_{tap} = 8.5 \times B$. Parameter α_{tap} is a slow varying function of the diffraction parameter B , and scales approximately to $B^{1/3}$. Analysis of the expression (1) shows that it has quadratic dependence in z for small values of z (limit of the wide electron beam), and linear dependence in z for large values of z (limit of the thin electron beam).

ANALYSIS OF TAPERING PROCESS

Seeded FEL

Red curve in Fig. 1 shows evolution of the average radiation power of seeded FEL along the optimized tapered undulator. Significant amount of particles is trapped in the regime of coherent deceleration (top plot in Fig. 2).

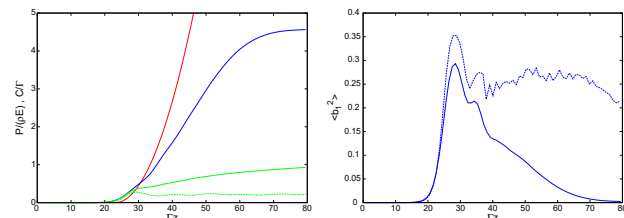


Figure 1: Left: Evolution along the undulator of the reduced radiation power $\hat{\eta} = W/(\rho W_{beam})$. Red and blue lines correspond to the case of tapered seeded and SASE FEL. Green dashed and solid lines refer the case of untapered seeded and SASE FEL. Right: Evolution along the undulator of the squared value of the bunching factor for the FEL amplifier with optimized undulator tapering. Dashed and solid line represent seeded and SASE FEL, respectively. Diffraction parameter is $B = 10$. Simulations are performed with code FAST [16].

The particles in the core of the beam are trapped most effectively. Nearly all particles located at the edge of the electron beam leave the stability region very soon. The trapping process lasts for a several field gain lengths when the trapped particles become to be isolated in the trapped energy band for which the undulator tapering is optimized further. For large values of the diffraction parameter $B \geq 10$ the trapping process is not finished even at three field gain lengths after saturation, and non-trapped particles continue to populate low energy tail of the energy distribution (see

FREQUENCY DOUBLING MODE OF OPERATION OF FREE ELECTRON LASER FLASH2

M. Kuhlmann, E.A. Schneidmiller, and M.V. Yurkov, DESY, Hamburg, Germany

Abstract

We report on the results of the first operation of a frequency doubler at free electron laser FLASH2. The scheme uses the feature of the variable-gap undulator. The undulator is divided into two parts. The second part of the undulator is tuned to the double frequency of the first part. The amplification process in the first undulator part is stopped at the onset of the nonlinear regime, such that nonlinear higher-harmonic bunching in the electron beam density becomes pronouncing, but the radiation level is still small to disturb the electron beam significantly. The modulated electron beam enters the second part of the undulator and generates radiation at the second harmonic. A frequency doubler allows operation in a two-color mode and operation at shorter wavelengths with respect to standard SASE scheme. Tuning of the electron beam trajectory, phase shifters and compression allows tuning of intensities of the first and the second harmonic. The shortest wavelength of 3.1 nm (photon energy 400 eV) has been achieved with a frequency doubler scheme, which is significantly below the design value for the standard SASE option.

INTRODUCTION

Free electron laser FLASH is equipped with two undulator beamlines [1]. Fixed gap undulator (period 2.73 cm, peak magnetic field 0.48 T, total magnetic length 27 m) is installed in the first beamline, FLASH1. The second beamline, FLASH2, is equipped with variable gap undulator (period 3.14 cm, maximum peak magnetic field 0.96 T, total magnetic length 30 m). With operating range of the electron beam energies of 0.4 - 1.25 GeV FLASH1 and FLASH 2 beamline cover wavelength range from 4 to 52 nm and 3.5 to 90 nm, respectively. Multiple scientific applications will benefit a lot with extension of the operating range of the facility deep into the water window spanning from 4.38 nm and 2.34 nm (K-absorption edges of carbon and oxygen).

One techniques to generate shorter wavelengths is by using the second harmonic afterburner [2–7]. Operating the afterburner at the 2nd harmonic has been tested successfully at LCLS with 5 final undulator modules retuned to the 2nd harmonic [7]. With long, variable gap undulator of FLASH2 it is possible to implement frequency doubler scheme. Here we demonstrate experimental results from FLASH2: with an appropriate optimization of undulator tuning it becomes possible to operate facility at visibly shorter wavelengths and organize two color mode of operation ($\omega + 2\omega$) with controllable radiation pulse intensities.

OPERATION OF FREQUENCY DOUBLER

The undulator is divided into two sections tuned to ω and 2ω frequencies. The plots in Fig. 1 illustrate general features of the operation of the frequency doubling scheme. Black dashed line shows evolution of the radiation power along the ω -section. The amplification process stops at some length, and then electron beam enters the 2ω -section tuned to the doubled frequency. Radiation with frequency ω does not interact with the electron beam in the 2ω -section, and just propagates forward. Radiation power produced in the ω -section at the second harmonic frequency is significantly suppressed [6, 8], thus only the beam density modulations at 2ω frequency can seed the 2ω -section.

We performed simulations of the amplification process for the full parameter space of the lengths of the ω and 2ω sections, and the results are summarized in Fig. 2. Despite the fact that simulations have been performed for specific sets of electron beam parameters, presentation of the results here is in normalized form to allow use of them for a wider range of parameters. The x-coordinate is radiation power is from the ω section normalized to the saturation power of SASE FEL operating at frequency ω . The y-coordinate is radiation power from the 2ω -section normalized to the

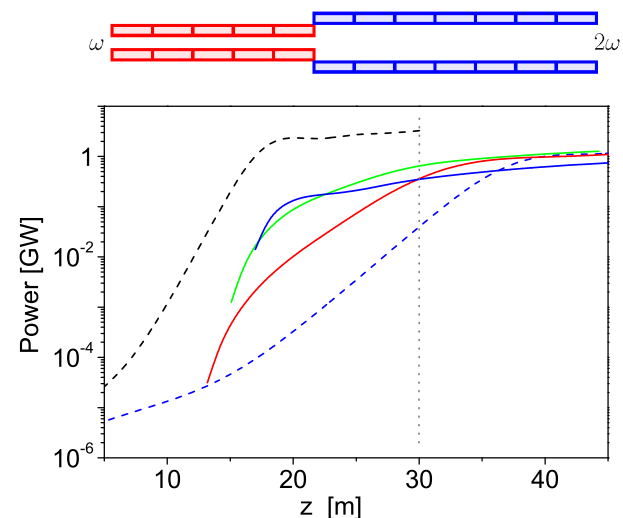


Figure 1: Top: Conceptual scheme of frequency doubler with variable gap undulator. Bottom: Evolution of the radiation power along FLASH2 undulator. Dashed curves correspond to SASE FEL operating at 8 nm (black) and at 4 nm (blue). Solid curves correspond to frequency doubler 8 nm \rightarrow 4 nm for different lengths of the ω undulator section (red, green, and blue colors). Gray dashed line at $z = 30$ m shows magnetic length of FLASH2 undulator. Electron energy is 1080 MeV, beam current is 1500 A, normalized rms emittance 1π mm-mrad, and rms energy spread 0.15 MeV. Simulations have been performed with code FAST [9].

OPPORTUNITIES FOR TWO-COLOR EXPERIMENTS AT THE SASE3 UNDULATOR LINE OF THE EUROPEAN XFEL

G. Geloni*, T. Mazza, M. Meyer, S. Serkez, European XFEL, Schenefeld, Germany
V. Kocharyan, E. Saldin, DESY, Hamburg, Germany

Abstract

As is well-known, the installation of a simple magnetic chicane in the baseline undulator of an XFEL allows for producing two-color FEL pulses. In this work we discuss the possibility of applying this simple and cost-effective method at the SASE3 soft X-ray beamline of the European XFEL. We consider upgrades of this method that include the further installation of a mirror chicane. We also discuss the scientific interest of this upgrade for the Small Quantum Systems (SQS) instrument, in connection with the high-repetition rate of the European XFEL, and we provide start-to-end simulations up to the radiation focus on the sample, proving the feasibility of our concept. Our proposed setup has been recently funded by the Finnish Research Infrastructure (FIRI) and will be built at SASE3 in 2020-2021. Detailed information is available at [1].

METHOD

The simplest way currently available to enable the generation of two closely separated (on the order of 50 fs) pulses of different wavelengths (which will later result in the two-colors) at X-ray Free-Electron lasers consists of inserting a magnetic chicane between two undulator parts as suggested in [2] and experimentally proven in [3,4]. The scheme is illustrated in Figure 1-a. We propose to split the baseline SASE3 soft X-ray undulator into two parts with a magnetic chicane. Both parts act as independent undulators and will be referred further as $U1$ and $U2$. The nominal electron beam enters the first undulator $U1$, tuned to the resonant wavelength λ_1 . After passing through $U1$, both electron beam and emitted Self-Amplified Spontaneous Emission (SASE) radiation enter the chicane. This magnetic chicane has two functions: first, it introduces a suitable delay between the electron beam and the radiation generated in $U1$. Delays from zero¹ up to the picosecond level can be obtained with a compact magnetic chicane of several meters length. Second, due to dispersion, the passage of the electron beam through the magnetic chicane smears out the microbunching at wavelength λ_1 . As a result, when the -after the magnetic chicane- delayed electron beam enters the second undulator $U2$, the SASE process starts from shot-noise again. Therefore, if the undulator $U2$ is tuned to the resonant wavelength λ_2 , then at the undulator exit one obtains a first radiation pulse at wavelength λ_1 followed by a second one with wave-

length λ_2 delayed by a time interval that can be varied by changing the strength of the chicane magnets.

One must ensure that the electron beam quality at the entrance of the second undulator $U2$ is still good enough to sustain the FEL process. This poses limits on the maximum total pulse energy that can be extracted from $U1$ and $U2$. In particular, the amplification process in $U1$ should not reach saturation. Optimization of the maximum pulse energy also poses limits on the wavelengths choices. The wavelength separation between the two pulses can theoretically span across the entire range made available by the undulator system, in the case of SASE3 between about 250 eV and 3000 eV. However, the impact of the FEL process on the electron beam quality depends on the radiation wavelength. Therefore, in order to maximize the combined radiation pulse energy that can be extracted, especially at large wavelength separations, the first pulse to be produced should be at the shortest wavelength. Moreover, the magnetic chicane strength should be large enough to smear out the microbunching at λ_1 , unless the separation between λ_1 and λ_2 is larger than the FEL bandwidth.

An easy way to increase the flexibility of the scheme is to introduce a compact optical delay line to have full control on the relative temporal separation between the two pulses as shown in Figure 1-(bottom). Since the photon beam transverse size at the position of the magnetic chicane is, roughly speaking, as small as the electron beam, i.e. a few tens of microns, the length of each mirror can be as short as several centimeters. In order to simplify the design of the mirror delay line, one may fix the optical delay to a few hundred femtoseconds, thus avoiding the use of moving mirrors, and subsequently tune the delay by changing the current in the magnetic chicane coils. Therefore, the introduction of an optical delay line would allow one to sweep between negative and positive delays at a cost of a smaller delay tuneability, caused by a lower limit of the chicane magnetic field (while the optical delay is inserted).

Even the simplest way of generating two-color pulses at the SASE3 beamline of the European XFEL, in combination with the high-repetition rate capabilities of the facility is expected to enable novel exciting science at the two soft X-ray instruments: Small Quantum Systems (SQS) [5] and Spectroscopy & Coherent Scattering (SCS) [6].

Here we limit ourselves to the analysis of one science case for the SQS instrument.

SQS SCIENCE CASE

The two-color operation mode enables a large number of scientific applications based on a pump-probe excitation

* gianluca.geloni@xfel.eu

¹ In our case, due to radiation slippage in the subsequent undulators, the effective minimum delay between the two pulses of different colors is of the order of several femtoseconds.

OVERVIEW OF THE SOFT X-RAY LINE ATHOS AT SwissFEL

R. Ganter[†], S. Bettoni, H.H. Braun, M. Calvi, P. Craievich, R. Follath, C. Gough, F. Loehl, M. Paraliev, L. Patthey, M. Pedrozzi, E. Prat, S. Reiche, T. Schmidt, A. Zandonella, PSI, Villigen PSI, 5232 Switzerland

Abstract

SwissFEL Athos line [1] will cover the photon energy range from 250 to 1900 eV and will operate in parallel to the hard X ray line Aramis. Athos consists of a fast kicker magnet, a dog leg transfer line, a small linac and 16 APPLE undulators. The Athos undulators follow a new design: the so called APPLE X design where the 4 magnet arrays can be moved radially in a symmetric way. Besides mechanical advantages of such a symmetric distribution of forces, this design allows for easy photon energy scans at a constant polarization or for the generation of transverse magnetic gradients. Another particularity of the Athos FEL line is the inclusion of a short magnetic chicane between every undulator segment. These chicanes will allow the FEL to operate in optical klystron mode, high brightness SASE mode, or superradiance mode. A larger delay chicane will split the Athos line into two sections such that two colors can be produced with adjustable delay. Finally a post undulator transverse deflecting cavity will be the key tool for the commissioning of the FEL modes. The project started in 2017 is expected to be completed by the end of 2020.

INTRODUCTION

Athos photon energy ranges from 250 eV to 1900 eV (or 6.5 – 49 Å) (Fig. 1) when assuming a maximum K value of 3.65. Such large range requires both a K variation and an electron energy variation. The electron energy at extraction point (270 m downstream electron source, Fig. 2) can be varied between 2.9 and 3.15 GeV. In addition, a small linac in the Athos branch can extend the beam energy range to 2.65 – 3.4 GeV.

The Athos undulator line is linked to the main linac of SwissFEL via a dogleg section (see Fig. 2). The SwissFEL injector will produce two bunches with 28 ns delay. The dogleg starts with the beam switching system, consisting of two kickers and three compensating dipoles. These kickers deflect the second beam vertically up by 1.75 mrad so that it enters a Lambertson septum magnets 10 mm above the Aramis axis [2]. The septum magnet deflects then the Athos bunch by 35 mrad horizontally. Kickers and septum deflecting angle must be very stable from bunch to bunch and a jitter of less than 0.3 μrad is expected. The rest of the dogleg should then close the vertical dispersion, collimate the beam in energy, compensate possible CSR kicks, align the beam tilt and energy acceptance by means of sextupoles and finally inject back the beam in the Athos undulator line parallel to the Aramis line at 3.75 m distance (Fig. 3). Downstream the dogleg, the beam can be accelerated / decelerated by four

C-band structures (+/- 250 MeV) followed by diagnostics (screens, wire scanner, beam arrival monitor) to characterize the beam before entering the undulator section. Sixteen undulator segments are distributed in a FODO period of 5.6 m length. Finally an X band deflecting transverse cavity [3] will be installed before the beam dump allowing a permanent monitoring of the electron energy loss when lasing [4] or to measure the slice emittance.

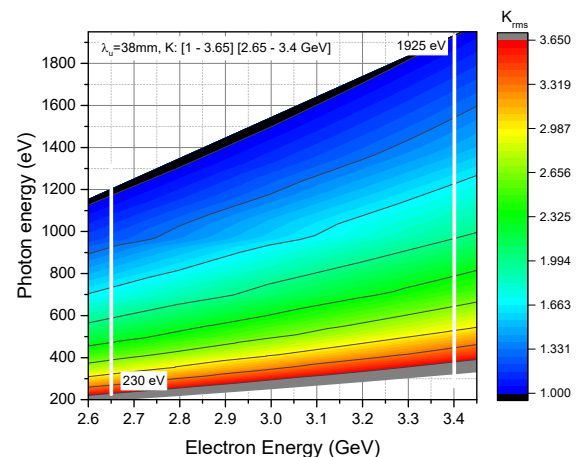


Figure 1: Photon energy range covered by the Athos FEL line (SIMPLEX [5]).

The Athos branch of SwissFEL is designed to operate in various modes of operation slightly different to standard SASE operation. The particularity of the Athos FEL lies in the permanent magnet chicanes present between every undulator segment. These chicanes allow operation in the optical klystron mode in which the microbunching process is speed up [6]. To generate terawatt – attosecond FEL pulses, a transversely tilted beam can also be shifted and delayed between every undulator segment thanks to the chicanes. In this mode, only a small portion of the beam is on the lasing trajectory and fresh electrons are supplied after a beam portion saturates [7]. The same chicanes can also be used to simply delay the bunch (without transverse shift) such that a given radiation slice (spike) will slip over a longer portion of the bunch and increase the cooperation length. This corresponds to the so called high-brightness mode [8,9] or purified SASE mode [10]. A larger magnetic chicane (2 meters length), with electromagnets, placed after the 8th undulator segment, will give the possibility to split the line and to generate two colors with adjustable time delay (0 to 500 fs). The Apple X undulator design can easily produce a transverse gradient which when used with a transversely tilted beam can produce a broadband FEL radiation of up to 10% bandwidth.

[†] romain.ganter@psi.ch

POSSIBLE METHOD FOR THE CONTROL OF SASE FLUCTUATIONS

N. R. Thompson*

ASTeC and Cockcroft Institute, STFC Daresbury Laboratory, Warrington, United Kingdom

Abstract

It is well known that because the SASE FEL starts up from the intrinsic electron beam shot noise, there are corresponding fluctuations in the useful properties of the output pulses which restrict their usability for many applications. In this paper, we discuss a possible new method for controlling the level of fluctuations in the output pulses.

INTRODUCTION

The output of a Self-Amplified Spontaneous Emission (SASE) Free-Electron Laser [1, 2] exhibits fluctuations in the temporal and spectral domains [3] because the FEL interaction grows from an initial bunching b_0 due to the intrinsic random shot noise in the electron beam. The fluctuations can be problematic for FEL applications, although if the FEL pulse properties are recorded on a shot-by-shot basis the experimental output data can often be appropriately normalised as a mitigation strategy. This paper presents a first examination of a proposed new method for damping shot-to-shot instability. One or more dispersive chicanes are added in between the undulator modules of a SASE FEL. The longitudinal dispersion of the chicane can be set to change the amount of bunching in the electron beam in a way that is anti-correlated with the energy spread. Because the FEL-induced energy spread is itself directly correlated to the FEL power this allows a simple, passive mechanism for single pass feedback and stabilisation.

DESCRIPTION OF METHOD

Following previous work optical on klystron enhancement to SASE FELs [4] it is useful to take into account the analytical treatment originally derived for HGHG [5] to provide a simple model for the method. The bunching factor at the n th harmonic after the dispersive section in HGHG is given by

$$b_n = \left| \exp \left(-\frac{1}{2} n^2 \sigma_b^2 k_r^2 R_{56}^2 \right) J_n \left(n \frac{\Delta\gamma}{\gamma_0} k_r R_{56} \right) \right| \quad (1)$$

where σ_b is the intrinsic relative energy spread, $k_r = 2\pi/\lambda_r$ is the resonant wavenumber, R_{56} is the dispersive strength of the chicane, J_n is the n th order of the Bessel function of the first kind and $\Delta\gamma$ is the energy modulation induced by the FEL prior to the chicane.

This function is plotted in Figure 1 for $\sigma_b = 1 \times 10^{-4}$, $\lambda_r = 2\pi/k_r = 100$ nm, $n = 1$, and $R_{56} = 60$ μm . The important point to note is that there are values of $\Delta\gamma/\gamma_0$ where the gradient of this plot is negative—these are highlighted in blue. The method for SASE stabilisation takes advantage of this negative gradient to introduce a feedback into the

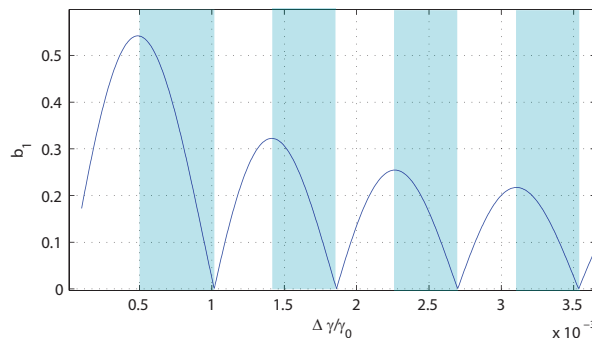


Figure 1: Plot b_n vs $\Delta\gamma/\gamma_0$ using Equation (1), for $\sigma_b = 1 \times 10^{-4}$, $\lambda_r = 2\pi/k_r = 100$ nm, $n = 1$, and $R_{56} = 60$ μm . The blue shading highlights regions where the gradient of the function is negative.

FEL growth. For example, if at the entrance to the chicane the initial bunching is small and the average induced energy spread over a number of SASE pulses is in the blue shaded region where $0.5 \times 10^{-3} \leq \Delta\gamma/\gamma_0 \leq 1 \times 10^{-3}$, then those pulses which had grown more strongly than average would have an induced energy spread higher than the average and would therefore acquire bunching after the chicane that was lower than average. Conversely, those pulses growing more weakly than average would have their bunching enhanced more than average. Overall, all the pulses would have their bunching increased in the chicane, giving stronger growth, but crucially, the weaker pulses would be boosted *more* than the stronger pulses, hence damping the shot-to-shot variation.

NUMERICAL RESULTS

The method was simulated using the three-dimensional FEL code Genesis 1.3. Two of the 240 MeV electron beam modes for the CLARA test facility [6] were used: ULTRASHORT mode which is a low charge velocity bunched mode intended to produce electron bunches suitable for lasing at 100 nm in single spike SASE regime; SHORT mode which is the default 250 pC mode for 100 nm SASE with peak current 400 A. For both modes the energy spread was set to $\sigma_b = 1 \times 10^{-4}$ and the dispersive strengths of the chicanes were within the design ranges of the facility.

ULTRASHORT Mode

The parameters of the method were empirically optimised to obtain the best stabilisation performance. The results are shown in Figure 2, which shows the pulse energy growth for a control SASE case, with 8 different shot noise seeds, and the results with the same seeds where chicanes are applied

* neil.thompson@stfc.ac.uk

COMMISSIONING OF FEL-BASED COHERENT ELECTRON COOLING SYSTEM*

V.N. Litvinenko^{1,2,#}, I. Pinayev¹, J. Tuozzollo¹, J.C. Brutus¹, Z. Altinbas¹, R. Anderson¹, S. Belomestnykh¹, K.A. Brown¹, C. Boulware³, A. Curcio¹, A. Di Lieto¹, C. Folz¹, D. Gassner¹, T. Grimm³, T. Hayes¹, R. Hulsart¹, P. Inacker¹, J. Jamilkowski¹, Y. Jing^{1,2}, D. Kayran^{1,2}, R. Kellermann¹, R. Lambiase¹, G. Mahler¹, M. Mapes¹, A. Marusic¹, W. Meng¹, K. Mernick¹, R. Michnoff¹, K. Mihara^{1,2}, T.A. Miller¹, M. Minty¹, G. Narayan¹, P. Orfin¹, I. Petrushina², D. Phillips¹, T. Rao^{1,2}, D. Ravikumar,^{1,2} J. Reich¹, G. Robert-Demolaize¹, T. Roser¹, B. Sheehy¹, S. Seberg¹, F. Severino¹, K. Shih^{1,2}, J. Skaritka¹, L.A. Smart¹, K. Smith¹, L. Snyderstrup¹, V. Soria¹, Y. Than¹, C. Theisen¹, J. Walsh¹, E. Wang¹, G. Wang^{1,2}, D. Weiss¹, B. Xiao¹, T. Xin¹, W. Xu¹, A. Zaltsman¹, Z. Zhao¹

¹Collider-Accelerator Department, Brookhaven National Laboratory, Upton, NY, USA

²Department of Physics and Astronomy, Stony Brook University, Stony Brook, NY, USA

³Niowave Inc., 1012 N. Walnut St., Lansing, MI, USA

Abstract

An FEL-based Coherent electron Cooling (CeC) has a potential to significantly boosting luminosity of high-energy, high-intensity hadron-hadron and electron-hadron colliders. In a CeC system, a hadron beam interacts with a cooling electron beam. A perturbation of the electron density caused by ions is amplified and fed back to the ions to reduce the energy spread and the emittance of the ion beam. To demonstrate the feasibility of CEC we pursue a proof-of-principle experiment at Relativistic Heavy Ion Collider (RHIC) using an SRF accelerator and SRF photo-injector. In this paper, we present status of the CeC systems and our plans for next year.

INTRODUCTION

An effective cooling of ion and hadron beams at energy of collision is of critical importance for the productivity of present and future colliders. Coherent electron cooling (CeC) [1] promises to be a revolutionary cooling technique which would outperform competing techniques by orders of magnitude. It is possibly the only technique, which is capable of cooling intense proton beams at energy of 100 GeV and above.

The CeC concept is built upon already explored technology (such as high-gain FELs) and well-understood processes in plasma physics. Since 2007 we have developed a significant arsenal of analytical and numerical tools to predict performance of a CeC. Nevertheless, being a novel

concept, the CeC should be first demonstrated experimentally before it can be relied upon in the up-upgrades of present and in the designs of future colliders.

A dedicated experimental set-up, shown in Fig. 1, has been under design, manufacturing, installation and finally commissioning during last few years [2-4]. The CeC system is comprised of the SRF accelerator and the CeC section followed by a beam-dump system. It is designed to cool a single bunch circulating in RHIC's yellow ring (indicated by yellow arrow in Fig. 1). A 1.5-MeV electron beam for the CeC accelerator is generated in a 113-MHz SRF quarter-wave photo-electron gun and first focussed by a gun solenoid. Its energy is chirped by two 500-MHz room-temperature RF cavities and ballistically compressed in 9-m long low energy beamline comprising five focusing solenoids. A 5-cell 704-MHz SRF linac accelerates the compressed beam to 15 MeV. The accelerated beam is transported through an achromatic dogleg to merge with ion bunch circulating in RHIC's yellow ring.

In the CeC beamline, interaction between ions and electron beam occurs in the common section, e.g. a proper coherent electron cooler. The CeC works as follows: In the modulator, each hadron induces density modulation in electron beam that is amplified in the high-gain FEL; in the kicker, the hadrons interact with the self-induced electric field of the electron beam and receive energy kicks toward their central energy. The process reduces the hadron's energy spread, i.e. cools the hadron beam. Fourteen quadrupoles

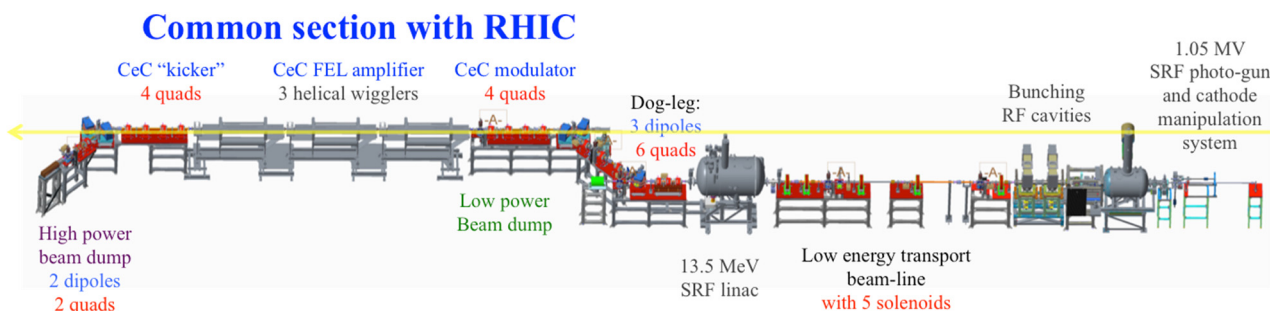


Figure 1: Layout of the CeC proof-of-principle system at IP2 of RHIC.

* Work is supported by Brookhaven Science Associates, LLC under Contract No. DEAC0298CH10886 with the U.S. Department of Energy, DOE NP office grant DE-FOA-0000632, and NSF grant PHY-1415252.

#vl@bnl.gov

Content from this work may be used under the terms of the CC BY 3.0 licence (© 2018). Any distribution of this work must maintain attribution to the author(s), title of the work, publisher, and DOI.

STATUS OF THE SEEDING DEVELOPMENT AT sFLASH

V. Grattoni*, R. Assmann, J. Bödewadt, I. Hartl, T. Laarmann, C. Lechner,
M. M. Kazemi, A. Przystawik, DESY, Hamburg, Germany
S. Khan, N. M. Lockmann, T. Plath, TU Dortmund, Dortmund, Germany
A. Azima, M. Drescher, W. C. A. Hillert, L. L. Lazzarino,
V. Miltchev, J. Rossbach, University of Hamburg, Hamburg, Germany

Abstract

sFLASH is the experimental free-electron laser (FEL) setup producing seeded radiation installed at FLASH. Since 2015 it has been operated in the high-gain harmonic generation (HGHG) mode. A detailed characterization of the laser-induced energy modulation, as well as the temporal characterization of the seeded FEL pulses is possible by using a transverse-deflecting structure and an electron spectrometer. In this contribution, we present the status of the sFLASH experiment, its related studies and possible developments for the future.

INTRODUCTION

Since 2005, the free-electron laser (FEL) facility in Hamburg, FLASH, at DESY has been operated as a user facility [1]. The wavelength range was upgraded in several steps to cover an interval from about 4.2 nm to 45 nm at the beamline FLASH1. Recently, a second undulator beamline, called FLASH2, was built and commissioned to serve simultaneously two user end stations [2]. Both the beamlines are operated in the self-amplified spontaneous emission (SASE) mode [3, 4].

As a SASE FEL starts up from the random shot noise in the electron beam, the FEL radiation has poor spectral stability and limited longitudinal coherence. Seeding the FEL with a fully coherent source such as a laser, offers an option to overcome these limitations as experimentally demonstrated in the FERMI FEL in Trieste, Italy [5].

At DESY, an experimental setup for seeding developments has been installed upstream of the FLASH1 main SASE undulator in 2010 [6]. After successful demonstration of direct-HHG seeding [7] at 38 nm in 2012 [8], the focus of the seeding R&D at FLASH has turned on HGHG [9] and echo-enabled harmonic generation (EEHG) [10] seeding [11, 12].

The results obtained at the sFLASH seeding experiment guide the design process of the proposed FLASH2 seeding option [13].

In this contribution, the performance of HGHG seeding at sFLASH is described and we present the current status of the FEL seeding developments at DESY.

EXPERIMENTAL SETUP

The sFLASH seeding experiment is installed at the FEL user facility FLASH [14]. Figure 1 shows the schematic layout of the sFLASH experiment.

The electron bunches arrive from the FLASH linear accelerator with a repetition rate of 10 Hz, a typical charge of 0.4 nC and an energy between 680 MeV and 700 MeV. At the exit of the energy collimator, the sFLASH section starts with two electromagnetic undulators (called modulators, labelled MOD1 and MOD2 in Fig. 1) with 5 full periods of period length $\lambda_u = 0.2$ m and orthogonal polarization [15], each followed by a magnetic chicane (labelled as C1 and C2). In the HGHG experiment, MOD1 and C1 are not used and the interaction of the seed laser pulse with the electron bunch takes place in MOD2. Here, the seed pulse generates a sinusoidal energy modulation in the electron bunch that afterwards is converted into a density modulation by chicane C2.

The Seed Laser

The 266 nm seed pulses are generated by third-harmonic generation (THG) of near-infrared (NIR) Ti:sapphire laser pulses. The maximum energy of these UV seed pulses at the entrance of the vacuum transport beamline to the modulator undulator is 500 μ J. At the interaction point with the electron beam, the Rayleigh length of the UV beam is between 1.5 and 3 m depending on the focus of the laser.

A single-shot cross-correlator for NIR and UV pulses in the laser laboratory enables to measure the UV pulse duration, that is typically between 250 and 280 fs FWHM. The NIR pulse duration is simultaneously measured with a single-shot auto-correlator and it is about 50 fs FWHM. The longitudinal position of the beam waist can be adjusted by changing the NIR focusing into the THG setup. Before and after MOD2, the seed beam position and size are measured using Ce:YAG fluorescence screens. In the configuration in which the beam waist coincides with the center of the modulator module, a characteristic value for the rms beamsize at the screen positions is $\sigma_r = 0.33$ mm.

Latest upgrades Until the end of 2016, the THG setup was installed in the FLASH tunnel, limiting maintenance access. Now, this setup is installed in the seed laser laboratory and can be accessed when needed which facilitates the optimization of the UV seed beam quality. In particular, thanks to the more generous spaces inside the laser laboratory, a second THG setup has been installed next to the existing one and the NIR laser transport system has been modified in order to obtain two properly focused pulses that enter each in one of the two triplers. The new UV beam is focused into MOD1 by a Galilean telescope that has been installed in the FLASH tunnel before MOD1 in July this year. The

* vanessa.grattoni@desy.de

PLASMA WAKEFIELD ACCELERATED BEAMS FOR DEMONSTRATION OF FEL GAIN AT FLASHFORWARD *

P. Niknejadi[†], A. Aschikhin, C. Behrens¹, S. Bohlen¹, J. Dale, R. D'Arcy, L. Di Lucchio, B. Foster¹, L. Goldberg¹, J.-N. Gruse¹, Z. Hu, S. Karstensen, A. Knetsch, O. Kononenko¹, K. Ludwig¹, F. Marutzky, T. Mehring, C. A. J. Palmer, K. Poder, P. Pourmousavi¹, M. Quast¹, J.-H. Röckemann¹, L. Schaper, J. Schaffran, H. Schlarb, B. Schmidt, S. Schreiber, S. Schroeder, J.-P. Schwinkendorf¹, B. Sheeran¹, M.J.V. Streeter, G. Tauscher¹, V. Wacker¹, S. Weichert¹, S. Wesch, P. Winkler¹, S. Wunderlich, J. Zemella, J. Osterhoff,
Deutsches Elektronen-Synchrotron DESY, Hamburg, Germany
V. Libov, A. Martinez de la Ossa, M. Meisel

Institut für Experimentalphysik, Universität Hamburg, Germany

A. R. Maier¹, Center for Free Electron Lasers, Hamburg, Germany

C. Schroeder, Lawrence Berkeley National Laboratory, California, USA

¹ also at Institut für Experimentalphysik, Universität Hamburg, Germany

Abstract

FLASHForward (FF▶▶) is the Future-ORiented Wakefield Accelerator Research and Development project at the DESY free-electron laser (FEL) facility FLASH. It aims to produce high-quality, GeV-energy electron beams over a plasma cell of a few centimeters. The plasma is created by means of a 25 TW Ti:Sapphire laser system. The plasma wakefield will be driven by high-current-density electron beams extracted from the FLASH accelerator. The project focuses on the advancement of plasma-based particle acceleration technology through the exploration of both external and internal witness-beam injection schemes. Multiple conventional and cutting-edge diagnostic tools, suitable for diagnosis of short electron beams, are under development. The design of the post-plasma beamline sections will be finalized based on the result of these aforementioned diagnostics. In this paper, the status of the project, as well as the progress towards achieving its overarching goal of demonstrating FEL gain via plasma wakefield acceleration, is discussed.

PLASMA WAKEFIELD ACCELERATORS

As opposed to conventional particle accelerators, where the accelerating electric gradients are generated by radio waves in superconducting (SRF) or nonsuperconducting (RF) structures, plasma wakefield accelerators (PWFA) employ a charged particle beam to create a charge-density "wake" in a plasma. With accelerating gradients on the order of 10-100 GeV/m, about three orders of magnitude greater than those produced by SRF methods, plasma wakefield accelerators allow for significant reduction of length, ultimately scaling down the size of future high energy accelerators for future light sources and colliders [1, 2]. Hence, PWFA is a promising alternative to conventional accelerators, worthy of further investigation.

FLASHFORWARD FACILITY

FLASHForward [3] is one of the few facilities in the world that is dedicated to studying and overcoming the technical and scientific challenges of beam-driven plasma wakefield acceleration. FLASHForward has as its main feature a new electron beamline in the FLASH2 tunnel, which consists of beam extraction, beam matching and focusing, a plasma cell, beam diagnostics, and undulator sections. This beamline is shown in Fig. 1. The first three sections of the beamline leading to the plasma cell are currently being installed. The project is planned in two phases so that progress and understandings gained in the first phase can benefit the second phase. Demonstration of high-quality electron beams, with small emittance and energy spread, is the goal of this first phase of the FLASHForward project. This phase will conclude with measurements of the longitudinal phase space of plasma-accelerated beams with femtosecond resolution via an X-band transverse deflecting cavity (XTDC) [4]. The design for the sections beyond the plasma cell, the diagnostics and undulator section, will be finalized after demonstration and characterization of PWFA beams. The commissioning of the second phase is expected to begin in 2020.

As previously mentioned, FLASHForward is an extension to the FLASH facility, to be operated in parallel with FLASH1 and FLASH2. As such, FLASHForward already benefits from features that are unique to linear accelerators designed for high-gain single-pass FEL sources. These features include a beam of sufficient quality to drive an FEL (up to 1.25 GeV energy, ~ 0.1% energy spread, ~ 2 μm transverse normalized emittance) with a peak current of 2.5 kA and variable current profile.

Through the use of FLASH bunches, which are already used to generate FEL pulses, the efficiency of a PWFA stage as an energy booster for FELs will be explored. In this scheme the FLASH beam will receive an energy boost via plasma acceleration while its qualities are preserved to produce FEL gain. Preservation of beam quality during accel-

* Work supported by Helmholtz ARD program and VH-VI-503

[†] pardis.niknejadi@desy.de

COMMISSIONING STATUS OF THE EUROPEAN XFEL PHOTON BEAM SYSTEM

F. Le Pimpec*, European XFEL, Schenefeld, Germany

Abstract

The European XFEL located in the Hamburg region in Germany, has finished its construction phase and is currently being commissioned. The European XFEL facility aims at producing X-rays in the range from 260 eV up to 24 keV out of three undulator beam lines that can be operated simultaneously with up to 27000 pulses/second. The FEL is driven by a 17.5 GeV linear accelerator based on TESLA-type superconducting accelerator modules. The accelerator has finished its first commissioning phase and is currently delivering photon beam to the experimental areas for commissioning in view of the user operation. This paper presents the status of the photon beam system from the undulators to the three experimental areas, as well as the status of the instruments.

INTRODUCTION

The European XFEL accelerator, operated by the DESY staff, has lased after 6 months of commissioning time [1, 2] and has reached the first set of design parameter as described in [3]. This success allows for the official start of the operation phase of the European XFEL. Although the machine would benefit of more time for a thorough commissioning of all its subsystems; the accelerator must provide x-ray (XR) laser type beam to the two instruments FXE (Femtosecond X-ray experiments) and SPB/SFX (Single Particles, clusters and Biomolecules /Serial Femtosecond Crystallography) located in the SASE 1 branch (see Fig.1). The technical commissioning of these two instruments, with and without beam, is in full swing in order to be ready to receive their first users in September 2017. The tight schedule allows a start of the exploitation phase with external users with a set of limited parameters for the electron and for the XR photon beams. The two other photon beamlines SASE 2 and 3 should be ready to receive beam in early 2018 and the instruments located at their end for user operation sometimes in late 2018.

ACCELERATOR OPERATION STATUS

The layout of the entire superconducting based Linear accelerator, including the 3 undulator sections and their respective electron beam dumps can be found in Figure 3 in the following reference [1]. Some of the design parameters of this machine and the value achieved at the beginning of August 2017 are given in Table 1. The normalized slice emittance measured with a bunch charge of 500 pC was 0.6 mm/mrad. The machine is now providing and tuning around a photon energy of 9.1 keV hence adjusting the gap

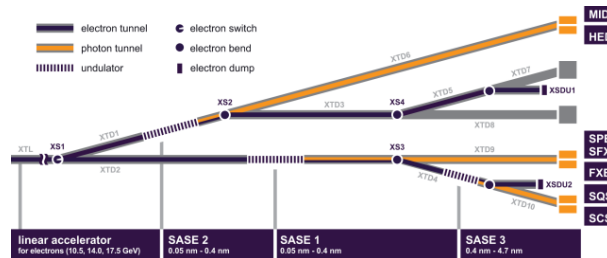


Figure 1: Photon beam system layout underlined by the orange color for the X-ray optics, diagnostics and beam transport

of the undulators according to needs based on the electron energy.

Table 1: European XFEL Design Parameters and Target Parameters Achieved at the Beginning of August 2017 [1].

Parameter		Design	Achieved
Energy	GeV	17.5	14.6
Bunch Charge	pC	20 - 1000	100-500
Macro Pulse Repetition Rate	Hz	10	10
Macro Pulse RF length	μ s	600	600
Inner pulse bunch frequency		1-2700	1-30
Max. beam power at LINAC end	kW	473	1.8
Peak Current	kA	3-5	5
Compression Factor		200-2000	200
Operating Temperature	K	1.9	1.9

It must be mentioned that the injector itself which finished its commissioning in 2016 could produce and drive to the injector dump (160 MeV) 2700 bunches per train at 10 Hz. The complex pattern of the European XFEL is reproduced in Fig.2. The warm RF gun could produce bunches with a charge varying from 20 pC to 1 nC [1].

In order to qualify the European XFEL facility to be ready to enter the operation phase, a set of parameters had to be achieved:

1. Photon Wavelength: < 0.2 nm
2. Peak brilliance: $> 10^{30}$ photons/s/mm²/mrad²/0.1 % BW
3. Dimension at sample: < 1 mm² (FWHM)
4. Positional stability: $< 50\%$ of beam size (RMS)
5. Photon energy stability: $< 0.1\%$
6. Shot-to-shot intensity fluctuation: $< 10\%$

* frederic.le.pimpec@xfel.eu

Content from this work may be used under the terms of the CC BY 3.0 licence (© 2018). Any distribution of this work must maintain attribution to the author(s), title of the work, publisher, and DOI.

PROGRESS OF DELHI LIGHT SOURCE AT IUAC, NEW DELHI*

S. Ghosh[†], B. K. Sahu, P. Patra, J. Karmakar, B. Karmakar, S. R. Abhilash, D. Kabiraj,
V. Joshi, N. Kumar, S. Tripathi, G. K. Chaudhari, A. Sharma, A. Pandey,
S. Kumar, G. O. Rodrigues, R. K. Bhandari, D. Kanjilal,
Inter University Accelerator Centre (IUAC), New Delhi, India
A. Aryshev, S. Fukuda, M. Fukuda, N. Terunuma, J. Urakawa,
High Energy Accelerator Research Organization, KEK, Tsukuba, Japan
U. Lehnert, P. Michel, Helmholtz Zentrum Rossendorf Dresden (HZDR), Dresden, Germany
V. Naik, A. Roy, Variable Energy Cyclotron Center, Kolkata, India
M. Tischer, Deutsches Elektronen-Synchrotron (DESY), Germany
T. Rao, Brookhaven National Laboratory, USA

Abstract

The first phase of the pre-bunched Free Electron Laser (FEL) based on the RF electron gun, has been initiated at Inter University Accelerator Centre (IUAC), New Delhi. The photoinjector-based electron gun made from OFHC copper was fabricated and tested with low power RF. The beam optics calculation by using ASTRA and GPT codes are performed and radiation produced from the pre-bunched electron bunches are being calculated. The high-power RF system was ordered and will be commissioned at IUAC by the beginning of 2018. The design of the laser system is being finalised and assembly/testing of the complete laser system will be started soon in collaboration with KEK, Japan. The initial design of the photocathode deposition system has been completed and its procurement/development process is also started. The first version of the undulator magnet design is completed and its further improvements are underway. The initial design of the DLS beam line have been worked out and various beam diagnostics components are being finalised. Production of the electron beam and THz radiation is expected by 2018 and 2019, respectively.

INTRODUCTION

A typical Free Electron Laser (FEL) accelerator is either based on the principle of oscillator or seeded amplifier or Self Amplified Spontaneous Emission. The length of most FEL facilities is extended to a few tens of metres which make the system complex as well as expensive. To reduce the length of the machine and, hence, to minimise the cost and complexity, the pre-bunched FEL [1,2] based on the photoinjector RF electron gun was planned to be developed at Inter University Accelerator Centre (IUAC), New Delhi. The name of the project is Delhi Light Source (DLS) [3] and it is divided into three phases. In the first phase, a photocathode based electron gun will produce low emittance electron beam with maximum energy of ~ 8 MeV which will be injected in to a compact, variable gap undulator

magnet to produce the coherent THz radiation in the range of 0.15 to 3.0 THz. During the second phase, a superconducting RF photo-injector will be developed and the electron beam will produce THz radiation with higher average power by an undulator magnet. In the third phase, the energy of the electron beam will be increased from 8 to 40 MeV and it will be injected in to longer undulator magnets to produce far-infrared and infrared radiation. The electron beam will be also used to produce soft X-rays by colliding it with a laser beam. Presently, the first stage of the DLS project is about to be commissioned at IUAC.

DEVELOPMENTAL STATUS OF MAJOR COMPONENTS OF PHASE-I OF DLS

A class 10000 clean room has been commissioned to accommodate the Phase-I of DLS. In addition to that, the photocathode deposition mechanism and all the experimental stations to perform experiments with electron and THz beam will be also installed inside the clean room. The stages of developments for various subsystems of the compact FEL is given in the following sections:

Simulation of Beam Optics and Radiation Production from the Undulator

The beam optics simulations are performed with the help of ASTRA [4] and GPT [5] code. In the first phase of DLS, the single laser pulse responsible to produce electron bunches will be split in to 2, 4, 8 or 16 micropulses. The maximum separation between 2, 4, 8 or 16 micropulses of laser and hence electrons will be ~ 6.6 ps, 2.2 ps, 950 fs or 333 fs respectively so that the total span of the microbunch train will occupy less than about 6.6 ps in an RF cycle of 2860 MHz. If the RF pulse width is adjusted to be at 3 μ sec, then 15 electron microbunch trains, each separated by 200 ns containing 2, 4, 8 or 16 micro-bunches will be accommodated within a RF pulse whose repetition rate is ~ 80 msec. For the case of 16 laser micro-bunches, a total number of 3000 electron micro-bunches ($16 \times 15 \times 12.5$) will be produced. If 15-pC electron charge can be accommodated inside a micro-bunch, the total charge of a macro-

[†] ghosh64@gmail.com

* The work is supported by Board of Research in Nuclear Science, India and Inter University Accelerator Center, India

DESIGN CALCULATION ON BEAM DYNAMICS AND THz RADIATION OF DELHI LIGHT SOURCE*

V. Joshi[†], J. Karmakar, N. Kumar, B. Karmakar, S. Tripathi, S. Ghosh, D. Kanjilal, R. Bhandari,
Inter University Accelerator Centre (IUAC), New Delhi, India
U. Lehnert, Helmholtz Zentrum Dresden Rossendorf (HZDR), Dresden, Germany
A. Aryshev, High Energy Accelerator Research Organization (KEK), Ibaraki, Japan

Abstract

The development of a compact light source facility, Delhi Light Source (DLS), based on pre-bunched Free Electron Laser has been initiated at Inter University Accelerator Centre (IUAC) [1-3]. A photocathode based normal conducting RF gun will generate a low emittance 'comb' electron beam with a maximum energy of ~ 8 MeV, which when injected into a 1.5 metre compact undulator magnet ($\sim 0.4 < K_{rms} < \sim 2$) will produce intense THz radiation in the frequency range of 0.15 to 3.0 THz. There will be provision to vary the spatial separation between the successive microbunches of the electron beam so that by varying the Undulator magnetic field and/or electron energy, the THz frequency can be tuned. The detailed information of the radiation to be generated from the facility along with the optimized beam optics results will be presented in the paper.

INTRODUCTION

Delhi Light Source (DLS) is a project initiated by Inter University Accelerator Centre to develop a compact THz radiation facility based on the principle of prebunched Free Electron Laser [1-3]. The facility will consist of a fibre laser system to generate 'comb' laser pulses with variable separation in frequency range of 0.15 to 3 THz which will be incident on the photocathode (Cu or Cs₂Te) to generate the electron micro-bunches. The electron beam generated from the photocathode will be accelerated by the normal conducting 2.6-cell copper cavity to produce an electron energy of ~ 8 MeV.

In this paper, we discuss the simulation results of generation of e-beam microbunches from the photocathode and its evolution through the beam line. General Particle Tracer [4] was used to track the electron beam from the photocathode to the exit of the undulator. The characteristics of the THz radiation to be produced from the wiggling electrons through the undulator was studied numerically by solving the Lienard-Wiechert fields for ensemble of charged particles, moving relativistically under the combined influence of the interaction fields and the undulator fields.

PRINCIPLE OF OPERATION OF DLS

The first phase of DLS is intended to produce THz radiation in the wavelength range of 0.15 to 3 THz. To reduce the cost and complication of the project, it was decided to design a compact facility with maximizing the peak elec-

tron current and peak intensity of radiation within a time width of a few hundreds of femtoseconds. This challenging goal can be achieved by producing thin slices of electrons called microbunches and then producing a train of those microbunches with a variable separation equal to the wavelength of the frequency range by varying the separation of the laser pulses. If the bunch length of the individual microbunches in the electron beam is extremely small with respect to the radiation wavelength, then the emitted radiation from individual electrons is added up in phases resulting in maximum radiation intensity and the bunches are called "super-radiant" [5]. Further, if each microbunch is super-radiant and inter microbunch separation is maintained at one radiation wavelength, then the radiation from each microbunch will be coherently added and the intensity will be proportional to the square of the total number of electron in e- beam. The total electric field [6] from the train of microbunches will be given by the following summation where k is the microbunch number, N_m is the total number of the microbunches, t_0 is the observation time for the radiation pulse from first microbunch and t_k is the temporal separation of the k th microbunch from the first microbunch. Since $\exp(-i\omega(t_0 + t_k))$ is a periodic function and $\exp(-i\omega(t_0 + t_k)) = \exp(-i\omega t_0)$ if $t_k = T_{\text{radiation}}$; therefore; the equation for total electric field will be reduced to $E_{\text{total}} = E_0 N_m N_e B_w$ where B_w is called bunching factor and the intensity will scale as $I \sim E_0^2 N_m^2 N_e^2 B_w^2$. Thus, pre-bunching should result in enhancement of the emission spectral energy for the frequency to be generated [5].

BEAM OPTICS SIMULATIONS

The beam optics simulations have been performed by using the GPT code and it includes the generation of the electron beam at the photocathode, its acceleration through the 2.6 cell RF cavity, transportation of the beam from the exit of the RF cavity up to the undulator exit with help of a solenoid magnet and a quadrupole magnet. To improve the quality of the e-beam, the simulation calculations have been performed a) to reduce the size, energy spread and emittance of the beam b) to maximize the bunching factor of the beam and c) to avoid the overlapping of the microbunch structure of the beam bunches starting from undulator entrance to exit. The beam optics calculations have been done with radial beam and important simulation parameters are given in Table 1.

The e- beam profile in x and y direction for the two extreme frequencies of 0.15 and 3THz from the photocathode

*This work is supported by Board of Research in Nuclear Sciences (BRNS) and IUAC.

[†] vipuljoshi92@gmail.com

A COMPACT THz FEL AT KAERI: THE PROJECT AND THE STATUS

S. Miginsky^{†1}, S. Bae, B. Gudkov, K. H. Jang, Y. U. Jeong, K. Lee, J. Mun, S. Saitiniyazi,
 Korea Atomic Energy Research Institute, Daejeon, Korea
 S. H. Park, Korea University Sejong Campus, Sejong, Korea
¹also at Budker Institute of Nuclear Physics, Novosibirsk, Russia

Abstract

A new compact THz free electron laser driven by a microtron is being developed recently at KAERI. It uses a hybrid electromagnetic undulator. A novel scheme of injection/extraction/outcoupling is developed. The machine is partially assembled and commissioned. Characteristic features and current state are described in the paper.

INTRODUCTION

About twenty years ago the first compact THz FEL at KAERI has been commissioned [1]. Since then a huge number of experiments using this FEL have been conducted [2, 3]. In addition, its parameters have been improved during this intensive operation. A number of user stations have been built at this machine. It operates now, but its resource is almost consumed and operation is not so stable. In this regard, a development of a new machine seems to be a good idea. Finally, technological progress over these years is significant, so a new FEL could provide much better characteristics. Thus, it was decided to develop a new FEL several years ago.

PROJECT

The basic scheme of the new FEL has been chosen similar to that of the previous one. It consists of a microtron, a beamline, and a FEL structure, as shown in Fig. 1.

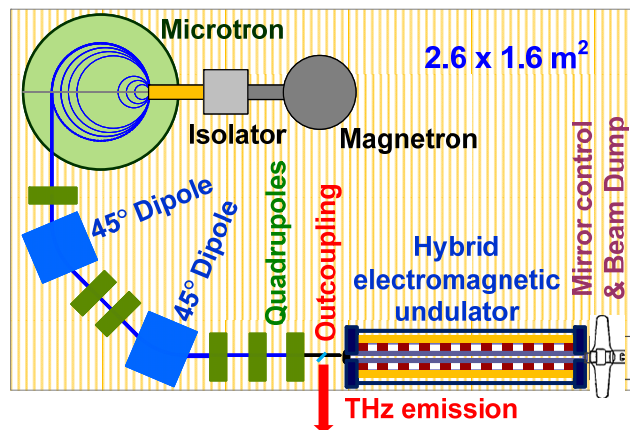


Figure 1: Schematic top view of the FEL.

The A microtron is an RF resonance electron accelerator with constant frequency and leading magnetic field, and variable harmonics number [4]. RF power is supplied by a magnetron in our case. A modulator for it is based on

storage capacities, solid state switches, and a high-voltage transformer. This combination seems to be the cheapest source of a comparably high quality electron beam of the energy of several MeV. Its basic parameters in our case are as follows:

- Electron kinetic energy 4.9 MeV
- Macropulse current 40 mA
- Macropulse duration 5 μ s
- Repetition rate up to 100 Hz
- Typical emittance x: 2 mm·mrad
y: 0.1 mm·mrad
- Typical energy spread $4 \cdot 10^{-3}$

The electron beam comes further through a beamline to the FEL structure. The beamline is used for matching the beam parameters to the optimal ones for the undulator. The matter is that the beam dispersion function and its derivative are not zero at the microtron exit while both should be zero in the undulator. Also, vertical and horizontal α - and β -functions are also far enough from the optimal ones in the undulator. Thus, one should match 6 parameters, so we used the very minimum number of quadrupoles. Two dipoles (but not one) were used to make the beamline more compact and avoid too big bending angles. This beamline provides the optimal beam parameters in the undulator at all expected entrance ones and the whole range of the undulator strengths.

A hybrid electromagnetic scheme has been selected for the undulator. This device contains magnetically soft poles and both permanent magnets and coils with electric current. Its design is similar to that of the existing machine. The strength is controlled by current in the coils. The main advantage of this design over the conventional hybrid one (without coils) is absence of moving parts. It means absence of heavy loaded precision mechanics (~1 ton) and permits to fasten a waveguide of an optical resonator precisely and reliably. In addition, compensation of the 1st and 2nd integrals of magnetic field at the entrance seems to be much easier in the chosen design.

There is no horizontal focusing in a perfectly planar undulator. In this case, it is impossible to conduct an electron beam through a narrow waveguide. To compensate for this, the poles were appropriately shaped to provide significant focusing. The two utmost poles were reshaped to compensate the integrals. The basic parameters of the undulator are as follows:

[†] email address Miginsky@gmail.com

Content from this work may be used under the terms of the CC BY 3.0 licence (© 2018). Any distribution of this work must maintain attribution to the author(s), title of the work, publisher, and DOI.

DEVELOPMENT OF COMPACT THz COHERENT UNDULATOR RADIATION SOURCE AT KYOTO UNIVERSITY*

Siriwan Krainara[†], Heishun Zen, Toshiteru Kii, Hideaki Ohgaki, Institute of Advanced Energy, Kyoto University, Gokasho, Uji, Kyoto 611-0011, Japan

Sikharin Suphakul, Department of Physics and Materials Science, Faculty of Science, Chiang Mai University, Chiang Mai 50200, Thailand

Abstract

A new THz Coherent Undulator Radiation (THz-CUR) source has been developed to generate intense quasi-monochromatic THz radiation at the Institute of Advanced Energy, Kyoto University. The system consists of a photocathode RF gun, bunch compression chicane, quadrupole magnets, and short planar undulator. The total length of this system is around 5 meters. At present, this compact accelerator has successfully started giving the THz-CUR in the frequency range of 0.16 - 0.65 THz. To investigate the performance of the source, the relationship between the total radiation energy, peak power and power spectrum as a function of bunch charge at the different undulator gaps were measured. The results are reported in the paper.

INTRODUCTION

At present, there are several THz sources such as quantum cascade lasers, solid state oscillators, optically pumped solid state or gas devices, electron tubes and accelerator based sources. They have been developed as the useful tools in many scientific fields [1]. At the Institute of Advanced Energy, Kyoto University, a THz Coherent Undulator Radiation (THz-CUR) source (Fig. 1), which consists of a photocathode RF gun, bunch compression chicane, quadrupole magnets, and short planar undulator, has been developed [2]. It is expected to generate a quasi-monochromatic THz beam with high peak power. This project has been started since 2008 and the construction was started in end of 2013. The 1.6-cell S-band BNL-type photocathode RF-gun designed and manufactured by KEK has been installed in 2014. The electron beam was firstly generated in 2015 with the electron beam energy of 4.6 MeV with the energy spread of 1.3% [3]. And the RMS normalized transverse emittance with the bunch charge of 50 pC was reported to be 6 and 8 mm-mrad for horizontal and vertical axis, respectively [4]. The first THz-CUR in this source was observed in August 2016.

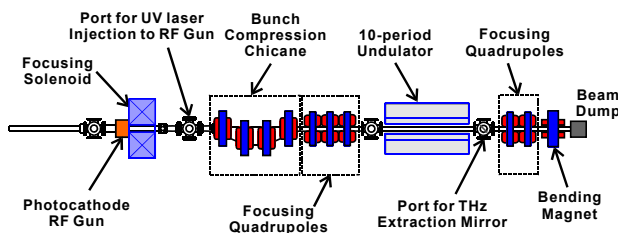


Figure 1: Layout of THz-CUR source at Kyoto University.

To investigate the performance of the THz-CUR source, the measurements of total radiation energy, the radiated peak power, and power spectrum were conducted as functions of bunch charge and the undulator gap. The results are presented and discussed.

THz-CUR PROPERTIES

The coherent undulator radiation (CUR) can be emitted when the electrons are propagating in undulator. The energy of CUR can be expressed in the formula [5]

$$W_{\text{coh}} = W_{1e} N_e^2 f(\omega, \sigma_z),$$

where W_{1e} is the total energy radiated by the single electron ($W_{1e} = \pi e^2 N_u K^2 \gamma^2 / 3 \epsilon_0 \lambda_u$), N_u is the number of undulator period, γ is the Lorentz factor. The undulator strength parameter K is $0.934 B_0 [T] \lambda_u [\text{cm}]$. B_0 is the magnetic field and λ_u is the period length of undulator. The bunch form factor $f(\omega)$ is defined as the square of the Fourier transform of the normalized longitudinal particle distribution. For a Gaussian bunch with the RMS width of σ_z , the form factor can be given as $f(\omega, \sigma_z) = \exp(-\omega^2 \sigma_z^2)$. The pulse energy is proportional to the square of electron number in the bunch. In order to have CUR, the longitudinal bunch length must be shorter than the radiation wavelength.

Up to now, the bunch length has not been measured, but it can be estimated by using General Particle Tracer (GPT) code [6]. The longitudinal bunch length is 1.0 ps in FWHM after compressing the electron bunch by using chicane magnets. As shown in Fig. 2, the bunch form factor gradually decreases to zero if the resonance frequency is higher than 0.8 THz and 0.5 THz for the bunch length of 1.0 ps and 1.5 ps, respectively.

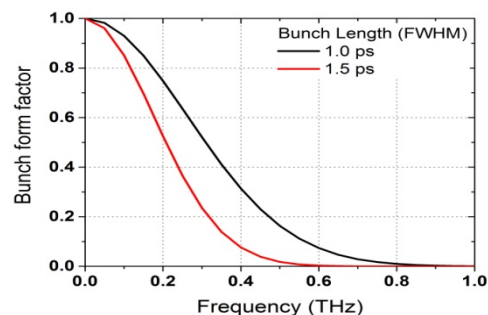


Figure 2: The bunch form factor with two bunch lengths of 1.0 and 1.5 ps in FWHM.

*This work supported by the MEXT/JSPS KAKENHI 26706026.

[†]siriwan.krainara.82r@st.kyoto-u.ac.jp

PRESENT STATUS OF INFRARED FEL FACILITY AT KYOTO UNIVERSITY*

H. Zen[†], J. Okumura, S. Tagiri, S. Krainara, S. Suphakul^{††}, K. Torgasin, T. Kii, K. Masuda,
and H. Ohgaki, Institute of Advanced Energy, Kyoto University, Uji, Japan

Abstract

A mid-infrared Free Electron Laser (FEL) named KU-FEL has been developed for promoting energy related research at the Institute of Advanced Energy, Kyoto University. KU-FEL can cover the wavelength range from 3.5 to 23 μm and routinely operated for internal and external user experiments. Recently a THz Coherent Undulator Radiation (CUR) source using a photocathode RF gun has been developed as an extension of the facility. As the result of commissioning experiment, it was confirmed that the CUR source could cover the frequency range from 0.16 to 0.65 THz. Present statuses of these infrared light sources are reported in this paper.

INTRODUCTION

An oscillator type Mid-Infrared Free Electron Laser (MIR-FEL) named as KU-FEL has been developed at the Institute of Advanced Energy, Kyoto University for promoting energy related research [1]. The FEL succeeded in its first lasing [2] and power saturation [3] in 2008. At that time, the tunable range of the FEL was not so wide (only 10 to 14 μm) because of the limited gain of the FEL and macro-pulse duration of the electron beam. In order to extend tunable range, the optical cavity mirrors and the undulator have been replaced in January 2012. Then the tunable range of KU-FEL has been extended to 5 – 15 μm [4]. The narrowest undulator gap has been reduced from 20 to 15 mm by replacing the vacuum duct of undulator section in 2013. As the result of commissioning experiment, it was confirmed that KU-FEL could cover the wavelength range from 5 to 21.5 μm [5]. After the replacement of the vacuum duct of the undulator, some efforts to optimize the operation parameter of KU-FEL have been made and now the tunable range was extended 3.5 – 23 μm .

Now, KU-FEL is routinely operated for internal and external user experiments. The layout of KU-FEL facility is shown in Fig. 1. There are three user stations available. The user station #1 is the FEL beam diagnostics and simple irradiation station. In this station, an MIR-monochromator, MIR-detectors, pyroelectric energy meters and some focusing optics are available. The user station #2 is the pump-probe experiment station. In the pump-probe station, ns-Nd:YAG laser (1064, 532 and 266 nm), ps-Nd:YVO₄ laser (1064 and 532 nm), and a closed-cycle cryostat with optical windows are available. Users

can perform the pump-probe experiment of solid samples with the lowest sample temperature of 12 K with various combinations of MIR-FEL and those solid state lasers. At this station, MIR induced mode-selective phonon excitation experiments of solid samples have been performed [6-8]. The station #3 is intended for multi-purpose application. There is an optical table and users can construct their experimental setup on the table.

In order to satisfy the user who wants to perform some nonlinear spectroscopy in MIR region, the photocathode operation of the KU-FEL has been demonstrated [9]. It was confirmed that the peak power of the FEL can be significantly increased by the photocathode operation with a significant reduction of the average power.

Recently, a THz Coherent Undulator Radiation (THz-CUR) source using a photocathode RF gun has been developed as an extension of the facility [10]. When the electron bunch length is shorter than the radiation wavelength, the radiations from each electron are coherently superposed. In the condition, the radiation intensity can be intense and the radiation has good longitudinal coherence. This radiation is called as “coherent” radiation. In the case of undulator radiation, it is called as CUR. In the THz region, some CUR sources have been developed so far [11-13]. Our THz-CUR source consists of a 1.6-cell photocathode RF gun, a bunch compression chicane, and 0.7-m Halbach type undulator. The total length of the machine is about 5 m. The THz-CUR source shares a photocathode driving laser system [14] and an RF source with a 4.5-cell RF gun of KU-FEL. The construction and commissioning of THz-CUR source were finished in August 2016. The layout of THz-CUR source is also shown in Fig. 1.

MIR-FEL

The oscillator type MIR-FEL named as KU-FEL consists of a 4.5-cell thermionic RF gun with a LaB₆ thermionic cathode which generates multi-bunch electron beams with the energy of 8.4 MeV, a dog-leg energy filtering section, a 3-m traveling-wave type accelerating structure, a bunch compressing 180-deg. arc section, a 1.8-m hybrid undulator, and a 5-m optical cavity. The typical characteristics of KU-FEL under the thermionic cathode operation are listed in Table 1. The available macro-pulse energies of KU-FEL measured at the user station #1 are shown in Fig. 2.

The shortest wavelength of KU-FEL (3.5 μm) is limited by the maximum available electron beam energy and the undulator period length which are 40 MeV and 33 mm, respectively. We can generate FEL with bit shorter wavelength by increasing available electron beam energy of the facility. The reason why the longest wavelength is

* This work was partially supported by the MEXT/JSPS KAKENHI Grant Number 26706026

[†] e-mail address zen@iae.kyoto-u.ac.jp

^{††} present affiliation Department of Physics and Materials Science, Faculty of Science, Chiang Mai University, Chiang Mai, Thailand

POLISH IN-KIND CONTRIBUTION TO EUROPEAN XFEL: STATUS IN SUMMER 2017*

J. A. Lorkiewicz[#], K. Chmielewski, Z. Golebiewski, W. C. Grabowski, K. Kosinski, K. Kostrzewa,
P. Krawczyk, I. M. Kudla, P. Markowski, K. Meissner, E. Plawski, M. Sitek, J. Szewinski,
M. Wojciechowski, Z. Wojciechowski, G. Wrochna,
National Centre for Nuclear Studies (NCBJ), 05-400 Otwock-Swierk, Poland
J. Sekutowicz, Deutsches Elektronen Synchrotron (DESY), 22-607 Hamburg, Germany
M. Duda, M. Jezabek, K. Kasprzak, A. Kotarba, K. Krzysik, M. Stodulski, M. Wiencek,
J. Swierblewski,
Institute of Nuclear Physics, Polish Academy of Sciences (IFJ PAN), 31-342, Krakow, Poland
P. Grzegory, G. Michalski, Kriosystem, 54-424 Wroclaw, Poland
P. Borowiec, Jagiellonian University, 30-392 Krakow, Poland
M. Chorowski, P. Duda, J. Fydrych¹, A. Iluk, K. Malcher, J. Polinski, E. Rusinski,
Wroclaw University of Science and Technology (WUST), 50-370 Wroclaw, Poland
J. Glowinkowski, M. Winkowski, P. Wilk, Wroclaw Technology Park, 54-424 Wroclaw, Poland
¹ also at European Spallation Source, 221 00 Lund, Sweden

Abstract

In the years 2010-2017 some of the Polish research institutes - members of the European-XFEL consortium, took responsibility for production and delivery of components, test infrastructure and procedures for the superconducting (sc) linear electron accelerator (LINAC) and PLC units of slow control system for the first experimental instruments of the European XFEL at DESY (Hamburg). The paper briefly summarizes the output of these works.

INTRODUCTION

European X-ray Free Electron Laser (Eu-XFEL) is dedicated to advanced studies of the structure of matter. It is based on a linear sc electron accelerator (LINAC) constructed by DESY (Deutsches Elektronen Synchrotron) and its partners of international XFEL consortium. The LINAC in its final version is composed of 97 modules. Each module contains 8 sc, nine-cell niobium cavities based on TESLA technology, placed in a liquid helium vessel and a single magnet package with a sc, super-ferric quadrupole magnet and two dipole magnets inside it [1]. The magnet packages are placed in liquid helium bath too. Every cavity is equipped with two high order mode (HOM) couplers. Parasitic high order modes (HOMs) in RF field are excited by e⁻ beam. They have to be coupled out by coaxial HOM couplers and sent

via cables to loads outside the module [1]. In addition a single beam line absorber (BLA) is installed in interconnectors between the modules to absorb the travelling HOMs. Each cavity is equipped with a pick-up (PU) antenna – a field probe in RF control system to regulate the amplitude and phase of the accelerating field. The activities of Polish groups which contributed in-kind to the project are briefly described below.

Wroclaw University of Science and Technology (WUST) was in charge of design and Wroclaw Technology Park (WPT) with its subcontractors were responsible for manufacturing and installation of a 165 m long XATL1 cryogenic transfer line for supercritical helium transport from the HERA refrigerator at DESY to Accelerator Module Test Facility (AMTF) hall and of two vertical cryostats for low power acceptance tests of cavities.

A group of National Centre for Nuclear Research (NCBJ) was in charge of design, production, testing and delivery of 1648 HOM couplers, 824 PU antennae with output lines and 108 HOM beam-line absorbers (BLAs).

A team of Institute of Nuclear Physics (IFJ-PAN, Krakow) was responsible for preparation and performance of acceptance tests for XFEL-type cavities, complete accelerator modules, sc magnets and their current leads.

Another group of NCBJ now contributes to the production of programmable logic controller (PLC) units for slow control system of the first experimental instruments to be installed at the ends of XFEL photon lines. The status of these tasks on the eve of XFEL facility startup is presented in the following sections.

*Supported by Polish Ministry of Science and Higher Education

[#]email address: jerzy.lorkiewicz@ncbj.gov.pl

FIRST OBSERVATION OF COHERENT THZ UNDULATOR RADIATION DRIVEN BY NSRRC HIGH BRIGHTNESS PHOTO-INJECTOR

M. C. Chou[#], K. T. Hsu, S. Y. Hsu, N. Y. Huang, C. S. Hwang, J. Y. Hwang, J. C. Jan,
 C. K. Kuan, W. K. Lau, A. P. Lee, C. C. Liang, G. H. Luo, I. C. Sheng
 NSRRC, Hsinchu, Taiwan
 Y. H. Wen, NTHU, Hsinchu, Taiwan

Abstract

Generation and characterization of coherent undulator radiation (CUR) in the THz region using the NSRRC S-band photo-injector linac system is achieved. The system consists of a laser-driven photocathode rf gun and one 5.2-m long S-band accelerating linac. Electron bunches in the linac can be accelerated and compressed simultaneously by velocity bunching. In this work, narrow-band tunable fully-coherent THz radiation can be produced from a U100 planar undulator when it is driven by a 100-pC electron bunch with effective bunch length of 90 fs. The experimental setup and the measurement of the power and the frequency spectrum of the coherent THz undulator radiation are reported.

INTRODUCTION

Terahertz (THz) radiation has recently attracted a lot of attention in the scientific applications, such as spectroscopy, imaging, communications and elementary excitations (e. g. excitation of phonons in solids). The THz frequency which is defined as 0.1 to 10 THz (wavelengths of 3 mm to 30 μm) covers the gap between microwaves and infrared light. Development of THz technologies is hindered by the so-called “THz-gap” which reflects the lack of THz sources in the electromagnetic wave spectrum. Over the past decade, the fruitful development of laser-based THz sources as well as nonlinear optics leads to a partial fill up of the THz-gap.

Accelerator-based THz radiation sources attract much attention in recent years [1, 2]. It is well-known that a relativistic electron beam emits temporal coherent synchrotron radiation when its bunch length is much shorter than the radiation wavelength [3]. For example, recalled that the wavelength of a 1 THz wave is 300 μm , a 100-fsec electron bunch can be used to generate coherent radiation in the THz regime such that the radiation intensity is proportional to the square of electron number in the bunch. Realization of a fully coherent THz light is possible if an ultrashort and simultaneously a low-emittance electron beam is available. For modern photo-injector, the beam transverse emittance is usually much smaller than that of the photon beam and therefore, radiation with excellent spatial coherence can be achieved.

A high brightness photo-injector equipped with a laser-driven photocathode rf gun and a 2998-MHz, 5.2-m-long

traveling-wave rf linac has been developed at NSRRC several years ago. In this report design of tunable narrow-band THz coherent undulator radiation (CUR) with this photoinjector and a 10-cm period length planar permanent magnet undulator (U100) has been studied. In addition, first observation of the THz CUR driven by this machine is also reported.

COHERENT UNDULATOR RADIATION

It is well known that relativistic electrons moving in a magnetic field emit synchrotron radiation as they are accelerated by the magnetic force which is always perpendicular to the electron orbits. Undulators can be used to produce synchrotron radiation with significantly higher brightness at narrow spectral bandwidth. Coherent synchrotron radiations (CSR) from bending magnets and undulators are possible as long as the bunch length is much shorter than the radiation wavelengths. When the electron beam emittance is smaller than the radiation photon emittance, a spatially coherent beam or diffraction limited radiation can be produced. Furthermore, a temporal coherent radiation can be achieved when the radiation fields from electrons that are randomly distributed in the bunch of length σ_t add up constructively when $c\sigma_t \leq \lambda$.

In general, the radiation spectrum of the electron bunch can be described as

$$\left. \frac{d^2W}{d\Omega d\omega} \right|_{\text{multi}} = \{N[1 - F(\omega)] + N^2F(\omega)\} \left. \frac{d^2W}{d\Omega d\omega} \right|_{\text{single}},$$

where N is the number of electrons in the bunch and $F(\omega)$ is the form factor which is the Fourier transform of

Table 1: Predicted Performance of THz CUR from U100

CUR from U100		
Electron charge	100 pC	100 pC
E-beam energy (MeV)	18.3 – 33.5	33.5
bunch length (fs, rms)	90 – 223	90
Undulator strength K	4.6	3.2 – 4.6
THz frequency (THz)	0.67 – 2.2	2.2 – 4.3
Bandwidth	5.6%	5.6%
THz pulse energy (μJ)	0.5 – 2.7	0.1 – 2.7
Repetition rate (Hz)	10	10
Average power (μW)	5 – 27	1 – 27
Peak power (MW)	0.02 – 0.32	0.02 – 0.32

[#]chou.mc@nsrc.org.tw

HIGH SPECTRAL DENSITY COMPTON BACK-SCATTERED GAMMA-RAY SOURCES AT FERMILAB *

D. Mihalcea¹, B. Jacobson², A. Khizhanok³, A. Murokh², P. Piot^{1,4}, and J. Ruan⁴

¹ Department of Physics and Northern Illinois Center for Accelerator & Detector Development, Northern Illinois University, DeKalb, USA

² Radiabeam Technologies, Santa Monica, USA

³ Department of Mechanical Engineering, Northern Illinois University, DeKalb, USA

⁴ Fermi National Accelerator Laboratory, Batavia, USA

Abstract

A ~ 1.2 MeV gamma-ray source is planned to be built at Fermilab following the completion of the ~ 300 MeV superconducting linac. The high energy photons are back-scattered from the interactions between electrons and high intensity IR laser pulses. In this contribution we discuss some of the experiment design challenges and evaluate the performances of the *gamma*-ray source. We expect the peak brilliance to be of the order of 10^{23} photons/[s-(mm mrad)² 0.1% BW] and the spectral density of the radiation in excess of 2×10^5 photons/s/eV.

INTRODUCTION

Gamma-ray sources are extensively used in various fields from biomedical and fundamental research applications to industry and national defense. The required performances of the γ -ray sources are dictated by the application, but for most cases, large values of peak brightness, photon flux, and a small energy bandwidth are desired. Typically, high precision experiments would require high brightness sources and others, like biomedical and industrial applications, would mostly benefit from higher beam fluxes.

Gamma-ray sources consisting of back-scattered radiation resulting during the collisions of energetic electrons and laser pulses [1], process also known as Inverse Compton Scattering (ICS), became attractive due to the progress in producing high quality GeV-class electron beams and very high intensity lasers. The size and the cost of these γ -sources are mostly driven by the electron beam accelerator. Recent progress in the field of laser plasma wakefield accelerators (LPWA) [2] made possible building compact γ -ray sources with very high brightness [3, 4] but with relatively low photon flux due to the low operating frequency (~ 10 Hz). To overcome this problem our approach is to use the superconducting 300 MeV Fermilab injector to be built at FAST facility, which can deliver up to 15,000 electron pulses per second.

In this paper we present the design of the proposed γ -ray source and the expected performances based on simulations.

* This work was sponsored by the DNDO award 2015-DN-077-ARI094 to Northern Illinois University. Fermilab is operated by Fermi Research Alliance, LLC, for the U.S. Department of Energy under contract DE-AC02-07CH11359.

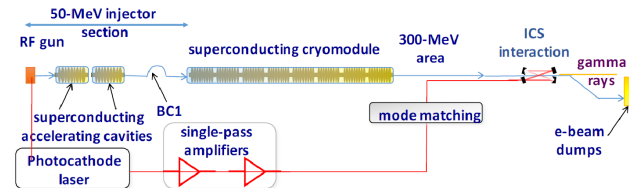


Figure 1: Linac layout at FAST facility.

ICS EXPERIMENT SETUP

The most relevant components of the FAST linac are shown in Fig. 1. The electrons are extracted by photoemission from a CsTe₂ cathode illuminated with picosecond long UV laser pulses. The acceleration is performed by a normal conducting RF gun, two superconducting TESLA cavities and a superconducting cryomodule consisting of eight TESLA cavities. The operating RF frequency is 1.3 GHz the final electron energy is up to 300 MeV and the charge of each electron pulse is up to 5 nC. More details about the linac and beam dynamics simulations can be found in Refs. [5, 6]. The low energy section of the linac, consisting of the gun and the two booster cavities, was successfully tested in the summer of 2016 and the full completion, testing and some experiments are expected to take place in the summer of 2017.

The laser system, already functional, can produce up to $10 \mu\text{J}$ IR pulses at 3 MHz sampling rate. The IR laser pulses are split in two components: the first component contains about 10% of the total energy and it is sent to the photocathode via two stages of frequency doubling crystals. The second component is further amplified to about 0.5 mJ/pulse and sent to the ICS experimental area. Up to five equally spaced RF macropulses are generated each second. The duration of each macropulse is 1 ms and trains of about 3,000 electron bunches can be emitted during this time.

The LINAC components most relevant for this experiment are those used for the final focus of the electron beam. Thirty centimeters upstream of the interaction point (IP) there are three permanent magnetic quadrupoles (PMQs) (Fig. 2) manufactured by Radiabeam. They are hollow cylinders with outer radius 15 mm, inner radius 4 mm and lengths 3 cm, 6 cm, and 3 cm respectively. The spacing between them is 5 cm. The lens strengths of the PMQs in the preliminary design are -150 m^{-1} , 150 m^{-1} and -150 m^{-1} . Symmetrically, there are three more identical PMQs downstream of

Content from this work may be used under the terms of the CC BY 3.0 licence (© 2018). Any distribution of this work must maintain attribution to the author(s), title of the work, publisher, and DOI.

CLARA FACILITY LAYOUT AND FEL SCHEMES

D. J. Dunning* on behalf of the CLARA team
STFC Daresbury Laboratory and Cockcroft Institute, Daresbury, UK

Abstract

CLARA is a new FEL test facility being developed at STFC Daresbury Laboratory in the UK. Commissioning has started on the front-end (photo-injector and first linac) while the design of the later stages is still being finalised. We present the latest design work, focusing on the layout and specification of components in and around the undulator sections. We give an overview of the design and modelling of the FEL schemes planned to be tested.

INTRODUCTION

The UK is constructing a new FEL test facility called CLARA [1] which will be a dedicated accelerator R&D facility focused around demonstrating FEL schemes that can be applied to enhance the capabilities of X-ray FEL facilities - including a potential UK XFEL [2]. It will operate with 250 MeV maximum energy and $\lambda_r=100\text{-}400$ nm fundamental FEL wavelength (see Fig. 1 for layout). The front end (up to 50 MeV) is being commissioned and the second phase (up to 150 MeV) is being assembled while design of the later stages continues - aiming for FEL lasing in 2022.

While CLARA will serve as a test-bed for various accelerator technologies, the focus of this paper is on the FEL schemes and the implications for the layout of the FEL section. The design of the FEL section will be finalised in September 2017 prior to initiating purchasing of the undulators. The main aims dictating design choices for the CLARA FEL section are:

- To demonstrate novel FEL capabilities that could be applied at X-ray FEL facilities, specifically ultra-short pulses, improved pulse quality, stability and synchronisation. For ultra-short pulses the aim is for pulse durations in the 1-100 fs range, which would correspond to 1-100 as when translated from the 100 nm minimum wavelength of CLARA to ~ 0.1 nm facilities.
- To gain experience with schemes for a future UK XFEL including those already demonstrated elsewhere.
- To produce a flexible design that can accommodate new ideas and future upgrades.

Given the above we aim to keep the focus on energy/wavelength-independent aspects of the FEL concepts and so minimise energy/wavelength-specific difficulties so far as possible. Key drivers for the wavelength choice were therefore the availability of single-shot diagnostic techniques for the characterisation of the output and availability of suitable seed sources for interacting with the electron beam. To suit single-shot temporal diagnostics it is proposed to study short pulse generation for FEL wavelengths in the range 250-400 nm, where suitable

non-linear materials are available. For schemes requiring only spectral characterisation the operating wavelength range will be 100-266 nm. While it was previously planned to use seed/modulating laser sources throughout the range from 800 nm-100 μm [1], on further consideration it is more straightforward (i.e. requires less laser R&D) to avoid the range from $20 \mu\text{m} \lesssim \lambda_{\text{mod}} \lesssim 70 \mu\text{m}$ and to cluster FEL schemes around a few select wavelengths.

FEL SCHEMES

The CLARA FEL team maintains an ongoing review of FEL schemes that have been proposed and demonstrated worldwide and assesses their compatibility with the aims and layout of CLARA. Some of these are listed below, categorised into what is foreseen to be the initial/major CLARA projects and others that impact the layout through maintaining as options of high interest.

Initial Projects

Schemes under consideration for the early stages of CLARA are those that are expected to be relatively less demanding at least in not requiring external laser modulation or synchronisation. This includes single-spike SASE [3], tapering (assessed for CLARA in [4]), two-colour schemes via undulator tuning and testing novel undulator technology [5] in a designated afterburner section.

Major Projects

These are listed in a potential running order where elements of the layout would be introduced incrementally:

High-brightness SASE The high-brightness SASE scheme [6] employs chicanes between undulator modules to increase the slippage of the radiation relative to the electron bunch and so improve the temporal coherence of the emitted radiation pulse. In simulations the scheme has been shown to perform more effectively for undulator modules shorter than the FEL gain length. It requires no laser seeding/modulation.

Mode-locked FEL The mode-locked FEL concept [7] uses chicane delays between undulator sections to allow pulses with duration much shorter than the FEL co-operation length, $l_c = \lambda_r/4\pi\rho$ (where the FEL parameter $\rho \approx 10^{-4} - 10^{-3}$), which is a lower limit for many schemes. The number of cycles per pulse can be reduced from hundreds to approximately the number of periods in an undulator module, N . For demonstration on CLARA the number of periods per undulator module should therefore be minimised, without negatively impacting other schemes: this has been set to 27 periods. While preliminary results could be achieved

* david.dunning@stfc.ac.uk

SCLF: AN 8-GEV CW SCRF LINAC-BASED X-RAY FEL FACILITY IN SHANGHAI

Z.Y. Zhu¹, Z.T. Zhao^{2†}, D. Wang², Z. Liu¹, R.X. Li³, L.X. Yin² and Z.H. Yang² for the SCLF Team

¹ShanghaiTech University, Shanghai 201210, China

²Shanghai Institute of Applied Physics, CAS, Shanghai 201800, China

³Shanghai Institute of Optics and Fine Mechanics, CAS, Shanghai 201800, China

Abstract

The Shanghai Coherent Light Facility (SCLF) is a newly proposed high repetition-rate X-ray FEL facility, based on an 8-GeV CW superconducting RF linac. It will be located at Zhangjiang High-tech Park, close to the SSRF campus in Shanghai, at the depth of ~38m underground and with a total length of 3.1 km. Using 3 phase-I undulator lines, the SCLF aims at generating X-rays between 0.4 and 25 keV at rates up to 1MHz. This paper describes the design concepts of this hard X-ray user facility.

INTRODUCTION

We are currently witnessing a rapid progress in X-ray free electron laser (XFEL) development across the globe, among which the superconducting RF (SCRF) linac based high-repetition-rate XFELs are leading ones. European XFEL [1] achieved its first lasing in early May 2017, and started operational phase in early July 2017. The LCLS-II [2] construction is now under way, and is scheduled to become operational in 2020. An energy upgrade proposal to LCLS-II, the LCLS-II-HE project, has also been initiated [3]. Considering this international context, and in response to the rapidly growing demands from Chinese science community on the high peak and high average brightness X-ray sources, and the needs from Zhangjiang Comprehensive National Science Center in Shanghai, a high repetition-rate XFEL, the Shanghai Coherent Light Facility (SCLF), was proposed.

SCRF linac. As shown in Fig. 1, it will be located at the Zhangjiang High-tech Park of Shanghai Pudong, closely connected to the campuses of the Shanghai Synchrotron Radiation Facility, the Shanghai Advanced Research Institute and the ShanghaiTech University. The SCLF major facility will be installed in the tunnels at the depth of ~38m underground and with a maximum length of 3.1 km.

The SCLF will have five shafts, one accelerator tunnel and three parallel undulator tunnels and the following three beamline tunnels, with each undulator tunnel capable to accommodate two undulator lines. In its initial phase, the SCLF consists of an 8 GeV CW SCRF linac, three undulator lines, three following FEL beamlines, and ten experimental end-stations. The end-stations are distributed in the near experimental hall (NEH) in Shaft 4 and the far experimental hall (FEH) in Shaft 5. The initial three undulator lines will be located in two undulator tunnels. Using these three undulator lines, the SCLF aims at generating brilliant X-rays between 0.4 and 25 keV at pulse repetition rates up to 1 MHz.

The proposed SCLF project is planned to start its civil construction within one year immediately after its preliminary design report is approved by the central government. The whole SCLF project is expected to be completed in 7 years, and then the user experiments can start right after the completion of the beamline and experimental station commissioning.

MACHINE LAYOUT AND MAIN PARAMETERS

Figure 2 shows the layout of the SCLF. The SCLF accelerator complex comprises the following two parts: a photo-injector which generates a bright electron beam with repetition rate up to 1 MHz and accelerates it to ~100 MeV; The main SCRF linear accelerator, where the electron beam is accelerated to about 8 GeV and longitudinally compressed to about 1.5 kA with two compressors working at energies of 270MeV and 2.1GeV respectively.

The photo-injector is based on the VHF photocathode gun similar to that developed at LBNL [4]. On the basis of LCLS-II experience, the design draws heavily to produce a 10ps (FWHM) long pulse with 100 pC bunch charge and a RMS normalized transverse emittance of 0.4 mm-mrad at 90-120 MeV. The bunch repetition rate is designed up to 1 MHz during the operation. The SCLF injector includes a 216 MHz photocathode VHF gun, a 1.3 GHz buncher, a 1.3 GHz single 9-cell cavity cryomodule, a 1.3 GHz eight 9-cell cavities standard cryomodule, a laser heater, and the beam diagnostics. A laser heater system is employed to

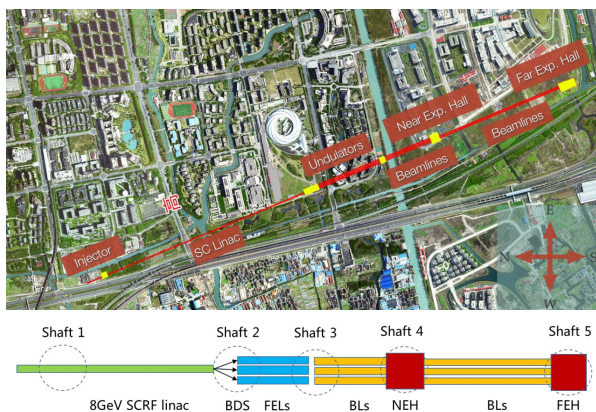


Figure 1: Aerial view of the SCLF project.

This proposal was officially approved by the central government of China in April 2017. The SCLF is an X-ray FEL facility based on an 8 GeV continuous-wave (CW)

† zhaozt@sinap.ac.cn

Content from this work may be used under the terms of the CC BY 3.0 licence (© 2018). Any distribution of this work must maintain attribution to the author(s), title of the work, publisher, and DOI.

DESIGN OF APPARATUS FOR A HIGH-POWER-DENSITY DIAMOND IRRADIATION ENDURANCE EXPERIMENT FOR XFEL APPLICATIONS

S. P. Kearney*, D. Shu, T. Kolodziej, K.-J. Kim, R. Lindberg, S. Stoupin†, D. A. Walko, J. Wang, Y. Shvyd'ko, Argonne National Laboratory, Lemont, IL 60439, USA

Abstract

We have designed apparatus for an irradiation setup capable of achieving greater than 10 kW/mm^2 power density of x-rays on a diamond single crystal under ultra-high-vacuum conditions. The setup was installed at the 7-ID-B beamline at the Advanced Photon Source (APS) for an irradiation experiment, demonstrating the capability of diamond to endure x-ray free electron laser oscillator (XFEL) levels of irradiation ($\geq 10 \text{ kW/mm}^2$) without degradation of Bragg reflectivity [1]. Focused white beam irradiation ($50 \mu\text{m} \times 20 \mu\text{m}$ spot size at 12.5 kW/mm^2 power density) of a diamond single crystal was conducted for varying durations of time at different spots on the diamond in a vacuum environment of 1×10^{-8} Torr and an additional irradiation spot in a “spoiled” vacuum environment of 4×10^{-6} Torr. Here we present the apparatus used to irradiate the diamond consisting of multiple subassemblies: the fixed masks, focusing optics, gold-coated UHV irradiation chamber, water-cooled diamond holder, chamber positioning stages (with sub-micron resolution), and the scattering detector.

DIAMOND IRRADIATION APPARATUS

A type IIa single crystal diamond in the [100] orientation was irradiated with focused white beam x-rays ($50 \mu\text{m} \times 20 \mu\text{m}$ spot size at 12.5 kW/mm^2 power density) to demonstrate the capability of diamond to endure XFEL levels ($\geq 10 \text{ kW/mm}^2$) of irradiation without degradation of Bragg reflectivity [1]. The diamond was irradiated at different spots on the diamond for varying durations and environments, which required scanning stages. In addition, two vacuum environments were tested, 1×10^{-8} Torr and a single irradiation spot with a “spoiled” vacuum environment of 4×10^{-6} Torr.

Figure 1(a) shows the entire apparatus, which was temporarily installed at the 7-ID-B beamline at the Advanced Photon Source (APS) [2]. The main components of the apparatus are identified in Fig. 1(a) and will be discussed in detail. Figure 1(b) is a diagram of the entire beamline layout showing the distances of the main components from the x-ray source.

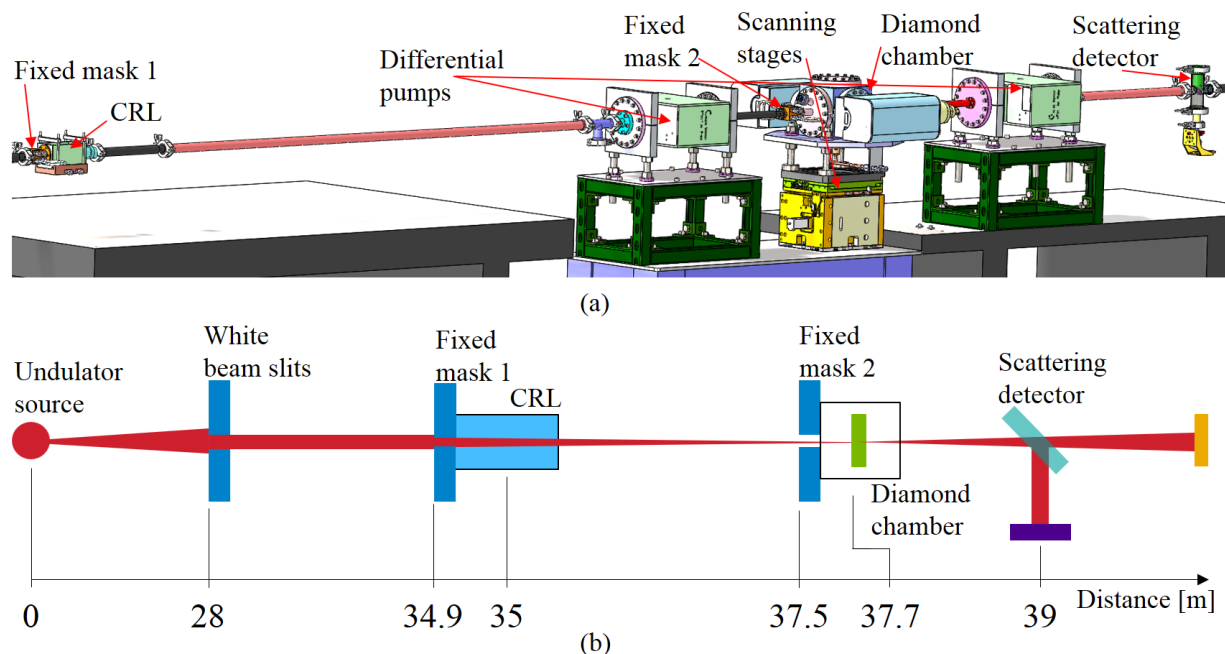


Figure 1: (a) Model of the diamond irradiation apparatus. The beam direction is from left to right and the main components are identified. (b) Diagram of the setup showing the distances from the source of the main components.

* skearney@aps.anl.gov

† Now at Cornell High Energy Synchrotron Source, Cornell University, Ithaca, NY 14853, U.S.A.

SYNCHRONIZED MID-INFRARED PULSES AT THE FRITZ HABER INSTITUTE IR-FEL

R. Kießling, S. Gewinner, W. Schöllkopf, M. Wolf, A. Paarmann
Fritz-Haber-Institut der Max-Planck-Gesellschaft, Berlin, Germany

Abstract

The combined application of FEL radiation and femtosecond table-top lasers for two-color spectroscopy demands an accurate pulse synchronization. In order to employ the infrared FEL at the Fritz Haber Institute for non-linear and time-resolved experiments, an RF-over-fiber-based timing system has been established. Using a balanced optical cross-correlation scheme, we determined an FEL micro-pulse timing jitter of 100 - 200 fs (rms). The long-term timing drift was found to be well correlated to the energy fluctuations of the accelerated electron bunches.

By means of sum-frequency generation cross-correlation, we directly measure the FEL pulse shape at different cavity detunings. For large cavity detuning, narrowband IR radiation ($\sim 0.3\%$ FWHM) can be generated and utilized for high-resolution non-linear spectroscopy. On the other hand, sub-picosecond pulses are provided at small detuning, which are well-suited for time-resolved measurements. At intermediate detuning values, we observe the build-up and dynamics of multipulses that result in the well-known limit-cycle power oscillations.

INTRODUCTION

Vibrational excitations are a fundamental property of molecules, clusters and solids and therefore contain material-specific information. Modes of vibrations carry kinetic energy of few meV, consequently optical excitation demands infrared (IR) wavelengths. Since its first demonstration, free-electron lasers are an ideal tool for infrared spectroscopy due to the frequency-tunable narrow-bandwidth radiation output. So far, the infrared FEL at the Fritz Haber Institute (FHI) has been used to investigate (static) vibrational spectra of gas-phase ions, bio-molecules, metal-clusters and polar dielectrics. Further investigations will employ the intense FEL IR radiation also for non-linear and time-resolved two-color spectroscopy experiments. To that end, an accurate synchronization of FEL and table-top laser pulses is required for sub-ps resolved measurements. In the following, the concept, timing stability and first application of the synchronized laser system is presented.

EXPERIMENTAL SYSTEM

Free-Electron Laser

Since the start of user operation in 2013, the mid-IR free-electron laser oscillator at the FHI provides intense, pulsed radiation in the wavelength region from 3 to 50 μm [1]. The electron bunches emitted from a thermionic cathode are accelerated by two subsequent normal-conducting linacs to

kinetic energies between 15 and 50 MeV, depending on the desired IR spectral range. The master oscillator (MO), an 2.99 GHz RF source, drives the electron gun at the third sub-harmonic, producing few-ps short micro-bunches of 1 GHz repetition rate within $\sim 10\ \mu\text{s}$ long macro-bunches at a 10 Hz rate. The following electron wiggling in a planar hybrid-magnet undulator with parameter $K = 0.5 - 1.6$ generates linearly polarized, ps-long IR pulses with a gap-scan tunable wavelength. Besides a 1 GHz micro-pulse rate, reduced repetition modes of 27.8 MHz and 55.5 MHz are available that are required for time-resolved studies. Adjustment of the optical cavity length is an additional degree of freedom to set the spectrum bandwidth as low as 0.3 %.

Synchronization Setup

As table-top laser we employ a high-power Terbium-doped fiber oscillator (FO) providing ~ 100 fs, near-infrared ($\lambda = 1055$ nm) pulses with up to 50 nJ pulse energy. The repetition rate of 55.5 MHz is matched to a reduced electron micro-bunch rate, corresponding to two FEL pulses circulating in the 5.4 m long FEL cavity simultaneously. For high-precision synchronization, the MO signal of 2.99 GHz is distributed from the FEL vault to the user lab via a stabilized RF-over-fiber link approximately 100 m long. This reference clock transfer system is a low-jitter (rms < 7 fs [10 Hz-10 MHz]) and low-drift (< 40 fs/day) RF transmission turn-key solution utilizing optical fiber connections [2].

The FO is locked to the MO using the 54th harmonic of the table-top laser output. Adjustment of the FO repetition-rate is done by temperature control of the fiber cage for coarse tuning and a piezo motor for fine setting of the fiber cavity length. In order to manage multiple synchronized situations due to phase-locking of the table-top laser to a higher frequency reference clock, a phase-shifter of the 2.99 GHz signal is added using the photodiode signal of the FO and a separately fiber-link transferred 55.5 MHz RF signal from the FEL machine (superperiod-lock). The shifter is used to adjust the temporal overlap of the optical pulses in the experimental setup. The fiber cables of the synchronization system going along the beamline from the FEL vault to the user lab are subject to ambient temperature and humidity fluctuations, which are compensated by the system.

Balanced Optical Cross-Correlation

Characterization of the synchronization stability of the FEL-table-top laser system is performed by two-color balanced optical cross-correlation (BOC) [3]. Utilizing a non-linear crystal (GaSe) for sum-frequency generation (SFG), the FEL and fiber oscillator pulses are overlapped twice within the same crystal, but with slightly different temporal

X-RAY REGENERATIVE AMPLIFIER FREE-ELECTRON LASER CONCEPTS FOR LCLS-II

G. Marcus, Y. Ding, J. Duris, Y. Feng, Z. Huang, J. Krzywinski, T. Maxwell, D. Ratner,
T. Raubenheimer, SLAC, Menlo Park, USA
K.-J. Kim, R. Lindberg, Y. Shvyd'ko, ANL, Argonne, USA
D. Nguyen, LANL, Los Alamos, USA

Abstract

High brightness electron beams that will drive the next generation of high repetition rate X-ray FELs allow for the possibility of optical cavity based feedback. One such cavity based FEL concept is the Regenerative Amplifier Free-Electron Laser (RAFEL). This paper examines the design and performance of possible RAFEL configurations for LCLS-II. The results are primarily based on high-fidelity numerical particle simulations that show the production of high brightness, high average power, fully coherent, and stable X-ray pulses at LCLS-II using both the fundamental and harmonic FEL interactions.

INTRODUCTION

XFELs such as the LCLS, based primarily on Self-Amplified Spontaneous Emission (SASE), are capable of producing extremely bright, transversally coherent, ultra-short pulses suitable for the investigation of ultra-fast chemical and physical processes that operate on the time and length scales of atomic and molecular motion [1, 2]. A characteristic feature of single-pass SASE FELs, however, is poor longitudinal coherence, which results from the initial amplification of incoherent radiation shot-noise [3, 4]. Improvement of the longitudinal coherence is of great practical importance and has been the subject of many recent investigations. Longitudinal coherence can be obtained by seeding the FEL amplifier with sufficiently narrow bandwidth radiation well above the effective shot noise power in the electron beam. Examples of this include self-seeding [5], which has been successfully implemented at LCLS in both the hard [6] and soft X-ray [7] spectral regimes and externally seeded schemes, which are currently being vetted as possible upgrade paths for LCLS-II soft X-rays [8]. Self-seeding, however, nominally suffers from low seed power in an attempt to preserve the electron beam properties important for lasing and is fundamentally still dependent on the noisy SASE process leading to large (100%) seed power fluctuations. External seeding necessarily requires high-harmonic conversions that have inherent challenges [9]. The RAFEL concept, studied here, offers an alternative pathway to the production of stable, fully coherent, high brightness, and high average power X-ray radiation.

Similar to an XFEL oscillator [10], a RAFEL consists of a high repetition rate electron beam, a short undulator and an X-ray crystal cavity (in the case of hard X-rays) to provide optical feedback (see, for example, Fig. 1). However, unlike an oscillator, which operates as a low-gain FEL in a

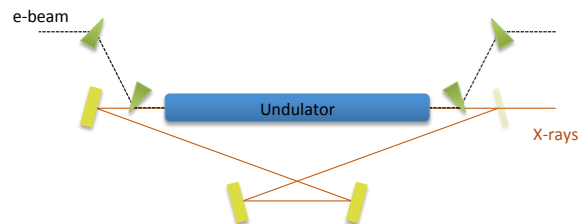


Figure 1: RAFEL concept where the X-ray cavity is wrapped around the entire undulator.

low output coupling cavity, the RAFEL is a high-gain FEL that reaches saturation in only a few round trips in a high output coupling cavity. The RAFEL concept exhibits many additional distinct advantages over an oscillator when considering challenges associated with potential cavity design. The high-gain FEL should be less sensitive to X-ray induced cavity optics degradation and the small number of cavity passes should relax the longitudinal alignment tolerances relative to what is expected with an oscillator cavity. In addition, the RAFEL cavity does not serve the function of defining the transverse radiation mode since the dominant amplified mode is gain guided. This substantially relaxes the cavity opto-mechanical stability and crystal positioning requirements. The main responsibility of the cavity is to recirculate the radiation, which, in turn, seeds successive electron bunches. This optical feedback also allows for a reduced undulator length relative to SASE and can ultimately produce longitudinally coherent X-ray pulses close to the Fourier Transform limit.

This paper reports the results of preliminary RAFEL studies within the context of the LCLS-II project. Numerical particle simulations using the FEL code GENESIS [11] are used to explore, in an ideal sense, possible RAFEL performance at LCLS-II in both the soft and hard X-ray spectral regimes. Results from lasing at both the fundamental FEL resonance wavelength as well as harmonics, using harmonic lasing [12–14], are presented.

SIMULATION STRATEGY

The high repetition rate LCLS-II FEL has been thoroughly studied and the challenges associated with generating, accelerating, and transporting high brightness electron beams to the undulators are well understood and documented (e.g. see [15–17] and references therein). Global optimizations of the electron beam delivery system and SASE FEL performance for charge distributions that span the planned opera-

X-RAY FEL OSCILLATOR SEEDED HARMONIC AMPLIFIER FOR HIGH ENERGY PHOTONS

W. Qin*, IHIP, Peking University, Beijing 100871, China
K.-J. Kim, R. R. Lindberg, ANL, Argonne, IL 60439, USA
J. Wu, SLAC, Menlo Park, CA 94025, USA

Abstract

High power, high energy X-ray pulses in the range of several tens of keV have important applications for material sciences. The unique feature of an X-ray FEL Oscillator (XFEL) makes it possible to seed a harmonic amplifier to produce such high energy photons. In this paper, we present simulation studies using 14.4-keV output pulses from an XFEL to generate harmonics at 43.2 keV (third harmonic) and 57.6 keV (fourth harmonic). Techniques such as undulator tapering and fresh bunch lasing are considered to improve the amplifier performance.

INTRODUCTION

High power, high energy hard X-ray free-electron lasers (XFELs) have important applications for exploring the dynamic properties of materials under extreme conditions. Generation of such high energy photons can be realized using conventional self-amplified spontaneous emission (SASE) [1, 2] scheme and advanced harmonic lasing [3] and fresh-slice technique [4] to improve the performance. An alternative way is to use the proposed XFEL [5], which successively amplifies X-ray pulse trapped in a low loss cavity, to produce coherent, stable hard X-ray as the seed for a high gain harmonic generation (HGHG) [6] type FEL, which is possible to generate stable pulses with high intensity and narrow bandwidth. This concept was studied for third harmonic of 14-keV XFEL and fourth harmonic of 15-keV XFEL using ideal beam [7, 8] for the Matter-Radiation Interactions in Extremes (MaRIE) [9]. Here we use the output from a start-to-end simulated 14.4-keV XFEL operating in fundamental mode [10] to investigate the harmonic performance at third harmonic (43.2 keV) and fourth harmonic (57.6 keV).

LAYOUT

The layout of the proposed scheme is illustrated in Fig. 1, where two photoinjectors are used to generate high brightness interleaved electron bunches for the XFEL and the harmonic amplifier, respectively. Electron beams are kicked from the linac at 8 GeV into the XFEL to generate a 14.4-keV seed. With a proper delay, the seed is sent into a modulator to modulate the 12-GeV, 3.4-kA electron beam. The energy modulation can be converted to density modulation via a small magnetic chicane or a detuned undulator. In a subsequent radiator tuned at third or fourth harmonic of

the modulation wavelength, high energy photons are emitted. Fresh bunch technique, where a fresh electron bunch is delayed to interact with the FEL radiation generated in the first part of the radiator, is used to reduce the effect of the increased energy spread after modulation on the FEL performance. The fresh bunch can be provided by accelerating two bunches in one RF bucket, as in Ref. [11], and the delay between two bunches is tens of femtosecond, which can be reached using a small magnetic chicane. Although the XFEL pulse is much longer than the delay of the two bunches, one of the two bunches can be tuned to off resonant in the modulator through energy difference between the two bunches due to wakefields, so that one bunch is modulated and the other remains fresh. Bunch charge is 100 pC for all cases. Normalized emittance is 0.2 μm for 12-GeV ideal Gaussian beam. For the XFEL simulation, the emittance is 0.25 μm . More machine parameters used in this study are listed in Table 1.

Table 1: Electron beam and FEL parameters. Bunch charge is 100 pC for all cases. Normalized emittance is 0.2 μm for 12 GeV ideal Gaussian beam. For the XFEL simulation, the emittance is 0.25 μm .

Parameter	XFEL	Mod.	43.2 keV	57.6 keV
FEL K	1.48	2.79	1.44	1.03
E_b [GeV]	8	12	12	12
I_{pk} [A]	120	3400	3400	3400
σ_s [fs]	317	12.5	12.5	12.5
σ_E [MeV]	0.2	1.8	1.8	1.8
λ_u [cm]	2	1.94	1.55	1.55
L_u [m]	20	8	70	70
harmonic	1	1	3	4

THE XFEL

The XFEL uses high reflectivity, narrow spectral bandwidth crystals as mirrors for the X-ray pulses. In this study we adopt the four crystal configuration as proposed in Ref. [12] to allow for wavelength tunability and C(733) is used for 14.4-keV radiation. GINGER [13] simulation is conducted to evaluate the XFEL performance, with its temporal profile and spectrum shown in Fig. 2. The power of the XFEL output reaches about 37 MW after saturation and the FWHM bandwidth is about 3.4 meV, which is two orders narrower than hard X-ray self-seeding machine.

* qinweilun@pku.edu.cn, also at SLAC.

AN EXPERIMENTAL SETUP FOR PROBING THE THERMAL PROPERTIES OF DIAMOND REGARDING ITS USE IN AN XFELO*

C. P. Maag, I. Bahns, J. Rossbach, P. Thiessen[†], Universität Hamburg, Hamburg, Germany
H. Sinn, European XFEL GmbH, Hamburg, Germany
J. Zemella, Deutsches Elektronen Synchrotron (DESY), Hamburg, Germany

Abstract

This work presents an optical pump-probe setup for measuring the thermal evolution of diamond crystals at cryogenic temperatures under the heat load conditions of an X-ray free-electron laser oscillator (XFELO). As an XFELO is based on a cavity using diamond Bragg reflectors and these reflectors are subjected to intense heat loads during operation, the correct understanding of the thermal evolution in diamond plays a major role in the correct modeling of an XFELO. *Stoupin et al.* [1] did a room temperature x-ray diffraction measurement on the nanosecond transient thermal response of diamond to an optical pulse. The measurements presented in this paper for the first time incorporate effects due to the very short penetration depth of only a few μm of an XFELO pulse in combination with the high mean free path in diamond at cryogenic temperatures. While at room temperature the heat equation based on Fourier's law accurately fits the measured results, this vastly changes due to the onset of ballistic processes at cryogenic temperatures. These changes, which are hard to predict theoretically, show the necessity of measurements of the thermal evolution in diamond with special regard to a correct mimicking of the heat load in an XFELO.

INTRODUCTION

Current hard X-ray free-electron laser (FEL) facilities all use the self-amplified spontaneous emission (SASE) scheme for operation. While these sources produce very brilliant femtosecond X-ray pulses with excellent transverse coherence, they suffer from a lack of longitudinal coherence. A promising approach for reaching full longitudinal coherence in the hard X-ray regime proposed by *Kim et al.* in 2008 [2] is the X-ray free-electron-laser oscillator (XFELO). This scheme is based on using a rather short undulator with a length of less than 15 m and a highly reflective cavity based on very pure diamond crystals serving as Bragg reflectors. As these Bragg reflectors also act as spectral filters an XFELO promises a spectral bandwidth in the order of the crystals bandwidth ($\Delta\omega/\omega \approx 10^{-5} - 10^{-7}$) and therefore orders of magnitude better than SASE-FELs. Furthermore, as the radiation field is built up over many cavity round trips, very low shot-to-shot fluctuations can be expected, even making the XFELO a promising candidate for X-ray quantum optics (XQO) [3]. With the recently commissioned European XFEL the realization of an XFELO becomes in reach. This is due to the facility's excellent electron beam

properties and especially due to its very high bunch repetition rate of 4.5 MHz in pulsed-mode [4] which enables resonator lengths of only 33 m.

A major issue one needs to address when dealing with an XFELO is the effect of the light-matter interaction between the X-ray field and the Bragg reflectors. This is due to the high requirements for the angular and spatial stability [5,6] as well as the necessity of very stable Bragg conditions.

As shown by *Zemella et al.* in 2012 [7] even an XFELO with a designedly limited saturated pulse energy of $\approx 250 \mu\text{J}$ circulating with a rate of 4.5 MHz leads to a considerable heating of the Bragg reflectors and thereby to their thermal expansion. This thermal expansion may lead to vibrations of the crystal, change of the wavelength satisfying the Bragg's law [7] and the generation of ultrasonic pulses [1,8]. The last effect is studied by *Bahns et al.* [9] also at this conference.

Owing to the importance of keeping these effects as low as possible, it has already been concluded that diamond at cryogenic temperatures is the ideal candidate for an XFELO [10,11], due to its very high thermal conductivity, its low thermal expansion coefficient as well as high radiation hardness and a Bragg reflectivity over 99%. Nonetheless, even with diamond at 50 K, heating of the crystals does not seem negligible [7]. Consequently, in order to properly predict the behavior of an XFELO at the European XFEL and the effect of the thermal load, the diamond reflectors' thermal response need to be understood and especially measured as will be shown in the following. Our approach is to mimic an XFELO by a UV laser which deposits roughly the same energy into a diamond crystal at the same penetration depth as an saturated XFELO pulse. Such an experimental setup is presented in this work.

QUASI-BALLISTIC HEAT TRANSPORT

As discussed above, diamond is the ideal candidate for Bragg reflectors in an XFELO. However, when treating thermally highly conductive materials, especially at low temperatures where the phonon-phonon Umklapp scattering is freezing out, one has to take into account size effects which lower the predictive power of the heat equation based on Fourier's law. The latter is based on the assumptions of local thermal equilibrium and time- and length scales of interest larger than the typical scattering time or mean free path of a phonon, respectively. As the mean free path in diamond is of the order of hundreds of microns at $T = 50 \text{ K}$ and still of the order of tens of microns at $T = 100 \text{ K}$, these assumptions begin to fail and size dependent ballistic processes begin to occur.

* Work supported by BMBF (FKZ 05K13GU4 + FKZ 05K16GU4)

[†] patrick.thiessen@desy.de

FREE ELECTRON LASERS IN 2017

P. J. Neyman*, W. B. Colson, S. C. Gottshalk, A. M. M. Todd
Compass Scientific Engineering, Fremont CA 94539 USA

J. Blau, K. Cohn

Physics Department, Naval Postgraduate School, Monterey CA 93943 USA

Abstract

Forty-one years after the first operation of the free electron laser (FEL) at Stanford University, there continue to be many important experiments, proposed experiments, and user facilities around the world. Properties of operating and proposed FELs in the terahertz (THz), infrared (IR), visible, ultraviolet (UV), and X-ray regimes are tabulated and discussed.

LIST OF FELS IN 2017

The following tables list existing (Tables 1 and 2) and proposed (Tables 3 and 4) relativistic free electron lasers (FELs) in 2017. Some FELs in Tables 1 and 2 may not be currently operating, but are still included until we have been notified they are decommissioned. Tables 2 and 4, denoted as “Short Wavelength”, contain FELs that are designed to operate in the UV and X-ray regimes (400-nm or shorter wavelength), while Tables 1 and 3, denoted as “Long Wavelength”, contain all other FELs. The first column lists a location or institution, and the FEL’s name in parentheses. References are listed in Tables 5 and 6; another useful reference is the following website: http://sbfel3.ucsb.edu/www/v1_fel.html.

The second column of each table lists the operating wavelength λ , or wavelength range. The longer wavelength FELs are listed at the top and the shorter wavelength FELs at the bottom of each table. The seven orders of magnitude of operating wavelengths indicate the flexible design characteristics of the FEL mechanism.

In the third column, t_b is the electron bunch duration (FWHM) at the beginning of the undulator, and ranges from almost continuous-wave to short sub-picosecond time scales. The expected optical pulse length in an FEL oscillator can be several times shorter or longer than the electron bunch depending on the optical cavity Q, the FEL desynchronization and gain. The optical pulse can be many times shorter in a high-gain FEL amplifier, or one based on self-amplified spontaneous emission (SASE). Also, if the FEL is in an electron storage ring, the optical pulse is typically much shorter than the electron bunch. Most FEL oscillators produce an optical spectrum that is Fourier-transform limited by the optical pulse length.

The electron beam kinetic energy E and peak current I are listed in the fourth and fifth columns, respectively.

* pneyman@ccicms.com

The next three columns list the number of undulator periods N , the undulator wavelength λ_0 , and the rms undulator parameter $K = eB\lambda_0/2\pi mc^2$ (cgs units), where e is the electron charge magnitude, B is the rms undulator field strength, m is the electron mass, and c is the speed of light. For an FEL klystron undulator, there are multiple undulator sections as listed in the N-column; for example, 2x7. Some undulators used for harmonic generation have multiple sections with varying N , λ_0 , and K values as shown. Some FELs operate at a range of wavelengths by varying the undulator gap as indicated in the table by a range of values for K . The FEL resonance condition, $\lambda = \lambda_0(1+K^2)/2\gamma^2$, relates the fundamental wavelength λ to K , λ_0 , and the electron beam energy $E = (\gamma - 1)mc^2$, where γ is the relativistic Lorentz factor. Some FELs achieve shorter wavelengths by using coherent harmonic generation (CHG), high-gain harmonic generation (HG), or echo-enabled harmonic generation (EEHG).

The last column lists the accelerator types and FEL types, using the abbreviations listed after Table 4.

The FEL optical power is determined by the fraction of the electron beam energy extracted and the pulse repetition frequency. For a conventional FEL oscillator in steady state, the extraction can be estimated as $1/(2N)$; for a high-gain FEL amplifier, the extraction at saturation can be substantially greater. In a storage-ring FEL, the extraction at saturation is substantially less than this estimate and depends on ring properties.

In an FEL oscillator, the optical mode that best couples to the electron beam in an undulator of length $L = N\lambda_0$ has a Rayleigh length $z_0 \approx L/12^{1/2}$ and has a fundamental mode waist radius $w_0 \approx (z_0\lambda/\pi)^{1/2}$. An FEL typically has more than 90% of its power in the fundamental mode.

At the 2017 FEL Conference, new lasings were reported at DESY, PSI, SACLAL, Pohang, and SINAP. These are all large X-ray FEL facilities, showing there is significant worldwide interest in short wavelength FEL applications. Various other facilities reported updated parameters for existing FELs, and there are several newly proposed short-wavelength FELs around the world.

ACKNOWLEDGMENT

The authors are grateful for the support of Compass Scientific Engineering.

Content from this work may be used under the terms of the CC BY 3.0 licence (© 2018). Any distribution of this work must maintain attribution to the author(s), title of the work, publisher, and DOI.

RECENT FEL EXPERIMENTS AT FLASH

Evgeny A. Schneidmiller, Siegfried Schreiber*, and Mikahil V. Yurkov, DESY, Hamburg, Germany

Abstract

The FLASH free-electron laser user facility at DESY (Hamburg, Germany) provides high brilliance SASE FEL radiation in the XUV and soft X-ray wavelength range. With the recent installation of a second undulator beamline (FLASH2), variable gap undulators are now available. They now allow various experiments not possible with the FLASH1 fixed gap undulators. We report on experiments on tapering, harmonic lasing, reverse tapering, frequency doubling at FLASH2 and experiments using double pulses for specific SASE and THz experiments at FLASH1.

INTRODUCTION

Since summer 2005, FLASH, the free-electron laser (FEL) user facility at DESY (Hamburg), delivers high brilliance XUV and soft X-ray FEL radiation for photon experiments [1, 2]. In 2013/14, the facility has been upgraded with a second undulator beamline (FLASH2), being the first FEL facility worldwide operating simultaneously two undulator lines [3, 4]. The FLASH2 beamline is equipped with modern variable gap undulators allowing now a variety of FEL experiments which have not been possible before. The 12 planar undulators have a period of 31.4 mm, a length of 2.5 m each with an adjustable $K_{\text{rms}} = 0.7$ to 1.9.

A planar electromagnetic undulator, installed downstream of the FLASH1 SASE undulators, provides THz radiation for user experiments [5, 6]. In order to facilitate THz-XUV pump-probe experiments, double pulse lasing has been developed to provide SASE and/or THz pulses with a variable and shorter delay in the nanosecond scale than the usual 1 μs .

More details of the FLASH facility are described in [3, 4, 7, 8] and references therein. An overview on photon science at FLASH can be found in the publication list of [9].

The amplification process in a free-electron laser (FEL) can be effectively controlled by means of changing its resonance properties along a gap tunable undulator with integrated phase shifters. Novel schemes for the generation of FEL radiation with improved properties based on the use of variable gap undulators have been developed at DESY and demonstrated at FLASH2. In particular, we report on the first operation of the Harmonic Lasing Self-Seeded (HLSS) FEL [10–13] that allows to improve longitudinal coherence and spectral power of a SASE FEL. We were able to successfully demonstrate the validity of the reverse tapering concept [14–16] that can be used to produce circularly polarized radiation from a dedicated afterburner with strongly suppressed linearly polarized radiation from the main undulator. This scheme can also be used for an efficient background-free production of harmonics in an afterburner. We performed

experiments on the frequency doubling scheme [17, 18] and were able to extend the photon energy range of FLASH down to Nitrogen K-edge (400 eV), far below original design parameters. The described FEL schemes can easily be implemented at large scale X-ray FEL facilities [19–22], and the scientific community will definitely benefit from these innovative extensions.

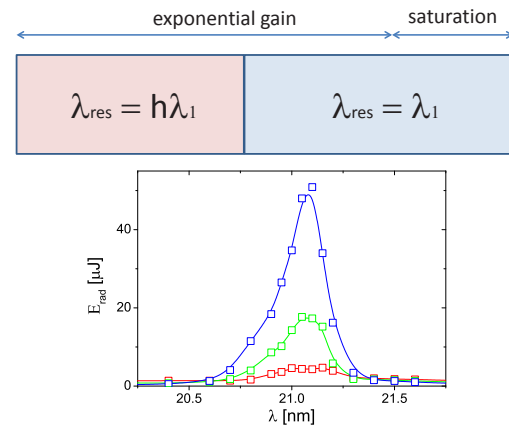


Figure 1: Top: conceptual scheme of a harmonic lasing self-seeded FEL. Bottom: operation of HLSS at FLASH2. Scan of the resonance wavelength of the first part of the undulator consisting of one undulator section (red), two sections (green), and three sections (blue). Pulse energy is measured after the second part of the undulator tuned to 7 nm.

HARMONIC LASING SELF-SEEDED FEL

In addition to well-known seeding and self-seeding techniques with enhanced spectral brightness [23–25], there are schemes without using optical elements. One of them is based on the combined lasing on a harmonic in the first part of the undulator with increased undulator parameter K , and on the fundamental in the second part [11]. In this way the second part of the undulator is seeded by a narrow-band signal generated via harmonic lasing in the first part (top plot in Fig. 1). This concept was named HLSS FEL (Harmonic Lasing Self-Seeded FEL). The enhancement factor of the coherence length (or, bandwidth reduction factor), that one obtains in an HLSS FEL in comparison with a reference case of lasing in SASE FEL mode in the whole undulator, is $R \approx h[L_w^{(1)}L_{\text{sat},h}]^{1/2}/L_{\text{sat},1}$ [11]. Here h is harmonic number, $L_{\text{sat},1}$ is the saturation length in the reference case of the fundamental lasing with the lower K -value, $L_w^{(1)}$ is the length of the first part of the undulator, and $L_{\text{sat},h}$ is the saturation length of harmonic lasing. Despite that the bandwidth reduction factor is significantly smaller than of traditional self-seeding schemes [23–25], the HLSS FEL scheme is very simple and robust, and it does not require any addi-

* siegfried.schreiber@desy.de

SUPPRESSION OF THE CSR EFFECTS AT A DOGLEG BEAM TRANSPORT USING DBA LATTICE

Toru Hara[†], Takahiro Inagaki, Kazuaki Togawa, Hirokazu Maesaka, Yuji Otake, Hitoshi Tanaka
 RIKEN SPring-8 Center, Sayo-cho, Hyogo 679-5198, Japan
 Chikara Kondo, Kenji Fukami
 JASRI, Sayo-cho, Hyogo 679-5149, Japan
 Shingo Nakazawa, Taichi Hasegawa, Osamu Morimoto, Masamichi Yoshioka
 SPring-8 Service Co., Ltd., Tatsuno-shi, Hyogo 679-5165, Japan

Abstract

Multi-beamline operation is an important issue of linear accelerator based XFELs to improve usability and efficiency of a facility. At SACLA, the multi-beamline operation had been tested since 2015 using two XFEL beamlines, BL2 and BL3. But the CSR effects at a 3-degree dogleg beam transport of BL2 caused projected emittance growth and instability of the electron beam orbit due to a high peak current of 10 kA and short bunch duration of SACLA. Consequently, stable lasing was obtained only for elongated electron bunches with low peak-currents below 3 kA. To suppress the CSR effects, the beam optics of the BL2 dogleg was replaced to that based on two DBA structures. In the new beam optics, the transverse effects of CSR are cancelled out between four bending magnets. To avoid the bunch length change, the electron beam passes an off-center orbit at the quadrupole magnets

of DBA. After the modification of the beam optics, stable lasing has been successfully obtained with 10-kA electron bunches. The parallel operation of the two beamlines will be started in autumn 2017 for user experiments.

INTRODUCTION

To meet the increasing demands from XFEL (X-ray Free-Electron Laser) users, the parallel operation of multiple beamlines is an important issue for improving the usability and efficiency of a facility [1].

Figure 1 is a schematic layout of SACLA (SPring-8 Angstrom Compact free-electron LASer) [2]. The undulator hall of SACLA can accommodate up to five undulator beamlines, and three of them have been installed so far. BL1 is a soft x-ray FEL beamline driven by a dedicated linear accelerator, SCSS+, which was originally build as a prototype of SACLA [3, 4]. BL2 and BL3 are XFEL

[†] toru@spring8.or.jp

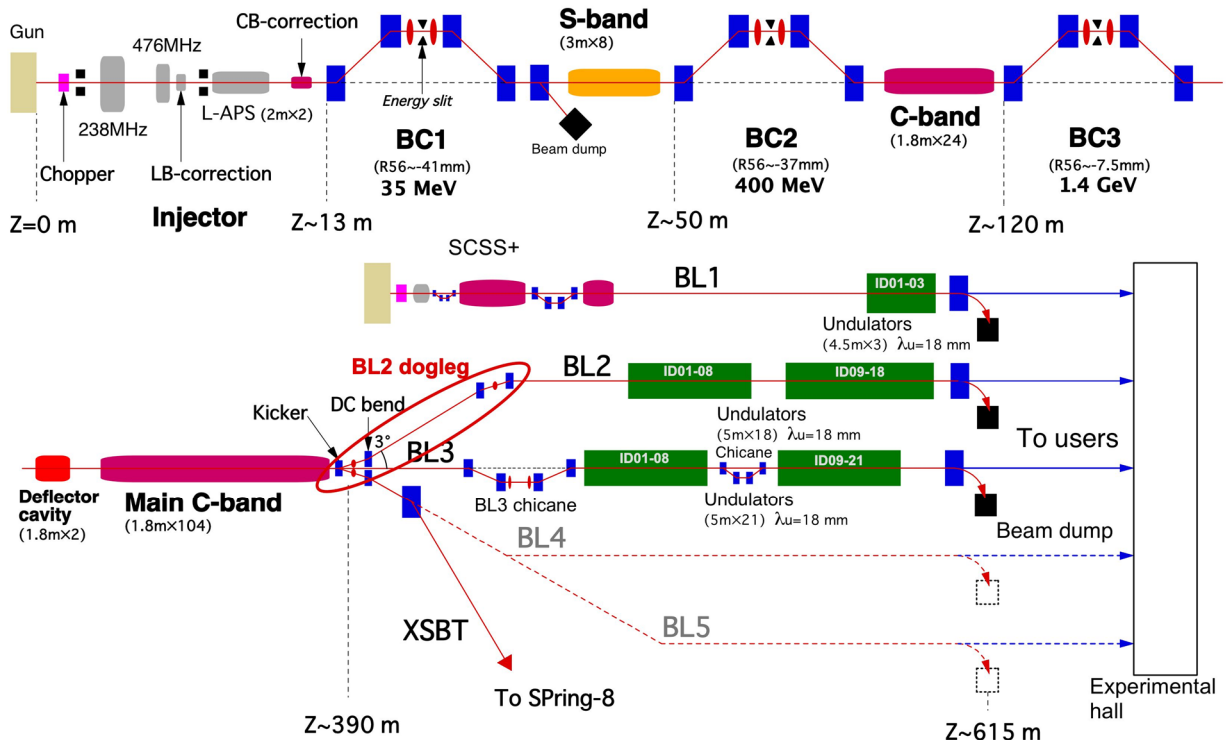


Figure 1: Schematic layout of SACLA.

Content from this work may be used under the terms of the CC BY 3.0 licence (© 2018). Any distribution of this work must maintain attribution to the author(s), title of the work, publisher, and DOI.

SEEDING EXPERIMENTS AND SEEDING OPTIONS FOR LCLS II

E. Hemsing[†], R. Coffee, G. Dakovski, W. Fawley, Y. Feng, B. Garcia, J. Hastings,
 Z. Huang, G. Marcus, D. Ratner, T. Raubenheimer, and R. W. Schoenlein
 SLAC National Accelerator Laboratory
 G. Penn

Lawrence Berkeley National Accelerator Laboratory

Abstract

We discuss the present status of FEL seeding experiments toward the soft x-ray regime and on-going studies on possible seeding options for the high repetition soft x-ray line at LCLS-II. The seeding schemes include self-seeding, cascaded HGHG, EEHG, and possible hybrid methods to reach the 1-2 nm regime with the highest possible brightness and minimal spectral pedestal. We describe relevant figures of merit, performance expectations, and potential issues.

INTRODUCTION

The general motivation for FEL seeding arises from the need for control over the longitudinal coherence. At soft x-rays, the ability to trade-off time-resolution (10-60 fs) and spectral resolution (180-30 meV) at close to the Fourier transform limit will open new dimensions in X-ray science.

Many seeding methods have been proposed to produce transform limited pulses down to soft x-rays. The three leading candidates are soft x-ray self seeding (SXRSS), Cascaded high gain harmonic generation (HG HG), and Echo Enabled Harmonic Generation (EEHG). SXRSS uses the monochromatized output from an upstream section of the FEL to seed the downstream section to saturation. It is currently the most mature technology in the 1-2 nm regime, as it has been demonstrated and delivered to users at LCLS for several years [1]. Cascaded HG HG uses external lasers to generate harmonic bunching and is in regular use at the FERMI FEL at Sincrotrone Trieste on the FEL-2 line where it is used to reach the 4-nm water window with peak fluences of order 10 μ J [2]. FERMI is currently operating as a user facility and has proved to be attractive for experiments that require wavelength tunability, multicolor pulses, polarization tunability, and higher coherence than is generally available from SASE-based FELs. EEHG also uses external lasers [3-8] and has been experimentally tested at wavelengths down to 32 nm [9], but has yet to demonstrated at soft x-rays, though efforts are underway [10, 11].

We have recently conducted studies on seeding for the high repetition soft x-ray line at LCLS-II. We find that the most promising candidates at this stage are SXRSS and EEHG as judged by anticipated performance, sensitivity, and flexibility, though there are clear challenges with both schemes. We show and compare their expected performance both in the case of ideal beams and more realistic start-to-end (S2E) beams. Other seeding methods like cascaded HG HG

[†] ehmsing@slac.stanford.edu

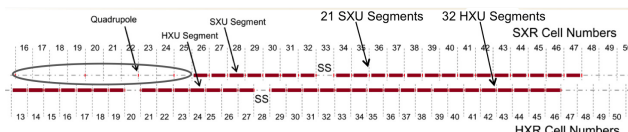


Figure 1: Layout of LCLS-II soft x-ray (top) and hard x-ray (bottom) undulators.

or even direct high harmonic generation (HHG) seeding are not among the most promising candidates at this stage due to anticipated poor performance or lack of current technical maturity. For example, we find through detailed simulations that cascaded HG HG is highly sensitive to the electron beam phase space distribution and that the spectral quality is comparable to SASE at the 1-2 nm level. The HHG technique is even more limited in its ability to access the required performance criteria due to poor ($\leq 10^{-6}$) harmonic conversion efficiency at shorter wavelengths. Upcoming proof-of-principle experiments on hybrid schemes like cascaded EEHG or EEHG/HG HG combinations, or on alternate techniques like coherent inverse Compton scattering may provide key information on their use as potential options, but currently these concepts are only in the preliminary experimental stages.

PERFORMANCE GOALS

The expectation for any seeding scheme in LCLS-II is the production of temporally coherent pulses with sufficient spectral brightness to address the photon science requirements. These requirements include several features that favor a seeded FEL with many characteristics inherent to optical laser systems:

- **Enhanced Control:** Precision control of the central wavelength well within the SASE bandwidth, as well as the ability to control the coherent bandwidth.
- **Minimal Spectral Pedestal:** The microbunching instability (MBI) is predicted to be a significant effect at the LCLS-II. It is believed to be responsible for the limited resolving power (roughly 2000-5000) of the SXRSS at LCLS [1, 12, 13]. Recent studies indicate that EEHG has a reduced sensitivity to MBI under certain conditions [14].
- **Coherent Two/Multi Color Operations:** Several different schemes to produce two-color x-ray pulses with variable pulse energy separations and timing delay have

ASU COMPACT XFEL*

W. S. Graves[†], J. P. J. Chen, P. Fromme, M. R. Holl, R. Kirian, L. E. Malin, K. E. Schmidt,
J. C. H. Spence, M. Underhill, U. Weierstall, N. A. Zatsepin, C. Zhang,
Arizona State University, Tempe, USA
P. D. Brown, K. H. Hong, D. E. Moncton, MIT, Cambridge, USA
E. A. Nanni, C. Limborg-Deprey, SLAC, Menlo Park, USA

Abstract

Arizona State University (ASU) is pursuing a concept for a compact x-ray FEL (CXFEL) that uses nanopatterning of the electron beam via electron diffraction and emittance exchange to enable fully coherent x-ray output from electron beams with an energy of a few tens of MeV. This low energy is enabled by nanobunching and use of a short pulse laser field as an undulator, resulting in an XFEL with 10 m total length and modest cost. The method of electron bunching is deterministic and flexible, rather than dependent on SASE amplification, so that the x-ray output is coherent in time and frequency. The phase of the x-ray pulse can be controlled and manipulated so that new opportunities for ultrafast x-ray science are enabled using attosecond pulses, very narrow line widths, or extremely precise timing among multiple pulses with different colors. These properties may be transferred to large XFELs through seeding with the CXFEL beam. Construction of the CXFEL accelerator and laboratory are underway, along with initial experiments to demonstrate nanopatterning via electron diffraction. An overview of the methods and project are presented.

INTRODUCTION

ASU has embarked on a multiphase effort to develop powerful compact x-ray sources, beginning with the compact x-ray light source [1] (CXLS) that is now under construction and will be operational by end of 2017. CXLS uses an x-band photoinjector, standing wave linac, and high power lasers to produce x-rays via inverse Compton scattering (ICS) with projected flux of about 10^8 photons per shot at the high repetition rate of 1 kHz. The 35 MeV linac is expected to produce photon energies in the range 1-35 keV with pulse length of 100 fs to 1 ps. CXFEL is the planned second phase of development and is closely based on CXLS equipment. CXFEL will transform the incoherent ICS emission of CXLS into a fully coherent x-ray laser by creating ‘nanobunches’ using a combination of methods including diffraction of the electron beam from a patterned silicon crystal [2–5] at energy of 4-10 MeV and transformation of the resulting spatial pattern, or density modulation, into the longitudinal dimension using emittance exchange (EEX) [6]. CXLS is designed to be easily upgraded to CXFEL by reconfiguring the bunch compression chicane into a double dogleg EEX

line. All of the electron optics and equipment needed to pattern the electron beam, with the exception of the EEX line, are included in the phase 1 CXLS, enabling preliminary experiments to study and understand the generation and manipulation of patterned electron beams.

TECHNICAL DESCRIPTION

The CXFEL components are shown in Figure 1. Beginning at the right end of the figure is the 4.5 cell x-band photoinjector [7] that accelerates the beam to 4 MeV. Following ports for the cathode laser is the first of three short 35 cm long linac sections, each of which is an innovative 20-cell standing-wave linac [8] adapted to our 9.3 GHz RF frequency. SLAC spinoff company Tibaray LLC is producing the photoinjector and linac. The first linac section L1 can accelerate the beam up to 12 MeV and/or adjust the time-energy chirp for optimum diffraction in the thin silicon crystal that sits just downstream of it. After the crystal the two linac sections L2 and L3 are jointly powered and phased to accelerate the beam to a maximum of 35 MeV. The photoinjector and linac L1 are powered by one RF transmitter with high power waveguide attenuator and phase shifter to arbitrarily split RF amplitude and phase among the two devices. A second RF transmitter powers L2 and L3 as well as the deflector cavity in the downstream EEX line. The RF transmitters are Scandinova solid-state K1A modulators driving L3 L6145-01 9.3 GHz klystrons capable of 6 MW output power in 1 microsecond pulses at repetition rates up to 1 kHz. The transmitters are now in final testing at the vendor and have demonstrated better than 100 ppm RMS voltage stability.

Following L3 is a set of 4 quadrupoles (Q1-Q4) arranged as a variable demagnification telescope to image the electron beam at the crystal plane to a downstream point. For electron microscopy studies the beam is spatially imaged onto a profile monitor PRO6 in the EEX line. The imaging requirement is different to generate nanobunches at the output of the EEX line. In this case the spatial image of the silicon grating is never formed, but rather a matching condition with tilted ellipses [2] is generated at the entrance to the EEX line so that the original modulation created by the crystal is transferred to the longitudinal dimension at the EEX output. The EEX line consists of the 4 bend magnets B1-B4, an RF deflector cavity and accelerator cavity that are independently phased and powered, along with sextupoles S1-S3 and octopole O1 for aberration correction. Following the EEX line is a quadrupole triplet (Q5-Q7) that focuses

* This work was supported by NSF Accelerator Science award 1632780, NSF BioXFEL STC award 1231306, DOE contract DE-AC02-76SF00515, and ASU.

[†] wsg@asu.edu

RECENT ON-LINE TAPER OPTIMIZATION ON LCLS*

Juhao Wu^{1†}, Kun Fang^{1‡}, Xiaobiao Huang¹, Guanqun Zhou^{1§}, Axel Brachmann¹,
 Claudio Emma^{1¶}, Chunlei Li^{1||}, Eric Li², Haoyuan Liu³, Weihao Liu^{4,1}, Alberto Lutman¹,
 Tim Maxwell¹, Claudio Pellegrini¹, Weilun Qin^{1**}, Tor O. Raubenheimer¹, Alexander Scheinker⁵,
 Cheng-Ying Tsai¹, Bo Yang⁶, Chuan Yang^{1††}, Moohyun Yoon^{1‡‡}, Brandon W. Zhang⁷
¹SLAC, Stanford University, Stanford, USA, ²Palo Alto High School, Palo Alto, USA,
³Boston University, Boston, MA, USA, ⁴NSRL, University of Science and Technology of China,
 Hefei, Anhui, China, ⁵LANL, Los Alamos, USA, ⁶Dept. of Mechanical & Aerospace Engineering,
 University of Texas at Arlington, Arlington, USA ⁷Lakeside School, Seattle, USA

Abstract

High-brightness XFELs are in high demand, in particular for certain types of imaging applications. Self-seeding XFELs can respond to a heavily tapered undulator more effectively, therefore seeded tapered FELs are considered a path to high-power FELs in the terawatt level. Due to many effects, including the synchrotron motion, the optimization of the taper profile is intrinsically multi-dimensional and computationally expensive. With an operating XFEL, such as LCLS, the on-line optimization becomes more economical than numerical simulation. Here we report recent on-line taper optimization on LCLS taking full advantage of nonlinear optimizers as well as up-to-date development of artificial intelligence: deep machine learning and neural networks.

TAPERED FEL TO REACH HIGH POWER

Ultra-fast hard X-ray Free electron laser (FEL) pulse providing atomic and femtosecond spatial-temporal resolution [1,2] makes it a revolutionary tool attracting world-wide interests for frontier scientific research. Among these, single particle imaging is one of the applications demanding terawatts (TW) level peak power [3]. To reach TW FEL peak power, using a tapered undulator to keep the FEL further extracting kinetic energy from the high energy electron bunch is an active research direction [4]. However, the FEL after exponential growth saturation has to have good temporal coherence to better respond to a heavily tapered undulator [5]. While the SASE FEL provides high spatial coherence, the

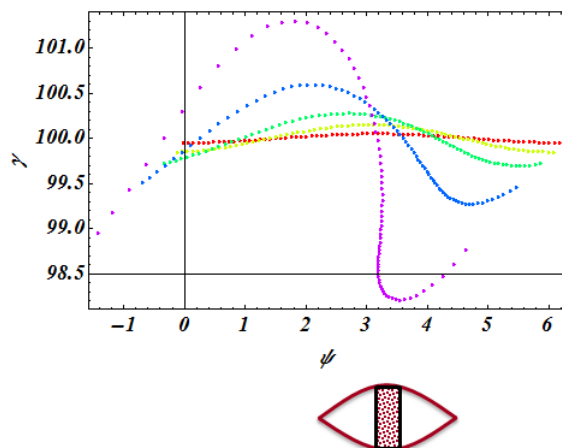


Figure 1: The electrons experience a quarter of a synchrotron motion period and microbunch with a central phase of $\psi \sim \pi$.

temporal coherence is rather poor at exponential growth saturation point. To improve the temporal coherence, seeding approaches: both external [6, 7] and self-seeding [8, 9] and Slippage-enhanced SASE (SeSASE) [10–13] can produce an FEL pulse with good temporal coherence at the exponential growth saturation region. In this paper, we conduct our study with a self-seeding tapered FEL [14–17].

The physics changes from high-gain to low-gain FEL after the exponential growth saturates. In the high-gain region, the FEL power grows exponentially [18]:

$$P_{\text{FEL}}(z) = P_0 \exp[z/L_G], \quad (1)$$

where P_0 is the start-up power, L_G is the power gain length, and z is the coordinate along the electron forward traveling direction in the undulator. The electrons experience a quarter of a synchrotron motion period from red, yellow, green, blue, and purple; they eventually microbunch with a central coordinate of $\psi \sim \pi$ as shown in Fig. 1. The electrons together with the FEL bucket are illustrated in the lower part of Fig. 1 indicating microbunching at $\psi \sim \pi$.

After the exponential growth saturation, the FEL system evolves into coherence emission. Assuming a transversely round electron beam, a constant bunching factor b_1 , and no

* Work supported by the US Department of Energy (DOE) under contract DE-AC02-76SF00515 and the US DOE Office of Science Early Career Research Program grant FWP-2013-SLAC-100164.

† jhwu@SLAC.Stanford.EDU

‡ now at Wells Fargo & Co., San Francisco, CA, USA

§ Ph.D. student from Institute of High Energy Physics, and UCAS, Chinese Academy of Sciences, Beijing, China

¶ Ph.D. student from UCLA, Los Angeles, USA

|| now at Shanghai Institute of Applied Physics, Chinese Academy of Sciences, Shanghai, China

**Ph.D. student from Peking University, Beijing, China

††Ph.D. student from NSRL, University of Science and Technology of China, Hefei, Anhui, China

‡‡on sabbatical leave from Department of Physics, Pohang University of Science and Technology, Pohang, Korea

POLARIZATION CONTROL OF STORAGE RING FELS USING CROSS POLARIZED HELICAL UNDULATORS *

J. Yan^{1,†}, H. Hao¹, S. Mikhailov¹, V. Popov¹, S. Huang², J. Y. Li³,
V. N. Litvinenko⁴, N. A. Vinokurov⁵, Y. K. Wu^{1,‡}

¹DFELL/TUNL, and Department of Physics, Duke University, Durham, NC, USA

²Institute of Heavy Ion Physics, Peking University, Beijing, China

³Institute of High Energy Physics, Chinese Academy of Sciences, Beijing, China

⁴Department of Physics and Astronomy, Stony Brook University, Stony Brook, USA

⁵Budker Institute of Nuclear Physics, Novosibirsk, Russia

Abstract

For more than two decades, accelerator researchers have been working to gain control of polarization of synchrotron radiation and FELs using non-optical means. In 2005, using mixed linear and helical undulators, the first experimental demonstration of polarization control of an FEL beam was realized with the Duke storage ring FEL. With the recent upgrade of the undulator system, the Duke FEL can be operated with up to four helical undulators simultaneously. Using two sets of helical undulators with opposite helicities, for the first time, we have demonstrated full control of the polarization of a storage ring FEL, including helicity switching and rotatable linear polarization. The helicity switching of the FEL beam has been realized with good lasing up to a few Hertz. The generation of a linearly polarized FEL beam using a set of cross polarized helical undulators has been demonstrated with a high degree of polarization ($P_{\text{lin}} > 0.95$). The FEL polarization direction can be fully controlled using a buncher magnet. Furthermore, the use of non-optical means to control the FEL polarization allows us to extend polarization control to γ -ray beams via Compton scattering. For the first time, we have produced linearly polarized Compton γ -ray beams with the rotatable polarization direction using helical undulators.

INTRODUCTION

Control of the polarization of light is of great importance to certain scientific research. For example, in the optical regime, a circularly polarized radiation source with switchable handedness can be used for magnetic dichroism experiments [1, 2]. In addition, some polarization-dependent spectroscopy techniques require the radiation sources to have switchable linear polarizations (typically two orthogonal linear polarizations). Polarization of light can be manipulated using polarizing optics in the visible regime. However, for the short wavelength regions such as vacuum ultraviolet (VUV) or extreme ultraviolet (EUV) where polarizing optics are either not available or have very limited capabilities, controlling polarization without the need of using polarizing optics is critical. In fact, non-optical polarization control

of the accelerator based light sources was proposed about 30 years ago, initially for the third-generation storage ring based synchrotron sources. A common approach to realize polarization control is to employ an undulator with multiple arrays of mechanically movable permanent magnets [3–5]. A specific polarization state can be obtained by translating one or more arrays of the magnets to a specific configuration. However, the manufacturing of such an undulator is typically very complicated and costly. Another method to obtain variable polarization is based upon the coherent superposition of two orthogonal polarization states. This idea (referred to as the crossed undulator configuration) was first proposed for planar undulators [6], where two identical planar undulators are used with the first one aligned to produce horizontally polarized radiation and the second one rotated by 90° to produce the vertically polarized radiation. The phase delay between two orthogonally polarized radiation beams is varied using a phase retarder positioned between two undulators, and elliptical polarization with arbitrary ellipticity can be obtained after a monochromator.

Polarization control is also a critical feature for FELs. Since the idea of the crossed undulator configuration was first introduced to the FEL field in the early 2000s [7], FEL polarization control was first experimentally demonstrated on a storage ring FEL at Duke University [8]. Later on, the development of polarization control using crossed undulators was proposed for several linac based FEL projects [9, 10]. In the past few years, some have experimentally realized polarization control using either variable-polarization undulators [11, 12] or crossed planar undulators [13, 14]. In Ref [7], Kim also proposed to use crossed helical undulators to produce linearly polarized radiation with controllable direction of the linear polarization. Its feasibility was theoretically confirmed by Dattoli *et al.* soon after [15, 16]. However, since most FELs do not have the configuration of crossed helical undulators, no experimental demonstration was done until the recent work at FERMI, a linac based high-gain FEL, in 2015 [14].

In 2005, the Duke storage ring FEL achieved polarization control using two planar undulators and two helical undulators [8]. By mixing the linearly polarized radiation from the OK-4 undulators and circularly polarized radiation from the OK-5 undulators with their relative FEL gains controlled by

* Work supported in part by the US DOE grant no. DE-FG02-97ER41033.

† junyan@fel.duke.edu, 1-919-660-2667.

‡ wu@fel.duke.edu, 1-919-660-2654.

THERMAL AND MECHANICAL STABILITY OF BRAGG REFLECTORS UNDER PULSED XFEL-RADIATION*

I. Bahns^{1†}, P. Thiessen, C. Maag, J. Rossbach, Universität Hamburg, Germany
J. Zemella, DESY, Hamburg, Germany
V. Sleziona, H. Sinn, European XFEL, Hamburg, Germany

Abstract

Free-electron laser (FEL) x-ray radiation can deliver pulses with a huge amount of energy in short time duration. X-ray optics like Bragg reflectors therefore must be chosen in a way that they can withstand radiation-material interaction without getting damaged so that they can maintain their technical functionality. Therefore thermal and mechanical reactions of Bragg reflectors to the radiation induced thermal strain and force (radiation pressure) have been considered in this study. The theory of thermoelasticity has been used to simulate the strain conditions at saturation of the amplifying process in an X-ray free-electron laser oscillator (XFELO). One aim of this study was to investigate, if the radiation pressure could be an effect that gives a considerable contribution to the strain propagation. The results of the simulations have shown that, if Bragg backscattering of the X-ray pulse by a diamond crystal with 99% reflectivity and 1% absorptivity is assumed, the value of the thermally induced strain is about two magnitudes higher than the radiation pressure induced strain. Also a measurement method which could be used to detect the simulated strain is shortly discussed at the end of this document.

INTRODUCTION

The European XFEL is under commissioning, the first lasing was achieved in May 2017. The facility provides radiation with high peak brilliance on the order of 10^{33} photons $[(s^{-1} mm^{-2} mrad^{-2}) / (0.1\% BW)]$, with up to 27000 photon pulses s^{-1} , which are delivered in 600 μs long pulse trains with a repetition rate of 10 Hz [1]. These conditions give the possibility for the realization of an X-ray free-electron laser oscillator (XFELO) [2]. With the integration of an XFELO at the European XFEL longitudinally full coherent pulses and an increase of the peak brilliance by one order magnitude should be achievable. The bandwidth would reduce to a value of $\frac{\Delta E}{E} = 1.6 \cdot 10^{-6}$. The amount of energy in saturation of these photon pulses would be about 300 μJ to 1 mJ. The small bandwidth is in the order of the Darwin width and therefore nearly the whole amount of energy per photon pulse would be Bragg reflected. Shvyd'ko et al have shown that nowadays diamond crystals are available, which have reflectivity of more than 99% in case of Bragg reflection [3]. Hence, by considering such a Bragg reflector for saturated XFELO radiation the maximum amount of pulse energy which is absorbed inside the penetration depth (extinction length) can be at most 1%.

Under these radiation conditions the thermal and mechanical stability of Bragg-reflectors, which are necessary for the XFELO, have to be considered in detail. Therefore simulations of the strain induced by X-ray radiation in a diamond crystal have been performed in this study. Strain has a direct influence on the lattice parameter and therefore changes the Bragg reflection conditions, which can influence the stability of an XFELO.

When energy of electromagnetic radiation is interacting with a solid body in the timespan of femtoseconds, the system moves out of thermal equilibrium. Theoretical and experimental studies [4] [5] have shown that the dynamics of this thermal expansion, apart from heat transfer, can be explained as a mechanical disturbance. The absorbed energy creates thermal stress which is propagating as a longitudinal wave with the speed of sound into the irradiated material [6].

Besides the creation of a thermally induced strain wave, the radiation pressure could also create such a strain propagation. This could be important in cases where the amount of reflected energy is large and the absorbed portion is small. These conditions exist for Bragg reflected radiation that a saturated XFELO would deliver, because the thermal expansion is directly influenced by the amount of energy that is absorbed whereas radiation pressure occurs for absorption as well as for reflection. However, the force which is induced by radiation pressure is very small due to the small impulse of a photon and therefore the thermal effects are normally dominating this effect.

Mechanical deflection of micro beams caused by the radiation pressure have been investigated theoretically and experimentally by several authors [7–10]. However, in the present study the strain propagation and not the deflection is the parameter of interest. To the best knowledge of the authors this kind of strain propagation has not been considered by any other theoretical or experimental investigation so far.

PROBLEM FORMULATION

Stoupin *et al.* [11] have done experimental studies on the strain propagation caused by a ≈ 8 ps laser pulse in diamond. The strain has been assumed to propagate only along the z direction (Fig. 2 a), which is valid for $\sqrt{A} \gg d$, where A is the radiated area of a crystal with the thickness d. In case of a low-flux laser pulse the heat dissipation can be neglected for the first tens nanoseconds after the radiation-material interaction and the formulas of thermoelasticity [12] yields:

* Work supported by BMBF FKZ 05K16GU4

† immo.bahns@desy.de

ENHANCEMENT OF RADIATIVE ENERGY EXTRACTION IN AN FEL OSCILLATOR BY POST-SATURATION BEAM ENERGY RAMPING

H. S. Marks[†], A. Gover, Tel Aviv University, Tel Aviv, Israel
 Yu. Lurie, E. Dyunin, Ariel University, Ariel, Israel

Abstract

We present results of experiments and simulations showing a greater than 50% increase in post-saturation radiation power extraction from a Free Electron Laser oscillator based on an electrostatic accelerator. Electrostatic accelerator free electron laser oscillators have the potential for CW operation. Present day operating oscillators rely on long pulses of electrons, tens of microseconds in duration, they generate correspondingly long radiation pulses, at a single longitudinal mode after a mode competition process. The post-saturation power extraction enhancement process is based on temporal tapering (up-ramping) of the beam energy, enabling a large synchrotron oscillation swing of the trapped electron bunches in passage along the interaction length. We further discuss the theoretical limits of the temporal tapering efficiency enhancement process.

INTRODUCTION

Of the FEL oscillators operating in the world [1], few operate with an electrostatic accelerator [2-6], one of them is the Israeli Electrostatic Accelerator FEL (EA-FEL). Generally, in FEL only a small proportion of the electron kinetic energy is extracted in the form of radiation. One way of increasing the efficiency of extraction is use of a tapered wiggler. That is, when the undulator period and or magnetic field are modified [7-10]. This ensures that as electrons lose kinetic energy their interaction with the radiated electric field remains strong [11]. Spatial undulator tapering has been proved already in experiments with an amplifier FEL [12-13]. All these works are connected to single-pass Self-Amplified Spontaneous Emission (SASE) amplifier FELs.

Oscillator FELs are multi-pass radiation systems. The out-coupling of the resonator can be modified until the optimum energy balance with the resonator internal losses is found for maximum radiative output power [14]. Pre-bunching the electron beam has also been shown to increase the extraction efficiency of radiative power [15].

Another way to increase the extraction of useful radiative energy is to positively-ramp the kinetic energy of the electron beam entering the resonator post-saturation. This temporal tapering of the electron parameters serves to raise the electrons, in terms of their potential to radiate, onto a more energetically favourable synchrotron oscillation path. Such a scheme was demonstrated via experiment and simulation for the first time [16].

Figure 1 shows a schematic of the Israeli Tandem EA-FEL. A thermionic cathode e-gun is biased to -40 kV and provides electron beam pulses with currents in the range 0.7-3 A and up to 100- μ s duration. These electron beam pulses are accelerated up to around 1.4 MeV where they enter an equipotential region where they are focused by quadrupoles for optimal entrance into the resonator (which is encompassed by a planar Halbach wiggler [17]). After passing through the resonator the electrons are again focused by quadrupoles before entry into the deceleration tube, at the end of the deceleration tube they are collected. Under regular operation the resonator and wiggler are at the same potential as the sections with the quadrupoles between the acceleration and deceleration tubes. The main properties of the EA-FEL are summarised in Table 1, and described in a previous publication [14].

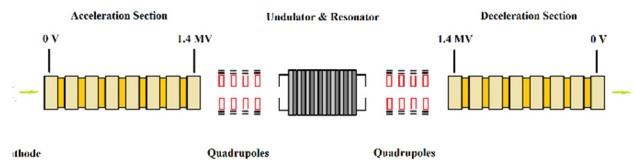


Figure 1: Schematic of the Israeli EA-FEL based on a Tandem Van-der-Graaf generator.

Table 1: Properties of the EA-FEL

Beam Current	0.7-3 A
Beam Energy	1.35-1.45 MeV
Wiggler Period	44.4 mm
Effective No. of Wiggler Periods	24
Wiggler field Amplitude	1.93 kG
Waveguide Fundamental Mode	HE11
Radiation Frequency	95-110 GHz
Optical Length of Resonator	1.514 m
Free Spectral Range of Resonator	100 MHz

A voltage ramping device (VRD) was built to compensate for falling accelerating voltage due to electrons hitting the walls of the beam line. The VRD is an electronic circuit composed of a 20-kV bipolar power supply that is remotely triggered to charge a capacitive load through selectable resistors producing an exponential pulse of rise time $\tau = RC$ that is nearly linear for time $t < \tau$. The first purpose of the

START-TO-END SIMULATIONS FOR AN X-RAY FEL OSCILLATOR AT THE LCLS-II AND LCLS-II-HE

W. Qin*, S. Huang, K. X. Liu, IHIP, Peking University, Beijing, China

K.-J. Kim, R. R. Lindberg, ANL, Argonne, USA

Y. Ding, Z. Huang, T. Maxwell, K. Bane, G. Marcus, SLAC, Menlo Parck, USA

Abstract

The proposed high repetition-rate electron beam from the LCLS-II and LCLS-II High Energy (LCLS-II-HE) upgrade are promising sources as drivers for an X-ray FEL Oscillator (XFEL) operating at both the harmonic and fundamental frequencies. In this contribution we present start-to-end simulations for an XFEL operating at the fifth harmonic with 4 GeV LCLS-II beam and at the fundamental with 8 GeV LCLS-II-HE beam. The electron beam longitudinal phase space is optimized by shaping the photoinjector laser and adjusting various machine parameters. The XFEL simulations show that high-flux output radiation pulses with 10^{10} photons and 3 meV (FWHM) spectral bandwidth can be obtained with the 8 GeV configuration.

INTRODUCTION

X-ray free-electron lasers (XFELs) such as the LCLS [1] in self-amplified spontaneous emission (SASE) [2, 3] mode are now generating unprecedentedly bright X-ray pulses for wide range of applications. Reaching fully coherent, stable hard X-ray pulses is still challenging due to the stochastic nature of the SASE process. Hard X-ray self-seeding [4] improved the temporal coherence and brightness but still relies on a SASE seed. The transition to the era of high repetition rate XFELs provides promising opportunities for the linac based X-ray FEL oscillator (XFEL) [5–8], which is characterized with full coherence, ultra narrow bandwidth, and stable X-ray pulses. The XFEL relies on successive low gain amplification of X-ray pulses trapped in an optical cavity with crystal mirrors. Since the spectral acceptance of the crystal mirror is about ~ 10 meV, high quality electron beams with low emittance, low energy spread are required.

Feasibility study of the 5th harmonic XFEL utilizing the LCLS-II [9] was carried out with an ideal 4 GeV beam for 14.4 keV photon energy [10, 11]. The proposed high energy upgrade of LCLS-II to 8 GeV LCLS-II-HE [12] enables driving the same wavelength in the fundamental mode. The performance of XFEL is strongly affected by the longitudinal phase space flatness due to the narrow spectral acceptance of the crystals. Linearizing longitudinal phase space via current shaping was studied [13]. Here, we present the start-to-end simulations for an XFEL based on both 4 GeV LCLS-II beam and 8 GeV LCLS-II-HE beam.

LAYOUT

The layout of the proposed linac-XFEL is sketched in Fig. 1. A photoinjector is used to generate high-brightness electron beams, and the 1.3 GHz superconducting linac cavities accelerate the beam to 4 GeV for LCLS-II and 8 GeV for LCLS-II-HE. Since the XFEL usually operates at lower current compared with high gain FELs, two stages of bunch compression are used to compress the beam to 100 A level current. A 3.9 GHz harmonic cavity is located before the first compressor to linearize the longitudinal phase space. The accelerated beam is transported for 2 km to the Beam Switch Yard (BSY) and directed to End Station A (ESA), a possible location for the XFEL. Since there is a beam energy chirp after the transport, a passive, parallel-plate corrugated dechirper [14, 15] is employed to cancel the energy chirp before entering the XFEL. The X-ray cavity is in the four crystal configuration as proposed in Ref. [6]. Diamonds are used as high reflectivity mirror for X-rays. For the harmonic setup, phase shifters are used to suppress the fundamental wavelength [7].

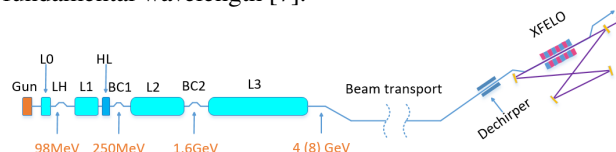


Figure 1: Layout of the proposed XFEL at the LCLS-II.

INJECTOR SIMULATION

Baseline of the LCLS-II injector [16] is based on the Advanced Photoinjector Experiment (APEX) [17] design, consisting of a normal conducting rf (NCRF) gun at 186 MHz with up to 20 MV/m gradient, one 1.3 GHz 2-cell buncher, two emittance compensation solenoids and one standard cryomodule with eight 9-cell superconducting cavities. Laser pulses of 40 ps flat-top are irradiated to a semiconductor cathode to generate 100 pC electrons bunches. The beam energy exiting the gun is 750 keV and reaches about 100 MeV at the exit of the injector. Genetic optimization based on NSGA-II algorithm was applied in the design of the injector to minimize the beam emittance [18]. Figure 2 shows the ASTRA [19] simulated electron longitudinal phase space, current, slice energy spread, and slice emittance of the 100 pC baseline case at the exit of the injector. The beam emittance is about $0.3 \mu\text{m}$. The electron beam exhibits a Gaussian-like current profile.

To get flat final longitudinal phase space, one approach is to shape the beam current by shaping the drive laser pulse profile at the injector. Since the NCRF gun setup compresses

* qinweilun@pku.edu.cn, also at SLAC.

NUMERICAL STUDIES ON RF-INDUCED TRAJECTORY VARIATIONS AT THE EUROPEAN XFEL

T. Hellert, B. Beutner, N. Walker, W. Decking, DESY, Hamburg, Germany

Abstract

At the European X-Ray Free-Electron-Laser, superconducting TESLA-type cavities are used for acceleration of the driving electron bunches. Due to the high achievable duty cycle, a long radio frequency (RF) pulse structure can be provided, which allows to operate the machine with long bunch trains. The required pointing stability of the FEL radiation places stringent restrictions on the acceptable trajectory variations of individual electron bunches. Therefore a transverse intra-bunch-train feedback system (IBFB) is located upstream of the undulator section. However, intra-bunch-train variations of RF parameters and misalignments of RF structures induce significant trajectory variations that may exceed the capability of the IBFB. In this paper we give an estimate of the expected RF induced intra-bunch-train trajectory variation for different machine realizations and investigate on methods for their limitation.

INTRODUCTION

The European X-Ray Free-Electron Laser (EuXFEL) Facility [1–3] is built in Hamburg and is currently undergoing commissioning [4]. It will provide FEL radiation with wavelengths from 0.05 nm to 5 nm. Acceleration of the driving electron bunches is achieved by using superconducting TESLA-type [5] cavities. The long RF pulse structure allows to provide long bunch-trains adapted to the needs of the experiments. Up to 2700 bunches are accelerated within one RF pulse with a pulse repetition rate of 10 Hz and a bunch spacing down to 222 ns, thus 27000 bunches per second can be used for the experiments.

The designated pointing stability of the photon beam leads to a stability requirement of 3 μm maximum trajectory spread within one bunch-train in the undulator section. A conservative estimate predicts worst case beam trajectory perturbations, e.g. from magnet vibrations or spurious dispersion, of about $\pm 100 \mu\text{m}$ assuming a beta function of 30 m [6]. This magnitude of amplitude can be corrected for individual bunches at the entrance to the undulator section by the transverse intra-bunch-train feedback system (IBFB) [7]. However, RF-induced trajectory variations have not been considered in the design studies of the IBFB.

At EuXFEL, several cavities with individual operational limits [8] are supplied by one RF power source. Within the bunch-train, the low-level-RF system (LLRF) [9, 10] is able to restrict the variation of the vector sum of the accelerating gradient of one RF station sufficiently [11]. However, individual cavities have an intrinsic variation of RF parameters within one bunch train, caused by the effects of beam loading and Lorentz force detuning [12]. Misaligned cavities in combination with variable RF parameters induce

intra-bunch-train trajectory variations [12]. Coupler kick variations caused by variations of the detuning are additional beam dynamics perturbations within one bunch train. In this paper we investigate their magnitude for different machine realizations and present methods for their limitation.

MODEL SETUP

A detailed description of the utilized beam dynamics model can be found in Ref. [12]. We use a combination of axially symmetric beam transport matrices [13] and discretized coupler kicks [14]. Misalignments are modeled by coordinate system transformations. The EuXFEL linear accelerator increases the electron beam energy up to 17.5 GeV in three separate sections: L1, L2 and L3, each consisting out of 4, 12 and 84 accelerating modules, respectively. Each module contains eight cavities and a quadrupole magnet, providing a FODO lattice in the accelerating sections. Initial beam energy is 150 MeV for L1, 600 MeV for L2 and 2.4 GeV for L3. If not stated differently, for each machine seed the following model parameters are randomly created within their range: variation of amplitude $\Delta V = 2 \text{ MV m}^{-1}$ and phase $\Delta\phi = 4^\circ$ of the accelerating field and the detuning $\Delta f = 20 \text{ Hz}$ of individual cavities within the bunch train. Furthermore the offset $\Delta u_{\text{cav}} = 0.5 \text{ mm}$ and tilt $\Delta u'_{\text{cav}} = 0.25 \text{ mrad}$ of cavities and modules, $\Delta u_{\text{mod}} = 0.5 \text{ mm}$ and $\Delta u'_{\text{mod}} = 0.2 \text{ mrad}$, respectively. The above values are expected for nominal machine operation.

BEAM DYNAMICS SIMULATIONS

Before conducting a statistical analysis of each accelerating section, tracking results of one random machine realization are presented. Figure 1 shows the intra-bunch-train trajectory variation for the horizontal and vertical plane as it could be recorded at the beam position monitors at each module at EuXFEL. Mean bunch train offsets are subtracted. The lower row of Figure 1 additionally shows the normalized trajectory variation $\Delta\tilde{u}$. It will be defined as the maximum possible offset variation at a point with zero divergence and $\beta_u = 30 \text{ m}$, where u stands for x and y , respectively. The normalized trajectory variation evolves non-monotonically throughout the machine. The correlation of particular misalignments of cavities and their RF parameters can affect the initial trajectory variation at the entrance of the cavity constructively or destructively. An accurate consideration must involve statistical methods.

The accumulated normalized intra-bunch-train trajectory variation $\Delta\tilde{u}$ is calculated for L1, L2 and L3 independently. 10^5 random sets of misalignments and RF parameters are evaluated. Figure 2 shows a histogram of $\Delta\tilde{u}$, as induced in each linac. Critical trajectory variation is defined as the

FIRST BEAM HALO MEASUREMENTS USING WIRE SCANNERS AT THE EUROPEAN XFEL

S. Liu[†], V. Balandin, B. Beutner, W. Decking, L. Fröhlich, N. Golubeva, T. Lensch, DESY, Hamburg, Germany

Abstract

Beam halo measurements and collimations are of great importance at the European XFEL, especially for the operation at high repetition rates (27000 pulses/s). First beam halo measurements have been performed during the commissioning using the wire scanners installed before and after the ~200 m long post-linac collimation section. We present the measurement results and the comparison of beam halo distributions before and after the collimation section.

INTRODUCTION

The European XFEL [1] is driven by a ~1.7 km long superconducting linear accelerator followed by three undulator systems called SASE1, SASE2 and SASE3 with 35, 35 and 21 undulator segments (each 5 m long), respectively. It operates in bunch train mode with 10 Hz of repetition rate and a maximum number of 2700 electron bunches can be generated per macro pulse with a spacing of 220 ns. The maximum beam power can be generated is more than 500 kW. It is well known that, a common issue for high power machines is the control of beam losses, since the beam losses can cause damages to different components of the machine. In the case of European XFEL, the main concern is the damage to the undulators. Therefore, a ~200 m long post-linac collimation (CL) section is designed to collimate the beam halo and dark current before the undulator section [2].

The CL section has two arcs and one straight section in between as phase shifter. The betatron functions at the collimator locations can be varied by tuning the quadrupoles in the matching sections before and after the collimation section, and in the phase shifter. This tuning includes also the possibility of FODO-like transport through the whole collimation section. This feature brings the flexibility to operate the collimation section in different optics modes. At the beginning of the commission, the FODO-like mode is used. Recently, another two optics modes have also been tested. One is the mode A optics: the standard collimation optics with beta functions (of about 200m) at the collimator locations, and the other is the mode B optics (see Fig.1): the relaxed optics with smaller beta functions (of about 100m) at the collimator locations.

The efficiency of beam halo collimation has been studied in simulations during the design of the collimation section [2] and also for the implementation of Hard X-ray self-seeding, where a diamond crystal will be inserted close to the beam in the undulator sections [3]. For the experimental study, different instruments can be used to

measure the beam halo (e.g. YAG:Ce screen [4], diamond detector [5] and wire scanners [6]). At the European XFEL, the wire scanners (WS's) [7] installed before and after the collimation section can be used. In this paper, we present the design and commissioning of the WSs followed by the first beam halo measurements using the WSs with the collimation optics mode B.

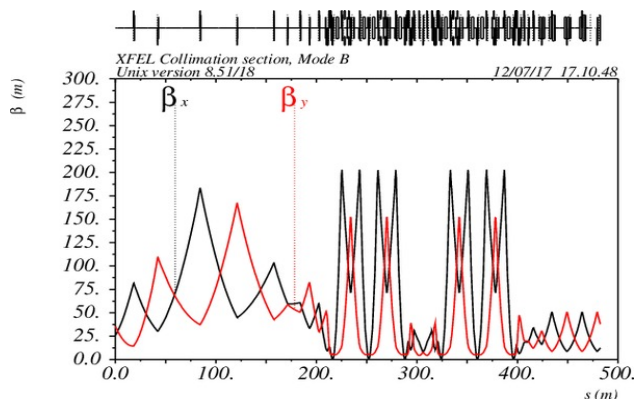


Figure 1: Betatron functions in the collimation section for optics mode B.

WIRE SCANNERS AT THE EUROPEAN XFEL

At the European XFEL, there are in total 4 sets of WSs installed in L3 (before CL), TL (after CL), T1 (before SASE2) and T4 (before SASE3), respectively. Each set of WS consists of three WS units, and each unit has one horizontal and one vertical WS stage. The WSs are installed in the optics matching sections, this allows for emittance measurement and optics matching purposes (especially at high repetition rate) in complementary to the measurements using the scintillation screens [5] (usu-

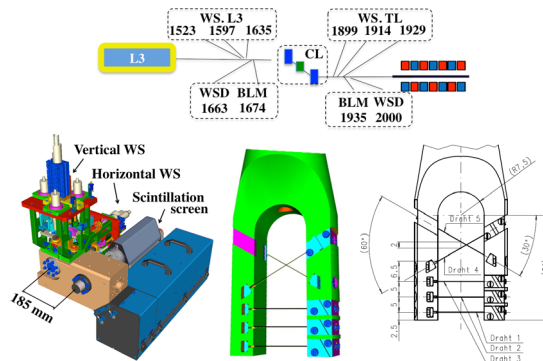


Figure 2: Two WS sets before and after CL section and their detectors (top), the number indicates their location from the gun in meters. Layout of WS stations with scintillation screen layout (bottom-left) and the wire scanner fork with tungsten wires (bottom-right).

[†] shan.liu@desy.de

LONGITUDINAL PHASE SPACE OPTIMIZATION FOR THE HARD X-RAY SELF-SEEDING

S. Liu[†], W. Decking, G. Feng, V. Kocharyan, I. Zagorodnov, DESY, Hamburg, Germany
 G. Geloni, S. Serkez, European XFEL, Schenefeld, Germany

Abstract

For the implementation of Hard X-Ray Self-Seeding (HXRSS) at European XFEL, short electron bunches (FWHM ≤ 50 fs) are preferred to mitigate spatio-temporal coupling effect and to fit to the seeding bump width. Therefore, operations with low charges (< 250 pC) are of interest. Longitudinal phase space optimization has been performed for the 100 pC case by flattening the current distribution. Start-to-end simulations show that, with the optimized distribution, for the photon energy of 14.4 keV, the HXRSS output power, pulse energy and spectral intensity can be increased by a factor of two compared to the nominal working point.

INTRODUCTION

The European XFEL [1] is driven by a superconductive linear accelerator operated with three bunch compressors (see Fig. 1 top) to enable operation with high peak current (~ 5 kA) and low transverse emittance at different charges (20 pC – 1 nC). Since the injector laser pulse length is the same for all the charges, the smaller the charge is, the larger compression is required to keep the same peak current. Different compression scenarios have been studied for the European XFEL to maximize the RF tolerances and minimize collective effects [2-4].

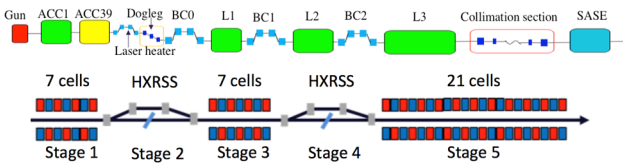


Figure 1: Schematic layout of European XFEL beam line (top) and HXRSS in SASE2 (bottom).

Hard X-ray Self-Seeding (HXRSS) is a well-known scheme to increase the X-ray longitudinal coherence and brightness simultaneously [5]. It has been successfully demonstrated at LCLS in 2012 [6]. The HXRSS at the European XFEL is planned to be implemented in the SASE2 beam line in 2018 (see Fig.1 bottom) [7, 8]. For the implementation of HXRSS at European XFEL, short electron beam bunches (FWHM ≤ 50 fs) are preferred to mitigate spatio-temporal coupling effect [9] and to fit to the seeding bump width. HXRSS simulations have been performed for several cases with different electron beam charges (100 pC and 250 pC) and output photon energies (9 keV-14.4 keV) [10, 11]. In these simulations, the input electron beam distributions used were, however, not fully optimized for self-seeding.

[†] shan.liu@desy.de

One example of the current profile and longitudinal phase space obtained from start to end (S2E) simulation is shown in Fig. 3 (top right, before undulator) for the 100 pC case with the nominal compression parameters. One can see a relatively narrow spike (FWHM ≈ 12 fs) with a peak current of ~ 5 kA. This spike is much more pronounced for lower charges than for higher charges due to the larger compression. Due to this spike, the lower charges suffer more from CSR effects in the bunch compressors, especially in BC2 and in the collimation section, which causes a nonlinear energy distribution along the bunch. The nonlinearity in the longitudinal phase space can seriously deteriorate the HXRSS performance. It results in multi-peaks in the final output power (if tapering is not applied) and in the spreading in photon spectrum. Thus, for the HXRSS, it is preferable to have a “flat top” current distribution, which mitigates the CSR energy loss in the bunch compressors and avoids long head or tails to obtain both higher spectral intensity and pulse energy. In the following sections, we present the study of the longitudinal phase space optimization for the 100-pC case with beam dynamics simulations including HXRSS.

OPTIMIZATION PROCEDURES

At the European XFEL, a third harmonic RF cavity ACC39, which is installed in the injector right after the booster cavity ACC1 (see Fig.1, top), is used to linearize the energy profile and to control the shape of the current profile. The combination of RF parameters of ACC1 and ACC39 defines the 1st derivative p' (chirp), the 2nd derivative p'' (curvature) and the 3rd derivative p''' (skewness) of the momentum p before the first bunch compressor BC0 as follows [3]:

$$\begin{bmatrix} 1 & 0 & 1 & 0 \\ 0 & -k & 0 & -(nk) \\ -k^2 & 0 & -(nk)^2 & 0 \\ 0 & k^3 & 0 & (nk)^3 \end{bmatrix} \cdot \begin{bmatrix} V_{1,1} \cos \phi_{1,1} \\ V_{1,1} \sin \phi_{1,1} \\ V_{1,3} \cos \phi_{1,3} \\ V_{1,3} \sin \phi_{1,3} \end{bmatrix} = \begin{bmatrix} 1 \\ p_0^{(1)} \\ p_0^{(2)} \\ p_0^{(3)} \end{bmatrix} \quad (1)$$

where k is the wave number of the fundamental RF, n is the harmonic number (in our case, $n=3$), $V_{1,1}$, $V_{1,3}$, $\phi_{1,1}$, $\phi_{1,3}$ are the voltage amplitude and phase of fundamental and third harmonic RF, respectively.

The parameter that plays the main role in our optimization is the skewness p''' , since it changes the ratio of compression in different parts of the bunch (i.e. the flatness). After changing p''' , one can adjust the curvature p'' to control the symmetry of the current distribution. Since the goal is to add more compression to the head and tail particles. In the new configuration, we significantly decreased the 3rd derivative p''' from -226.3 to -5.05×10^4 ,

STUDIES OF THE TRANSVERSE BEAM COUPLING IN THE EUROPEAN XFEL INJECTOR

M. Scholz*, B. Beutner, DESY, Hamburg, Germany

Abstract

Coupling between the transverse planes leads to an increase of the horizontal and vertical electron beam emittances. The coupling can be measured with dedicated multi quadrupole scans while the correlations of the beam are observed on a screen. In this paper we show the results from first coupling studies in the European XFEL injector.

INTRODUCTION

SASE FELs like the European XFEL [1] depend strongly on the emittance, thus it is significant to investigate and optimize this parameter. Earlier multi quad scans revealed hints for transverse coupling of the electron beam thus we started further investigations. The technique how to measure the coupling between the transverse planes with multi quadrupole scans was e. g. demonstrated at the SwissFEL Injector Test Facility (SITF) [2]. This method was also used for the coupling measurements in the injector. Additional information can be found in [3]. In this paper, we present measurements of the transverse coupling in the European XFEL injector.

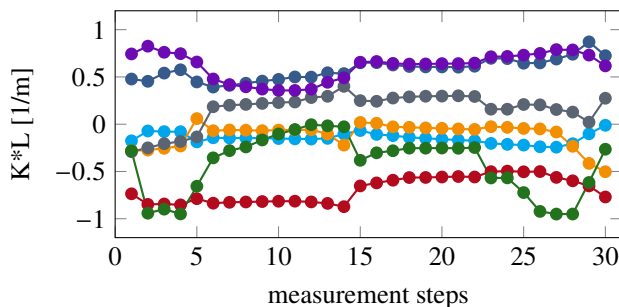


Figure 1: Normalized integrated strength of all quadrupole magnets used for the scan.

EUROPEAN XFEL INJECTOR

A schematic layout of the European XFEL injector is presented in Fig. 4. Two superconducting accelerating modules are installed in the linac, a 1.3 GHz module and the third harmonic module, which operates with 3.9 GHz, to linearize the longitudinal phase space of the particle distributions. The design beam energy downstream these modules is 130 MeV. A subsequent diagnostic section including a transverse deflecting cavity as well as four screens [4] and a spectrometer allow to study the electron beam quality. All quads in the diagnostics section are equipped with individual bipolar power supplies.

* matthias.scholz@desy.de

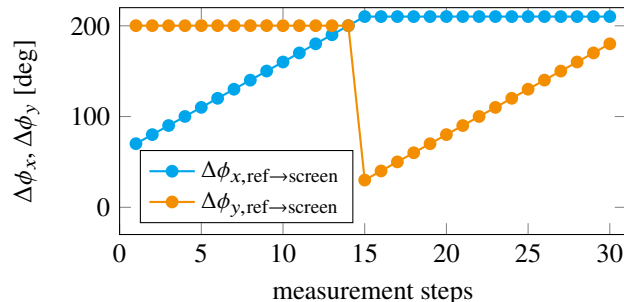


Figure 2: Phase advances in horizontal and vertical plane between optics reference position and the screen plotted for all scan steps.

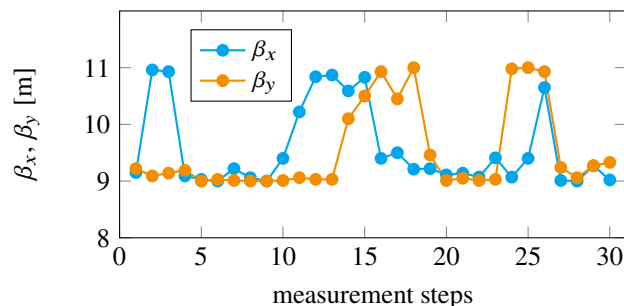


Figure 3: Horizontal and vertical beta functions at the screen for all steps of the phase scan.

MULTI-QUADRUPOLE SCANS

The basic requirements on the quad scan for these measurements is to scan the phase advance between the optics reference position and the measurement screen in one plane over 180 degree (if possible) and keep it constant in the second one. Then the second plane has to be scanned while phase advance in the first plane is constant. In addition, the beam sizes should be kept preferably constant on the screen in order to ensure the same resolution for all measurement steps. A list with $k \times n$ entries of quadrupole strengths, fulfilling the described requirements mentioned above, has to be prepared. The number of measurement steps is k , here $k = 30$, and the number of quads is n , here $n = 7$. All k quadrupole settings are then applied one by one to the machine. For each setting, the transverse particle distribution at the measurement screen is saved for evaluation. For the quad scan discussed in this paper, all 7 quadrupole magnets between the laser heater chicane and the last screen in the diagnostics section were used. Figure 1 shows the integrated strengths of all seven quads and for all 30 measurement steps. The phases advances of the quad scan are shown in Fig. 2.

THE EFFECT OF TRANSVERSE SPACE CHARGE ON BEAM EVOLUTION AND PHOTON COHERENCE

Q. Marksteiner, Los Alamos National Laboratory, Los Alamos, USA

Abstract

An electron beam experiences a transverse electric field which tests to act like a defocusing force on the beam. This defocusing force will act with different strengths at different locations in the electron beam because the current varies along the beam. A single, quasi-analytic method is presented to calculate the impact of this force on beam projected emittance.

INTRODUCTION

The effect of transverse space charge on the transverse emittance of the beam in the MaRIE [1] accelerator is estimated. The dominant effect of transverse space charge is that it causes an extra defocusing term in the electron beam transverse evolution. This defocusing is different at different locations along the electron beam, because electron current is different at different locations of the beam. This will cause the beam to go through different betatron oscillations along the accelerator, which will increase the projected emittance.

THE MaRIE ACCELERATOR

Figure 1 shows a schematic of the MaRIE accelerator [2]. The accelerator consists of three accelerator sections, L1, L2, and L3, with two bunch compressors, BC1 and BC2. The initial current after the photocathode is 15 A. After BC1, the current is compressed to 150 A, and after BC2, the current is compressed to 3 kA. The final energy of the electron beam is 12 GeV. The accelerating gradients of the three sections are all slightly different, with the accelerating gradient in L2 being much lower than the accelerating gradient in the other two accelerator sections. The gradient in L2 is lower because the beam is accelerating off crest in order to provide a chirp for the BC2 bunch compressor.

The effect of the transverse space charge decreases as the beam accelerates, but increases with current. Because of this, the effect of the transverse space charge is strongest right after the bunch compressors.

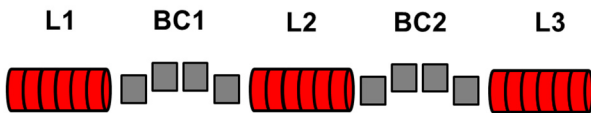


Figure 1: A simple schematic of the MaRIE accelerator.

EQUATIONS OF MOTIONS

Beam Evolution

In order to examine the effect of transverse space charge, we must first look at the transverse dynamics of a single

electron that is being accelerated at a constant rate. The time derivative of the radial component of an electron under the force of a radial electric field is given by $d/dt(\gamma m \dot{r}) = (eE_{r,l})/\gamma^2$. Here \dot{r} is the time derivative of the electron's radial coordinate, $E_{r,l}$ is the radial field, as described in the lab frame of reference, and γ is the relativistic factor.

For a long bunch ($\gamma l \gg a$) with a constant radial current density, given in the lab frame by $\rho_l(z)$ (z is the location along the electron bunch) we can estimate the radial electric field using Gauss's law. Then we have

$$d/dt(\gamma m \dot{r}) = er\rho_l(z)/(2\epsilon_0\gamma^2).$$

Next, we expand out the derivative, replace \dot{r} with $\beta cr'$, substitute in the Alven current $I_A = (4\pi\epsilon_0 mc^3)/e$, replace the current density with the total line current ($\rho_l(z) = I(z)/(\pi R^2 \beta c)$), and rearrange to get:

$$r'' = \frac{2I(z)}{\beta^3 \gamma^3 R^2 I_A} r - \frac{\gamma'}{\gamma} r'. \quad (1)$$

Equation (1) describes the motion of a single electron under acceleration, with no external focusing. We next want to solve for the evolution of the rms value of the radius of the electron beam: $R^2 = \langle r^2 \rangle$, when the electron beam is under constant acceleration. We use the radial envelope equation (3):

$$R'' = \frac{\langle rr'' \rangle}{R} + \frac{\epsilon_r^2}{R^3}. \quad (2)$$

Next, we solve for $\langle rr'' \rangle$. Using equation 1, we get:

$$\langle rr'' \rangle = \frac{2I(z)}{\beta^3 \gamma^3 I_A} - \frac{\gamma'}{\gamma} RR'. \quad (3)$$

Then we can use the approximation that the normalized slice emittance remains constant in an accelerator: $\epsilon_n = \gamma\epsilon$. Plugging this and equation (3) into equation (2) gives:

$$R'' = \frac{2I(z)}{I_A} \frac{1}{R\beta(s)^3\gamma(s)^3} - \frac{\gamma'(s)}{\gamma(s)} R' + \frac{\epsilon_{nr}^2}{\gamma(s)^2 R^3}. \quad (4)$$

Here s represents the distance along the accelerator. Equation (4) can be used to calculate the evolution of electron beams with different values of electron current $I(z)$.

Beam Evolution

In this paper, we analyse the evolution of the transverse size of the electron beam at different locations of the electron beam. We assume that the electron current profile is a Gaussian, given by $I(z) = I_0 \exp(-z^2/(2\sigma^2))$.

DOUBLE-BUNCHES FOR TWO-COLOR SOFT X-RAY FREE-ELECTRON LASER AT THE MAX IV LABORATORY

J. Björklund Svensson*, O. Lundh, Department of Physics, Lund University, Sweden
J. Andersson, F. Curbis, M. Kotur, F. Lindau, E. Mansten,
S. Thorin, S. Werin, MAX IV Laboratory, Lund, Sweden

Abstract

The ability to generate two-color free-electron laser (FEL) radiation enables a wider range of user experiments than just single-color FEL radiation. There are different schemes for generating the two colors, the original being to use a single bunch and two sets of undulators with different K-parameters. An alternative scheme was recently shown, where two separate bunches in the same RF bucket are used for lasing at different wavelengths in a single set of undulators. We here investigate the feasibility of accelerating and compressing a double-bunch time structure generated in the photocathode electron gun for subsequent use in a soft X-ray FEL at the MAX IV Laboratory.

INTRODUCTION

The MAX IV Linear Accelerator \mathbb{T} is a warm S-band electron accelerator serving as full-energy injector for the 1.5 and 3 GeV storage rings [2] as well as the Short Pulse Facility (SPF) [3], where the electron bunches are compressed to 100 fs at an emittance of $\lesssim 1$ mm mrad and a bunch charge of 100 pC. A compact overview of the linac is shown in Fig. 1. The layout of the MAX IV facility is such that the SPF houses three available slots, located downstream of the transfer line to the 3 GeV storage ring. The end of the linac, from the second bunch compressor and downstream, is shown in Fig. 2, with the existing sections and possible extensions on white and orange background, respectively. Simulations indicate that it is possible to compress the bunches to well below 100 fs and still keep the emittance low [4].

The Soft X-ray Laser (SXL) project, currently in the early conceptual design phase, is a collaboration between many Swedish research groups with experience from both user and accelerator sides [5]. The idea is to use one of the SPF beamlines to house a soft X-ray free-electron laser (FEL) operating in the 0.25-1 keV energy range at pulse lengths below 100 fs, paired with unique pumping, detection and imaging schemes. Strong scientific interest has also been expressed towards a two-color radiation operation mode.

Two-color FEL radiation pulses are a way of extending the experimental range at an FEL by producing two radiation pulses with a certain variable separation in energy and time. The original implementation [6] of the concept for X-rays used a single electron bunch and two differently tuned undulator sections to achieve lasing at two different wavelengths, while a more recent development [7, 8] uses two electron bunches, accelerated in the same RF period, and only one

undulator section. Benefits of using the double-bunch technique include allowing both colors to reach saturation intensity and a simpler undulator setup. Double electron bunches can be obtained in a few different ways, but we will focus on generation by tailored laser pulses in the photo-cathode electron gun.

Generating the double-bunch time structure in the photocathode gun at MAX IV would require some additional work on the laser system [9, 10], but no further addition to the accelerator or lattice seems necessary, potentially making this technique a cost-effective extension of the operational capabilities of the SPF. Because of the layout of the facility, see Fig. 2, this could synergetically enable experiments on beam-driven plasma-wakefield acceleration (PWFA) [11]. We have used the particle tracking code *elegant* [12] to simulate the acceleration and compression of a double-bunch beam in the MAX IV Linear Accelerator.

BUNCH COMPRESSION

Compression and Linearization

To compress the bunches longitudinally, the MAX IV linac employs two double achromat compressors, see e.g. [4], which have a positive first-order momentum compaction, R_{56} . This means that a positive chirp, with respect to longitudinal coordinate z , is required for compression. This is achieved with a positive off-crest phase in the RF voltage. The naturally positive second-order momentum compaction, T_{566} , has been optimized with sextupoles in such a way that it cancels out the longitudinal phase-space curvature imposed by the RF field. This means that the phase space linearization is done using the optics alone; no higher-order harmonic cavity is employed. This compressor scheme is simple, reliable and economical.

One effect of this compression scheme is that the first bunch, which arrives closer to the peak of the RF voltage, will in many cases obtain a smaller (and less linear) chirp than the second bunch, particularly in the first linac section, L0-L1b (see Figure 1). This can lead to weaker compression of the first bunch, yielding a beam where the second bunch is shorter than the first. The second bunch curvature can also become over-compensated, leading to asymmetric compression. Part of the tuning process involves minimizing these effects.

Wakefields and Coherent Synchrotron Radiation

Short-range geometric longitudinal wakefields can influence the bunch chirp in the linac [13]. The effects of these wakefields increase with both bunch charge and degree of

* jonas.bjorklund@fysik.lth.se

EXPERIENCE AND INITIAL MEASUREMENTS OF MAGNETIC LINEARISATION IN THE MAX IV LINAC BUNCH COMPRESSORS

S. Thorin, J. Andersson, M. Brandin, F. Curbis, L. Isaksson, M. Kotur,
F. Lindau, E. Mansten, D. Olsson, R. Svärd, S. Werin, MAX IV Laboratory, Lund, Sweden
J. Björklund Svensson, Lund University, Lund

Abstract

The MAX IV Linac is now in routine operation for injection into two storage rings, and as a high-brightness driver for a Short Pulse Facility (SPF). In short-pulse mode the electron bunch is created in a photo cathode gun and compressed in two double achromat bunch compressors that also linearise longitudinal phase space with the second order transfer matrix element T566. T566 in the compressors can be tweaked with weak sextupoles located at high dispersion. In this paper we present the current experience from operating the bunch compressors at MAX IV and results from initial measurements of longitudinal phase space using our version of the the zero-crossing method.

BACKGROUND

The MAX IV facility [1] is the successor of the MAX-lab accelerators at Lund University and include two storage rings, a full energy linac and a Short Pulse Facility (SPF) [2]. The rings are operated at 1.5 and 3 GeV. The SPF is a single pass linac lightsource, producing sub-ps spontaneous X-ray pulses. The linac injector is flexible enough to drive both injection and top-up for the storage rings, and produce high brightness pulses for the SPF. Recently plans for a soft X-ray FEL has developed [3] and the long term strategic plan for the facility include an X-ray FEL. The linac was developed to be fully prepared to handle the high demands for an FEL driver.

The MAX IV linac is now operating mainly to deliver beam to both storage rings and to the Short Pulse Facility. Some commissioning work still remains, to the most part concerning bunch compression.

MAX IV LINAC GENERAL DESIGN

For injection and top up to the storage rings a thermionic gun with a pulse train chopper system is used [4]. In high brightness mode we use a 1.6 cell photo cathode gun capable of producing an emittance of 0.4 mm mrad at a charge of 100 pC [5]. The gun is operated together with a kHz Ti:sapphire laser at 263 nm [6].

The acceleration is done in 39 warm S-band linac sections together with 18 RF units, each consisting of a 35 MW klystron and a solid state modulator. The klystrons are operated at the lower power of 25 MW which reduces the operational cost and gives a total redundancy in energy of 0.6 GeV. The RF power is doubled with a SLED.

The beam is kicked out for injection into the storage rings at 1.5 and 3 GeV. Bunch compression is done in double achromats [7] at 260 MeV and at full energy, 3 GeV, after

extraction to the storage ring. A schematic view of the linac layout can be seen in Figure 1.

Linearising double achromat compressors

The magnetic double achromats used as bunch compressors in the MAX IV injector has a positive R56 unlike the commonly used magnetic chicane which has a negative R56. We have thus to work on the falling slope of the RF voltage. Both types of bunch compressors naturally have a positive T566 and a positive T566 has a linearising effect in the achromat case. We can thus choose the optical parameters in the achromat to get optimal linearisation without needing to have a harmonic linac for this purpose. A sextupole is needed to minimize the second order dispersion at the end of the achromat. This sextupole, positioned at the achromat middle, is rather weak and could be compared with the chromaticity compensating sextupoles in a storage ring.

The natural T566 of the double achromats is actually over-linearising the RF induced curvature and the sextupoles work in the opposite direction of the natural T566, to compensate for the over-linearisation. To achieve full linearisation of longitudinal phase space, the sextupole strength has to be increased. This can be done in such a way that second order dispersion is still closed at the end of the BC, but the energy derivative of dispersion becomes large, leading to increased emittance. For a spontaneous source like the SPF this is however not a problem. But even without over-tuning the sextupoles, a satisfying linearisation can be achieved to produce low emittance pulses, although at a lower peak current.

Table 1: Electron Bunch and Measurement Parameters

Compression energy	265 MeV
Final energy	9.98 GeV
Compression phase	0-50°
Initial electron bunch length rms	3 ps
Charge	100 pC
Dispersion at the screen	0.34 m
Sextupole strength	18/35 m ⁻³

BUNCH LENGTH MEASUREMENT USING A VARIANT OF THE ZERO-CROSSING METHOD

One single achromat will also induce some other second-order effects acting in the transverse direction. Many of the relevant ones are energy-dependent and thus linear in angle or position. The introduction of a double achromat, the

COHERENT TRANSITION RADIATION FROM TRANSVERSELY MODULATED ELECTRON BEAMS

A. Halavanau^{1,2}, D. Mihalcea¹, P. Piot^{1,2}, S. P. Antipov^{3,4}, J. G. Power³, W. Liu⁴,
 E. Wisniewski³, C. Whiteford³, N. Neveu^{3,5}, A. Benediktovitch^{6,7}, A. V. Tyukhtin⁸, S. N. Galyamin⁸

¹ Department of Physics and Northern Illinois Center for Accelerator & Detector Development, Northern Illinois University DeKalb, IL, USA

² Fermi National Accelerator Laboratory, Batavia, IL, USA

³ Argonne Wakefield Accelerator, Argonne National Laboratory, Lemont, IL, USA

⁴ Euclid Techlabs LLC, Bolingbrook, IL, USA

⁵ Illinois Institute of Technology, IL, USA

⁶ Belarusian State University, Department of Theoretical Physics and Astrophysics, Minsk, Belarus

⁷ Center for Free Electron Laser Science, DESY, Hamburg, Germany

⁸ Saint Petersburg State University, Saint Petersburg, Russia

Abstract

A transverse laser-shaping optical setup using microlens arrays (MLAs), previously developed and employed at Argonne Wakefield Accelerator (AWA), allows the formation of both highly uniform and modulated (patterned) beams. In the latter case, transverse modulation is imposed in the sub-millimeter scale. In the present study, we report the simulations of backward coherent transition radiation (CTR) emitted from a transversely modulated beam. We compare the case of a uniform round beam against different transverse modulation wavelengths by generating CTR on a steel target and measuring the autocorrelation function of the resulting radiation with an interferometer. We particularly focus on the differences between round and patterned beam distributions and discuss possible future applications of this setup in THz radiation generation.

INTRODUCTION

Microlens arrays (MLAs) are commonly known in laser technology as light condensers and are often used for transverse laser beam homogenization. An alternative application of the MLAs is the generation of patterned beams that can be used in photoinjectors for multiple purposes [1].

Microlens array consists of periodically placed lenses forming a rectangular, honeycomb, or circular pattern. The resulting modulated light distribution mimics the microlens array geometry. The modulated pattern generated at the photocathode can be preserved and propagated downstream of the accelerator, while the spacing between the beamlets is controlled via solenoid and quadrupole lenses. Such an experimental setup was recently established at Argonne Wakefield Accelerator (AWA) facility [1], see Fig. 1.

Coherent transition radiation (CTR) is commonly used in temporal profile diagnostics [2–8]. An experimental setup usually consists of a retractable metallic screen and radiation diagnostics operating in the THz regime. Such a setup is depicted in Fig. 1 (a) and was recently built at AWA facility.

The goal of this study is to utilize MLA setup to introduce transverse modulation in the electron beam and observe its effect on the resulting CTR spectrum.

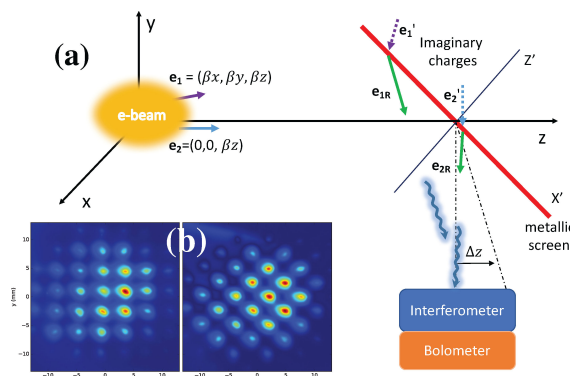


Figure 1: (a) Schematic of the experiment: an electron beam is incident on a metallic screen positioned at 45 deg. The resulting transition radiation photons are received in bolometer via interferometer transport to perform an auto-correlation scan. (b) An example of MLA-formed electron beam patterns observed at $\gamma = 100$.

SIMPLIFIED ANALYTICAL CALCULATION

A detailed analytical derivation of the transition radiation from a point charge as a solution of Maxwell's equations between two media can be found in classical textbooks [9, 10]. The electromagnetic field of a point charge falling onto a metallic plate can be calculated using the “method of images” [11], where for every charge incident on an infinite plane (q, \mathbf{e}_i) there is a “mirror” charge (q', \mathbf{e}'_i) behind the plane forming a pair of real and image charges. When a virtual pair of charges approaches the plane, it emits radiation that is mathematically equivalent to the transition radiation from a point charge [10]¹.

¹ Additionally, an analytical expression for a TR EM-field in case of a finite metallic plane can be found in [12].

Content from this work may be used under the terms of the CC BY 3.0 licence (© 2018). Any distribution of this work must maintain attribution to the author(s), title of the work, publisher, and DOI.

BEAM-DYNAMICS ANALYSIS OF LONG-RANGE WAKEFIELD EFFECTS ON THE SCRF CAVITIES AT THE FAST FACILITY*

Young-Min Shin[#], Northern Illinois Univ., Dekalb, IL, and FNAL, Batavia, IL, USA

Randy M. Thurman-Keup, Jinhao Ruan, Alex H. Lumpkin, FNAL, Batavia, IL, USA

Frank L. Krawczyk, Kip A. Bishofberger, Bruce E. Carlsten, LANL, Los Alamos, NM, USA

Abstract

Long-range wakefields in superconducting RF (SCRF) cavities create complicated effects on beam dynamics in SCRF-based FEL beamlines. The driving bunch excites effectively an infinite number of structure modes (including HOMs) which oscillate within the SCRF cavity. Couplers with loads are used to damp the HOMs. However, these HOMs can persist for long periods of time in superconducting structures, which leads to long-range wakefields. Clear understanding of the long-range wakefield effects is a critical element for risk mitigation of future SCRF accelerators such as XFEL at DESY, LCLS-II XFEL, and MaRIE XFEL. We are currently developing numerical tools for simulating long-range wakefields in SCRF accelerators and plan to experimentally verify the tools by measuring these wakefields at the Fermilab Accelerator Science and Technology (FAST) facility. A particle-in-cell (PIC) simulation model for the FAST 50 MeV beamline indicates strong bunch-by-bunch variations of beam parameters with the operating conditions at 9 MHz bunch rep-rate along a macro-pulse and 500 pC, 1 nC, and 2 nC per bunch. This paper previews the experimental conditions at the FAST 50 MeV beamline based on the simulation results.

INTRODUCTION

An ILC type cryomodule, consisting of nine 1.3 GHz, 9-cell SCRF cavities, is considered standard for future SCRF accelerators. The XFEL at DESY in Germany and the LCLS-II XFEL in USA are being constructed with these cryomodules with only minor modifications and the same cryomodule is included in the pre-conceptual design of the MaRIE XFEL. In such SCRF cavities, the driving bunch excites effectively an infinite number of structure modes (including higher-order modes (HOMs)) which oscillate within the superconducting cavity, with some even propagating into other cavities. Couplers with loads are used to damp the HOMs. However, these HOMs can persist for long periods of time in superconducting structures, which leads to long-range wakefields. The signals measured via a HOM-detector [1] indicated that the ILC HOM dampers do not act fast enough to damp out the long-range wake-fields and their effects need to be considered for closely spaced electron bunches. Energy in the HOMs clearly persists for at least a few μ secs, and is particularly large over the first few 10^3 's of nanosecs after

the drive bunch, which is the time scale for the bunch spacing within burst pulses of high rep-rate X-Ray FELs, e.g. MaRIE XFEL.

Particle tracking simulations with the numerical code Lucretia [2] indicated that HOM couplers are not capable of damping all HOMs: while some are well damped, a limited number of modes remain poorly damped. In this calculation, only the five modes most destructive to the beam are damped to the level of $Q = 10^5$, with the rest of modes having $Q = 10^6$. A train of 500 bunches was injected at a 3 MHz repetition rate and with an offset of 6 μ m. Tracking this beam through the linac indicated that a single 9-cell cavity would generate 3 - 5 % of emittance growth for the bunches at the end of the train, which is catastrophic, given that there are on the order of a thousand cavities in a linac for an XFEL and even more for a collider. The duration of the HOM power and its possible effect on an electron bunch from this scoping calculation strongly indicate that more detailed analysis and measurements are needed. Importantly, the alignment of individual cavities in the ILC cryomodules is limited to about 0.2 mm due to the fabrication technique, far larger than the offset used in this scoping calculation.

The experiment to verify the long-range wake effect for the first time was planned at the FAST facility. The beamline consisting of two SCRF capture cavities and a full 8-cavity ILC cryomodule is designed to operate with up to 3000 bunches per macro-pulse, up to 9 MHz in bunch repetition rate, and up to 3 nC per bunch at beam energies from 50 MeV to 300 MeV with several high-resolution beam diagnostics tools, including BPMs and a streak camera. The facility fits well for the long-range wakefield experiment. The experiment is currently scheduled for the 2017 FAST runtime.

As a part of the plan, we have been developing simulation tools for accurately assessing SCRF long-range wakefield effects on beam dynamics and comparing it to the diagnostic capabilities at the FAST 50 MeV beamline. Bunch-to-bunch deviations of the longitudinal and transverse beam profiles are analyzed for the current FAST beamline setup. In this paper, the simulation results are discussed with the measurable range of the instruments installed in the 50 MeV beamline.

OVERVIEW

In the FAST beamline (Fig. 1), the two capture cavities (CC1 and CC2) are ILC superconducting cavities. Last year beam commissioning was conducted through the diagnostic stations after CC2 (with up to a 50-MeV electron beam). The 9-cell cavities, operating with 25

* Work supported by the subcontract (contract No: G2A62653) of LANL-LDRD program and DOE contract No. DEAC02-07CH11359 to the Fermi Research Alliance LLC.

[#] yshin@niu.edu

MODELING AND OPTIMIZATION OF THE APS PHOTO-INJECTOR USING OPAL FOR HIGH EFFICIENCY FEL EXPERIMENTS*

C. C. Hall[†], D. L. Bruhwiler, S. W. Webb, RadiaSoft LLC., Boulder, USA
Y. Sun, A. Zholents, Argonne National Laboratory, Argonne, IL, 60439, USA
P. Musumeci, Y. Park,
Department of Physics and Astronomy, UCLA, Los Angeles, California 90095, USA
A. Murokh, RadiaBeam Technologies Inc., Santa Monica, CA 90404, USA

Abstract

The Linac Extension Area (LEA) is a new beamline planned as an extension of Argonne's APS linac. An S-band 1.6-cell copper photo-cathode (PC) RF gun has been installed and commissioned at the APS linac front end. The PC gun will provide a beam to the LEA for accelerator technology development and beam physics experiments, in interleaving with a thermionic RF gun which provides a beam for APS storage ring operations. Recently an experiment was proposed to demonstrate the TESSA high-efficiency concept at LEA. In support of this experiment, we have begun simulating the photo-injector using the code OPAL (Object-oriented Particle Accelerator Library). In this paper, we first benchmark OPAL simulations with the established APS photo-injector optimization using ASTRA and ELEGANT. Key beam parameters required for a successful high-efficiency TESSA demonstration are discussed.

OVERVIEW

The Advanced Photon Source (APS) linac provides electrons at up to 500 MeV for operation of the APS storage ring. The end of the APS linac beamline has been extended to create a new beamline called the Linac Extension Area (LEA) that will be fed by an alternate photo-injector operating in-between top-up cycles for the synchrotron. The LEA beamline will serve as an area for performing a variety of experiments requiring flexible, high-brightness electron beams.

* Work supported by the United State Department of Energy, Office of Scientific Research, under SBIR contract number DE-SC0017161.

[†] chall@radiasoft.net

The Tapering Enhanced Stimulated Superradiant Amplification (TESSA) concept [1] is a novel FEL scheme that allows for extremely high extraction efficiencies (as much as 50%). Design of an undulator to test the TESSA concept at 266 nm is underway, with plans to perform a proof-of-principle experiment at the LEA beamline.

We will discuss simulation studies of the photo-injector and APS linac to ensure that sufficient beam quality can be achieved to meet requirements for TESSA. We first show comparisons between the code ASTRA, previously used for the injector modeling, and OPAL, which is now being used. We then look at the electron beam requirements for TESSA and some of the challenges to meeting these requirements.

LEA and the APS Linac

The APS linac, shown in Fig. 1, serves as the start of the accelerator chain feeding the APS light source. When operating in this capacity a thermionic rf gun (RG2) is used, electron bunches are accelerated to 450 MeV in the linac and fed into the booster. During normal top-up operation the linac is only used for twenty seconds every two minutes. During the downtime on this interval the linac will be used to feed electron bunches from the photocathode gun (PCG) to the Linac Extension Area (LEA). The timing structure for LEA/APS operation is shown in Fig. 2.

Beam from the PCG will reach the L2 linac at 40 MeV where it will then be using the same lattice as beam from thermionic guns. Previous efforts at APS have optimized lattice settings that can accommodate the disparate properties of both PCG and RG2 beams [2]. From L2 the beam is

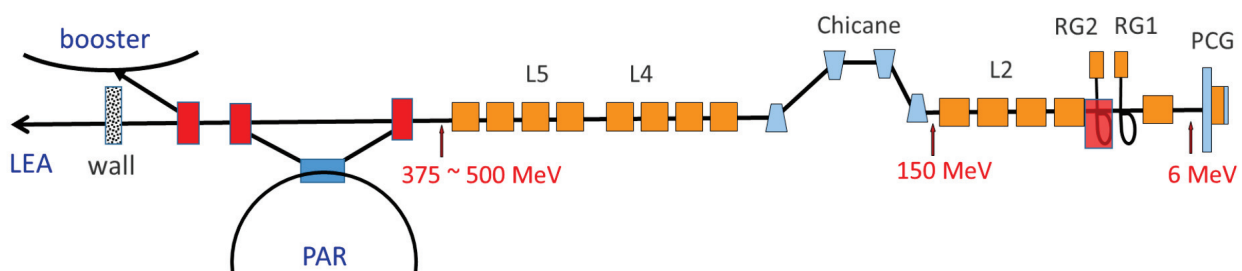


Figure 1: Schematic of the APS beamline showing the thermionic rf guns (RG1 and RG2), photocathode gun (PCG), accelerating sections (L2, L4 and L5), and Linac Extension Area (LEA) at the end of the beamline.

Content from this work may be used under the terms of the CC BY 3.0 licence (© 2018). Any distribution of this work must maintain attribution to the author(s), title of the work, publisher, and DOI.

RECENT DEVELOPMENTS AND PLANS FOR TWO BUNCH OPERATION WITH UP TO 1 μs SEPARATION AT LCLS*

F.-J. Decker, K.L.F. Bane, W. Colocho, A.A. Lutman, J.C. Sheppard, SLAC, Menlo Park, USA.

Abstract

Two electron bunches with a separation of up to 1 μs at the Linac Coherent Light Source (LCLS) is important for LCLS-II developments. Two lasing bunches with up to 220 ns separation have been demonstrated. Many issues must be solved to get that separation increased by a factor of 5. The typical design and setup for one single bunch has to be redressed for many devices. RF pulse widths must be widened, BPM diagnostics can see only one bunch or a vector average, feedback systems must be doubled, the main Linac RF likely needs to be un-SLEDed, and special considerations must be done for the Gun and L1X RF.

INTRODUCTION

Since the first two bunch test in 2010 [1], many photon experiments have been performed in recent years [2,3]. They can be categorized into pump-probe and probe-probe experiments. The first typically excites the sample and then probes it, using different photon energies for the two bunches, the first above and the second below an absorbing K-edge. Probe-probe experiments have identical bunches only differentiated by arrival time. They study the natural time evolution of the sample without disturbing it with the first pulse.

SHORTER BUNCH SEPARATION

Operation up to about 25-ns bunch separation is already considered “standard” procedure. However, attention is needed as different experiments require special setups. A typical setup for probe-probe experiments is described followed by a description of pump-probe setups, wherein the first bunch typically has a higher photon energy above a K-edge and is absorbed while the lower energy second bunch goes through and its scattering pattern is detected.

Same Bunch Performance, Just Delayed

To make two bunches with different time separation, two pulses from independent lasers are combined on the cathode, typically in S-band bucket intervals (0.35 ns). When they overlap in time, an interference pattern is generated on the gun cathode (see Fig. 1 in Ref. [4]); the temporal overlap reduces the total charge emitted from cathode by 10%. The BPM response for different delays shows a beating, determined to be an artefact of the BPM processing frequency (1/140 MHz = 7 ns) (see Fig. 2 in Ref. [4]) [5].

RF Setup The RF timing must be set up so that the two bunches have a flat energy gain versus time, this is especially problematic for long separations (over 100 ns).

Wakefield Kicks It was observed that at certain bunch separations the second bunch did not lase (Fig. 1). The rms beam trajectory in the undulator must be less than 40 μm to produce significant FEL energy.

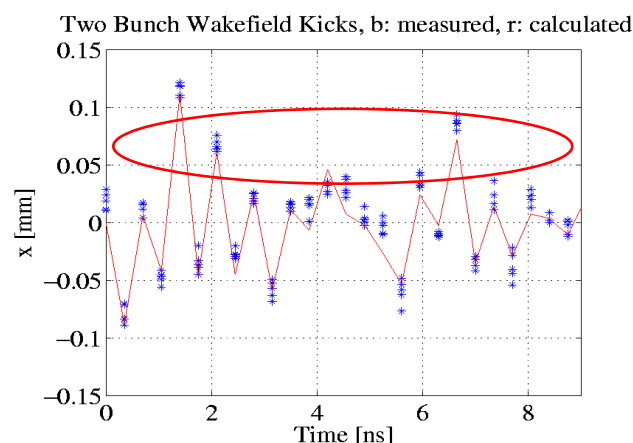


Figure 1: Timing scan of the second bunch. At certain bunch separations, the second bunch gets kicked by wake-fields and has therefore enough transverse displacement in the undulator so that it does not produce FEL radiation.

A two-mode wakefield calculation predicted a too simplistic picture of the transverse kick which slowly increases up to 2.5 ns, then decoheres around 5 ns, and recoheres afterwards [6]. The observed behaviour was consistent with the 5-ns decoherence where both bunches typically lase. But the kicks are more complicated (see Fig. 3 in Ref [4]). With a two-bucket separation, both bunches always lase since the second bunch does not get kicked. A new time-domain wakefield calculation revealed that modes 3, 6 and 10 are important and produce the observed kicks. The peak wakefield at 1.4 ns is $W_x = -2\text{V}/(\text{pC}\cdot\text{m}\cdot\text{mm})$ for an S-band structure. The X-band cavity, L1X, has 16 times larger transverse wakefields, which decohere faster; the only significant effects are at one and two bucket separation ($W_x = +38$ and $-16 \text{ V}/(\text{pC}\cdot\text{m}\cdot\text{mm})$).

* Work supported by U.S. Department of Energy, Contract DE-AC02-76SF00515.

Content from this work may be used under the terms of the CC BY 3.0 licence (© 2018). Any distribution of this work must maintain attribution to the author(s), title of the work, publisher, and DOI.

STOCHASTIC EFFECTS FROM CLASSICAL 3D SYNCHROTRON RADIATION

B. Garcia*, T. O. Raubenheimer, SLAC, Menlo Park, USA
 R. Ryne, Lawrence Berkeley National Laboratory, Berkeley, USA

Abstract

In most cases, the one-dimensional coherent synchrotron radiation wakefield gives an excellent approximation to the total coherent effect due to classical synchrotron radiation in bend magnets. However, full particle Liénard-Wiechert simulations have revealed that there is non-numerical, stochastic noise which generates fluctuations about the approximate 1D solution. We present a model for this stochastic term in which this noise is due to long-range interaction with a discrete number of synchrotron radiation cones. The nature of this noise and how it depends on the 3D dimensions of the beam are explored.

INTRODUCTION

Much study has focused on the so-called Coherent Synchrotron Radiation (CSR) effect in bend magnets [1] [2] [3] [4]. Radiation from the tail of the electron bunch catches up with the head electrons where it exchanges energy with them. This leads to a well-known, one-dimensional wakefield which is a deterministic function of the longitudinal distance along the bunch.

While this wakefield is often undesirable and can lead to emittance growth in bend magnets [5], it is a deterministic function and can therefore in principle always be removed. Other effects which can cause emittance degradation are stochastic in nature, and thus provide an irreversible heating of the beam. Two effects are especially important in the context of bending magnet systems: Incoherent Synchrotron Radiation (ISR) [6] and Intra-Beam Scattering (IBS) [7]. ISR is caused by the quantum nature of the synchrotron radiation emission process, and its effect on the beam grows strongly with electron beam energy. By contrast, IBS is caused by multiple small-angle Coulomb scattering events and increases with electron beam density.

Computational results in the past few years have suggested that the CSR wakefield result also contains a stochastic component [8] [9]. Recently, an analytical model has been developed which explains this stochastic noise term [10]. The goal of this paper is to compare the analytical theory with computational results obtained from full 3D Liénard-Wiechert simulations.

THEORY OVERVIEW

The full theory on the stochastic origin of the CSR noise is presented in [10], so we first briefly present the main results. The analytical theory is based on a 3D extension of the steady state two-dimensional CSR model developed

by Huang, Kwan, and Carlsten [11]. In this work they noticed a long-ranged, narrow cone of longitudinal synchrotron radiation trailing behind the electron. It is this feature of the radiation profile which is ultimately responsible for the noise.

We describe the electron bunch and radiation via the scaled coordinates $\alpha = s/R$, $x = \chi/R$, and $y = \Upsilon/R$, where s is the arclength along a circular trajectory of radius R , χ is the physical radial displacement, and Υ the physical vertical displacement. It is found that this long-ranged longitudinal radiation component has magnitude $E_s^T \approx \frac{-q\beta^2\gamma^4}{\pi\epsilon_0 R^2}$ for a beam with relativistic factor γ . The net effect of this region integrated over a uniform electron beam is found to be zero. However, counting statistics on the number of particles contained within this region leads to a stochastic variation in the total field.

This field region does not decay in the radial dimension but opens up in the vertical plane. This leads to two distinct regimes characterized by the parameter $\Xi \equiv \frac{\gamma^4\sigma_y^4}{\sigma_x^2}$, where $\sigma_{x,y}$ are the (scaled) rms beam sizes for a Gaussian electron distribution. The case of $\Xi \ll 1$ is essentially a 2-D beam, while for $\Xi \gg 1$ the beam's vertical size is much larger than the radiation extent.

The probability f that an electron in a group of N_p electrons will be contained within the trough can be computed analytically. There will therefore be a variance in the total (longitudinal) field due to this finite number of contained electrons which can be expressed as,

$$\sigma_{E_s} = g E_s^T \sqrt{f N_p}, \quad (1)$$

where g is an $O(1)$ geometric factor related to the non-constant value of the field across the trough ($g = 4/9$ for a parabolic profile, for example). While the exact expression is complicated, the scaling of this field variance with energy can be written down in the two Ξ regimes as,

$$\sigma_{E_s} \sim \begin{cases} \gamma^2 & \Xi \gg 1 \\ \gamma^{2.5} & \Xi \ll 1 \end{cases}. \quad (2)$$

The above result is derived for the variations in the field at the center of the electron bunch. However, one can easily generalize the electron fraction f for an off-radial electron with displacement $a = x/\sigma_x$. The resulting ratio of f factors

Content from this work may be used under the terms of the CC BY 3.0 licence (© 2018). Any distribution of this work must maintain attribution to the author(s), title of the work, publisher, and DOI.

* bryantg@stanford.edu

CANCELLATION OF COHERENT SYNCHROTRON RADIATION KICKS AT LCLS

D. Z. Khan[†], T. O. Raubenheimer, SLAC, Menlo Park, USA

Abstract

In this paper, we look at a phase advance manipulation technique used for the Coherent Synchrotron Radiation (CSR) emittance growth cancellation pioneered by D. Douglas [1]. The idea was then further developed by R. Hajima in the matrix formalism and later extended in the Courant-Snyder formalism by S. Di Mitri [2,3]. With the ever-growing demands of high energy, short wavelength Electron Storage Rings (ESR) and Free Electron Laser (FEL) drivers, the CSR effect has proven to be a detrimental factor in emittance stability. Under linear approximation, it has been shown that the CSR induced dispersive kicks in successive bending magnet systems can, with careful balancing of the linac optics, cancel each other to nullify the bend plane emittance growth. This technique of optics balancing in the constant bunch length regime is the focus of this paper. We will present our findings, analytically and numerically, of the emittance measurements for the current Linac Coherent Light Source (LCLS) dogleg system (DL2).

INTRODUCTION

Bending systems in linear accelerators are essential for beam transport and bunch compression. When electrons travel in curved orbits in the bending magnets of an accelerator they emit synchrotron radiation [4]. For longer bunches, the electrons radiate independently and the radiation is incoherent with a power scaling of N , the number of electrons in the bunch. The situation is vastly different when the bunch length becomes ultra-short and comparable to the radiation's wavelength; the electrons begin to radiate as a unit and the radiation is coherent with a power scaling of N^2 . The dramatic increase in radiation power for the coherent case has the ability to induce a sizable energy chirp along the beam which will, consequently, dilute the transverse emittance of the beam as its transported through the linac [5]. Conserving the transverse emittance is essential in delivering high brightness electron beams. The CSR radiation induces a variation of the electron energy that is correlated along the longitudinal bunch coordinate (barring transverse effects). It is in this correlation that we may manipulate and attempt to suppress the CSR driven transverse emittance dilution.

The LCLS at the Stanford Linear Accelerator Center (SLAC) is one of the world's premiere X-ray free-electron laser (XFEL) facilities. It is the source of the brightest coherent radiation in the sub-nanometer wavelength regime and has remarkable capabilities in the bio-

logical, chemical, material science and the molecular research fields [6-8]. After injection, the beam transport line consists of a two-stage bunch compression system with three accelerating sections, as shown in Figure 1. The bunch length at the second bunch compressor is short ($\sim 10 \mu\text{m}$) and the radiation emitted in the dipoles is coherent for the wavelengths comparable to the electron bunch length.

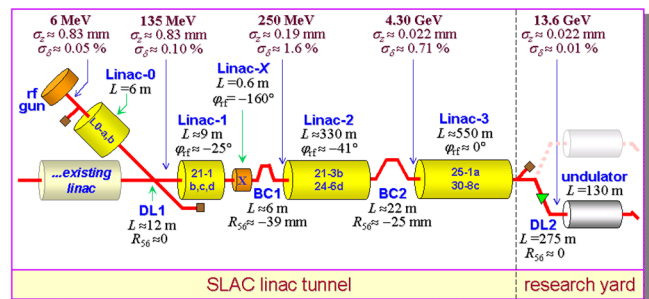


Figure 1: LCLS beamline schematic.

At the end of the 3rd linac section is a dogleg (DL2) bending system implemented to transport the electron bunch to the undulator beamline. It is at this location where we will conduct our studies of CSR emittance growth cancellation via optics balancing. As we will see, with careful balancing of the optics in between the dispersive CSR kicks in BC2 and DL2, we can orient the kicks to cancel each other and preserve transverse emittance along the beam line.

OPTICS BASED BALANCING OF CSR DISPERSIVE KICKS

We first acquaint ourselves with Hajima's first order matrix approach to the analysis of CSR induced transverse emittance growth [3]. To the first order, the bend plane space coordinates can be written as $x(s) = (x, x', \delta_0, \kappa L_B, \kappa)^T$ where x is the deviation from the on energy path, x' is derivative of the deviation with respect to the ideal path, δ_0 is the initial relative energy deviation, L_B is the magnet length, and κ is the normalized CSR wake potential in a bend magnet measured in [eV/m]. In this formalism, the CSR energy deviation is found by $\delta_{\text{CSR}} = \kappa L_B$. When a particle gains or loses energy within a bending system, its transverse coordinates are altered with respect to the on-energy path as $\Delta x = R_{16}\delta$ and $\Delta x' = R_{26}\delta$, where the matrix terms R_{16} and R_{26} are the first order dispersion and its slope. The corresponding bend magnet matrix can then be constructed via the Green's function method to include the effect of CSR [9]:

*Work supported by the U.S. Department of Energy under contract No. DE-AC03-76SF00515

[†] donish@SLAC.stanford.edu

APPROXIMATED EXPRESSIONS FOR THE COHERENT SYNCHROTRON RADIATION EFFECT IN BENDING MAGNETS

D. Z. Khan[†], T. O. Raubenheimer, SLAC, Menlo Park, California, USA

Abstract

In today's X-ray free-electron laser (XFEL), the ultra-bright radiation's strict dependence on emittance has motivated research on advanced electron accelerator techniques. Understanding mechanisms borne in the linac that could jeopardize FEL radiation is important to ensure maximal potential of the machine. One such mechanism, is the Coherent Synchrotron Radiation (CSR) effect. The effect is prominent in latter stages of the linac where the bunch length is short, the peak current is high and the synchrotron radiation emitted in curved sections is temporally coherent. Though, the CSR effect has been comprehensively studied, it still must be quantified for any accelerator system, and requires care in circumventing [1-9].

In this paper, we describe the development of simple and compact analytic expressions for the relative CSR RMS induced energy spread resulting from two typical bending magnet situations in electron particle accelerators. The expressions are compared with the CSR wake field integral expressions derived for a electron bunch with arbitrary linear density, λ_s [10, 11]. Then, the accuracy of each expression is compared against ELEGANT's CSR computational algorithm with the simulation of several idealized examples [15].

INTRODUCTION

The standard derivation of the CSR wakefield begins with the Liénard-Wiechert fields for two electrons traveling along the *same* circular trajectory, ignoring any transverse extent of the beam [10]. The energy transfer due to the electric field of the trailing electron onto the advancing electron is simply given by $dE/d(ct) = e\vec{\beta} \cdot \vec{E}$. The wakefield is inversely proportional to the distance between the two electrons and contains a singularity when the electron separation approaches zero. The singularity is removed by the "normalization process" developed by Saldin *et al.* [10] by subtracting off the contribution of two electrons along a straight-line trajectory. The resulting two electron kernel for the CSR wakefield can then be integrated over any longitudinal bunch distribution to give the collective effect under a wide range of scenarios one might find in a typical accelerator environment. In particular, we concern ourselves with two highly prominent cases found in XFEL applications: First, a linearly chirped electron bunch entering a bending magnet and compressing into the steady-state regime, and second, an electron bunch exiting a bend into the subsequent drift section, both cases of which, are in the ultra-relativistic regime ($\gamma \rightarrow \infty$). The complete mathematical expressions

for the two situations under the 1-D projected model are as follows [10]:

$$\frac{dE}{dz} \Big|_{\text{bend}} = \frac{4}{R\phi} (\lambda(s - S_L) - \lambda(s - 4S_L)) + \dots \frac{2}{(3R^2)^{\frac{1}{3}}} \int \frac{d\lambda(s')}{ds'} \left(\frac{1}{(s-s')^{\frac{1}{3}}} \right) ds' \quad (1)$$

$$\frac{dE}{dz} \Big|_{\text{drift}} = \frac{4}{R} \left(\frac{\lambda(s-S_M)}{\theta_B + 2x} \right) + \dots \frac{4}{R} \left[\int \frac{d\lambda(s')}{ds'} \left(\frac{1}{\phi + 2x} \right) ds' \right] \quad (2)$$

where R is the bending radius, θ_B is the total bend angle, x is the subsequent drift coordinate, ϕ is the bend angular displacement, λ_s is the normalized longitudinal distribution of the bunch, s and s' are the internalized bunch coordinate of the front and back electron, respectively, and S_L , S_M are the slippage conditions inside the bend and in the subsequent drift, respectively [11]. In the ultra-relativistic regime, the slippage conditions reduce to:

$$S_L = s - s' = \frac{R\phi^3}{24} \quad (3)$$

$$S_M = s - s' = \frac{R\phi^3}{24} \frac{R\phi + 4x}{R\phi + x} \quad (4)$$

The RMS energy deviation (normalized to the beam energy) that the CSR induces onto the bunch is an important parameter in beam dynamics. Let us now look at the induced CSR energy spread for the specific case of an electron bunch traversing a bending magnet. In this case, when the bunch is fully contained in the magnet, all trailing electron fields will catch-up and interact with advancing electrons (for a given "s" coordinate) and the slippage condition effectively approaches infinity, $S_L \rightarrow \infty$. Under this condition, the first two terms on the right of eq. 1, the "transient" terms, tend to zero and the lower bound of the integral spans the entire bunch tail domain i.e. the energy transfer is constant along the trajectory dz . In this steady-state regime, the relative CSR RMS energy spread induced on a beam with a Gaussian longitudinal distribution was derived to be [12]:

$$\sigma_{CSR} = 0.22 \frac{r_e N L_B}{\gamma \rho^{2/3} \sigma_s^{4/3}} \quad (6)$$

The above expressions can also take into account the evolution of the longitudinal profile of the electron bunch in compression scenarios assuming that the bunch length is short compared to the slippage. We substitute the constant σ_s terms with one that evolves via the R_{56} of the system and energy chirp, h , of the beam to incorporate

*Work supported by the U.S. Department of Energy under contract No. DE-AC03-76SF00515

[†] donish@SLAC.stanford.edu

AN EMITTANCE-PRESERVATION STUDY OF A FIVE-BEND CHICANE FOR THE LCLS-II-HE BEAMLINE

D. Z. Khan[†], T. O. Raubenheimer, SLAC, Menlo Park, CA, USA

Abstract

The Linac Coherent Light Source II (LCLS-II) is an upgrade intended toward advancing on the great success of its predecessor, LCLS, to maintain its position at the forefront of X-ray science. The introduction of a niobium metal superconducting linac for LCLS-II not only increases the repetition rate to the MHz level (from 120 Hz) but also boasts an average brightness many orders higher ($\sim 10^4$) than that of LCLS. Though, these improvements do not come without a price: the peak brightness suffers by a factor of 10 in part due to the impact of Coherent Synchrotron Radiation (CSR) diminishing the peak current of the beam in the second bunch compressor (BC2) [1]. In this paper, we discuss the impact of implementing a plug-compatible 5-bend chicane for BC2 on the beam's emittance dilution for a high energy, low emittance configuration of LCLS-II (LCLS-II-HE). The results are compared with that of a standard 4-bend chicane under various settings in ELEGANT and CSRTrack [2, 3].

INTRODUCTION

The detrimental effects of CSR in the accelerator environment is one of most challenging problems to study, let alone counter, for current free electron laser (FEL) facilities. The CSR energy chirp induced by the beam onto itself from traveling along arced sections of the beam line has direct consequences on the beam's bend-plane emittance. The issue is exacerbated by the push to produce even shorter and more compact electron bunches for ultra-brilliant FEL radiation in the X-ray regime at facilities such as the European XFEL at DESY, Spring-8 Angstrom Compact Free Electron laser (SACLA), Pohang Accelerator Laboratory X-ray Free Electron Laser (PAL-XFEL) and the LCLS-II, which is currently being construction. The ceiling of producing such radiation is in the painstaking details of the beam transport line, in particular, the latter stage bunch compression systems [4]. Many techniques have been researched and developed but, as the limits are continually pushed, new solutions are needed to adjust with the demand.

LCLS-II HIGH ENERGY (HE)

The LCLS-II high-rate FEL can generate X-ray pulses from 200 eV to 5 keV at MHz repetition rates [5]. The electron beam for the FEL is generated in an RF gun and accelerated in a superconducting RF (SCRF) linac to a beam energy of 4 GeV. While the beam is accelerated, it is compressed to a peak current of 400 to 1000 Amps,

depending on the bunch charge. Over much of the photon energy range, the LCLS-II electron beam will generate X-rays with peak powers of roughly 10 GW [6].

While the average brightness of the LCLS-II X-ray laser will be many orders-of-magnitude higher than that of the LCLS operating at 120 Hz, the peak brightness will be a factor of 10 or more lower. For comparison, the LCLS routinely produces X-ray pulses with over 200 GW using a 5 kA electron bunch and beam shaping techniques [7].

There are two reasons for the relatively poor peak performance of the LCLS-II: first, the peak current of the LCLS-II electron bunch is 5 to 10 times lower than that in the LCLS and, second, the beam energy is a factor of 2 to 3 times lower than that in the LCLS. The reduced peak current is largely due to the impact of Coherent Synchrotron Radiation (CSR) and Longitudinal Space Charge (LSC) which are exacerbated by a lower beam energy at the second bunch compressor (BC2) of 1.6 GeV versus roughly 5 GeV. These effects are further amplified in the 2-km long bypass transport line which, at the 4 GeV beam energy, lead to a significant micro-bunching instability [8].

To extend the photon energy range to upwards of 20 keV and improve the X-ray pulse performance, the LCLS-II-HE was proposed with a high energy upgrade from 4 to 8 GeV and a possible lower beam emittance where the gun emittance is reduced from 0.4 to 0.1 μm . The upgrade will increase the beam energy in the 2 km Bypass line from 4 to 8 GeV, significantly reducing the impact of the largest LSC contribution. However, the energy of BC2 will be roughly the same, increasing from 1.6 to 1.9 GeV, leaving the impact of CSR on the beam comparable and diluting the beam emittance significantly. In December 2016, the LCLS-II-HE concept received CD0 from the DOE. Further details on the upgrade can be found in the supporting documentation at https://portal.slac.stanford.edu/sites/conf_public/lclsiihe2017/Pages/default.aspx.

LCLS-II Bunch Compressor 2 (BC2)

The LCLS-II second stage bunch compressor, BC2, is a standard 4-bend chicane with its main features listed in Table 1. It is responsible for the final compression of the beam before its transported to the undulators. It is here that the peak current reaches its maximum value thus making BC2 a salient area for CSR driven emittance growth.

Current methods for mitigating BC2's CSR emittance growth are centered on linac optics optimization. First method of which, balances the RF chirp, $h = (1/E_0) (dE/dz)$, and the compression factor amongst the bunch compressors to find a minimization of the CSR induced emittance growth. Generally, allocating the linac's R_{56} , so that much of the compression work can be done

*Work supported by the U.S. Department of Energy under contract No. DE-AC03-76SF00515

[†] donish@SLAC.stanford.edu

DESIGN OF A DOGLEG BUNCH COMPRESSOR WITH TUNABLE FIRST-ORDER LONGITUDINAL DISPERSION

W.K. Lau, N.Y. Huang, M.C. Chou, A.P. Lee, NSRRC, Hsinchu, Taiwan
 J. Wu, SLAC National Accelerator Laboratory, Menlo Park, CA 94025, USA

Abstract

A nonlinear bunch compressor has been designed for the proposed NSRRC VUV FEL facility. It is a double dog-leg configuration that provides a first order longitudinal dispersion function (i.e. R_{56}) with a sign opposite to that of a conventional four-dipole chicane. A large variation in the bunch length or the peak current for various operation conditions can be done by tuning R_{56} . This can be realized by changing the longitudinal positions of the outside dipoles and adjusting the quadrupoles and sextupoles settings for desired bunch compression. Residual energy chirp left after bunch compression as revealed from ELEGANT simulation can be corrected by a capacitive dechirper structure when the bunch is slightly over-compressed.

INTRODUCTION

A high brightness S-band injector system equipped with a laser-driven photocathode rf gun has been developed in house at NSRRC [1]. This system has been operated regularly in the Accelerator Test Area (ATA) for light source R&D. Recently, the possibility of establishing a free electron laser facility which delivers high intensity tunable coherent VUV radiation in the range of 66.5-200 nm is being investigated. The baseline design is a 4th harmonic high gain harmonic generation (HGHG) FEL driven by a 325 MeV driver linac system [2]. By making maximum use of existing hardware, a driver linac system has been designed [3]. One unique part of this design is that the bunch compressor is a single-stage double dogleg, which allows a control of nonlinear beam dynamics for efficient bunch compression. In this report, the analysis of nonlinear bunch compressors is recalled and the design this dogleg compressor for the 325 MeV high brightness linac system is studied. Tunability of bunch length and peak current by controlling R_{56} of this compressor is also discussed.

NONLINEAR BEAM DYNAMICS IN BUNCH COMPRESSORS

Consider an electron moving in the traveling-wave field of a constant-gradient linac structure. The energy gain of this electron is

$$\Delta E = eV_0 \cos(\omega t - kz + \varphi_0), \quad (1)$$

where V_0 , ω , k , φ_0 are the peak voltage, frequency, wave vector and initial phase of the wave which is propagating

in the $+z$ direction with phase velocity of $V_p = \omega/k = c$ respectively. The electron is also moving in the $+z$ direction with velocity $v_e = \beta c$.

When an electron enters the linac structure at $\phi_0 = 0$, acceleration of electron is maximized as it rides on the crest of the wave. It is worth noting that if an electron in a bunch passes a fixed location in space earlier (later) than all other electrons in time, it must be at the very front (end) of this bunch and it defines the location of bunch head (tail). For a bunch of electrons moving with the traveling wave in a linac along the direction of the $+z$ axis, the bunch head always has a positive value with respect to the bunch center.

Nonlinear Energy Chirps

Generally speaking, in a split photo-injector configuration, the associated rf linac structure is operated at a phase (i.e. the rf crest) to minimize beam energy spread and a subsequent chirper linac is used to produce the required energy chirp for the bunch compression in the dispersive section located downstream. Therefore, it is reasonable to assume the correlated energy spread of the electron beam at the entrance of the chirper linac is small and the energy deviation of an electron from the designed value at chirper linac exit (i.e. $\delta(z) = (E_f(z) - E_{f0})/E_{f0}$) can be expressed by means of Taylor series expansion as

$$\delta(z) = a\delta_i + h_1 z + h_2 z^2 + h_3 z^3 + \dots \quad (2)$$

where $E_f(z)$ is the central beam energy at the entrance of chirper linac, δ_i the deviation of electron energy from the designed value with initial uncorrelated energy spread, z the particle's initial longitudinal coordinate relative to the bunch center. E_{f0} is the central beam energy after the chirper linac, $a = E_{i0}/E_{f0}$ is the damping factor and

$$\begin{cases} h_1 = \frac{keV_0}{E_{f0}} \sin \varphi_0, \\ h_2 = -\frac{k^2 eV_0}{2E_{f0}} \cos \varphi_0, \\ h_3 = -\frac{k^3 eV_0}{6E_{f0}} \sin \varphi_0, \end{cases} \quad (3)$$

are the first, second and third order energy chirps respectively. It is clear that the signs of the 1st order and the 3rd

NOVEL ASPECTS OF BEAM DYNAMICS IN CEC SRF GUN AND SRF ACCELERATOR

I. Petrushina*¹, T. Hayes, Y. Jing, D. Kayran, V.N. Litvinenko¹, G. Narayan,
I. Pinayev, F. Severino, K.S. Smith, G. Wang¹, K. Shih¹, K. Mihara¹
Brookhaven National Laboratory, Upton, NY 11973, USA
¹ also at Stony Brook University, Stony Brook, NY 11794, USA

Abstract

A 15 MeV CW SRF accelerator has been commissioned at Brookhaven National Laboratory to test the Coherent electron Cooling concept. The accelerator consists of an SRF 113 MHz photoemission gun, two 500 MHz bunching cavities and a 704 MHz 5-cell SRF linac. In this paper, we describe our experience with this system with focus on unusual phenomena, such as multipacting in the SRF gun. We also discuss issues of wakefields in the CeC accelerator.

CEC ACCELERATOR

Coherent electron Cooling (CeC) is an advanced method of beam cooling which is based on electrostatic interactions between electron and ion beams amplified by a high-gain free electron laser (FEL) [1]. This promising method would significantly reduce cooling time of a hadron beam compared to the other known techniques. The CeC Proof of Principle (PoP) experiment is currently undergoing commissioning at Brookhaven National Laboratory, and the layout of the CeC beamline is illustrated in the figure at the top of the next page [2]. The accelerating section of the system consists of a 113 MHz superconducting photo-injector followed by the first focusing solenoid, two 500 MHz normal conducting bunching cavities, a transport section with 5 solenoids, and a 704 MHz superconducting accelerating 5-cell cavity. After the electron beam is accelerated to the velocity matching the velocity of the hadron beam circulating in RHIC, it is directed by the dogleg into the common section, where the beams co-propagate. In this paper, we present the observations during the system commissioning alongside with the simulation results, and we discuss our future plans for the wakefields and beam dynamics simulations.

113 MHz SRF PHOTO-INJECTOR

The 113 MHz photo-injector is based on a quarter-wave resonator which provides 1.05 MV of accelerating voltage, and can generate an electron bunch with charge up to 4 nC (see Fig. 1) [3–5]. This year, the gun was generating an electron beam at the third subharmonic of the RHIC revolution frequency, which is 26 kHz for the hadron's energy of 26.5 GeV/u. For the Run'18 the gun will be retuned to operating at a harmonic of RHIC revolution frequency e.g. 78 kHz. During the last run, the photo-injector demonstrated excellent performance, which showed significant improvements compared to the results of the Run'16, which was

challenged by the presence of strong multipacting (MP) barriers.

Multipacting

Multipactor discharge was a major limiting factor during the previous year of commissioning. We observed that vacuum activity due to the MP would significantly increase in the presence of the external magnetic field of the first solenoid (especially for a magnetic field of about 400 Gs). The most dangerous MP level was found to be at 40 kV of accelerating voltage, which would become worse when the CsK₂Sb photocathode was inserted into the cavity. This MP level would lead to serious vacuum excursions, which were rather damaging to the quantum efficiency of the photocathode—it would deteriorate from 2-8 % to 0.01-0.1 %.

After a comprehensive study of the MP in the gun using Track3P [6], it was confirmed that the external magnetic field increases the strength of MP in the gap of the fundamental power coupler (FPC), with stable trajectories moving from the cavity side of the gun towards the bellow (see Fig. 1). The simulation results showed that the stubborn MP level at 40 kV is localized in the front rounding of the cavity and is a 1st-order multipactor discharge. See [7, 8] for a more detailed discussion of the simulation results.

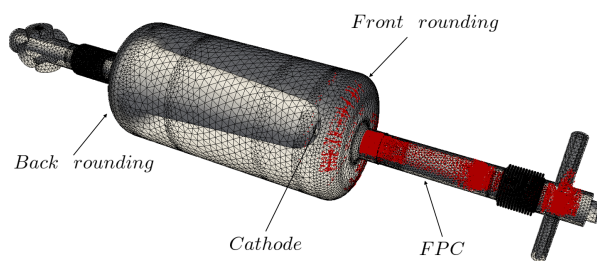


Figure 1: Geometry of the CeC photo-injector. Areas of the cavity affected by MP are shown in red.

With the knowledge of the main MP levels and their locations, operation of the gun became very intuitive. When bringing the cavity to the operating voltage, we would keep the first solenoid at zero current, and insert the FPC into position with the maximum achievable coupling using full 4 kW of available RF power in order to overcome the 40 kV MP level. After passing a voltage of about 100 kV there was no significant MP activity, and we were able to bring the cavity to the operational level by adjusting coupling via FPC position in a phase-lock loop mode.

* ipetrushina@bnl.gov

CSR WAKE FIELDS AND EMITTANCE GROWTH WITH A DISCONTINUOUS GALERKIN TIME DOMAIN METHOD*

D. A. Bizzozero[†], H. De Gersem, E. Gjonaj

Institut für Theorie Elektromagnetischer Felder, TU Darmstadt, Germany

Abstract

Coherent synchrotron radiation (CSR) is an essential consideration in modern accelerators and related electromagnetic structures. We present our current method to examine CSR in the time domain. The method uses a 2D Discontinuous Galerkin (DG) discretization in the longitudinal and transverse coordinates (z, x) with a Fourier decomposition in the transverse coordinate y . After summation over modes, this treatment describes all electromagnetic field components at each space-time coordinate (z, x, y, t). Additionally, by alignment of mesh element interfaces along a source reference orbit, DG methods can handle discontinuous or thin sources in the transverse x direction. We present an overview of our method, illustrate it by calculating wake functions for a bunch compressor, and discuss a method for estimating emittance growth from the wake fields in future work.

PROBLEM STATEMENT

In a continuation of earlier work [1–3], we examine the generation of CSR by an ultra-relativistic electron bunch in a vacuum chamber of rectangular cross-section. For a simplified model, we only consider motion of the bunch in a planar orbit with Cartesian coordinates (Z, X, Y) in the midplane $Y = 0$. Additionally, we only model vacuum chambers with planar horizontal boundaries at $Y = \pm h/2$ where h is the height of the chamber and only consider perfectly electrically conducting (PEC) boundary conditions on the chamber walls. An example of a chamber with a planar orbit is shown in Figure 1 (top), corresponding to the bunch compressor DESY BC0.

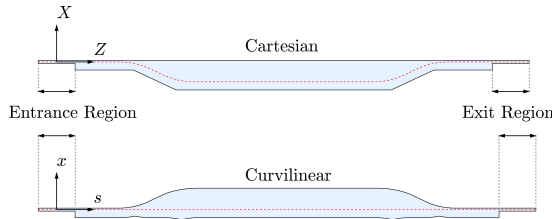


Figure 1: DESY BC0 vacuum chamber domain in (Z, X) (top) or (s, x) (bottom) coordinates with reference orbit (red dashed). The entrance region is the same in both systems.

To study CSR wake fields, we seek to time-evolve the Maxwell field equations for \mathbf{E} and \mathbf{H} inside the chamber:

$$\frac{\partial \mathbf{E}}{\partial \tau} = Z_0 \nabla \times \mathbf{H} - Z_0 \mathbf{j}, \quad \frac{\partial \mathbf{H}}{\partial \tau} = -\frac{1}{Z_0} \nabla \times \mathbf{E}, \quad (1)$$

* Work supported by DESY.

[†] bizzozero@temf.tu-darmstadt.de

where $\tau = ct$, with speed of light c , vacuum impedance Z_0 , and current density \mathbf{j} .

Given a smooth reference orbit parametrized by its arc length $\mathbf{R}_r(s) = (Z_r(s), X_r(s), 0)$, we transform the (Z, X, Y) coordinate system to a curvilinear system (s, x, y) with the inverse transformation of:

$$\begin{aligned} Z(s, x, y) &= Z_r(s) - xX_r'(s), \\ X(s, x, y) &= X_r(s) + xZ_r'(s), \\ \text{and } Y(s, x, y) &= y, \end{aligned} \quad (2)$$

using the signed curvature: $\kappa(s) = Z_r''(s)X_r'(s) - Z_r'(s)X_r''(s)$ and length scale factor: $\eta(s, x) = 1 + x\kappa(s)$. In the (s, x, y) coordinate system, the reference orbit is the straight line $(x, y) = (0, 0)$. Furthermore, this coordinate mapping is well-defined if $\eta > 0$ throughout the domain; where the transformation is unique. See Figure 1 (bottom) for a depiction of the curvilinear transformation of the geometry in the case of DESY BC0.

In the (s, x, y) coordinate frame, we assume a current density of the form: $\mathbf{j} = (qc\lambda(s - \tau)\delta(x)G(y), 0, 0)$ with Gaussian longitudinal and transverse distributions λ and G , and a Dirac distribution in the x -coordinate. We choose σ_s , the bunch length, such that the bunch is supported only in the entrance region to machine precision at $\tau = 0$.

We now use the parallel plate geometry of $y = \pm h/2$ to introduce a Fourier decomposition in y for all fields:

$$\begin{aligned} f(s, x, y, \tau) &= \sum_{p=1}^{\infty} f_p(s, x, \tau) \phi(\alpha_p(y + h/2)) \\ \text{and } f_p(s, x, \tau) &= \frac{2}{h} \int_{-h/2}^{h/2} f(s, x, y, \tau) \phi(\alpha_p(y + h/2)) dy, \end{aligned} \quad (3)$$

with $\alpha_p = \pi p/h$, f representing $E_s, E_x, E_y, H_s, H_x, H_y$ or G , and $\phi(\cdot)$ is $\sin(\cdot)$ for E_s, E_x, H_y, G or $\cos(\cdot)$ for E_y, H_s, H_x . If the initial fields and $G(y)$ are symmetric about $y = 0$, then the even p modes for all fields vanish. We denote the Fourier series modes with the subscript p .

To numerically treat the singularity at $x = 0$ in the current \mathbf{j} term on the right-hand-side of (1), we apply an additional transformation on the H_{yp} field component: $\tilde{H}_{yp} = H_{yp} - qcG_p\lambda(s - \tau)\Theta(x)$ where $\Theta(x)$ is the Heaviside function. Additional transformations can be made to transform the source to arbitrary degree of smoothness [4]; however, for a DG method with element edges which align along the discontinuity, this is not required.

Applying the curvilinear coordinate transformation in (2), the Fourier series decomposition in (3), and the transforma-

EXPERIMENTS IN ELECTRON BEAM NANOPATTERNING*

C. Zhang[†], W.S. Graves, L.E. Malin and J.C.H. Spence, ASU, Tempe, USA
 R.K. Li, E.A. Nanni, X. Shen, S.P. Weathersby and J. Yang, SLAC, Menlo Park, USA
 D. Cesar, J. Maxson, P. Musumeci and A. Urbanowicz, UCLA, Los Angeles, USA

Abstract

We report on experiments in nanopatterning electron beams from a photoinjector as a first step toward a compact XFEL (CXFEL). The nanopatterning is produced by Bragg diffraction of relativistic electron beams through a patterned Si crystal consisting of alternating thick and thin strips to produce nanometer-scale electron density modulations. Multi-slice simulations show that the target can be oriented for a two-beam condition where nearly 80% of the elastically scattered electron beam is diffracted into the 220 Bragg peak. An experiment at the two-beam condition measurement has been carried out at the SLAC UED facility showing this effect with 2.26 MeV electrons. We successfully proved a large portion of the main beam is diffracted into 220 spot by tuning the orientation of the sample. Future plans at UCLA are to observe the nanopatterned beam, and to investigate various grating periods, crystal thicknesses, and sample orientations to maximize the contrast in the pattern and explore tuning the period of the modulation. The SLAC measurement results will be presented along with design of the UCLA experiments.

INTRODUCTION

Research to develop compact XFEL [2, 3] based on inverse Compton scattering are being carried on at ASU. We proposed to use a Si grating to generate nanometer scale bunched beam [7, 9] which can be an ideal source for seeding a room-size XFEL. The method depends on diffracting electrons through a thin silicon grating structure to produce a transverse modulation, and then transferring this modulation into the time domain via emittance exchange [5]. The high reproducibility and determinability of electron bunches generated by grating diffraction method will greatly improve the coherence of X-ray output. Proof-of-principle experiments [4, 6] have been performed at SLAC's UED facility [8], and new experimental data presented here shows a close match of simulation and experiment showing that the photoinjector beam quality and the stability of the accelerator are adequate to achieve nanopatterning.

We present the results of these studies and discuss plans to carry out grating diffraction experiments at UCLA's Pegasus laboratory in the near future, and study associated beam dynamics.

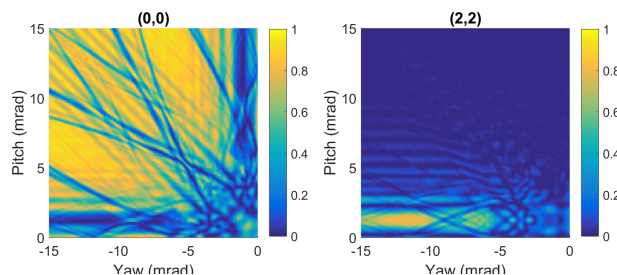


Figure 1: Simulated intensity maps of 200 nm thick planar Si membrane. The color of each pixel represents the normalized intensity of the selected beam. Left is the intensity map of (000) beam, right is the map of (220) beam.

SLAC RESULTS

Previous simulation of Si crystal electron diffraction using multislice method [4] showed a possibility to find a two-beam condition where 80% of the diffracted electron beam is in a single Bragg peak. In the laboratory frame we use pitch and yaw angles with respect to the horizontal electron beam to denote the angular deviation of the beam from the [001] normal to the silicon crystal. The aim of these experiments is to measure the variation in the transmitted (000) and (220) Bragg beams as the diffraction conditions are varied around the exact (220) Bragg condition. To determine the relation between pitch/yaw angle and diffraction intensity, 2D intensity maps shown in Fig. 1 have been created to predict the exact position where we can find the two-beam condition. To create the maps, scans of the pitch (rotation about x-axis) and yaw (rotation about the y-axis) angles have been performed while recording the diffraction pattern and then we processed the images to find the intensity of different Bragg spots as maps of pitch and yaw.

The (000) beam intensity map in Figure 1 shows a dark gap near pitch = 1 mrad, yaw = -12 mrad which is corresponding to the bright strips in the (220) beam map where the direct beam has been mainly diffracted into Bragg spots.

To make a precise measurement, careful calibrations of all rotation angles of the system are needed. The roll angle of the sample corresponding to holder pitch and yaw has been mounted less than 1 degree. Then the sample is aligned in both pitch and yaw angle within ± 0.02 degrees to normal position.

A fine 2D scan over the area of interest was performed to search for the two-beam condition. Figure 2 shows representative patterns of a two-beam condition where the majority of electron beam are scattered into either the forward (000)

* This work was supported by NSF Accelerator Science awards 1632780 and 1415583, NSF BioXFEL STC award 1231306, and DOE contract DE-AC02-76SF00515.

[†] czhan178@asu.edu

Content from this work may be used under the terms of the CC BY 3.0 licence (© 2018). Any distribution of this work must maintain attribution to the author(s), title of the work, publisher, and DOI.

ELECTRON BEAM REQUIREMENTS FOR COHERENT ELECTRON COOLING FEL SYSTEM*

G. Wang[#], Y.C. Jing, V. N. Litvinenko and J. Ma, BNL, Upton, NY 11973, USA.

Abstract

The proof of coherent electron cooling (CeC) principle experiment is currently on-going and due to the limitations of the 5-cell SRF accelerating LINAC, the final achievable energy of the electron beam is 15 MeV, i.e. 68% of its originally designed value, 22 MeV [1]. Consequently, all evaluations and simulation results need to be revisited for the reduced beam energy. This work focuses on the requirements of the electron beam quality in order to achieve the desired amplification from the FEL amplifier of our CeC system.

FEL AMPLIFIER OF THE PROOF OF CEC PRINCIPLE EXPERIMENT

As shown in Fig. 1, the FEL amplifier of the CeC system consists of three helical undulators. Illustrated in Fig. 2, the length of each undulator is about 2.49 meters. The separations between any two adjacent undulators are 42.25 cm where phase shifters are installed to match the phase of electrons with that of the radiation [2]. The undulator period is 4 cm and for the current set-up, the undulator field on axis is 0.134 T, which correspond to an undulator parameter of $a_w = 0.5$. The originally designed gain in the bunching factor is 100, requiring peak current about 100 A for 22-MeV electron beam with normalized RMS emittance smaller than 5 mm.mrad and RMS energy spread within 0.1%.

During RHIC run 17, the CeC system is commissioned and it is found that the cavity voltage of the 5-cell SRF LINAC is limited to 13.5 MeV and hence the maximal achievable energy of the electron beam is 15 MeV. Apart from all necessary modifications of the diagnostic system, the cooling process needs to be re-visited and here we present our preliminary studies of the requirements on the electron beam qualities for achieving the desired gain from the FEL amplifier.

*Work supported by Brookhaven Science Associates, LLC under Contract No.DE-AC02-98CH10886 with the U.S. Department of Energy.
[#]gawang@bnl.gov

TOOLS AND SIMPLIFICATIONS

Since the FEL amplifier consists of three undulators with no quadruples in between, the beta functions vary along the amplifier section. Figure 3 (orange) shows the designed beta functions, which give minimal variation of the electron beam size along the amplifier.

We use Genesis 1.3 to investigate what are the requirements on electron beam quality to achieve the bunching gain about 100 [3]. For a preliminary estimate, we simplify the FEL amplifier as a single undulator of 7.5-m long with the undulator period of 4 cm and undulator parameter of 0.5.

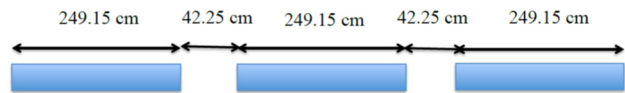


Figure 2: Illustration of the FEL amplifier of the CeC experiment.

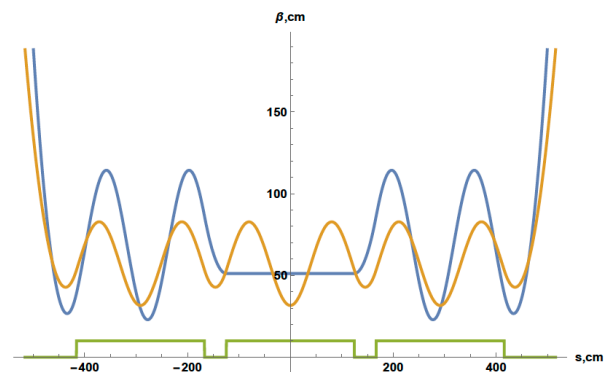


Figure 3: Variation of beta function along the FEL amplifier. Orange: the designed beta function of the amplifier, which gives minimal variation of electron beam size. Blue: one of the un-optimized lattice designs where the beta function is matched at the middle undulator but the overall variation of beam size is large.

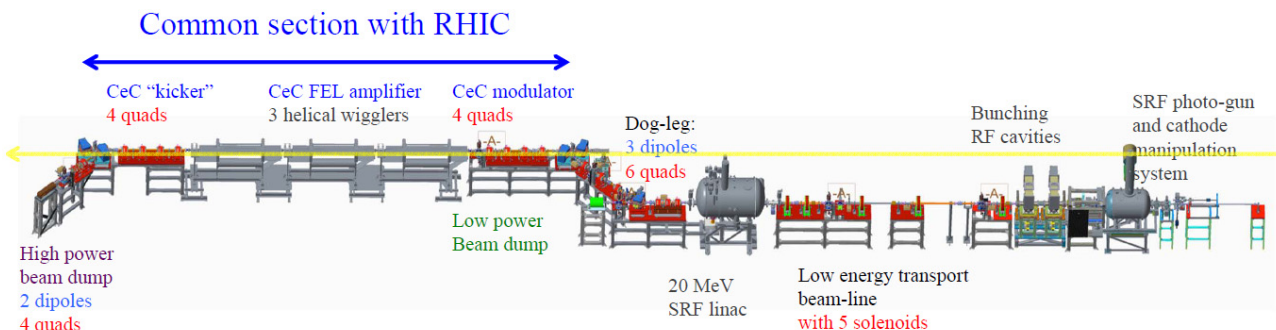


Figure 1: Layout of the proof of CeC principle experiment at RHIC IP2.

DETERMINATION OF THE SLICE ENERGY SPREAD OF ULTRA-RELATIVISTIC ELECTRON BEAMS BY SCANNING SEEDED COHERENT UNDULATOR RADIATION*

J. Bödewadt[†], R. Aßmann, M. M. Kazemi, C. Lechner, DESY, Hamburg, Germany
 L. L. Lazzarino, T. Plath[‡], J. Roßbach, University of Hamburg, 22671 Hamburg, Germany

Abstract

Modern high-gain free-electron lasers make use of the high-brightness ultra-relativistic electron beams. The uncorrelated energy spread of these beams is, upon creation of the beam, in the sub-permille range and below the resolution of state-of-the-art diagnostics. One method to determine the slice energy spread is to use an external seed laser to imprint a coherent microbunching structure that gives rise to coherent radiation processes different than radiation sources such as transition radiation, synchrotron radiation, or undulator radiation and others. Here, we present a method and show measurements to determine the slice energy spread using an external seed laser with a 266 nm wavelength to produce coherent undulator radiation at higher harmonics. The distribution of these harmonics allows to retrieve the electron beams slice energy spread with high precision.

INTRODUCTION

The invention of the high-gain x-ray free-electron laser has enabled the study of the dynamics and structure of matter on the atomic and molecular level and for time scales on the order of atto- and femtoseconds [1–4]. As these devices are driven by high-brightness ultra-relativistic electron beams, the operation requires sophisticated beam and bunch diagnostics in order to be able to measure and control the properties of the electron beam parameter. One of the crucial beam parameters for the performance of an FEL is the uncorrelated energy spread σ_E . Modern high-brightness electron sources are known to generate electron bunches with uncorrelated energy spread in the order of one keV. The direct measurement of this parameter is extremely challenging as typical diagnostic tools are resolution limited at a few keV. Nevertheless, processes which directly depend on σ_E can be used to indirectly determine this value. At the SDUV-FEL facility in Shanghai, a method using laser-seeded radiation with coherent harmonic generation (CHG) was used to determine the slice energy spread [5]. Here, the seed laser power and the longitudinal dispersion of the bunching chicane of the CHG setup was scanned in order to retrieve the local energy spread using the second harmonic of the initial seed laser wavelength. Similar to that, it is possible to scan the harmonic number instead of changing the dispersion and laser power. Fitting the measurements to simulation data by using the energy spread σ_E and modulation amplitude ΔE

as free parameter, we are able to retrieve these values in a similar way. The measurements were performed at the experimental seeding setup sFLASH at the free-electron laser user facility FLASH at DESY.

METHOD

Imprinting a periodic modulation of the longitudinal current density to the electron bunches allows the production of coherent radiation at harmonics of the fundamental frequency. The radiating process can e.g. be synchrotron radiation from a dipole, diffraction or transition radiation from screens, or undulator radiation. By overlapping an external laser pulse (wavelength λ) with the electron beam of beam energy E_0 and with a slice energy spread σ_E inside an undulator, it is possible to induce a periodic modulation of the beam energy with modulation amplitude ΔE . Transporting this energy-modulated beam through a section with longitudinal dispersion (R_{56}), a periodic current modulation forms. A Fourier analysis of the current density is used to extract the bunching coefficients for higher harmonic orders [6]:

$$b_n = \exp \left[-\frac{1}{2} n^2 B^2 \right] \cdot J_n(-nAB) \quad (1)$$

where $A = \Delta E / \sigma_E$ is the normalized modulation amplitude, $B = 2\pi\sigma_E R_{56} / (\lambda E_0)$ the normalized dispersive strength of the chicane, and n the harmonic number. For a laser pulse with an electric field envelope $\mathcal{E}(t)$, the modulation amplitude also will be a function of time $\Delta E(t)$. Assuming a constant energy spread along the modulated fraction of the electron bunch we can calculate the bunching distribution $b_n(t)$ after the chicane. Sending the electron beam with this bunching distribution through an undulator of length L_u tuned to the n^{th} harmonic will lead to the emission of coherent undulator radiation with a power profile proportional to $\rho_{FEL} |b_n(t)|^2 L_u^2$ [7]. For simplicity, we assume that the initial bunch current is low enough to neglect exponential FEL amplification. Integrating the power profile over time we can now calculate the photon pulse energy from the coherent harmonic generation for different harmonic numbers.

SIMULATION

For accurate simulation of the CHG process, the time-dependent FEL simulation code *GENESIS1.3* has been used [8]. The simulation parameters are similar to the experimental settings summarized in table 1. Figure 1 exemplary shows the result of the simulated bunching distributions for different harmonic numbers n and for an energy spread of

* Supported by the Federal Ministry of Education and Research of Germany under contract 05K13GU4, 05K13PE3, and 05K16PEA

[†] contact: joern.boedewadt@desy.de

[‡] present address: TU Dortmund University, Dortmund, Germany

INTERFERENCE-BASED ULTRAFAST POLARIZATION CONTROL AT FREE ELECTRON LASERS

S. Serkez*, G. Geloni, European XFEL GmbH, Schenefeld, Germany
 E. Saldin, DESY, Hamburg, Germany

Abstract

X-Ray Free Electron Lasers (XFELs) provide short high power pulses of X-rays with a high degree of polarization, where polarization properties are determined by the undulator magnetic field. Fast control of these properties would allow for unique experiments. Here we propose a scheme to modulate the polarization of FEL radiation (polarization shaping) or generate on average non-polarized radiation with FELs. This scheme is based on “crossing” APPLE-X helical undulators.

INTRODUCTION

X-ray Free Electron Lasers (XFELs) opened up the possibility of obtaining polarized X-ray pulses with unprecedented power and femtosecond-order duration. In recent years there has been a growth of demand for pump-probe schemes that deliver FEL radiation for both pump and probe with variable wavelength and delay.

At the LCLS the generation of two pulses with variable polarization and delay was demonstrated after installation of a helical undulator, following the main planar undulators [1]. In the current paper we propose another, alternative scheme to shape the polarization of FEL radiation on 100-femtosecond timescale and exemplify it for the SASE3 beamline of the European XFEL. This scheme does not require any special hardware, but only the components already being proposed for installation at this facility, namely:

- Emittance spoiler (slotted foil).
- Soft X-ray Self-Seeding monochromator (optional).
- Corrugated structure located upstream the SASE3 undulator.
- Two APPLE-X helical undulators located downstream the baseline SASE3 undulator, separated by a phase shifter.

The main elements of the proposed setup are the two helical APPLE-X undulators [2], tuned to the same resonant frequency ω , but with opposite polarization direction (as a basis for reasoning, the first undulator is tuned to produce radiation with right-handed circular polarization as defined from the point of view of the source (negative helicity), while the second one - left-handed (positive helicity).

PROPOSED METHOD

Two radiation beams with mutually orthogonal polarizations can be generated and naturally overlapped by propagating an electron beam through two planar undulators with the

orthogonal polarization planes located one after the other. If the electron beam is delayed by $\lambda/4$ between these undulators, the combined radiation would be circularly polarized, as illustrated on Fig. 1, first column. This was studied in [3] for synchrotron facilities. Later this approach was extended for FELs [4], experimentally demonstrated [5] and is currently referred to as the “crossed undulator technique”.

We consider the case, when, instead of linearly polarized radiation, two circularly polarized pulses with equal intensities, opposite helicity and a phase shift $\Delta\phi$ with respect to each other are generated. Then the resulting radiation will be always linearly polarized, with a polarization plane depending on the phase shift value $\Delta\phi$ (see Fig. 1, second column).

When the carrier frequency of the second pulse is shifted by $\Delta\omega$, then the phase difference $\Delta\phi$ varies linearly along the radiation pulses. In other words, one pulse has linear phase chirp with respect to the other. Then the polarization plane of the resulting linearly polarized radiation would gradually and periodically change its orientation (i.e. rotate) with frequency $\Delta\omega/2$, as schematically shown on Fig. 1, third column.

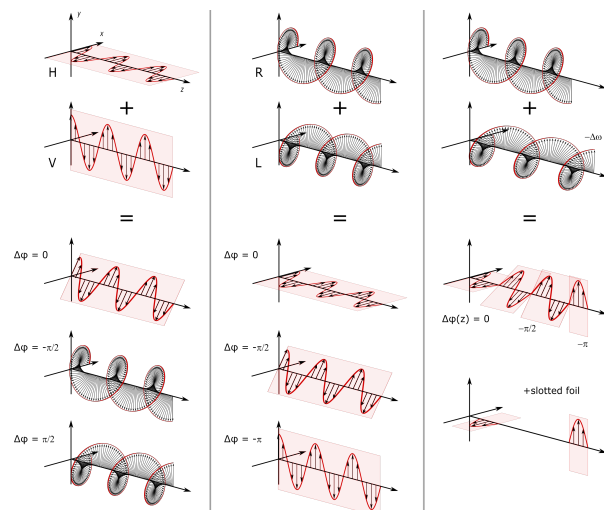


Figure 1: Combination of radiation pulses with different polarization: two linearly polarized (left column), two circularly polarized (central column), and two circularly polarized with linear phase chirp (right column). Note that for illustration purposes the depicted radiation carrier frequency is small, while the actual frequency would be much higher compared to rate of the polarization plane rotation. The same remark applies to radiation after slotted foil introduction.

On the large timescales this radiation is not polarized, since due to rotation of the Stokes vector its averaged length

* svitozar.serkez@xfel.eu

BEAM DRIVEN ACCELERATION AND RF BREAKDOWN IN PHOTONIC BAND GAP TRAVELLING WAVE ACCELERATOR STRUCTURES

J. Upadhyay and E. Simakov
Los Alamos National Laboratory, Los Alamos, NM 87545, U.S.A.

Abstract

We report the results of an experiment to demonstrate excitation of wakefields and wakefield acceleration in a photonic band gap (PBG) accelerating structure. The experiment was conducted at Argonne Wakefield Accelerator (AWA) facility. For modern X-ray Free Electron Lasers (FELs), preservation of the electron beam quality during the beam acceleration is of crucial importance. Therefore, new accelerating structures must be designed with careful attention paid to the suppression of wakefields. PBG structures are widely studied due to their ability to exclude higher order modes. A 16-cell travelling-wave normal conducting PBG structure operating at 11.7 GHz is installed at the AWA beam line. We passed a high-charge single bunch and a multiple bunch train through the structure that generated wakefields and evaluated the effect of these wakefields on a low charge witness beam.

INTRODUCTION

Photonic band gap (PBG) structures are periodic structures (metallic, dielectric or both) which confine the drive mode and damp higher order modes. PBG structures have great potential in reducing higher order modes (HOM) and long range wakefields. The problem associated with the high beam current accelerators needed for the future light sources and high luminosity colliders are the wakefields and HOM related beam breakup instabilities. PBG structures might be the technology needed for a compact and inexpensive high beam current accelerators. This raises the needs for the test of acceleration and wakefield suppression in PBG structures. To date only one test of the acceleration in a PBG structure was performed [1].

TWO-BEAM COLLINEAR WAKEFIELD ACCELERATION EXPERIMENTAL SETUP

The experiment is conducted at Argonne Wakefield Accelerator (AWA) at Argonne National Lab. In AWA facility, an L-band photocathode rf electron gun is used to produce electron beam. The electron gun uses a cesium-telluride photocathode. Six seven-cell accelerating structures are used to raise the electron energy up to 65 MeV. The beam can be split into different bunches and bunch charge of each bunch can be varied. This is achieved by splitting the laser pulse used in electron gun and varying the energy of the laser pulse. In our experiment, a high bunch-charge beam is used to excite the longitudinal wakefield in the PBG structure and hence is referred to as

a drive beam, while low charge beam used to probe the field excited by the drive beam is known as a witness beam. When the drive and witness beams travel through the same structure, it is called a collinear configuration. More details of the facility are given in [2].

A normal temperature traveling-wave PBG accelerating structure operating at 11.7 GHz was built and successfully tested for wakefield suppression at Argonne Wakefield Accelerator. This structure has 9 times the operational frequency of the AWA facility. The PBG structure is electroformed and could not be brazed due to internal stresses, a vacuum compatible epoxy was used to attach the components. Due to the use of epoxy, the vacuum chamber containing the PBG structure could not reach ultra-high vacuum to isolate and protect the Cesium telluride photocathode used in the photo injector in AWA facility, the vacuum chamber containing the PBG structure is separated from the beamline with a thin Beryllium (Be) window of the thickness of 178 microns. The experiment on wakefield suppression was conducted at AWA [3].

In the wakefield-suppression experiment [3], a good fraction of electron beam was hitting the front of the PBG structure and not entering the beam pipe of PBG structure due to high thickness of Be window. In order to understand how to send the beam through the PBG structure a series of experiment were done at AWA facility with three different thickness (30, 75, and 127 micron) Be windows. The beam size was measured before and after these windows with different charges and different beam energies. Based on these experiments, a 30-micron Be window was chosen. This 30-micron thick Be window was used during our two-beam collinear wakefield acceleration experiment.



Figure 1: The experimental setup on the beam line at Argonne Wakefield Accelerator (AWA).

THE ACHIP EXPERIMENTAL CHAMBERS AT PSI

Eugenio Ferrari*¹, Rasmus Ischebeck, Nicole Hiller, Simona Borrelli, Franziska Frei, Cigdem Ozkan-Loch, Micha Dehler, Eduard Prat, Simona Bettoni, Sven Reiche, Albert Romann, Jörg Raabe, Blagoj Sarafinov, Saha Susmita, Marco Calvi, Terence Garvey, Volker Schlott, Vitaliy A. Guzenko, Christian David, Martin Bednarzik, Hans-Heinrich Braun, Leonid Rivkin¹, Paul Scherrer Institut, Villigen PSI, Switzerland
Joshua McNeur, Peter Hommelhoff, FAU Erlangen Nurnberg, Erlangen, Germany
¹also at École Polytechnique Fédérale de Lausanne EPFL, Lausanne, Switzerland

Abstract

The Accelerator on a Chip International Program (ACHIP) is an international collaboration, funded by the Gordon and Betty Moore Foundation, whose goal is to demonstrate that laser-driven accelerator on a chip can be integrated to fully build an accelerator based on dielectric structures. PSI will provide access to the high brightness electron beam of SwissFEL to test structures, approaches and methods towards achieving the final goal of the project. In this contribution, we will describe the two interaction chambers installed on SwissFEL to perform the proof-of-principle experiments. In particular, we will present the positioning system for the samples, the magnets needed to focus the beam to sub-micrometer dimensions and the diagnostics to measure beam properties at the interaction point.

INTRODUCTION

With the potential of delivering acceleration of particles with gradients in excess of more than one order of magnitude larger than conventional RF technology, dielectric laser acceleration (DLA) [1] represents one of the most promising candidates for the realization of table top accelerators and for reducing the dimensions of future high energy colliders. The technique is based on the interaction between charged particles and the electric field of a laser, mediated by a dielectric microstructure. It is capable of exceeding the conventional technology as it implies dielectrics instead of metals. Dielectric materials are capable of supporting much higher electrical fields before breakdown happens.

The Accelerator on a Chip International Program (ACHIP) [2], an international collaboration between seven Universities, three National Laboratories and a private company, has been established with the support of the Gordon and Betty Moore Foundation to advance the DLA technology. The final goal is the realization of an all-on-a-chip particle accelerator. The role of EPFL/PSI in the collaboration is to investigate DLAs at relativistic electron beam energy and perform proof-of-principle experiments, in particular using the electron beam of SwissFEL [3].

Our goal is to demonstrate gradients in excess of 1 GV/m for a dielectric length of 1 mm, resulting in an acceleration of 1 MeV [4] for the electrons.

INJECTOR CHAMBER

Installed at meter 89 of the SwissFEL injector [5] is a chamber dedicated to experiments, see Fig. 1 where a breakout 3D representation of the setup is shown. It is composed of in vacuum manipulator, operated through a feedthrough by a stepper motor for the vertical translation and equipped with a camera box for detecting the electron beam signal on the screens (blue box on the left). Two different targets for transverse beam measurements (YAG:Ce and OTR foil) are installed on the manipulator as well as four different sample holders for the samples. Using the manipulator the samples can be inserted into the SwissFEL electron beam depending on the request of the different experiments.

A load-lock pre-chamber allows for installation of the samples on the sample holders without breaking the accelerator vacuum. A summary of the relevant parameters is reported in Table 1. Notice that in the low energy chamber the installation of a laser is not planned, hence the DLA studies are focused on the investigation of the wakefields induced by the microstructures on the electron beam and on assessing the radiation hardness of the materials used for the microstructures.

The chamber has been successfully commissioned and has been already used to perform a number of different experiments (see in the following).

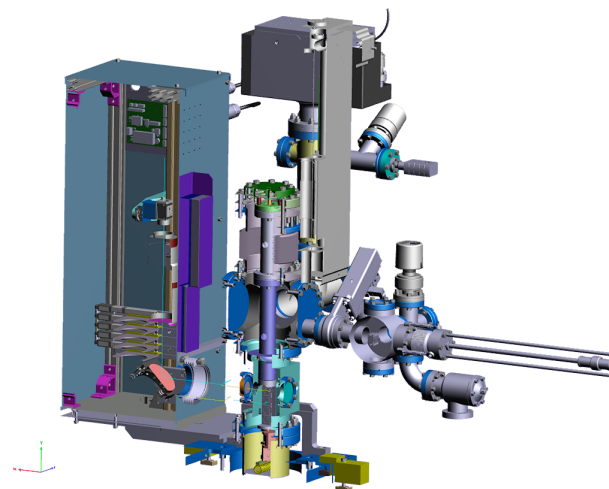


Figure 1: 3D breakout model of the ACHIP injector chamber.

* eugenio.ferrari@psi.ch

PREPARATIONS FOR INSTALLATION OF THE DOUBLE EMITTANCE-EXCHANGE BEAMLINE AT THE ARGONNE WAKEFIELD ACCELERATOR FACILITY*

G. Ha¹, J. G. Power², M. Conde², D. S. Doran², W. Gai²

¹Pohang Accelerator Laboratory, Pohang, Korea

²Argonne National Laboratory, Argonne, USA

Abstract

Preparations to upgrade the single EEX beamline at the Argonne Wakefield Accelerator (AWA) facility to a double EEX beamline are underway. The single EEX beamline recently demonstrated exchange-based longitudinal bunch shaping (LBS) which has numerous applications including high energy physics linear colliders, X-ray FELs, and intense radiation sources. The exchange-based method can generate arbitrary LBS in the ideal case but has limitations in the real case. The double EEX beamline was proposed as a means to overcome the limitations of single EEX due to transverse jitter and large horizontal emittance. In this paper, we present the current status of beamline design and installation and simulation results for the planned experiments: collinear wakefield acceleration with tailored beams and tunable bunch compression without the double-horn feature.

DOUBLE EEX BEAMLINE AT AWA

The Argonne Wakefield Accelerator (AWA) is an accelerator facility dedicated for future accelerator R&D [1]. This facility consists of three RF photoinjector beamlines for carrying out future accelerator research; wakefield applications [2-4], beam manipulation [5], field emission study [6] etc. The main beamline has a 1.5 cell RF gun generating a very high charge beam (up to 100 nC for single bunch) and 6 accelerating cavities to accelerate the beam up to 70 MeV. Downstream of the beamline is a flexible experimental area including a straight section and a single emittance exchange (EEX) beamline.

The EEX beamline was recently used to demonstrate property exchange and longitudinal profile shaping (LPS) [5]. Although the experiment was successful, the single EEX beamline has two important limitations [7] for practical usage. First, the single EEX beamline exchanges the (typically) large longitudinal emittance for the small transverse yet most applications benefit from a small transverse emittance. Second, both initial timing and energy jitters become a horizontal offset jitter after the single EEX beamline.

These limitations can be overcome with a double EEX beamline where a second EEX beamline is added after the first (Fig. 1). The first EEX exchanges transverse and longitudinal phase spaces; this enables the manipulation of the longitudinal phase space by altering the transverse beam properties in the middle section. Afterward, the second EEX exchanges these phase spaces again to return the emittances. Upstream longitudinal jitters become transverse jitters after the first EEX, but go back to longitudinal jitters after the second one [7,8].

The double EEX (DEEX) beamline at the AWA is going to have two double dogleg type EEX beamlines [5] with ~ 3 m separation for the transverse manipulation using quadrupoles and masks. Each dogleg uses 20 degree bending angle and 1.5 m separation between dipoles. The dispersion of the dogleg is ~ 0.77 m, and the corresponding deflecting cavity (TDC) strength needed is 1.3 m^{-1} . This beamline also has many YAG screens for transverse measurements, ICTs for the charge level, and two TDCs for longitudinal diagnostic. A single dipole magnet is followed by each TDC to measure the longitudinal phase space. Approximately a 1-m space is reserved at the upstream, middle, and downstream of the double EEX beamline for various EEX applications (e.g. THz radiation [9], wakefield applications [10], etc.).

In the remainder of the paper, we present a study of the CSR-effect in EEX and some preliminary simulation results for applications.

CSR SUPPRESSION IN DOUBLE EEX BEAMLINE

CSR is a well-known limitation for dispersive beamlines (e.g. chicane) and it comes as no surprise that it strongly impacts the DEEX beamline which consist of eight dipole magnets with large bending angles and (some) applications that require a high charge beam. We have found a simple method to partially suppress the CSR-effect for some applications [11], but we still have significant emittance growth along the beamline [7].



Figure 1: AWA drive beamline configuration with a double EEX beamline.

Content from this work may be used under the terms of the CC BY 3.0 licence (© 2018). Any distribution of this work must maintain attribution to the author(s), title of the work, publisher, and DOI.

MEASUREMENT OF SHORT-WAVELENGTH HIGH-GAIN FEL TEMPORAL COHERENCE LENGTH BY A PHASE SHIFTER

G. Zhou^{1,2,3†}, J. Wu^{1‡}, M. Yoon^{1,4}, C-Y. Tsai¹, C. Yang^{1,5},
 W. Liu^{1,5}, W. Qin^{1,6}, B. Yang⁷, T. Raubenheimer¹

¹SLAC National Accelerator Laboratory, Menlo Park, U.S.A

²Institute of High Energy Physics, Chinese Academy of Science, Beijing, China

³University of Chinese Academy of Science, Beijing, China

⁴Department of Physics, Pohang University of Science and Technology, Pohang, Korea

⁵University of Science and Technology of China, Hefei, Anhui, China

⁶Peking University, Beijing, China

⁷University of Texas at Arlington, Arlington, USA

Abstract

Short-wavelength high-gain free-electron lasers (FELs) are now well established as ultra-fast, ultra-bright, longitudinally partial coherent sources. Since coherence is one of the fundamental properties of a light source, continuous efforts on high-gain free electron laser coherence measurements are made. In this work, we propose a possible approach, employing a phase shifter to induce electron beam delay to measure the temporal coherence length. Simple analysis, numerical simulation and preliminary experimental results are presented. This approach can be robust and independent of frequency.

INTRODUCTION

Free-electron lasers (FELs) greatly benefit fundamental research in physics, chemistry, materials science, biology, and medicine by producing intense tunable radiation ranging from the infrared to hard x-ray region [1]. Approaches like coherent x-ray diffraction imaging (CXDI), x-ray holography and nano-crystallography promise important new insights in biology, condensed matter physics and atomic physics [2]. Therefore, coherence property plays an important role in these experiments. Furthermore, [3-4] indicate that small deviations from perfect coherence can be considered in the CXDI method if the degree of coherence is known. Thus, a pre-knowledge of FEL coherence properties would help.

Young's experiment [5] is one of the most widely used methods for characterization of coherence, the transverse coherence properties could be measured with the interference pattern. Previous work regarding measurements of transverse coherence properties of FEL sources has been done earlier [6-8]. The other important statistical characteristic of the FEL radiation is its temporal coherence. Due to the FEL instabilities leading to partial coherence, the FEL pulses are not fully coherent in the time domain.

In addition, the slippage effect in FEL results in the radiation pulse consisting of several spikes with a width of about the temporal coherence length. These longitudinal modes can be correlated and interfere with each other, which affects the temporal coherence length, which was recently observed experimentally [9]. Several optical methods are proposed to measure the FEL temporal coherence length. In the extreme ultraviolet regime, the feasibility of autocorrelation methods using laser beam splitter has been proved in [10]. Experimental measurement employing two-beam interference, analyzing the contrast of these interference fringes to get the temporal coherence length has been reported [11].

In this paper, we make use of high-gain FEL process to measure temporal coherence length. By introducing phase difference between the radiation field and the electron beam, the resultant radiation field can be represented by two waves with a constant phase difference, in which two-wave temporal interference should be expected [see Theory Section]. Based on this analysis, we propose a possible approach to measure the FEL temporal coherence length. In the theory part, we obtain solutions of high-gain FEL including phase shift in time domain. We further prove the feasibility of our approach with supports of numerical simulation. In the on-going experiment part, preliminary experimental results at Linac Coherent Light Source (LCLS) are presented and further experimental investigation is on our schedule.

THEORY

Following [12], we start from a one-dimension linear model described by:

$$\frac{\partial A(\bar{z}, \bar{s})}{\partial \bar{z}} + \frac{\partial A(\bar{z}, \bar{s})}{\partial \bar{s}} = B(\bar{z}, \bar{s}), \quad (1)$$

$$\frac{\partial B(\bar{z}, \bar{s})}{\partial \bar{z}} = P(\bar{z}, \bar{s}), \quad (2)$$

$$\frac{\partial P(\bar{z}, \bar{s})}{\partial \bar{z}} = iA(\bar{z}, \bar{s}). \quad (3)$$

*Work supported by the US Department of Energy (DOE) under contract DE-AC02-76SF00515 and the US DOE Office of Science Early Career Research Program grant FWP-2013-SLAC-100164

†gzhou@SLAC.Stanford.EDU

‡jhwu@SLAC.Stanford.EDU

SLIPPAGE-ENHANCED SASE FEL*

Juhao Wu^{1†}, Kun Fang^{1‡}, Claudio Pellegrini^{1§}, Tor Raubenheimer¹, Guanqun Zhou^{1¶},
 Axel Brachmann¹, Agostino Marinelli¹, Cheng-Ying Tsai¹, Chuan Yang^{1||}, Moohyun Yoon^{1**},
 Heung-Sik Kang^{2††}, Gyu Jin Kim², Inhyuk Nam², Andrew Chen³,
 Claire Davidson-Rubin⁴, Alexandra Li⁵, Nancy Munoz⁶, Bo Yang⁷

¹SLAC, Stanford University, Stanford, CA, USA,

²PAL-XFEL, Pohang University of Science and Tech., Pohang, Korea,

³Mission San Jose High School, Fremont, CA, USA,

⁴UC San Diego, La Jolla, CA, USA,

⁵Saratoga High School, Saratoga, CA, USA,

⁶Texas Tech University, Lubbock, TX, USA

⁷UT Arlington, Arlington, TX, USA

Abstract

High-brightness XFELs are in demand for many users, in particular for multiple types of imaging applications. Seeded FELs including self-seeding XFELs were successfully demonstrated. Alternative approaches by enhancing slippage between the x-ray pulse and the electron bunch were also demonstrated. This class of Slippage-enhanced SASE (SeSASE) schemes can be unique for FEL spectral range between 1.5 keV to 4 keV where neither grating-based soft x-ray self-seeding nor crystal-based hard x-ray self-seeding can easily access. SeSASE can provide high-brightness XFEL for high repetition rate machines not suffering from heat load on the crystal monochromator. We report start-to-end simulation results for LCLS-II project and preliminary experimental results for PAL-XFEL project.

SLIPPAGE-ENHANCED SASE (SESASE)

Free electron lasers (FEL) are perceived as the next-generation light source for many frontier scientific researches. Ultra-fast hard-X-ray FEL pulses, providing atomic and femtosecond spatial-temporal resolution, makes them a revolutionary tool attracting world-wide interest [1,2]. While an FEL provides high spatial coherence due to gain selection, *i.e.*, only the transverse mode which has the highest gain will dominate at the end of the undulator; the temporal coherence is rather poor. The temporal structure is spiky with coherent spikes with random relative phase among them [3]. In the high-gain region, the FEL group velocity

is $v_g = \omega_0 / (k_0 + 2k_u/3)$ and the electron longitudinal velocity is $v_l = \omega_0 / (k_0 + k_u)$ where $\omega_0 = k_0 c = 2\pi c / \lambda_0$ with c speed of light in vacuum, λ_0 the FEL resonance wavelength; and $k_u = 2\pi / \lambda_u$ with λ_u the undulator period. So, the coherent spike duration, the cooperation duration, is only $\tau_s \approx N_u \lambda_0 / (3c)$ where N_u is the total undulator period for the FEL to reach saturation. The so-called cooperation length is $Z_c = \tau_s c$. For the LCLS 1.5-Å FEL, $N_u \approx 2000$ to reach saturation, so $\tau_s \approx 0.3$ fs, which is much shorter than the electron bunch duration on the order of 10 to 100 fs.

To improve the temporal coherence, seeding approaches: both external [4,5] and self-seeding [6,7] have been actively pursued. Another approach along this line is to try to increase the slippage between the electron bunch and the FEL pulse. Such Slippage-enhanced SASE (SeSASE) [8–11] can produce bandwidth much narrower than that of a conventional SASE. The first preliminary experimental results was reported in Ref. [10].

ONE-DIMENSIONAL THEORY

To understand the SeSASE mechanism, let us work with a 1-D theory here. Such analysis is very similar to those developed in Refs. [12–14].

The coupled Maxwell-Vlasov equations for the FELs can be written as [14]:

$$\left(\frac{\partial}{\partial z} - 2ik_u \eta v \right) F(v, \eta, z) = \kappa_1 A(v; z) \frac{\partial}{\partial \eta} V(\eta), \quad (1)$$

$$\left(\frac{\partial}{\partial z} - i\Delta v k_u \right) A(v; z) = \kappa_2 \int F(v, \eta; z) d\eta, \quad (2)$$

where z is the coordinate along the undulator system; $\eta = (\gamma - \gamma_0) / \gamma_0$ the relative energy deviation with γ_0 the electron resonant energy; $v = \omega / \omega_0$ with ω the radiation frequency which is different from the FEL resonant frequency ω_0 ; $\Delta v = v - 1$ the detuning parameter; $F(v, \eta, z)$ is the electron bunch bunching factor; $A(v; z)$ is the slow varying envelop function of the FEL field, and $V(\eta)$ is the

* Work was supported by the US Department of Energy (DOE) under contract DE-AC02-76SF00515 and the US DOE Office of Science Early Career Research Program grant FWP-2013-SLAC-100164.

† jhwu@slac.stanford.edu

‡ Now at Wells Fargo & Co., San Francisco, CA, USA

§ Also as UCLA., Los Angeles, CA, USA

¶ Visiting Ph.D. student from Institute of High Energy Physics, and UCAS, Chinese Academy of Sciences, Beijing, China

|| Visiting Ph.D. student from NSRL, University of Science and Technology of China, Hefei, Anhui, China

** On sabbatical leave from Department of Physics, Pohang University of Science and Technology, Pohang, Korea

†† hskang@postech.ac.kr

ALTERNATIVE ELECTRON BEAM SLICING METHODS FOR CLARA AND X-RAY FELS

D. J. Dunning*, D. Bultrini, H. M. Castañeda Cortés, S. P. Jamison,
T. A. Mansfield, N. R. Thompson, D. A. Walsh
STFC Daresbury Laboratory and Cockcroft Institute, Daresbury, UK

Abstract

Methods to generate ultra-short radiation pulses from X-ray FELs commonly slice a relatively long electron bunch to feature one (or more) short regions of higher beam quality which then lase preferentially. The slotted foil approach spoils the emittance of all but a short region, while laser-based alternatives modulate the electron beam energy, improving potential synchronisation to external sources. The CLARA FEL test facility under development in the UK will operate at 100-400 nm, aiming to demonstrate FEL schemes applicable at X-ray wavelengths. We present laser-based slicing schemes which may better suit the wavelength range of CLARA and provide options for X-ray facilities.

INTRODUCTION

CLARA is a new FEL test facility being developed at STFC Daresbury Laboratory in the UK [1], which will operate with 250 MeV maximum energy and $\lambda_r=100-400$ nm fundamental FEL wavelength. Commissioning is underway on the front-end while design of the later stages is still being finalised. An overview of the facility layout and FEL schemes is given in [2] but briefly the aim is to demonstrate novel FEL capabilities that could be applied at X-ray FEL facilities such as high-brightness SASE [3], mode-locking [4], mode-locked afterburner [5], optically slicing a single SASE spike [6] and others. It will have a flexible design that can accommodate new ideas and future changes.

A common feature of many FEL schemes including [4–6] is so called ‘slicing’ of the electron beam. It refers to applying a longitudinal variation in electron beam properties such that one (or more) short regions of the bunch lase preferentially, thereby generating shorter photon pulses for use in experiments. For example, the slotted foil method [7, 8] spoils emittance in all but a short section of the beam, while [6] defines the lasing part of the beam via a specific energy chirp.

Given the aims of CLARA it is desirable to keep the focus on wavelength-independent aspects of the FEL concepts and so minimise wavelength-specific difficulties where possible. For example, to suit single-shot temporal diagnostics it is proposed to study short pulse generation for FEL wavelengths in the range 250-400 nm. A similar argument applies for the seed/modulating lasers. Initially it was planned that both mode-locking and slicing with chirp/taper would be carried out with an applied energy modulation of period $\lambda_{\text{mod}} \approx 50 \mu\text{m}$ [1]. However it has since been recognised

that wavelengths outside the range $20 \mu\text{m} \lesssim \lambda_{\text{mod}} \lesssim 70 \mu\text{m}$ would require less laser R&D to deliver suitable sources.

Modeling shows that mode-locking can be achieved with $\lambda_{\text{mod}} = 20 \mu\text{m}$ while the transverse apertures of the modulation section have been specified to transport wavelengths up to $100 \mu\text{m}$ to retain these options. However, another option could be to use a shorter wavelength seed (e.g. 800 nm) to replace some of the functionality of the $20 \mu\text{m} \lesssim \lambda_{\text{mod}} \lesssim 100 \mu\text{m}$ range - this paper reports studies of two such methods.

MODE-LOCKING WITH BEAT MODULATION

The mode-locked FEL concept [4] uses chicane delays between undulator sections to allow pulses with duration much shorter than the FEL co-operation length, $l_c = \lambda_r/4\pi\rho$ (where the FEL parameter $\rho \approx 10^{-4}-10^{-3}$), which is a lower limit for many schemes. The number of optical cycles in the pulse can be reduced from hundreds to approximately the number of periods in an undulator module, $N = 27$ for CLARA. The electron beam energy (or other electron-beam properties [9] such as current [10]) needs to be modulated with period $\lambda_{\text{mod}} = S_e N \lambda_r$, where a slippage enhancement factor [4] $S_e \approx 4-8$ has commonly been used, corresponding to $\sim 30-60 \mu\text{m}$ for CLARA. While it might not be straightforward to deliver a suitable laser source operating in this range, it might nevertheless be possible to modulate the electron beam energy on this scale through a laser induced beating modulation, as has already been demonstrated for various purposes at the FERMI FEL [11].

Modulation Stage

For initial studies the modulation stage was approximated by directly applying a superposition of two sinusoidal energy modulations of different period to the electron beam. Wavelengths of $\lambda_1 = 800$ nm and $\lambda_2 = 816$ nm were used to give a beat modulation period $\lambda_{\text{beat}} = 40 \mu\text{m}$ as shown in Fig. 1. This is plotted alongside a typical sinusoidal energy modulation (with $\lambda_{\text{mod}} = 40 \mu\text{m}$) as would normally be used. In both cases it would be expected for FEL pulses to develop at $s = 20/60/100 \mu\text{m}$, etc. where the energy variation is minimised. The beat modulation case can in fact be anticipated to give cleaner output since the normal sinusoidal modulation generates secondary spikes at the maxima of the energy modulation where the energy chirp is also minimised [9].

* david.dunning@stfc.ac.uk

STUDY OF THE ELECTRON TRANSPORT IN THE COXINEL FEL BEAMLINE USING A LASER-PLASMA ACCELERATED ELECTRON BEAM*

T. Andre[†], I. Andriyash, F. Blache, F. Bouvet, F. Briquez, M.-E. Couprie, Y. Dietrich,
J.-P. Duval, M. El-Ajjouri, A. Ghaith, C. Herbeaux, N. Hubert, C. Kitegi, M. Khojayan,
M. Labat, N. Leclercq, A. Lestrade, A. Loulergue, O. Marcouillé, F. Marteau,
P. Ngotta, P. Rommeluere, E. Roussel, M. Sebdaoui, K. Tavakoli, M. Valléau

SOLEIL, Gif-sur-Yvette, France

S. Corde, J. Gautier, J.-P. Goddet, G. Lambert, B. Mahieu, V. Malka, K. Ta-Phuoc, C. Thaury
LOA, Palaiseau, France

S. Bielawski, C. Evain, C. Szwaj, PhLAM/CERLA, Villeneuve d'Ascq, France

Abstract

The ERC Advanced Grant COXINEL aims at demonstrating free electron laser (FEL) at 200 nm, based on a laser-plasma accelerator (LPA). To achieve the FEL amplification a transport line was designed to manipulate the beam properties. The 10-m long COXINEL line comprises a first triplet of permanent-magnet variable-strength quadrupoles (QUAPEVA), which handles the large divergence of LPA electrons, a magnetic chicane, which reduces the slice energy spread, and finally a set of electromagnetic quadrupoles, which provides a chromatic focusing in a 2-m undulator. Electrons were successfully transported through the line from LPA with ionization-assisted self-injection (broad energy spectra up to 250 MeV, few-milliradian divergence).

INTRODUCTION

Today, LPAs [1–3] can deliver over few millimeters of acceleration distances, relativistic electron beams with energies from hundreds MeV to few GeV [4] of few femtosecond durations and high peak currents in the multi-kiloAmps range. While transported and accelerated in the laser wake field, electrons acquire significant spread of the transverse and longitudinal momenta, leading to degradation of beam quality ($\sigma_{x'} \approx 1$ mrad and $\sigma_{\delta} \approx 1\%$ [5]). So far LPA-based undulator radiation has been observed [6–10] but application of such beams for FEL remains very challenging. The large divergence can be handled by means of high gradient quadrupoles or plasma lens [11, 12], while the energy spread can be reduced using a demixing magnetic chicane [13, 14] or being compensated in a Transverse Gradient Undulator [15, 16]. Among other LPA-based FEL projects [13, 17, 18], COXINEL [19–22] is part of the French FEL project LUNEX5 [23–25]. A transport line was designed to handle the large divergence of LPA electrons thanks to strong permanent magnet quadrupoles, a magnetic chicane permits to reduce the slice energy spread and a chro-

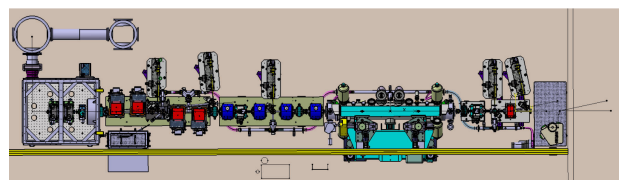


Figure 1: General top view of the COXINEL LPA demonstration set-up. From left to right: LPA chamber (gray) with the first set of quadrupoles, magnetic chicane dipoles (red), quadruplet of quadrupoles (blue), undulator (2-m U18 shown), dipole for beam dump (red), and UV-spectrometer (brown).

matic focusing in the undulator was developed to improve FEL performance [26].

TRANSPORT LINE DESCRIPTION

The transport line was designed, build and characterized at SOLEIL, then installed and aligned with the laser line of the “Salle Jaune” laser system of Laboratoire d’Optique Appliquée (see Fig. 1).

The laser plasma acceleration is performed with a Ti:Sa laser system that delivers 800 nm, 30 fs (FWHM), 30 PW pulses. A first triplet of quadrupoles, called QUAPEVA [27], is immediately installed after the source. These quadrupoles are built with permanent magnets, but have an original design for gradient variation and magnetic center adjustment for flexible refocusing [28, 29]. The beam is then manipulated in a magnetic chicane composed of four electromagnetic dipoles followed by a set of four electromagnetic quadrupoles (QEM) to provide electron beam focusing inside a cryo-ready U18 undulator [30, 31]. Electron diagnostics such as turbo-Integrated Current Transformer, cavity Beam Position Monitors, and multiple scintillating screens, are installed every 1–2 m along the beam line [32]. Two photons diagnostic devices, an under vacuum CCD camera and a photon spectrometer, are installed at the exit of the undulator.

* Work supported by ERC COXINEL (340015).

[†] thomas.andre@synchrotron-soleil.fr

Content from this work may be used under the terms of the CC BY 3.0 licence (© 2018). Any distribution of this work must maintain attribution to the author(s), title of the work, publisher, and DOI.

ELECTROMAGNETIC AND MECHANICAL ANALYSIS OF A 14 MM 10-PERIOD NBTI SUPERCONDUCTING UNDULATOR*

F. Trillaud[†], Instituto de Ingeniería, UNAM, CDMX, 04510, Mexico

G.A. Barraza-Montiel, Facultad de Ingeniería, UNAM, CDMX, 04510, Mexico

M. Gehlot, and G. Mishra, IDDL, Devi Ahilya University, Indore, MP 452001, India

Abstract

A 14 mm - 10 period NbTi superconducting undulator for the next generation of Free Electron Laser has been studied. The optimum electromagnetic pre-design was carried out using RADIA, an extension module of the commercial software Mathematica. For this pre-design, a variable gap was considered. Additionally, a thermo-mechanical study of one eighth of the superconducting undulator was conducted. This study utilized a thermal and mechanical contact model between the pancake coils and the carbon steel core. This coupled model allowed estimating the minimum pre-loading of the coil. This pre-loading ensures that the coil would remain stuck to its pole during cooling. Numerical results are presented for both studies.

INTRODUCTION

The new generation of light sources are expected to achieve greater luminosity benefiting from the advances in superconducting wires and tapes [1]. In the past 15 years, an increasing body of research has been dedicated to the development of superconducting insertion devices making use of state of the art commercial Low Temperature Superconductors operated in liquid helium [2]. Over the years, a few prototypes have been built and installed showing the applicability of the technology [3]. As the superconductivity gets more and more reachable to countries such as India which operates light sources, there is an increasing interest in exploring new technologies to upgrade their existing facilities [4]. It should be noted that the Mexican scientific community, users of light sources, have recently expressed their interest in the construction of a first light source in Mexico [5]. Addressing both interests in light sources and new technological developments for greater brightness, a small program to develop a first Indian 14 mm-10 period superconducting undulator operated in boiling liquid helium at 4.2 K has been launched in 2015 [6, 7], a technology that will certainly benefit the Mexican light source as well.

SCU are superconducting electromagnets wound on two ferromagnetic cores separated by a gap. The electromagnets are made of series-connected, impregnated coils with alternative winding to provide an oscillating magnetic field on axis [8]. The magnitude of the field is adjusted by the current intensity fed to the coils. Additionally, as the superconductor can carry large amount of currents without

losses, it is possible to achieve greater field allowing the construction of shorter period undulators at a greater brightness than any of the conventional technologies [9]. They are clear advantages over more conventional technologies such as permanent magnets (PPM) and hybrid undulators (HU).

The following work reports pre-studies carried out on a NbTi undulator to be operated at 4.2 K and its structure. The choice of the conductor was made on the basis of its well-understanding and its malleability compared to other technologies such as Nb₃Sn or the High Temperature Superconductors (HTS) [10, 11]. The electromagnetic pre-design, the conceptual design of the mechanical structure and cryogenic system needed to test the SCU and a mechanical pre-analysis to operate safely the device are presented. The current margin of the superconducting electromagnet and the pre-compression to ensure that the coils would not delaminate from their support were estimated. It is a first step allowing understanding the technology to be completed by more in depth studies.

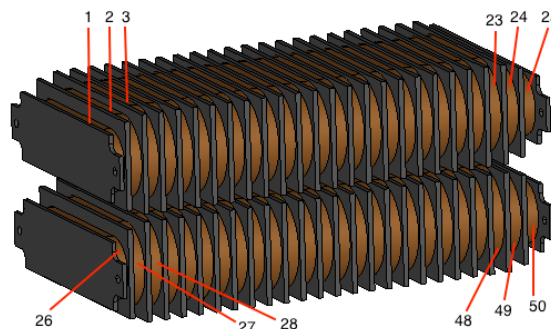


Figure 1: SCU structure with coil packs.

ELECTROMAGNETIC PRE-DESIGN

The NbTi superconducting undulator (SCU) is composed of two separated carbon steel cores, referred to as poles as it is shown in Fig. 1. Each pole holds 25 epoxy-impregnated racetrack coils connected in series with alternative winding. The coils are numbered from 1 to 50 over both poles (1-25 and 26-50). The first and last two coils of each pole are graded to smoother the magnetic flux density and lower the kick. The first and last coils (1 and 25, 26 and 50) are 1/4th of the height and width of the regular coil whereas the second and the penultimate coils (2 and 24, 27 and 49) are 3/4th. The regular coils, 3-23 and 28-48, have same dimensions along the pole length to generate a regular oscillating magnetic field. Figure 2 provides the dimensions of a regular coil and

* Work supported by the Dirección General Asuntos del Personal Académico (DGAPA) of the Universidad Nacional Autónoma de México (UNAM) under grant PAPIIT TA100617 and from SERB, India.

[†] ftrillaudp@iingen.unam.mx

DIELECTRIC LASER ACCELERATION SETUP DESIGN, GRATING MANUFACTURING AND INVESTIGATIONS INTO LASER INDUCED RF CAVITY BREAKDOWNS*

M. Hamberg[†], E. Vargas Catalan, M. Karlsson, D. Dancila, A. Rydberg, J. Ögren, M. Jacewicz,
Uppsala University, Uppsala, Sweden
M. Kuittinen, I. Vartiainen, Institute of Photonics, University of Eastern Finland, Finland

Abstract

Dielectric laser acceleration (DLA) is the technique utilizing strong electric fields in lasers to accelerate electrons in the proximity of nanoscaled dielectric gratings. The concept was recently demonstrated in experimental studies. Here, we describe the experimental DLA investigation setup design including laser system and scanning electron microscope (SEM). We also present the grating manufacturing methods as well as investigations into vacuum breakdowns occurring at RF accelerating structures.

INTRODUCTION

Accelerator physics plays an exponentially increasing role within the fields of natural sciences though the technology is generally spacious and expensive which hampers scientific progress [1]. Electrical breakdown inside of the acceleration cavities are limiting them in field strength and, therefore, size. Typical gradients are on the order of 10-50 MVm⁻¹ [2], which is less than the structures developed by the Compact Linear Collider (CLIC) collaboration, which operate up to 100 MVm⁻¹ [3]. To overcome these limits, alternative methods should be investigated.

Dielectric materials have proven superior properties regarding damage threshold of strong electric fields. Therefore, dielectric laser acceleration (DLA) where the strong electric fields from lasers are used for acceleration of charged particles at nanofabricated dielectric structures is a promising alternative [4]. The method has recently been proven in proof of principle studies for a large interval of energies ranging from non-relativistic and with acceleration gradients up to 690 MVm⁻¹ [4-7].

The technology is under development and promising, with gradients 10-100 times higher than current state of the art. Such increase in gradients would result in the corresponding size reduction and effectively more inexpensive accelerators rendering in higher scientific output when more accelerators can be built up. Challenges include timing, manufacturing of the dielectric structures regarding material and layout.

In this paper, we describe manufacturing of acceleration gratings made of diamond, construction of an acceleration test setup and how this setup can be utilized for vacuum breakdowns by high electric fields in metallic accelerator cavities (this is also previously described in [8]).

*Work supported by Stockholm-Uppsala Centre for Free Electron Laser Research.

[†]mathias.hamberg@physics.uu.se

DIAMOND GRATING MANUFACTURING AND LASER DAMAGE INVESTIGATIONS

For the dielectric acceleration grating structures we choose to work with 10 mm diameter and 300 μm thick polycrystalline diamond substrates from Element Six Ltd and Diamond Materials GmbH.

Recently, co-authors demonstrated an improved process utilizing electron-beam lithography, nano-replication using solvent assisted micro molding (SAMIM) [9,10]. The result of this process are replicas with line widths close to identical to the master grating pattern. The method furthermore includes inductively coupled plasma etching (ICP-RIE) with pure oxygen resulting in a lower sidewall angle [9].

As a first suitability test laser damage investigations of unprocessed diamond substrates were undertaken Friedrich-Alexander Universität (FAU) in Erlangen, Germany. The substrates were irradiated by a 1MHz laser with a wavelength of 1.93 μm, 600-fs pulse duration, and a 4-GVm⁻¹ peak field. No visible damage on the substrates was identified which motivated proceeding with the subsequent manufacturing steps.

Once the diamond structures are ready they will be tested for acceleration at FAU.

SEM TEST SETUP

We are constructing a DLA test bench based on a scanning electron microscope (SEM) Philips XL-30 (Fig. 1), with a similar design as at FAU. Such device can provide a well determined and precisely tuneable electron beam. Furthermore, the electron energies are typically in the tens of keV which arguably a very important energy range for investigation.

The design scheme in Fig. 2, illustrates where the electron beam passes near the acceleration grating. A laser beam is irradiating in transverse direction, exciting near fields which accelerate electrons in the right phase. An alignment microscope is used to read out the position of the laser spot on the diamond grating. Finally, an energy spectrometer is used for reading out the effect of the acceleration. It consists of two electrostatic plates bending the electron beam onto a micro channel plate (MCP).

The inside of the SEM of ~Ø300x200 mm leaves room for movable sample mount and energy spectrometer. The sample mount consists of three vacuum compatible

LUMINOSITY INCREASE IN LASER-COMPTON SCATTERING BY CRAB CROSSING*

Y. Koshiba[†], T. Takahashi, S. Ota, M. Washio, RISE, Waseda University, Tokyo, Japan
 K. Sakaue, WIAS, Waseda University, Tokyo, Japan
 T. Higashiguchi, Utsunomiya University, Tochigi, Japan
 J. Urakawa, KEK, Ibaraki, Japan

Abstract

Laser-Compton scattering X-ray (LCS-X) sources has been expected as a compact and powerful source, beyond X-ray tubes. It will enable laboratories and companies, opening new X-ray science. It is well known that luminosity depends on the collision angle of laser and electron beam. Head-on collision is ideal in the point of maximizing the luminosity, though difficult to create such system especially with optical enhancement cavity for laser. In collider experiments, however, crab crossing is a promising way to increase the luminosity. We are planning to apply crab crossing to LCS, to achieve a higher luminosity leading to a more intense X-ray source. Electron beam will be tilted to half of the collision angle using an rf-deflector. Although crab crossing in laser-Compton scattering has been already proposed [1], it has not been demonstrated yet anywhere. The goal of this study is to experimentally prove the luminosity increase by adopting crab crossing. In this conference, we will report about our compact accelerator system at Waseda University, laser system favorable for crab crossing LCS, and expected results of crab crossing LCS.

INTRODUCTION

Laser-Compton scattering (LCS) has been expected as an attractive X-ray source for years. Brilliance of almost 10^{10} has been achieved [2], and exceeding 10^{12} has been designed [3]. Comparing with magnetic undulators, LCS could be explained as “laser undulator”, which the undulator period equivalent to laser wavelength (~ 1 μm) while magnetic undulator is the order of cm. Figure 1 shows the comparison of undulator radiation and LCS.

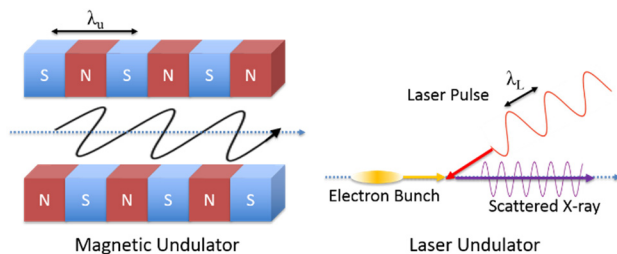


Figure 1: Comparison of undulator radiation and LCS.

* Work supported by Grant-in-Aid for JSPS Research Fellow.
[†] email address: advanced-yuya@asagi.waseda.jp

In order to produce 1-Å photons, LCS needs to provide a beam of 25-MeV energy, assuming 6 GeV for undulator radiation ($K = 1$, $\lambda_u = 2$ cm) and 4 GeV for synchrotron radiation ($\rho = 12$ m). Low required beam energy enable the whole system compact and low cost so that laboratories and hospitals may take care. The schematic drawing of LCS is shown in Fig. 2.

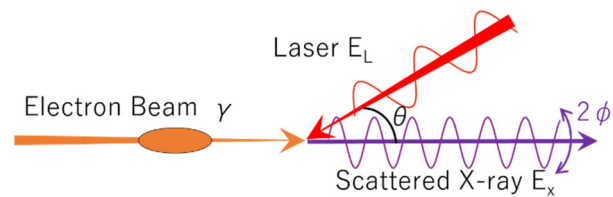


Figure 2: Schematic drawing of LCS.

In Fig. 2, γ , E_L , E_X , θ , ϕ represents the Lorentz factor of electron beam, energy of laser photon, energy of scattered X-ray, colliding angle, and scattering angle, respectively. The maximum X-ray energy E_X^{MAX} would be obtained along the electron beam axis $\phi=0$ and written as:

$$E_X^{MAX} \approx 2\gamma^2(1 + \beta \cos \theta)E_L, \quad (1)$$

where β is the velocity of electrons relative to the speed of light. We can see in Eq. (1) that scattered photon energy is tunable by controlling the beam energy or the collision angle.

The number of scattered photons is given by the product of cross section and luminosity:

$$N = \sigma L = \sigma P G. \quad (2)$$

Since the total cross section is unchangeable once the laser wavelength and beam energy is decided, it is necessary to increase the luminosity as much as possible. Luminosity can be expressed as the product of power factor (P) and geometric factor (G) as seen in Eq. (2). Power factor is the product of the number of electrons in a bunch and the number of photons in a laser pulse. Geometric factor is written as Eq. (3) when assuming Gaussian for both electron bunch and laser pulse. Here σ_x , σ_y , σ_z represents the electron bunch sizes of horizontal, vertical, and longitudinal respectively, and prime ones are those of laser pulse. We substitute our beam parameters, shown in Table 1, into the equation for the geometric factor,

Content from this work may be used under the terms of the CC BY 3.0 licence (© 2018). Any distribution of this work must maintain attribution to the author(s), title of the work, publisher, and DOI.

STUDY ON CHERENKOV LASER OSCILLATOR USING TILTED ELECTRON BUNCHES *

K. Sakaue[†], WIAS, Waseda University, Tokyo, Japan

M. Brameld, Y. Tadenuma, R. Yanagisawa, M. Washio, RISE, Waseda University, Tokyo, Japan

R. Kuroda, Y. Taira, AIST, Ibaraki, Japan

J. Urakawa, KEK, Ibaraki, Japan

Abstract

We have been studying a coherent Cherenkov radiation by using tilted electron bunches. Bunch tilting can enhance the radiation power about 10 times due to the wavefront matching of radiations. Recently, we investigated that this technique can produce high peak power THz pulses with sufficient pulse energy. The resulting pulse energy was more than 30 nJ/pulse and peak power was about 10 kW. Introducing the oscillator cavity with two concave mirrors can achieve lasing using tilted electron bunches. In the calculation we present, 1 μ J/micro-pulse and 100 μ J/macro-pulse broadband THz pulses are expected to achieve, which is powerful THz source compared with the existing THz FELs. In this conference, we will report the experimental results of coherent Cherenkov radiation, calculated results towards lasing and future prospective.

INTRODUCTION

Radiation in the terahertz (THz) frequency range is recognized to be useful for material science, medical use and other applications. The most useful feature of THz radiation its absorption spectrum of particular materials. This is the absorption of the vibration and/or rotation of molecules. Recently, the high peak power THz pulse was found to be useful for transforming the surface molecular using specific absorption [1]. The accelerator based THz source has an advantage in high peak power THz pulse generation with monochromatic and wavelength tunability. have useful properties. The photon energy of the THz radiation is several meV so that our electron accelerator system based on photocathode rf gun with 5-MeV energy is enough for the THz generation.

We have been studying on the coherent THz generation with Cherenkov radiation process [2]. In order to enhance the THz radiation power, we employed an electron bunch tilting. The relativistic electrons radiate a Cherenkov radiation when the velocity of electron is faster than the light in the medium at certain angle. Fig. 1 shows the schematic of Cherenkov radiation from electron (left) and tilted electron bunch (right). Electron radiates the Cherenkov radiation at several points in the medium but each radiation cannot be interacted with each other. When the electron bunch is perpendicular to the Cherenkov angle (right), radiation from different points of the medium can coherently overlap and enhance the pulse intensity [2].

* This work was supported by a research granted from The Murata Science Foundation and JSPS KAKENHI 26286083.

[†] kazuyuki.sakaue@aoni.waseda.jp

We successfully measured and enhanced the THz power, then started to design the oscillator cavity for lasing by Cherenkov radiation. This paper reports on the experimental results of coherent Cherenkov radiation, design and calculated results for constructing a laser, and future prospective.

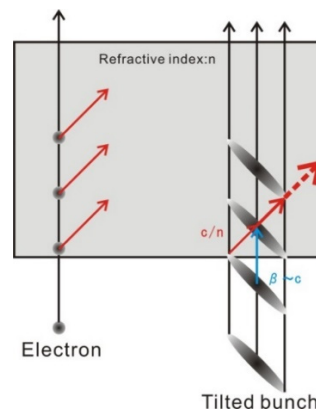


Figure 1: Generation of Cherenkov radiation from a tilted electron bunch.

EXPERIMENTS OF COHERENT CHERENKOV RADIATION

Experimental setup

Figure 2 shows the experimental setup of coherent Cherenkov radiation by electron bunch tilting. Electron bunch is produced by photocathode rf electron gun with energy of 4.5 MeV. Electron bunch is passed through the solenoid magnet for emittance compensation and focused by the quadrupole magnets. The focus size is the key parameter of the form factor in this experiment. After the quadrupole magnets, we installed an rf transverse deflecting cavity for tilting the bunch. Tilting angle can be controlled by regulating the rf power for the rf deflector.

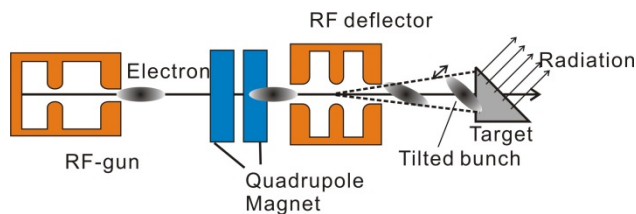


Figure 2: Experimental setup of coherent Cherenkov radiation by electron bunch tilting.

SIMULATING BEAM DYNAMICS IN COHERENT ELECTRON-COOLING ACCELERATOR WITH WARP

K. Shih[†], V. N. Litvinenko, I. Pinayev, Y. Jing, G. Wang, I. Petrushina, K. Mihara,
 Brookhaven National Laboratory, New York, USA
 Stony Brook University, SUNY, USA

Abstract

Coherent Electron Cooling (CeC) [1] is a novel cooling technique based on amplification of interaction between hadrons and electron by an FEL. If proven, this CeC could bring a revolution in hadron and electron-hadron colliders. A dedicated CeC proof-of-principle experiment is under way at RHIC collider (BNL) using a sophisticated SRF accelerator for generating and accelerating electron beam. This paper is dedicated to studies of beam dynamics in the CeC accelerator and specifically to emittance preservation in its ballistic compressions section. Two 500-MHz RF cavities are used for generating the necessary energy chirp leading in 1.56-MeV, 0.5-nsec-long electron bunched to compress them to 25-psec duration downstream. During the commissioning of the CeC accelerator we noticed that beam emittance can be strongly degraded when electron beam passes these 500 MHz RF cavities off-axis. We used a full 3D PIC code WARP to simulate effect of the off-axis beam propagation through these cavities.

INTRODUCTION

The CeC PoP experiment [2] is divided into two sections, the accelerator section and the cooling section (see Fig. 1). In the accelerator section, 1.05-MeV electron beam is first generated by a 113 MHz SRF gun. This electron beam is then “bunched” by two 500 MHz RF cavities and accelerated by a 704-MHz RF cavity to about 14.6 MeV. This acceleration provides the CeC electron beam with enough speed to match up with the RHIC’s hadron beam. After passing through a dogleg, electron beam will enter the cooling section.

The first part of the cooling section is the modulator, where the electron – hadron interaction takes place, the CeC electron beam will carry the density imprints of the RHIC’s hadron beam which will then be amplified by the

FEL undulators. At the end of cooling section, the electron beam will be allowed to merge with RHIC’s hadron beam and perform coherent electron cooling.

During the commissioning of CeC PoP machine, we allowed a 1.05-MeV electron off-axis electron beam to pass through two 500-MHz RF cavities. The cavities were aiming to provide an energy chirp for compressing a 0.5-nsec electron beam to 25 psec downstream. While we varied the phase of these cavities, a correlation between the phase and transverse positions of the off-axis electron beam following the cavities was observed. The data of transverse position of the off-axis electron beam was recorded by a beam-center position monitor (bpm) about 2 meters after the second 500 MHz RF cavity. The phase of both cavities was changed linearly in time, while a sine-wave like pattern of bpm readings were shown (see Fig. 2). This whole event was simulated by using the full-3D PIC code WARP. In WARP, an electron beam with the same initial condition to the experiment was used. It passed through two 500 MHz RF cavities with multiple offset values in the y-direction. The control comparison was also performed by allowing the same electron beam to pass through the same cavities at the center of the cavities. Details are shown in the next section.

ANALYSIS

We first simulated the effect of a single 500 MHz RF cavity to an off-axis electron beam. The beam had the same initial condition as with that of the experiment. The phase of cavity was set into zero-crossing (The phase with no total kinetic energy gain for the beam, but energy chirp). This was the default setting for the experiment. During the simulation, we allowed both the off-axis beam and the centered beam (electron beam without offset to the cavity center) to pass through this RF cavity. Multiple beam profiles

[†] kshih@bnl.gov

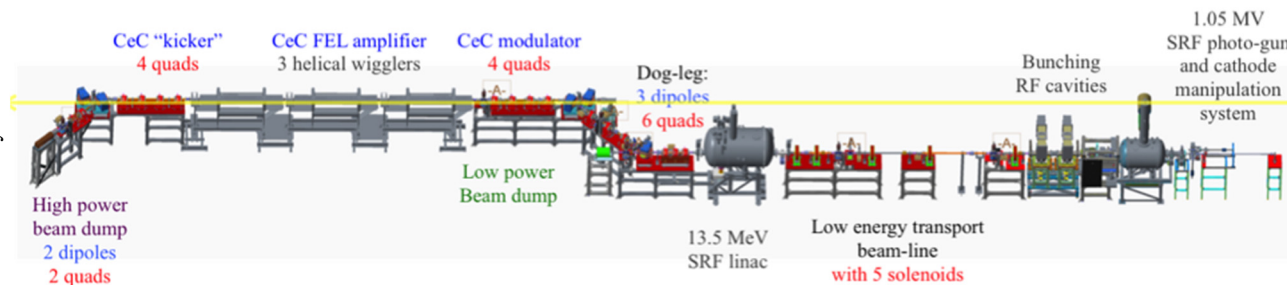


Figure 1: Schematic drawing of the CeC PoP Experiment machine. CeC electron beam travels from right to left.

Content from this work may be used under the terms of the CC BY 3.0 licence (© 2018). Any distribution of this work must maintain attribution to the author(s), title of the work, publisher, and DOI.

DEVELOPMENT OF MID-INFRARED PHOTOACOUSTIC SPECTROSCOPY SYSTEM FOR SOLID SAMPLES AT KYOTO UNIVERSITY FREE ELECTRON LASER FACILITY

J. Okumura[†], H. Zen, T. Kii, and H. Ohgaki,
Institute of Advanced Energy, Kyoto University, Uji, Japan

Abstract

A Photoacoustic Spectroscopy (PAS) system for solid samples using a Mid-Infrared Free Electron Laser (MIR-FEL) with a high-resolution grating monochromator is under development at Kyoto University Free Electron Laser Facility. Our target is to achieve 0.2% resolution in 10 μm . We designed a PAS cell whose internal volume was small for reducing the loss of the acoustic energy and by using cups for the sample holder to exchange the samples easily. We also conducted experiments to check the sensitivity of the developed PAS system using powdered $\text{CaSO}_4 \cdot 2\text{H}_2\text{O}$ and CaCO_3 as samples. The monochromator had the wavelength resolution of 0.015 μm (0.15% at 10- μm wavelength) in the experiments. As the result, we obtained quite high S/N ratio PAS signals with the FEL beam whose expected spectral width was 0.15% and whose power was reduced to one-eightieth by the monochromator.

INTRODUCTION

When material (whether solid, liquid or gas) is illuminated by light, acoustic wave is generated. This is called Photoacoustic effect. Especially with solid, this phenomenon is explained by RG Theory [1]. According to this theory, light is absorbed by the sample and its energy is converted to a thermal energy. The thermal energy causes the temperature distribution at the circumambient gas of the sample, and a pressure variation is arisen. Thus, the acoustic pressure wave is produced. Since the intensity of the acoustic pressure wave depends on the light absorption of the sample, we can directly obtain the absorption spectrum of the sample by measuring the intensity of pressure wave as the function of the illumination wavelength. This method is called Photoacoustic Spectroscopy (PAS).

When we use a pulsed infrared (IR) laser, PAS enables us IR absorption spectrum measurements of solid samples without pre-processing of samples such as the KBr pellet preparation and fine polish to very small thickness. As a feature of the PAS, its sensitivity and resolution depend on the intensity and spectral width of the IR light, respectively. Since a mid-infrared Free Electron Laser (MIR-FEL) is an intense, quasi-monochromatic and tunable laser in MIR region, the method of PAS with MIR-FEL (FEL-PAS) was proposed [2, 3]. In these previous works on the FEL-PAS, the spectral resolution was limited be

cause the used FEL beam had the spectral width of 1%. Therefore, they could not resolve sharp peaks in previous experiments. The spectral resolution can be significantly improved by inserting a monochromator on the optical path of the PAS system.

In order to realize this idea and targeting 0.02 μm resolution in 10 μm wavelength region, a high-resolution PAS system for solid samples using an MIR-FEL with a monochromator is under development at Kyoto University Free Electron Laser Facility (KU-FEL). We designed a new PAS cell and conducted demonstration experiments using this system to evaluate the system performance. In this paper, the outline of PAS system and demonstration experiments are briefly reported.

HIGH-RESOLUTION PAS SYSTEM

Figure 1 shows the outline of a high-resolution PAS system for solid samples. As the light source, we use KU-FEL [4]. A grating monochromator (DK240, CVI) whose grating was 75 groove/mm was put into the optical path. The monochromator had the wavelength resolution of 0.015 μm when the entrance and exit slit were adjusted to 0.3 mm. The FEL beam after passing through the monochromator was injected to a parabolic mirror and converted to the quasi-parallel beam. Then the FEL beam was split into two by a beam splitter. The transmitted light was monitored by a pyroelectric detector and the reflected light was focused on the sample within the PAS cell by the focusing mirror.

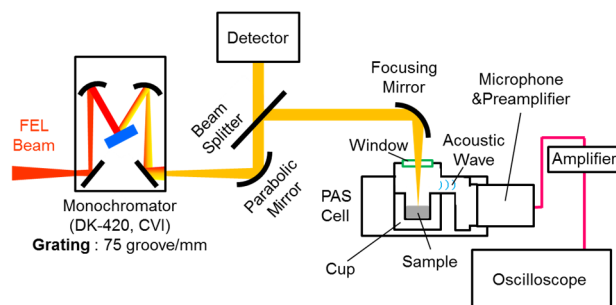


Figure 1: The outline of a high-resolution PAS system for solid samples using KU-FEL and monochromator.

[†] okumura.jumpei.24c@st.kyoto-u.ac.jp

Content from this work may be used under the terms of the CC BY 3.0 licence (© 2018). Any distribution of this work must maintain attribution to the author(s), title of the work, publisher, and DOI.

STUDY ON SECOND HARMONIC GENERATION IN SiC USING INFRARED FEL

S. Tagiri[†], H. Zen, T. Kii, and H. Ohgaki,
 Institute of Advanced Energy, Kyoto University, Uji, Japan

Abstract

Mode-selective phonon excitation (MSPE) is an attractive method for studying the lattice dynamics (e.g. electron-phonon interaction and phonon-phonon interaction). In addition, MSPE can control electronic, magnetic, and structural phases of materials. In 2013, we have directly demonstrated MSPE of a bulk material (6H-SiC) with MIR-FEL (KU-FEL) by anti-Stokes (AS) Raman scattering spectroscopy. Recently, we have certified that the Sum Frequency Generation (SFG) also occurs with AS Raman scattering. For distinguishing between the AS Raman scattering and SFG, we need to know the nonlinear susceptibility and the transmittance. The coefficients can be measured by the Second Harmonic Generation (SHG) spectroscopy. This paper outlines of the measurement system and reports preliminary results with a 6H-SiC sample.

INTRODUCTION

The electron-phonon interaction influences physical properties of solid-state materials. Thus, the clarification of the interaction is required for understanding basic physical properties of solid-state materials and developing high-performance devices [1,2]. To clarify the interaction, it is important to understand the relation between the electronic state and the excitation of a particular lattice vibration (phonon). Mode-selective phonon excitation (MSPE) is one of the attractive methods in the solid-state physics because it can be a powerful tool for the study of ultrafast lattice dynamics (e.g. electron-phonon interaction and phonon-phonon interaction). Not only for that, but MSPE can control electronic, magnetic, and structural phases of ma-

terials [3-5]. By irradiating a mid-infrared pulse laser tuned to the resonant wavelength of a specific phonon, the direct excitation of a specific phonon mode is available [3,5].

We have developed a technique which can directly observe the vibration of a particular phonon mode by using AS Raman scattering spectroscopy (Fig. 1) [6]. By using the technique, the MSPE induced by MIR-FEL has been directly demonstrated with a bulk material of 6H-SiC (Fig. 2)[7]. However, we have certified that SFG also occurs together with AS Raman scattering. For distinguishing between the AS Raman scattering and SFG, we need to know the nonlinear susceptibility and the transmittance. In the previous study at FHI-FEL [8], the wavelength dependence of nonlinear susceptibilities $\tilde{\chi}^{(2)}$ of 4H-SiC and 3C-SiC in MIR region have been experimentally characterized by the SHG spectroscopy.

The SHG intensity scales linearly with nonlinear polarization P , which can be given by the formula [9],

$$\vec{P}(2\omega) = \tilde{\chi}^{(2)}(2\omega, \omega, \omega) : \left(\vec{L}_1(\omega) \vec{E}_1(\omega) \right) \left(\vec{L}_2(\omega) \vec{E}_2(\omega) \right),$$

where ω denotes frequency of incident light. The frequency of SHG is twice as great as it of incident light. $\vec{L}_{1(2)}$ are the Fresnel transmission tensors for two incident beams representing the macroscopic local field corrections [10], and $\vec{E}_{1(2)}$ are the incident electric field vectors. The Fresnel transmission tensor can be evaluated by theoretical calculation. The nonlinear susceptibility must be experimentally determined by the equation of SHG spectroscopy in the reference [8]. The reflected second harmonic intensity is given by projecting the nonlinear polarization onto the field direction of the reflected [10].

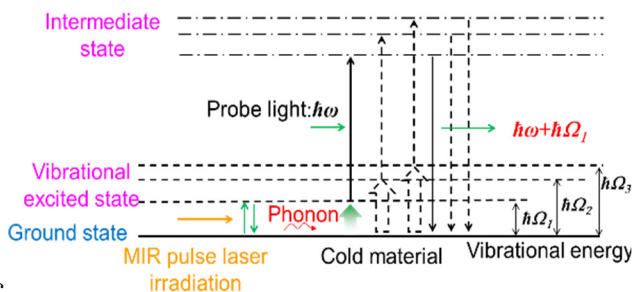


Figure 1: Schematic of the principle of demonstration experiment of MSPE induced by MIR-FEL irradiation. The anti-Stokes-Raman scattering was utilized to observe the excited state [3].

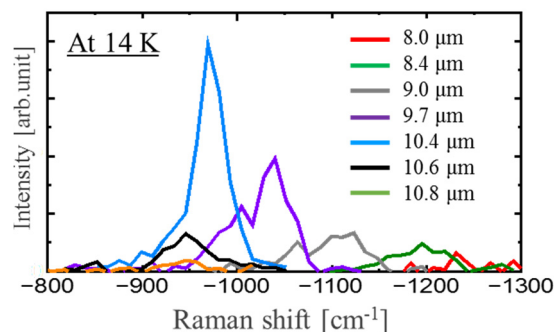


Figure 2: Anti-Stokes Raman scattering spectra measured with MIR-FEL and pico-second laser at 14K [7].

[†] tagiri.shunsuke.53a@st.kyoto-u.ac.jp

Content from this work may be used under the terms of the CC BY 3.0 licence (© 2018). Any distribution of this work must maintain attribution to the author(s), title of the work, publisher, and DOI.

SIMULATION OF PHASE SHIFTERS BETWEEN FEL AMPLIFIERS IN COHERENT ELECTRON COOLING*

Yichao Jing^{†,1}, Vladimir N. Litvinenko^{1,2}, Igor Pinayev¹

¹Collider-Accelerator Department, Brookhaven National Laboratory, Upton, NY, USA

²Physics Department, Stony Brook University, NY, USA

Abstract

Coherent electron Cooling (CeC) [1] is a proposed advanced beam cooling method that has the potential of reducing the ion beam emittance in significantly shorter amount of time compared to existing cooling methods. A high gain FEL, composed of three permanent magnet helical wigglers, is acting as an amplifier of the ion's signals picked up by electron beam in CeC. A self-consistent simulation which takes the space and possible phase shifts between wigglers into account is crucial in determining the performance of the FEL. The authors developed an algorithm based on the well-used GENESIS [2] code to treat the propagation of particles and radiations in between wigglers and predicted the FEL performance with different beamline layouts. The authors will present their simulation setup and results.

INTRODUCTION

The CeC beamline (Figure 1) consists of low energy beam transport (where electron beam is prepared and accelerated to a total energy of 14.6 MeV), a dogleg section to transport the beam to a common section where the electron beam is co-propagating with the hadron beam. In the common section, the electron beam is picking up information from hadron beam in modulator section (consists of four quadrupoles for beam optics tuning). Then the information is amplified in the FEL section and reacts back to the hadron beam with proper phase adjustment to cool the hadron beam, i.e., to reduce the hadron beam's energy spread and phase space areas. The performance of the CEC is highly dependent on the FEL gain and phase preservation. Thus, a self-consistent simulation of the FEL section is crucial in determining the required electron beam properties and in predicting the machine setups to characterize the cooling.

The FEL section consists of three helical wigglers composed of permanent magnets. The magnetic length for each wiggler is about 250 cm while the wigglers are separated by a drift space of about 42 cm. A schematic drawing of the detailed FEL can be found in Fig. 2 [3]. In between two wigglers, a three pole C-type chicane is used to properly delay the phases of the electron beam (to match

with the phases of the radiation fields) and potentially to change the gain of the FEL and thus to adjust the cooling time of the CeC. In the following section of this paper, the authors will explain a method to simulate the three wigglers together with the drifts in between wigglers. The authors will examine how to maximize the beam-field matching using the phase shifter. The authors will also discuss how this study is affecting the understanding of the gain and performance of the cooling.



Figure 1: Engineering drawing of CeC beamline (electron beam travels from right to left).

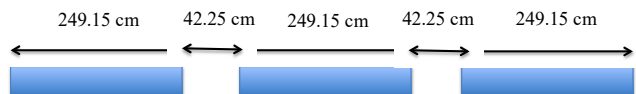


Figure 2: Schematic drawing of CeC FEL section (consisting of three wigglers and drifts in between).

FEL SIMULATION SETUP

The authors used GENESIS for the FEL process simulation. It is to our interest that the pondero-motive phases could be adjusted so that the relative phasing between the electron beam and the laser fields could be varied and FEL gain of signal could be studied under various beamline setups. In order to simulate such effect, the phase needs to be changed in a small fraction of the radiation wavelength. In GENESIS, the drifts and chicane models all result in integer steps of the radiation wavelength (tracking results are calculated and exported in steps of the radiation wavelength). Thus, for our study, the distributions of both electrons and fields at the end of each wiggler needs to be exported and reused as inputs for next section of wiggler simulation.

A transport which calculates the phase shifting for both particles and fields is fulfilled with external C++ code which reads in the binary files (.dpa and .dfl files) and generates new binary files with proper phase propagated in between the wiggler gaps. The electron beam parameters used in GENESIS for the studies in this paper is listed in Table 1 [4].

* Work is supported by Brookhaven Science Associates, LLC under Contract No. DEAC0298-CH10886 with the U.S. Department of Energy, DOE NP office grant DEFOA-0000632, and NSF grant PHY-1415252.

[†] yjing@bnl.gov

EUROPEAN XFEL INJECTOR COMMISSIONING RESULTS*

B. Beutner[†], DESY, Hamburg, Germany

on behalf of the European XFEL Accelerator Consortium and Commissioning Team

Abstract

In the first commissioning phase of the European XFEL SASE FEL driver linac, we demonstrated the design goals for the injector section. These goals include reliable operation of sub-systems and feasible beam parameters like emittance and bunch length of the beam produced by the RF gun. Of particular interest is the operation of long bunch trains with up to 2700 bunches with a 4.5 MHz repetition rate. In this presentation we will provide an overview of our experiences from the injector commissioning run including beam dynamics studies, diagnostics, and system performance.

INTRODUCTION

The European XFEL aims at delivering X-rays from 0.25 to up to 25 keV out of 3 SASE undulators lines [1, 2]. These undulators are driven by a superconducting linear accelerator based on TESLA technology [3]. European XFEL is build in an international collaboration of eleven countries.

In this paper we summarize results from the commissioning run of the injector in the first half of 2016, building on a previous report [4]. Results from the commissioning of the downstream part off the machine are summarised in [5].

The injector of the European XFEL consists of (compare Fig. 1) the RF gun, an booster and a lineariser accelerating module, a laser heater, and a diagnostic section. The main

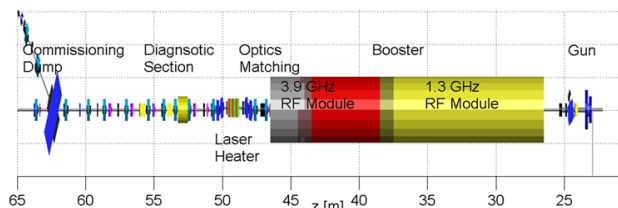


Figure 1: Injector of the European XFEL. Two RF stations (A1 at 1.3 GHz, and the AH1 at 3.9 GHz) are used for acceleration and longitudinal phase space shaping.

task of the injector is the production of low emittance beam at various charges ranging from 20 pC to 1 nC and the generation of a suitable longitudinal phase space correlation for downstream bunch compression. Nominal beam energy in the injector is 130 MeV.

As summarised in Table 1 we were able to demonstrate the design performance of the injector.

Time Structure

The unique feature of superconducting RF systems is the ability to generate long RF pulses and thus long bunch trains.

* Work supported by the respective funding agencies of the contributing institutes; for details please see <http://www.xfel.eu>

[†] bolko.beutner@desy.de

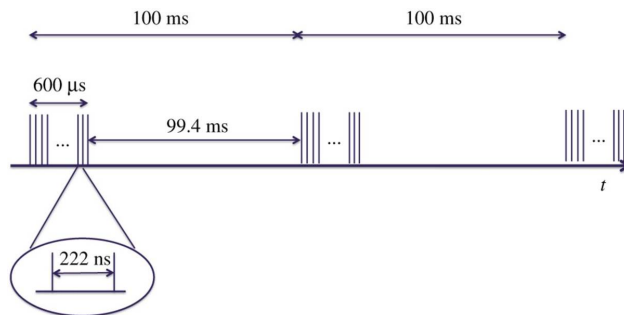


Figure 2: Time structure of the European XFEL bunch trains.

As visualised in Fig. 2 trains of up to 600 μs are generated with a 10 Hz repetition rate. With an intra train rate of up to 4.5 MHz the linac can deliver up to 2700 bunches per pulse. With a total of up to 473 kW beam power at full beam energy of 17.5 GeV. These bunches can be send to different undulator lines using fast kicker systems to allow flexible timing patterns for the user stations.

RF GUN

Gun Operation

During the injector run we restricted gun operation to limit the stress on the RF window. Either the gradient is driven to the maximum, for optimum emittance, or the pulse length is set to the design to demonstrate long train operation maintaining reasonable emittance. The parameters are shown in Table 2. These limitations are mainly imposed by the RF window. At PITZ¹ a setup with two RF windows is in operation allowing full design operation. For the time being we do not risk operation, however a later upgrade to a two-window setup is considered.

Fast Gun Start-up

Long RF pulses in the gun are challenging for gun operation. Up to 50 kW heat load are deposited in this normal conducting copper cavity from the RF. While the temperature stability requirements to keep the cavity on resonance is on the order of 0.05 deg C. Especially during startup the resonator is detuned since the RF load typically reacts much faster than the water regulation. The traditional solution to this problem is a slow increase of RF power. In such a operation, however, the startup takes about an hour with a risk of trips during the process. The process can be significantly accelerated by inducing an dynamic phase slope on the RF input signal. Such a slope is an effective frequency shift of the drive signal. A control system server is updating this phase slope according the determined detuning minimising the reflected RF power in the process [6]. With this

¹ Photo-injector test stand in DESY Zeuthen.

Content from this work may be used under the terms of the CC BY 3.0 licence (© 2018). Any distribution of this work must maintain attribution to the author(s), title of the work, publisher, and DOI.

MODEL OF PHOTOCATHODE FOR CW ELECTRON GUN

P. W. Huang[†], W. H. Huang, C. X. Tang, Tsinghua University, Beijing, China

Abstract

The rapid development of X-ray Free Electron Lasers (XFEL) requires continuous wave (CW) electron guns to provide high brightness electron bunch. Most of the proposed CW gun for free electron laser use semiconductors as photocathodes due to their high quantum efficiency and potentially low thermal emittance. We manage to establish a model to explain the photoemission of semiconductors with incident photon energy above or below the theoretical threshold and derive the expression for quantum efficiency and thermal emittance. For the incident photon energy near or below the threshold of the cathode, things will be subtle and we should be careful to consider the details we used to neglect. The results of quantum efficiency and thermal emittance agree well with the published work.

INTRODUCTION

The next generation of the XFEL is the most powerful scientific instrument for cutting edge research areas, such as material science and biology. To achieve the desired x-ray performance, many researches have been dedicated to making XFELs with high brightness and high repetition rate. This will give a great challenge to the fabrication and conditioning of the photocathode. High quantum efficiency (QE) is required to achieve high repetition rate. Thermal emittance is now of greater importance to high brightness, for it has gradually become the dominant term for beam emittance due to the development of electron gun technologies. Both characters are closely related to the photoemission of the cathode. Therefore, understanding the mechanism of photoemission will be helpful to the design of the cathode. Recently, some researchers [1, 2] have discovered that it is possible to obtain extremely low thermal emittance from semiconductors with photon energy lower than the emission threshold. These results cannot be explained by the previous model. In this paper, we would like to establish our photoemission model to explain the experimental results and explore the subtle nature near the threshold region.

MODEL OF SEMICONDUCTOR PHOTOCATHODE

Our model is shown in Fig. 1. We consider the photoelectrons provided by defect level and valance band. First, we define n_d as the ratio between the density of defect level and valance band. To estimate the value of n_d , we can do the following derivation. The electrons at defect level should follow the Fermi-Dirac statistics as

$$f(E_A) = \frac{1}{1 + 2 \exp((E_A - E_F) / k_B T)}, \quad (1)$$

where E_A is the energy of a defect level beyond the bottom of the valance band, and E_F is the Fermi energy. The factor 2 is required in the expression for defect levels or impurities, representing two spins. The electrons occupied at the defect level can be calculated as

$$N_{\text{defect}} = N_A \times f(E_A), \quad (2)$$

where N_A is the density of acceptors. To estimate the electron density of the valance band, we use the effective mass approximation. The energy of electrons can be transferred to the free particle form near the bottom or top of the band. The density of states $g(E)$ can be defined as

$$\frac{2}{8\pi^3} \int d^3k = \frac{1}{2\pi^2} \left(\frac{2m_e^*}{\hbar^2} \right)^{\frac{3}{2}} \int \sqrt{E} dE = \int g(E) dE. \quad (3)$$

Based on the expression of the density of states, we can normalize the contribution of the defect level as

$$n_d = \frac{N_{\text{defect}}}{(2m_e^* / \hbar^2)^{\frac{3}{2}} / 2\pi^2}. \quad (4)$$

Thus, the distribution of excited electrons with regard to the energy can be expressed as

$$N(E) = n_d \sqrt{E} \delta(E - \hbar\omega + E_g - E_A) + \sqrt{E(E - \hbar\omega + E_g)}. \quad (5)$$

When the photon energy is below the threshold, the contribution from defect level will become remarkable. The formation of defect level starts from the vacancies of atoms, which is very universal during the fabrication process. If the atom happens to be a positive ion, then the vacancy behaves as a negative charge. It will attract a hole

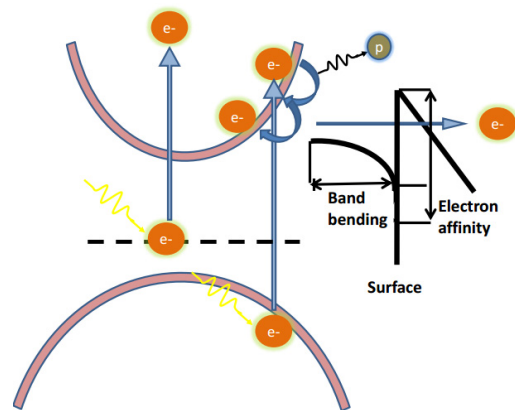


Figure 1: Model of photoemission for semiconductors.

[†] hpw17@mails.tsinghua.edu.cn

NOVEL CONCEPTS OF A HIGH-BRIGHTNESS PHOTOINJECTOR RF GUN

S.V. Kuzikov^{†,2,3}, O.A. Ivanov, A.A. Vikharev, A.L. Vikharev,

Institute of Applied Physics, Russian Academy of Sciences, Nizhny Novgorod, Russia

S. Antipov, Euclid Techlabs LLC, Bolingbrook, IL, USA

²Euclid Techlabs LLC, Bolingbrook, IL, USA

³Lobachevsky University of Nizhny Novgorod, Nizhny Novgorod, Russia

Abstract

We propose here a program to design and manufacture a high performance, advanced source of electrons having high beam brightness (over 10^{16} A/m²) and high bunch charge (~100 pC). Three innovations are being considered: (1) the use of a high peak cathode field, short-pulse RF gun; (2) the use of multi-layered diamond photocathode at low temperature; and (3) the utilization of THz ultrafast field emission gating. High peak cathode field is necessary to achieve a high brightness (low emittance) beam to be accelerated to relativistic energies before space-charge effects lengthen the bunch. The multilayered diamond photocathode is needed to obtain high QE with long wavelength laser in the first doped layer, beam cooling in the next layer, and negative electron affinity at the emission layer. High field single cycle THz pulses, produced by means of laser light rectification in a nonlinear crystal, allow to avoid a UV laser, provide high field emission charge (up to 1 nC) and ~1 GV/m pre-acceleration of sub picosecond bunches.

HIGH CATHODE-FIELD RESONATORS

A natural way to enhance brightness of beams emitted in a photoinjector gun is increasing of cathode fields in order to mitigate space charge effects [1,2]. The necessary high fields can be obtained avoiding a breakdown and a pulse heating by means of short high-power RF pulses. Because high brightness is extremely important parameter for XFEL applications, a possible solution could be to use an additional RF gun which emits short bunch train producing short high-power RF pulse. In recent experiments, it was shown that ~300 MW, 10 ns of RF power can be taken away from bunch train in ANL gun [3]. It is important that RF power in this case is phase locked with a laser of the first “driving” RF gun. The same laser can service the second high-brightness RF gun.

Note that high fields are necessary at near cathode area only because in the rest part of the resonator a flying beam is already relativistic one. That is why, we suggest a scheme of a gun consisted of two uncoupled cells powered independently (Figure 1). To obtain ~500 MV/m on the cathode surface in X-band, a large portion of RF power, about 70 MW, is directed into the half-cell section that has quality factor $Q \approx \pi \cdot f \cdot \tau$ of 370 ($f=11.7$ GHz, $\tau=10$ ns). RF is coupled in using a coaxial coupler and a choke

reflector. Approximately 20% of the power fed into the first section is required for the second 1-cell section to achieve an acceleration field of 150 MV/m. The power splitting between the two sections is done using a variable power attenuator and a variable phase shifter. The field structures in cells are shown in Figure 1.

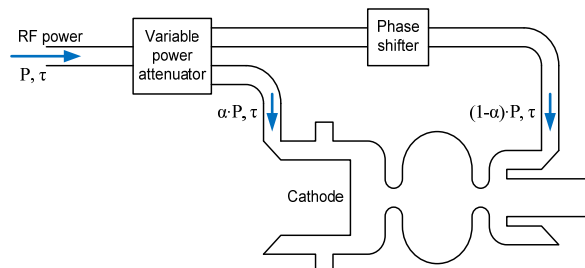


Figure 1: A schematic of the proposed two-cell photoinjector.

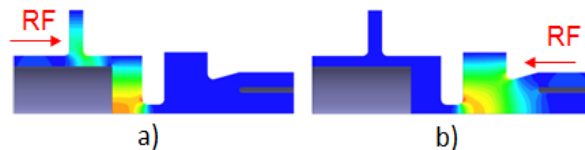


Figure 2: Field distribution in the first half-cell (a) and in the second cell (b).

ULTRAFAST FIELD EMISSION GATING

Another idea is to build a high brightness gun based on a gated picosecond flat field-emission cathode. Laser-based single-cycle THz pulse production by optical rectification and semiconductor switching yields high intensity, ~ 1 ps long THz pulses [4]. The 1 GV/m field strength of the THz pulse, combined with the RF gun accelerating field of ~100 MV/m, results in the emission of a short current pulse from the cathode. Compared to a standard photocathode, the beam brightness is increased due to the high additional accelerating field provided by the THz pulse. The proposed injection scheme does not require a UV laser, high emission charge (up to 1 nC) is emitted due to field emission at high THz fields for sub-picosecond bunch lengths.

In order to obtain the highest emission fields the THz pulse that is generated will be focused to the smallest possible size at the cathode by means of a parabolic mirror

[†] sergeykuzikov@gmail.com

HIGHER FIELDS AND BEAM ENERGIES IN CONTINUOUS-WAVE ROOM-TEMPERATURE VHF RF GUNS*

F. Sannibale[†], J. Byrd, D. Filippetto, M. Johnson, D. Li, T. Luo, C. Mitchell, J. Staples, S. Virostek, Lawrence Berkeley National Laboratory, 94720 Berkeley, CA,

Abstract

The development/proposal in the last decade of MHz-class repetition rate free electron lasers (FELs), inverse Compton scattering sources, and ultrafast electron diffraction and microscopy (UED/UEM), required the development of new gun schemes capable of generating high brightness beams at such high rates. The VHF-Gun, a 186 MHz room-temperature continuous wave RF photogun developed at the Lawrence Berkeley Lab (LBNL) was one of the answer to that need. The VHF-Gun was constructed and tested in the APEX facility at LBNL successfully demonstrating all design parameters and the generation of high brightness electron beams. A close version of the APEX VHF-Gun is in the final phase of fabrication at LBNL to operate as the electron source for the LCLS-II, the new SLAC X-ray FEL. The recently approved upgrade of the LCLS-II towards higher energies (LCLS-II HE), and the always brightness-starving UED and UEM applications, would greatly benefit from an increased brightness of the electron source. Such performance upgrade can be obtained by raising the electric field at the cathode and the beam energy at the gun exit. In this paper, we present and discuss possible upgrade options that would allow to extend the VHF-Gun performance towards these new goals.

INTRODUCTION

The last decade has been characterized by the formidable and successful development of several X-ray free electron laser (FEL) facilities capable to generate peak brightness of up to 9 orders of magnitude higher than the ones generated by 3rd generation light sources based on storage rings. More recently, a number of new FEL facilities were proposed targeting a similar dramatic performance increase also in terms of average brightness using superconducting RF (SRF) linacs operating in continuous wave (CW) mode. These facilities are designed to increase the repetition rate of the original FELs from hundreds of Hz to MHz. Among those, the LCLS-2 at SLAC was funded and it is now in the construction phase [1], and very recently, the Shanghai Coherent Light Facility (SCLF) project was approved in China [2].

The electron source is a key component in linac-based applications where it ultimately determines the maximum electron beam brightness and the facility overall performance. A high-repetition rate, high-brightness electron source was not readily available and several groups around the world started to propose and develop

new schemes or upgrades for electron guns that could address that need.

It is worth to remark that the availability of such a high-repetition rate, high-brightness source would also dramatically benefit other electron beam applications such as inverse Compton Scattering sources and ultrafast electron diffraction and microscopy (UED/UEM).

In response to that need, our group at the Lawrence Berkeley Laboratory (LBNL) developed in the framework of the Advanced Photoinjector EXperiment (APEX), the VHF-Gun, a room-temperature RF photo-gun resonating at 186MHz in the VHF frequency range and designed to operate in CW mode [3, 4]. During its commissioning, the gun successfully demonstrated reliable continuous wave RF operation at the design parameters [5] generating MHz electron beams with transverse emittances, longitudinal phase space and charge suitable for the operation of a high-repetition rate X-ray FEL such as the LCLS-II [6]. Also importantly, the APEX VHF-gun also demonstrated the low vacuum pressures required to operate high quantum efficiency semiconductor cathodes (Cs₂Te and CsK₂Sb) with acceptable lifetimes [7, 8].

At the present time, a close version of the APEX gun is in the final phase of fabrication at LBNL to serve in the LCLS-II injector, while the original APEX gun is now in operation as the electron source for HiRES, the LBNL high repetition-rate UED experiment [9].

In spite of these positive developments, there are already several high repetition-rate applications that would strongly benefit from an even further increase in beam brightness at high repetition rates. A notable example is the LCLS-II HE, the higher energy upgrade of the SLAC FEL [10], which already received CD-0 (the 1st approval level by the US Department of Energy. LCLS-II HE would require for its main mode of operation at 100 pC bunch charge, a normalized transverse emittance approaching 0.1 μm rms for further extending its lasing spectrum in the hard X-ray region. This is an about two-fold reduction with respect to the present LCLS-II emittance requirement. The additional electron beam coherence offered by the higher brightness would also greatly benefit UED/UEM applications.

The successful performance of the APEX VHF-Gun pushed our group to investigate the possibility of extending the VHF technology towards higher beam brightness while maintaining the operational functionality and reliability demonstrated by the present VHF-gun. In this paper, we present several concepts for possible gun configurations with the capability of achieving the desired enhanced performance. We will refer to these upgraded gun versions as the APEX-2.

*Work supported by the Director of the Office of Science of the US Department of Energy under Contract no. DEAC02-05CH11231

[†]fsannibale@lbl.gov

Content from this work may be used under the terms of the CC BY 3.0 licence (© 2018). Any distribution of this work must maintain attribution to the author(s), title of the work, publisher, and DOI.

R&D AT SLAC ON NANOSECOND RANGE MULTI MW SYSTEMS FOR ADVANCED FEL FACILITIES*

A. Krasnykh[†], A. Benwell, T. Beukers, and D. Ratner, SLAC, Menlo Park, CA, USA

Abstract

A nanosecond range, multi MW system containing TEM mode electrodynamic structures fed by controllable pulsers are needed for (1) an array of FEL beamlines powered by superconducting linear accelerators operating with close MHz bunch repetition rate and (2) fast injection systems in multi-bend achromat upgraded (MBA-U) storage rings. The R&D effort covers both: type (1) and (2) layouts.

INTRODUCTION

L-Band CW linacs with approximately MHz bunch trains powered by a photoinjector are a fundamental to next generation FELs [1]. Such FEL projects require MW peak power spreader kicker systems of a nanosecond range. These systems have to distribute GeV bunches from the superconducting CW linac into beamlines with independently configurable undulators. In the ideal case, such systems allow the option to pick out bunches with arbitrary time pattern from a MHz bunch train. This technology optimizes the flexibility of the FEL for end users.

US Storage Ring Upgrades [2] are another example where nanosecond range multi-MW peak pulsers are required. They are necessary for the injection/extraction system to swap “bad” bunches with the new ones without shaking up the neighbours. Similar requirements were specified for the injection/extraction system of the ILC damping rings [3]. A main difference between [2] and [3] pulser specification is repetition rates. The repetition rate to swap bunches in the storage ring is approximately four orders of a magnitude lower compared to the ILC damping rings pulser.

The MaRIE complex [4] with pRad, XFEL, and eRad beamlines and switchyards is discussed presently. The electron bunch trains of the XFEL and eRad SC linacs will be unevenly spaced during 100 μ s. The spacing between micro pulses is governed by the radiographic experiments. The unevenness in the bunch train formed in the photoinjector is a source of transients in the high Q accelerating structures. To avoid unwanted effects during accelerating mode, the MaRIE linac ends may contain a fast kicker system. The kicker system allows controlling the 12 GeV pulse train with the arbitrary bunch pattern. Pulses with fast rise/fall shapes are needed to knock out the unneeded bunches from the 100 μ s train.

Discussed above are motivations for MW peak power systems of a nanosecond range in the future. However, beamlines built now at SLAC LCLS-II XFEL may incorporate the pump-probe experiments with two bunches. A separation between bunches is approximately 10 ns. A

fast kicker system is required to control the bunch destination. The beamline layout is illustrated in Fig. 1.

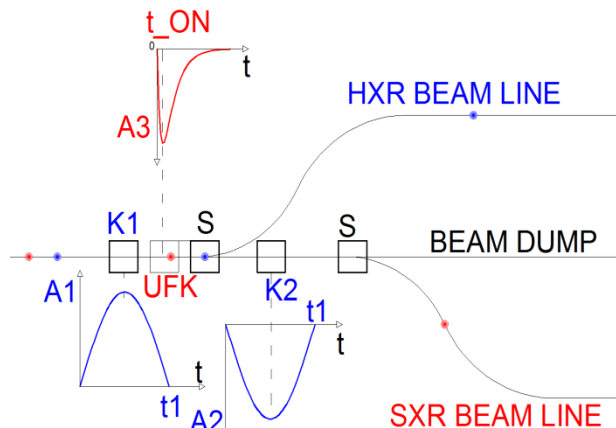


Figure 1: LCLS-II beamline scenario for pump-probe experiments. Red and blue dots represent two bunches, which propagate from the left to the right. K1 and K2 boxes are “slow” kicker magnets. Their transverse force (A1 and A2) vs. time (t) is shown in the blue curves. Two septum magnets (S) direct bunches into the hard or soft X-ray beamlines. The “fast” kicker system (UFK) is introduced into this beamline for the pump-probe experiments. The transverse force peak (A3) of the UFK vs. time (t) is shown in the red curve and cancels the kick K1. The system is activated when the separation between bunches is approximately 10 ns. The resulting x-rays, of different color, would be recombined for pump-probe experiments.

Figure 1 illustrates one possible scenario with a fast kick ON time (t_{ON}) and slow decay. The reader can find other scenarios with the fast kicker system in [5] where fast kick OFF time is discussed too.

GENERAL SPECIFICATIONS FOR FAST KICKER SYSTEM

Table 1 shows a general requirement for fast kicker system.

Table 1: Required Specifications

Parameter	Requirement	Unit
Deflection	0.75	mrad
Bunch Energy	4.0	GeV
Aperture	10	mm
Rise or/and Fall time	10.8 is good, 5.4 is better	ns
Repeatability	100	ppm rms
Availability	Low	
Pre-pulse/Post-	5	% of peak

* Work supported by US DoE contract DE-AC02-76SF00515

[†] e-mail address: krasnykh@slac.stanford.edu

LASER-TO-RF SYNCHRONIZATION WITH FEMTOSECOND PRECISION

T. Lamb*, Ł. Butkowski, E. Felber, M. Felber, M. Fenner, S. Jablonski,
T. Kozak, J. Müller, P. Prędki, H. Schlarb, C. Sydlo, M. Titberidze,
F. Zummack, Deutsches Elektronen-Synchrotron (DESY), Hamburg, Germany

Abstract

Optical synchronization systems are already in regular operation in many FELs, or they will eventually be implemented in the future. In FLASH and the European XFEL, phase-stable optical reference signals are provided by a pulsed optical synchronization system in order to achieve low timing jitter FEL performance. The generation of phase-stable RF signals from a pulsed optical synchronization system is still a field of active research. The optical reference module (REFM-OPT), designed at DESY for operation in both FELs, employs a laser-to-RF phase detector, based on an integrated Mach-Zehnder interferometer. The phase drift of the 1.3 GHz RF reference signals with respect to the optical pulses is measured and actively corrected within the REFM-OPT at multiple locations in the accelerator. Therefore the REFM-OPT provides phase stable 1.3 GHz RF reference signals at these locations. The short-term and long-term performance in the accelerator tunnel of the European XFEL is presented and carefully reviewed.

INTRODUCTION

Femtosecond stability has become a key requirement in modern large-scale free-electron lasers (FELs). Optical synchronization systems for femtosecond synchronization have been developed and built over the past years. The most recent application for such an optical synchronization system is the remote RF synchronization. RF reference signals are distributed and used as the phase reference for many accelerator sub-systems at the European XFEL and FLASH at DESY. Their performance requirements are driven by the low-level RF (LLRF) system, where the stability of the accelerating fields in the superconducting cavities depends on them. The field stability requirement of 0.01° at 1.3 GHz (or about 20 fs) leads to a stability requirement of the reference signals of about 10 fs [1].

An active system had to be implemented due to the size of the European XFEL and the number of devices connected. RF amplifiers are required to compensate cable losses. The phase stability of the RF reference signals is disturbed during their transport through the accelerator due to temperature and humidity induced drifts of the installed RF cables, amplifiers and auxiliary components. The 10 fs stability can therefore – especially in large scale FELs like the European XFEL – not be reached by conventional RF transport. The optical synchronization system however can supply laser pulse trains with femtosecond stability to any point in the

accelerator. A Laser-to-RF phase detector within the REFM-OPT is used to measure the phase drift of the 1.3 GHz RF reference signals with respect to the optical reference at dedicated locations. These drifts are actively corrected and the REFM-OPT can therefore supply RF reference signals with femtosecond stability.

THE OPTICAL SYNCHRONIZATION SYSTEM

The central component of the optical synchronization system is the redundant master laser oscillator (MLO) which generates a low jitter, 216.66 MHz repetition rate optical pulse train at a wavelength of 1550 nm. It is tightly phase-locked to the RF master oscillator of the facility. The MLO is located in a central synchronization laboratory close to the injector laser. Environmental parameters like temperature and humidity are carefully controlled in this synchronization laboratory.

The laser pulses are subsequently distributed to individual link stabilization units (LSUs) from where the fiberlinks to the individual end stations launch. The fiberlink stabilization is based on balanced optical cross-correlation. The length changes of the optical fibers are compensated by a piezo driven fiber stretcher for fast changes and an optical delay line for slow long-term drift correction. Thirteen stabilized fiberlinks are currently in permanent operation at the European XFEL. More information on the optical synchronization system can be found in [2]. The optical synchronization system supplies reference signals to three different types of end stations.

The bunch arrival time monitors (BAMs) are used to measure the electron bunch arrival time with femtosecond precision at dedicated locations along the accelerator. A more detailed description of the BAM system can be found at [3]. A feedback system to the LLRF controllers allows to stabilize the electron bunch arrival time based on the BAM measurement.

Laser-to-Laser synchronization using balanced two-color optical cross-correlation is employed to synchronize laser systems along the FEL to the optical synchronization system. This is especially crucial for the pump-probe lasers which need to be tightly synchronized to the FEL but it is also foreseen for the injector lasers. Further details on Laser-to-Laser synchronization is available at [4].

The third and newest application is the Laser-to-RF synchronization. The key component of the REFM-OPT is the Laser-to-RF phase detector. It is based on a commercial integrated Mach-Zehnder modulator in which the phase dif-

* Thorsten.Lamb@desy.de

OPTIMIZATION OF SUPERCONDUCTING UNDULATORS FOR LOW REPETITION RATE FELS

J. A. Clarke, K. Marinov, B. J. A. Shepherd, and N.R. Thompson,
STFC Daresbury Laboratory and Cockcroft Institute, Sci-Tech Daresbury, Warrington, UK
V. Bayliss, J. Boehm, T. Bradshaw, A. Brummitt, S. Canfer, M. Courthold, B. Green, T. Hayler,
P. Jeffery, C. Lockett, and D. Wilsher, STFC Rutherford Appleton Laboratory, Didcot, UK
S. Milward and E. C. M. Rial, Diamond Light Source, Didcot, UK

Abstract

Superconducting undulators (SCUs) optimized for storage rings and MHz-level FELs require an intermediate beam screen to intercept the power deposited by the electron beam, due to resistive wall wakefields, to prevent magnet quenching. This beam screen increases the magnet gap by around 2 mm which is a significant increase when compared to the typical electron beam aperture of around 5 mm. However, lower repetition rate FELs only deposit of the order of tens of mW/m and so the beam screen is no longer needed resulting in a significant reduction in undulator magnet gap. We have investigated the impact of this reduced magnet gap and found that the magnetic field level increases greatly. For example, an SCU with a 15-mm period and 5-mm aperture optimized for a low repetition rate FEL instead of a storage ring will generate a field of 2.1 T compared to 1.4 T. Such a major increase in undulator performance could have a significant impact on the optimization of FELs. This paper describes how an SCU optimized for application in a FEL will be able to generate magnetic field levels far beyond those currently foreseen for any other magnet technology.

INTRODUCTION

Despite the ongoing improvements in permanent magnet undulators (PMUs), there is still a clear margin in performance advantage to be gained through the application of superconducting materials and it is for this reason that several groups around the world have been actively pursuing the detailed development of short period, high field SCUs for light source applications over the past ten years or more [1]. This research and development effort has led to the construction of a few SCUs which are now installed and in daily use on storage ring light sources in Germany [2] and USA [3]. These particular examples have exhibited very good operational performance in terms of reliability, stability, and user experience and this has increased confidence within the accelerator community that national FEL light source facilities, such as LCLS-II, should carefully assess employing SCUs rather than permanent magnet alternatives in their baseline configurations [4].

This paper explores how and when the engineering of SCUs can be significantly simplified for FELs compared to storage rings and the impact this will have on the available undulator parameters compared against the most advanced PMU options today.

SCU OPTIMIZATION FOR FELS

International efforts on SCU developments have primarily focussed upon storage ring applications which have different constraints to FELs. One clear difference is the accelerator vacuum requirement which is radically different between a stored beam facility and a single pass facility, with the former being far more demanding. Another difference is the relatively large good field region required in the storage ring undulators to maintain an adequate dynamic aperture and to enable efficient off-axis injection. Neither of these issues is of importance for single pass FELs, enabling narrower good field regions to be fit for purpose and potentially further simplifying the engineering.

However, the most significant difference between the two types of facility is the heating due to the electron beam in the SCU itself. In a storage ring care must be taken to ensure no synchrotron radiation from upstream dipoles can impinge on the SCU cold surface which is not an issue in FELs. More importantly though, in a storage ring there is significant beam heating due to resistive wall wakefields (RWW) within the SCU. This power level is too high for the 4K undulator magnet to handle without quenching and so all storage ring SCUs employ an intermediate beam screen between the magnet poles, held at between 10 and 20K, to absorb this power safely. This beam screen also acts as the beam vacuum chamber, which is essential to separate the machine vacuum from the magnet's thermal insulating vacuum. Significant engineering efforts are made to make this vacuum vessel have as little impact on the SCU magnet gap as possible but even with wall thicknesses of ~0.5mm and similar insulating spacing between this surface and the SCU coils and poles the magnet gap is increased by typically ~2.0mm compared to the aperture needs of the electron beam itself.

Since the power deposited by these wakefields scales linearly with the number of bunches passing through the SCU, it is clear that as the bunch repetition rate is reduced there will be a point at which the SCU will not suffer from significant beam heating and the internal vacuum chamber can be completely removed from the design and instead be replaced by a thin high conductivity copper liner similar to that employed by all permanent magnet in-vacuum undulators (IVU).

UPDATE ON THE LIFETIME OF Cs₂Te CATHODES OPERATED AT THE FLASH FACILITY

S. Schreiber*, S. Lederer, DESY, Hamburg, Germany

L. Monaco, D. Sertore, P. Michelato, INFN Milano - LASA, Segrate (MI), Italy

Abstract

The photoinjector of the free-electron laser facility FLASH at DESY (Hamburg, Germany) uses Cs₂Te photocathodes. We give an update on lifetime and quantum efficiency of cathodes operated at FLASH during the last years. At the time of the conference, cathode 73.3 has been operated with a record of 933 days with a stable quantum efficiency of in average 8.8 %.

INTRODUCTION

Since 2005, FLASH [1–4], the free-electron laser user facility at DESY (Hamburg, Germany), successfully delivers high brilliance femtosecond short XUV and soft X-ray SASE radiation pulses to photon experiments.

A unique feature of FLASH is its superconducting accelerating technology. It allows to accelerate several thousand electron bunches per second. The bunches come in bursts with a repetition rate of 10 Hz. The maximal burst duration is 0.8 ms, the smallest distance between single bunches is 1 μs allowing a maximum number of 800 bunches per burst or 8000 bunches per second with a single bunch charge between 20 pC and a bit more than 1 nC. With a beam time of more than 8000 h per year, a maximum of about 200 C would be extracted from the cathode per year. In practice, not all users require maximum charge and maximum number of bunches per second so that the charge actually extracted is much lower and depends on the experimental requirements. The cathode of the electron source has to cope with these requirements.

THE ELECTRON SOURCE

The electron source of FLASH is a photoinjector based on a normal conducting L-band 1.5 cell RF-gun (1.3 GHz). [5] The RF-gun is version 3 (G3.1) with the usual race-track spring RF-contact between the gun backplane and the cathode. The RF-gun was built in 2005, conditioned at the PITZ facility (DESY, Zeuthen) in 2006 and finally installed in April 2013 as a preemptive maintenance measure replacing gun G4.1. The gun is operated with an RF power of 5 MW corresponding to a maximal accelerating field at the cathode of 52 MV/m, which leads to a beam momentum of 5.6 MeV/c. The gun is designed to provide the same RF-pulse length as the superconducting accelerator: the RF pulse flat top duration is up to 800 μs with a repetition rate of 10 Hz. The average RF power of 40 kW is efficiently cooled away by a dedicated water cooling system [6] keeping the gun temperature within 0.02 K [7].

* email: siegfried.schreiber@desy.de

The RF-gun and cathode system vacuum is pumped with several ion-getter pumps (IGP) most of them with a pumping speed of 60 l/s each. A few IGP's are equipped with an additional titanium-sublimation pump (TSP) adding 1000 l/s. The vacuum set-up is very similar to Fig. 4 in [5]. The base pressure without RF is kept below 2×10^{-10} mbar, with RF, the pressure increases roughly by a factor of 2. Note, that the pressure is not measured inside the gun body nor at the cathode surface.

To generate thousands of bunches per second with a charge in the nC-scale, we use a high quantum efficiency cathode. Cesium telluride (Cs₂Te) has been proven to be a reliable and stable cathode material with an excellent quantum efficiency (QE) for a laser wavelength around 260 nm [8–10]. The bunch charge required for FLASH operation is between 20 pC (for ultra-short SASE pulse operation) and a bit more than 1 nC (for efficient THz-generation).

Typical numbers are illustrated in the following example: We extract a charge of 1 nC with a laser pulse energy of 50 nJ having a QE of the Cs₂Te cathode of 10 %. The laser wavelength is 262 nm. For a burst of 800 pulses with 1 MHz and 10 bursts per second, this corresponds to a burst laser power of 50 mW. The laser pulse duration is 6.5 ps (sigma) leading to a peak power of 3 kW only. The laser spot shape is a truncated Gaussian with a diameter of 1.2 mm yielding a fluence in the burst of 4.4 mJ/cm², far away from typical damage thresholds of a few J/cm². These are all reasonable low laser power values which eases the design of the laser system and, damages or ablations of optical components or of the cathode thin film itself are avoided. The laser is sent to the cathode through a high quality fused-silica vacuum window [11] and is reflected to the cathode with a custom made mirror [12] inside the vacuum. For details on the FLASH injector laser systems, the reader is referred to [13] and references therein.

QUANTUM EFFICIENCY

For practical reasons, we define the quantum efficiency (QE) as the ratio of number of photons impinging the photocathode and the number of electrons emitted – while the RF-gun is operated at its nominal working point.

The nominal working point of the RF-gun is at a forward power of 5 MW which yields in an on-crest accelerating field of 52 MV/m. The launch phase is set to of 38° from the zero-crossing point. This phase has been chosen years ago and has been kept as a reference phase for all QE-data presented since then. The launch phase for SASE-operation is usually around 45°.

CALCULATIONS FOR A THz SASE FEL BASED ON THE MEASURED ELECTRON BEAM PARAMETERS AT PITZ

P. Boonpornprasert*, M.Krasilnikov, F. Stephan, DESY, Zeuthen, Germany

Abstract

The Photo Injector Test facility at DESY, Zeuthen site (PITZ), develops high brightness electron sources for modern linac-based Free Electron Lasers (FELs). The PITZ accelerator can also be considered as a suitable machine for the development of an IR/THz source prototype for pump-probe experiments at the European XFEL. Calculations of THz radiation by means of a SASE FEL based on the simulated and the measured beam profiles at PITZ for the radiation wavelength of 100 μm were performed by using the GENESIS1.3 code. The results of these simulations are presented and discussed in this paper.

INTRODUCTION

The Photo Injector Test facility at DESY, Zeuthen site (PITZ) has been established to develop, study and optimize high-brightness electron sources for modern linac-based short-wavelength Free-Electron Lasers (FELs) like FLASH [1] and the European XFEL [2].

The concept of generating IR/THz radiation by electron bunches from a "PITZ-like" accelerator for pump and probe experiments at the European XFEL was presented in [3]. PITZ has been considered as an ideal machine for the development of such IR/THz source. Start-to-end (S2E) simulations of the SASE FEL from a PITZ-like accelerator were performed and presented in [4]. An electron beam with 4 nC bunch charges was used for the FEL generation. Experimental optimization and characterization of 4 nC electron beams including time-resolved measurements were done and presented in [5].

In this paper, we present results of beam dynamics simulation using the actual PITZ beamline layout together with the results of electron beam measurements. Then, we performed SASE FEL simulations based on the simulated and the measured beam profiles for a radiation wavelength of 100 μm by using the GENESIS1.3 code. The initial seed for the random number generator used for particle phase fluctuation in the GENESIS1.3 code was scanned in order to simulate the FEL pulse energy fluctuation during the SASE FEL process.

BEAM DYNAMICS SIMULATION

Since works in [4] were studied by using only a PITZ-like beamline layout, the beam dynamics simulations with the actual PITZ layout were re-done. The actual PITZ beamline plus an extension for simulation studies for an IR/THz SASE FEL at the end of the beamline is shown in Fig. 1. The layout consists of a 1.6-cell L-band photocathode RF gun

surrounded by main and bucking solenoids, a CDS booster, a TDS cavity, screen stations, quadrupole and dipole magnets and an APPLE-II type undulator which is assumed to be placed at the end of the beamline. Dispersive sections (LEDA, HEDA1 and HEDA2) are used for electron beam momentum and longitudinal phase space (LPS) measurements.

The ASTRA code [6] is used for simulation of the electron beam with 4 nC bunch charge from the cathode to the undulator entrance. Space-charge effects were included in the simulation as well. Machine parameters used in this simulation are shown in Table 1. The RF gun phase was adjusted for the maximum mean momentum and the booster phase was adjusted for the minimum momentum spread. The quadrupole magnets along the beamline were used for beam transport and matching. The simulated beam parameters at the undulator entrance are listed in Table 2.

Table 1: Machine Parameters Used in Beam Dynamics Simulations and Measurements. PC means Photocathode.

Parameter	Sim.	Meas.
PC laser long. pulse shape	Flat-top	Gaussian
PC laser pulse duration (FWHM) [ps]	~20	~11
PC laser diameter on the cathode [mm]	5.0	3.7
Peak E-field in the gun [MV/m]	60.5	60.5
Peak E-field in the booster [MV/m]	9.8	9.8

Table 2: Electron Beam Parameters Resulted from Beam Dynamics Simulation and Measurements

Parameter	Sim. [§]	Meas. [†]
Bunch charge [nC]	4.0	4.0
Average momentum [MeV/c]	15.1	15.2
Momentum spread [keV/c]	134.7	50.9
Average slice momentum spread [keV/c]	6.2	28.5
Projected $\varepsilon_{n,x}$ [μm]	7.9	7.1
Projected $\varepsilon_{n,y}$ [μm]	7.6	11.1
Average slice $\varepsilon_{n,x}$ [μm]	3.1	10.9
Average slice $\varepsilon_{n,y}$ [μm]	3.1	-
Peak current [A]	195	183
Bunch length [mm]	2.0	3.0

[§] The simulated beam parameters at the undulator entrance

[†] The measured beam parameters at the measurement stations

* prach.boonpornprasert@desy.de

COAXIAL COUPLER RF KICK IN THE PITZ RF GUN

Y. Chen[†], H. Qian, M. Krasilnikov, I. Isaev, Q. Zhao¹, P. Boonpornprasert, J. Good, H. Huck, A. Oppelt, Y. Renier and F. Stephan, DESY, Platanenallee 6, 15738 Zeuthen, Germany
W. Ackermann, H. De Gerssem, TEMF, Technische Universität Darmstadt, Schlossgartenstraße 8, 64289 Darmstadt, Germany
M. Dohlus, DESY, Notkestraße 85, 22607 Hamburg, Germany

Abstract

We investigate a transverse RF kick induced by the transition between rectangular waveguide and coaxial line of the RF coupler in the 1.6-cell L-band normal conducting (NC) RF gun at the Photo Injector Test Facility at DESY, Zeuthen site (PITZ). A three-dimensional electromagnetic simulation shows the disturbed RF field distributions in the fundamental accelerating mode. Based on the 3D RF field map, an electron beam based characterization and quantification of the coaxial coupler RF kick in the PITZ gun is simulated. The current status of the investigation is presented.

INTRODUCTION

As a high brightness photoelectron source required for the operation of TESLA technology based FELs, the 1.6-cell 1.3-GHz NC RF gun at PITZ has been used at FLASH [1] and the European X-ray Free Electron Laser (XFEL) [2]. The RF power in the PITZ gun is supplied by a 10 MW multi-beam klystron. The power is coupled from the input waveguide (WG) via the door-knob transition into the rotationally symmetric coupler and the gun cavity. This is illustrated in Fig. 1. For a thorough description of the PITZ gun and its supporting RF system, the interested reader is referred to [3-6].

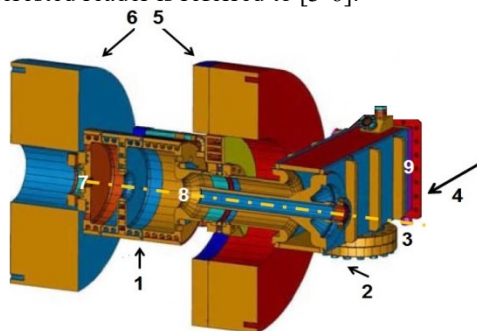


Figure 1: Sketch of the PITZ gun with coaxial RF coupler: 1-gun cavity, 2-door-knob transition, 3-cavity axis, 4-RF feeding direction, 5-main solenoid, 6-bucking solenoid, 7-cathode, 8-end of coaxial line and 9-reference position of WG port for simulations. Note that this sketch is rotated by 90 degrees compared to the computational model used in the follow-up simulations.

The rotationally symmetric coupler at PITZ is designed as a coaxial input coupler that couples to the gun cavity on the cavity axis [7-8]. The axial symmetry of the cavity thus stays undisturbed. Compared to the conventional input coupler aside the cavity [9], the asymmetric electromagnetic modes are strongly suppressed. This inhibits the emittance growth due to the RF field distortions caused by these asymmetric modes. The evanescent dipole modes, however, are not avoidable to be generated at the door-knob transition (see 2 in Fig. 1). The dipole modes may not be fully decayed till the end of the coaxial line and thus can disturb the cylindrical symmetry of the fundamental mode. The induced RF field asymmetries may create a transverse kick onto the electron bunch [10-11]. This occurs, more specifically, when the bunch is leaving the cavity through the inner conductor of the coaxial line (see 8 in Fig. 1). To first clarify the RF field asymmetries, three-dimensional electromagnetic field simulations are performed using CST Microwave Studio® (CST-MWS®) [12].

RF FIELD ASYMMETRY

The RF field in the gun is simulated using the frequency domain solver in CST-MWS®. To enable excitation, a standard WG port condition is applied at the boundary of the input WG. Based on a so-called mono-frequency excitation method, two principal matching conditions (i.e., broadband matching from WG to coaxial line and narrowband matching from coaxial line to cavity) are satisfied by slightly tuning the length of the inner conductor. This results in a reflection coefficient lower than -30 dB at the WG port position. The RF field is then calculated under such optimized conditions of the gun at its resonance frequency. Surface losses are taken into account. Based on the field simulation, a 3D RF field map is also extracted for later particle tracking simulations in ASTRA [13].

In Fig. 2, the RF field asymmetries are exemplarily visualized in the close vicinity of the coaxial coupler. One can recognize these asymmetries from the electric and magnetic field strength variation around the inner conductor, as well as from the on-axis zero-crossing positions of the fields.

[†] ye.lining.chen@desy.de

¹ on leave from IMP/CAS, Lanzhou, China

Content from this work may be used under the terms of the CC BY 3.0 licence (© 2018). Any distribution of this work must maintain attribution to the author(s), title of the work, publisher, and DOI.

Content from this work may be used under the terms of the CC BY 3.0 licence (© 2018). Any distribution of this work must maintain attribution to the author(s), title of the work, publisher, and DOI.

PRELIMINARY ON-TABLE AND PHOTOELECTRON RESULTS FROM THE PITZ QUASI-ELLIPSOIDAL PHOTOCATHODE LASER SYSTEM

J. Good[#], G. Asova[†], P. Boonpornprasert, Y. Chen, M. Gross, H. Huck, I. Isaev, O. Lishilin, D. Kalantaryan, X. Li, G. Loisch, M. Kraslinikov, D. Melkumyan, A. Oppelt, Y. Renier, H. Qian, T. Rublack, F. Stephan, Q. Zhao[¶], Deutsches Elektronen-Synchrotron, Zeuthen, Germany
 I. Hartl, S. Schreiber, Deutsches Elektronen-Synchrotron, Hamburg, Germany
 A. Andrianov, E. Gacheva, E. Khazanov, S. Mironov, A. Poteomkin, V. Zelenogorsky, Institute of Applied Physics, IAP, Nizhny Novgorod, Russia
 E. Syresin, JINR, Dubna, Moscow Region, Russia

Abstract

High brightness photoinjectors for superconducting linac-based FELs are developed, optimized and characterized at the Photo Injector Test facility at DESY in Zeuthen (PITZ). Simulations have previously shown that homogeneous ellipsoidal photocathode laser pulses allow the production of high brightness electron bunches with minimized emittance.

Correspondingly, a new prototype photocathode laser system capable of producing quasi-ellipsoidal laser pulses was installed last year and brought into active electron beam operation at the start of this year.

Several electron beam measurements have been made with pulse shaping. It was possible to show a beam quality improvement equivalent to that of conventional beam shaping techniques such as pulse stacking and beam shaping apertures. Further improvements were constrained due to a number of systematic limitations which are to be addressed in the redesign currently under construction.

INTRODUCTION

Low-emittance beams have been obtained using a flat-top temporal laser profile with 60 MV/m gradient in the RF gun [1], more recently with a Gaussian temporal laser profile and 53 MV/m [2]. In earlier simulations, it was found that uniform ellipsoidal charge distributions with sharp charge transition boundaries would produce even higher beam quality. Furthermore, it was shown that such electron bunches should also be less sensitive to machine parameter jitter [3] and therefore increase the reliability and stability – crucial parameters for single-pass FELs such as FLASH and the European XFEL.

QUASI-ELLIPSOIDAL PHOTOCATHODE LASER SYSTEM

Naturally, a homogenous ellipsoidal photocathode laser pulse is a first approximation to produce such charge distributions. Consequently, such a laser system has been developed for PITZ by the Institute of Applied Physics in Nizhny Novgorod, under the framework of a joint German-Russian research activity [4].

[#] james.david.good@desy.de

[†] on leave from BAS INRNE, 1784 Sofia, Bulgaria

[¶] on leave from IMP/CAS, 730000 Lanzhou, China

The system produces quasi-ellipsoidal laser pulses in the infrared through spatio-spectral amplitude masking of chirped Gaussian laser pulses.

The shaper is implemented by locating a modulator at the at the Fourier plane of a 4f - zero-dispersion stretcher-compressor. In this case the modulator is a Spatial Light Modulator (SLM) to act as an amplitude mask in the transverse-temporal domains (Fig. 1).

The pulses are passed through the shaping unit, rotated 90° about their propagation axis before being passed back through the shaper, and are then coupled out for frequency conversion to the ultraviolet.

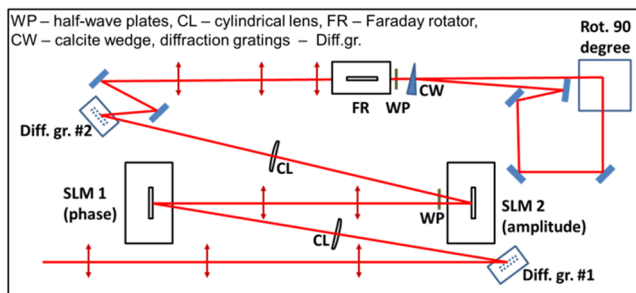


Figure 1: Schematic overview of the 3D shaper (phase mask currently omitted).

A number of diagnostic tools are implemented to characterize the laser pulses. The temporal envelope of the laser pulses is characterized by cross-correlator coupled cameras in the both the infrared, prior to frequency conversion, and in the ultraviolet afterwards. Furthermore, a slit-scanning spectrometer is used to acquire spectrographs of the pulses and reconstruct their profiles.

Finally, the laser is coupled into a shared laser transport beamline. A uTCA-based feedback loop is used to ensure synchronization to the RF systems which permitted the first electron beam quality measurements with the new laser system at PITZ.

SIMULATIONS

Simulations were done using the ASTRA [5] code to compare and contrast various pulse distributions (Fig. 2) for the 9.5 ps FWHM pulse durations which are currently available. These were done for the operating parameters of 0.5 nC bunch charge, 6.5 MeV/c momentum in the gun, and 22.3 MeV/c after the CDS booster.

ELECTRON BEAM ASYMMETRY COMPENSATION WITH GUN QUADRUPOLES AT PITZ

M. Krasilnikov*, I. Isaev, G. Amatuni¹, G. Asova², P. Boonpornprasert, Y. Chen, J. Good, B. Grigoryan¹, M. Gross, H. Huck, D. Kalantaryan, X. Li, O. Lishilin, G. Loisch, D. Melkumyan, A. Oppelt, H. Qian, Y. Renier, F. Stephan, Q. Zhao³, DESY, Zeuthen, Germany

¹on leave from CANDLE, Yerevan, Armenia

²on leave from INRNE, Sofia, Bulgaria

³on leave from IMP/CAS, Lanzhou, China

Abstract

The electron beam asymmetry observed at the Photo Injector Test Facility at DESY in Zeuthen (PITZ) was traced back to multipole kicks in the gun section, namely around the location of the coaxial power coupler and the main solenoid. Several dedicated studies have been performed to quantify the kick location and strength. Based on these studies, two designs of correction quadrupole coils were proposed. The coils were fabricated and tested with an electron beam. The second updated design implies a two-quadrupole setup on a frame installed around the gun coaxial coupler close to the main solenoid centre location. Skew and normal quadrupole magnets are powered independently, enabling flexibility in electron beam manipulations. By means of this setup, a more symmetric beam was obtained at several screens. This led also to more equal measured horizontal and vertical phase spaces and to even smaller overall emittance values. Some details of the gun quadrupole designs, magnetic measurements, and results of electron beam measurements including emittance optimization will be reported.

INTRODUCTION

Several dedicated experiments to investigate the observed asymmetry in the transverse distribution of electron beams in the rotationally symmetric PITZ photo injector have been performed. One of them, the so-called “Larmor angle experiment” [1] yielded a possible location of the kick onto the transverse phase space at the longitudinal position of ~ 0.2 m from the photocathode. A 45° orientation of the kick corresponds to a skew quadrupole-like impact. Additional studies were performed in order to characterize this source considering RF gun power coupler [2] and main solenoid aberrations due to anomalous quadrupole fields [3] as major candidates responsible for the observed distortions in the transverse electron beam shape. These studies yielded also the second location of the possible kick – namely around $z \sim 0.4$ m from the cathode [3].

In order to compensate the assumed kick integrally by a static quadrupole field, two sets of gun quadrupoles were designed and fabricated. The first are quadrupole air coils on an aluminium frame, tested at PITZ for both orientations – normal and skew. No universal settings of these coils were found to compensate the beam asymmetry for

both solenoid polarities. The second design consists of a pair of quadrupoles – normal and skew on the same frame. They were connected to two independent power supplies and were able to deliver symmetric beams for both solenoid polarities. Two parameter scans of the beam images at YAG screens as functions of the normal and skew gun quadrupoles currents were performed resulting in slightly different settings for various screens. Emittance measurements were performed for 0.5 nC beams without and with found settings of gun quadrupoles.

GUN QUADRUPOLES

The gun quadrupole design is based on an air coil concept, consisting of eight individual coils that form two separate quadrupoles: normal (Gun.Quad1) and skew (Gun.Quad2). Such combination of the skew and normal quadrupole fields provides an opportunity to perform a virtual rotation of the quadrupole field. Both quadrupole magnets are placed on the same aluminium frame of 108 mm inner diameter and 36 mm width. Each of eight air coils consists of 140 windings of 0.56 mm copper wire. The coils are powered independently by currents $I_{\text{Gun,Quad1}}$ and $I_{\text{Gun,Quad2}}$, respectively, with up to ± 3 A.

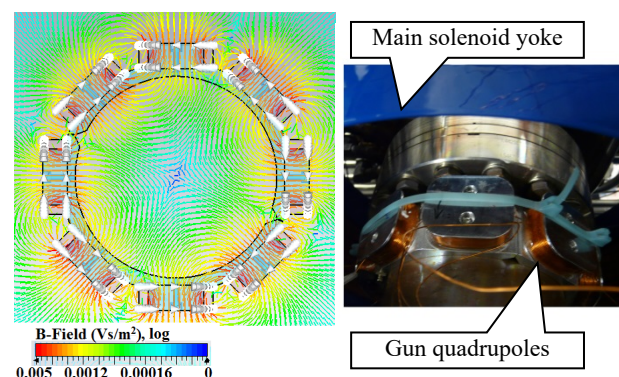


Figure 1: Compensating gun quadrupoles consisting of two air quadrupole coils: normal and skew. Magnetic field simulated with CST EM Studio for $I_{\text{Gun,Quad1}} = -0.5$ A and $I_{\text{Gun,Quad2}} = -0.6$ A (left). Photo of the quadrupole installed in the PITZ injector (right).

Before quadrupoles fabrication magnetic simulations using the CST EM Studio [4] were performed (Fig. 1, left). Thermal load for the maximum currents was estimated as well resulting in a maximum temperature of 75-

* mikhail.krasilnikov@desy.de

BEAM BRIGHTNESS IMPROVEMENT BY ELLIPSOIDAL LASER SHAPING FOR CW PHOTOINJECTORS

H. Qian[#], M. Krasilnikov, F. Stephan, DESY, Zeuthen, Germany

Abstract

High brightness photoinjectors operating in continuous wave (CW) mode are enabling many advanced applications, such as CW X-ray free electron laser (FEL), ERL light source, electron coolers for hadron beams and electron-ion colliders and so on. Now, three types of CW electron guns are available: DC gun, SRF gun, and normal conducting RF gun. Compared to pulsed guns, the CW gun beam brightness is compromised due to a lower acceleration gradient at the cathode. Flattop laser shaping and ‘cigar beam’ photoemission have been applied in CW guns to improve beam emittance. In this paper, ellipsoidal laser shaping is studied to further improve the beam brightness for CW photoinjectors towards $\sim 0.1 \mu\text{m-rad}$ at 100 pC.

INTRODUCTION

X-ray free electron lasers (XFEL) have seen great success in the past decades, increasing peak brightness of X-ray beams over synchrotron X-ray sources by as much as 11 orders of magnitude [1]. While all current XFELs are low repetition rate pulsed machines, with advances of CW SRF linac technology, new XFEL machines in CW mode are under design [2, 3]. The gradient of a CW SRF linac is lower than a pulsed linac, and thus CW XFEL linac energy is expected to be lower. To lase at the shortest photon wavelength with lower linac energy, an even brighter electron source is required, e.g. 100 pC bunch charge with $\sim 0.1 \mu\text{m-rad}$ transverse emittance and $\sim 20 \text{ A}$ peak current is wished [4].

The electron source brightness is limited by photoemission at the cathode, which can be described as [5, 6]:

$$B_{\perp}^{\text{pancake}} \propto \frac{E_0}{\sigma_{p\perp}^2}. \quad (1)$$

$$B_{\perp}^{\text{cigar}} \propto \frac{E_0^{3/2} t_{\text{laser}}}{\sqrt{R} \sigma_{p\perp}^2}. \quad (2)$$

where $B_{\perp}^{\text{pancake}}$ and B_{\perp}^{cigar} are the transverse beam brightness for pancake photoemission and cigar photoemission, resp., E_0 is the gradient at photoemission, t_{laser} is the cathode laser pulse duration, R is the laser spot radius on the cathode, and $\sigma_{p\perp}$ is the RMS transverse momentum after photoemission. Current CW guns, such as DC guns, SRF guns, and normal conducting guns, have a relatively low accelerating gradient at the cathode compared to pulsed guns. This makes it more difficult to

achieve a better beam brightness at CW guns. According to Eq. (1) and (2), to improve the electron source brightness with a relatively low gun gradient, low $\sigma_{p\perp}$, i.e. a low thermal emittance cathode becomes extremely important. Besides, for cigar beam photoemission, a long laser pulse duration and a smaller laser spot size can increase the transverse beam brightness by relaxing the peak current. This might be recovered by velocity or magnetic compression downstream the gun. Both methods have been applied in state of the art CW photoinjector designs.

Even with an optimized emittance at the gun, emittance growth along the linac has to be kept at a minimum. Without careful control of space charge effects, both the projected emittance growth due to slice mismatch and the slice emittance growth easily go beyond $0.1 \mu\text{m-rad}$. Flattop laser shaping has been used to improve space charge linearization in both pulsed and CW guns. An emittance of $\sim 0.2 \mu\text{m-rad}$ has been achieved at $\sim 200 \text{ pC}$ [7, 8]. To further increase the beam brightness, laser shaping for a uniform ellipsoidal beam has been proposed for 3D space charge linearization. Experimental realizations of an ellipsoidal beam have made a lot of progress in the past, both in the pancake beam regime through blowout emission and in the cigar beam regime through direct laser shaping [9-11].

In simulations, uniform ellipsoidal laser shaping has shown an emittance reduction of $\sim 30\%$ for a 1 nC beam compared to flattop laser shaping in high gradient pulsed guns [12]. In this paper, uniform ellipsoidal laser shaping will be applied in CW photoinjectors to check its benefit in improving the transverse emittance of a 0.1 nC beam for XFEL applications.

OPTIMIZATION TOOL

As shown in Eq. (2), the transverse beam brightness can be increased by relaxing the peak current. Besides, in CW photoinjector designs based on a DC gun or a normal conducting VHF gun, a buncher is used to control the beam peak current, trading transverse emittance.

Transverse emittance and bunch length are two compromising goals in photoinjector optimization, and a group of non-dominating optimal solutions of transverse emittance and bunch length form the Pareto front, which can be solved by multi objective genetic algorithm (MOGA) [13]. In this paper, a MOGA tool developed at LBNL is used to drive ASTRA simulations for photoinjector optimization [14]. 10000 macro particles are used in MOGA simulations, and interesting solutions are refined with 100000 macro particles in ASTRA for detailed analysis.

[#] houjun.qian@desy.de

A CRYOCOOLED NORMAL-CONDUCTING AND SUPERCONDUCTING HYBRID CW PHOTOINJECTOR

H. Qian[#], M. Krasilnikov, F. Stephan, DESY, Zeuthen, Germany

Abstract

Continuous wave (CW) photoinjectors have seen great progress in the last decades, such as DC gun, superconducting RF (SRF) gun and normal conducting (NC) VHF-band gun. New developments of CW guns are aiming higher acceleration gradient and beam energy for higher beam brightness. While a SRF gun being the natural CW gun technology for better performance, it has been technically limited by the compatibility between normal conducting high QE cathodes and superconducting (SC) cavity. In this paper, a high gradient and low voltage cryocooled CW NC gun is proposed to house the high QE cathode, and a half cell SRF cavity immediately nearby gives further energy acceleration. Preliminary RF design of the NC gun and ASTRA simulations of such a hybrid photoinjector are presented.

INTRODUCTION

Electron sources of both high peak brightness and high average brightness are wished for a lot of advanced applications [1]. Pulsed electron guns enjoy a high cathode gradient (60-200 MV/m), enabling electron beams with high 6D-brightness possible right at the cathode. Such high gradients are difficult to extend to a CW gun, due to cooling concerns, dark current, and other concerns. Current CW RF guns operate at cathode gradient around 20 MV/m [2,3], and beam transverse brightness are optimized by relaxing peak current at photoemission, which is recovered by velocity bunching or magnetic bunch compression [4,5]. To achieve higher beam brightness, higher cathode gradient and beam energy is wished [1]. The next generation of normal conducting VHF-band gun with over 30-MV/m cathode gradient is under study, and a major challenge is thermal loading (over 100 kW)[6].

Based on such a gun design, ASTRA simulations have shown that the emittance of a 100-pC beam can be improved towards $\sim 0.1 \mu\text{m}\cdot\text{rad}$ [6,7]. Besides, SRF guns have made great progress in the past decade, showing the possibility of high cathode gradient up to 60 MV/m [8]. The compatibility of a high-QE cathode and a high gradient SRF cavity is still a technical challenge. In most of cases, the SRF gun gradient is greatly reduced once a high QE photocathode is present inside the cavity. Besides, multipacting inside the gun can also kill the high QE cathode [9]. While engineering improvements have been implemented in the design of cathode insertion channels of SRF guns to mitigate multipacting and to avoid cathode contamination to SRF cavity surface, risks still exist due to the high sensitivity of SRF cavity surface.

Other special SRF gun designs are also under development. The DESY 1.5-cell L-band SRF gun uses superconducting metal cathodes, eliminating the gap between SRF cavity and NC high QE cathodes for potentially high-gradient performance [8]. The DC-SRF gun developed at Peking University puts the high-QE cathode inside the DC gun just before the SRF cavity, preventing the complex cathode channel design and cathode contamination to SRF cavity. The DC-SRF gun has demonstrated an average current of $\sim \text{mA}$ for CW operation [10].

Inspired by the DC-SRF gun, the DC acceleration of the hybrid gun is proposed to be replaced by a high-gradient NC-CW RF gun, forming a NC-SRF gun, so that beam brightness is not limited by the low cathode gradient. In this paper, the preliminary concept and RF design of such a gun is described, and the engineering considerations are not discussed. Based on the proposed NC-SRF gun concept, a CW photoinjector is optimized by ASTRA simulations.

NC-SRF GUN CONCEPT

The high gradient NC RF cavity is proposed to house the high QE cathode and support high brightness photoemission with high cathode gradient, and the main acceleration is still in the SRF cavity. The compatibility between high gradient NC RF cavity and high QE cathode has been well demonstrated in both pulsed and CW NC guns [11,12]. Since the NC cavity voltage is supposed to be low, to maintain the beam brightness from the NC cavity, the SRF cavity should be as close to the NC cavity as possible, same as in the DC-SRF gun. Since the NC cavity and SRF cavity will stay in the same cryomodule, the NC cavity should be cryocooled, and then the NC cavity RF heating should be minimized. The NC cavity should be high gradient with low cavity voltage, i.e. a thin gap cavity. A re-entrant cavity shape is considered for such a thin gap cavity. Scaling from the existing LBL VHF gun parameters [3], i.e. $\sim 100 \text{ kW}$ for 800 kV, the gun is assumed to be $\sim 1 \text{ kW}$ for 80 kV. Since the NC cavity will be cryocooled, the cavity quality factor will increase, and the RF heating will be even lower. Several cryocooled NC guns have been proposed for the purpose of ultrahigh gradient operation [13,14]. Microwave measurements at cryogenic temperature (20 K) has shown RF surface-resistance reduction of a factor of ~ 5 compared to room temperature at both S-band and C-band frequencies [15,16]. Applying the same reduction ratio to the assumed 80 kV NC cavity, the RF heating, i.e. cryogenic load at 20 K will be reduced from $\sim 1 \text{ kW}$ to $\sim 200 \text{ W}$.

[#]houjun.qian@desy.de

BEAM ASYMMETRY STUDIES WITH QUADRUPOLE FIELD ERRORS IN THE PITZ GUN SECTION

Q. Zhao^{†,1}, M. Krasilnikov, I. Isaev, H. Qian, P. Boonpornprasert, G. Asova², Y. Chen, J. Good, M. Gross, H. Huck, D. Kalantaryan, X. Li, O. Lishilin, G. Loisch, D. Melkumyan, A. Oppelt, Y. Renier, T. Rublack, C. Saisa-Ard³, F. Stephan, DESY, Zeuthen, Germany

Abstract

The Photo Injector Test Facility at DESY, Zeuthen site (PITZ) was built to test and optimize high brightness electron sources for Free Electron Lasers (FELs) like FLASH and the European XFEL. Although the beam emittance has been optimized and experimentally demonstrated to meet the requirements of FLASH and XFEL, transverse beam asymmetries, such as wing structures and beam tilts were observed during many years of operation with different generations of guns. These cannot be explained by simulations with the rotationally symmetric gun cavities and symmetric solenoid fields. Based on previous coupler kick, solenoid field imperfection studies and coupling beam dynamics, the beam asymmetries most probably stem from anomalous quadrupole field error in the gun section. A thin lens static quadrupole model is applied in the RF gun section simulations to fit the position and intensity of quadrupole field errors by comparing the beam asymmetry directions in experiments and ASTRA simulations. Furthermore, by measuring the laser position movement at the photocathode and the corresponding beam movement at downstream screens, the integrated quadrupole field strength can also be extracted.

INTRODUCTION

The RF gun of PITZ is a rotationally symmetric 1.6 cell L-band cavity. The electron beam is generated at the cathode by a laser and then accelerated by gun cavity RF fields and focused by the solenoid field. From beam dynamics simulation with $E_z(z)$ and $B_z(z)$ field map in ASTRA [1], the beam transverse distribution is symmetric anywhere downstream the gun cavity, which is not exactly matching to the experimental results. During several years of operation with different generations of guns, the imperfect beams were always observed from experiments [2-3], such as beam tilt from transverse images, beam wing structures, asymmetric x and y phase space distributions and not round beam transverse distributions observed during emittance measurements. One of the most obvious asymmetric features is the beam wing structure shown in Figure 1 from experiment. For Figure 1 the experiment results were taken at High1.Scr1 ($z = 5.277$ m from cathode) with beam momentum of 6.18 MeV/c, bunch charge 480 pC and two polarities of the main solenoid (I_{main}) but the same current. The beam wings are at

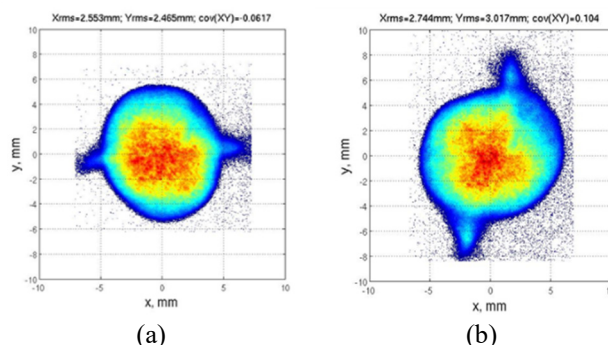


Figure 1: Beam images at High1.Scr1 (a) normal solenoid polarity ($I_{\text{main}} = -360$ A) and (b) opposite solenoid polarity ($I_{\text{main}} = +360$ A).

different orientations due to different rotation angle caused by different solenoid polarity.

From previous studies [4-5], the PITZ gun RF coupler kick was found from RF field simulations. In the transition region from the coupler to the gun, the RF field distribution is not uniform. The RF coupler kick optics can be modelled as a rotated quadrupole with focal length and rotation angle given in terms of complex voltage kicks. A rotated quadrupole near the coupler is effective at compensating for the coupler kicks, cancelling both the coupling emittance and the astigmatic focusing [6-7]. Another source of the beam asymmetries may come from solenoid field imperfections. Beam asymmetries from photo gun are also observed in other labs [8]. The feature of the beam transverse coupling from rotated quadrupoles can be observed from beam transverse distributions in experiment like the beam tilt in Figure 1. Linear coupling can be compensated in principle by additional rotated quadrupoles, but the beam dynamics for coupling effects must be known to perform a proper compensation [9].

QUADRUPOLE FIELD ERROR POSITION AND ROTATION ANGLE ESTIMATION

Experiments for Beam Wings Studies

For beam asymmetry studies, some dedicated experiments were done with different RF power in the Gun4.2 and solenoid current scan. Three values of power 5 MW, 3 MW and 1.5 MW in the gun were used. The beam wings appeared at High1.Scr1 by solenoid current scan and the clearest signals of beam wings are seen for I_{main} at 360 A, 290 A, 219 A respectively and other I_{main} s have shown the beam tilted images for both polarities. The

[†] quantang.zhao@desy.de

¹ on leave from IMP/CAS, Lanzhou, China

² on leave from INRNE, Sofia, Bulgaria

³ on leave from Chiang Mai University, Chiang Mai, Thailand

A 2.45 GHz PHOTOINJECTOR GUN FOR AN FEL DRIVEN BY LASER WAKEFIELD ACCELERATED BEAM*

S. V. Kuzikov[†], S. A. Bogdanov, E. I. Gacheva, E. V. Ilyakov, D. S. Makarov,
S. Yu. Mironov, A. K. Potemkin, A. P. Shkaev, A. A. Vikharev,
Institute of Applied Physics, Russian Academy of Sciences, Nizhny Novgorod, Russia

Abstract

The photoinjector of short electron bunches is a key element of investigations aimed on particle acceleration by pulses of the subpetawatt laser PEARL (10 J, 50-70 fs)[1]. Projected parameters of the photoinjector are the following: an electron energy of 5 MeV, charge >0.1 nC, bunch length of about 3 mm, transverse emittance no worse than $1 \text{ mm} \times \text{mrad}$, and an energy spread no more than $\sim 0.1\%$. The photoinjector is based on a 2.45-GHz klystron (model KIU-111 built by Toriy), with output power ~ 5 MW, pulse length $\sim 7 \mu\text{s}$, efficiency $\sim 44\%$, power gain ~ 50 dB. This klystron will feed a standard 1.5-cell gun resonator with removable photocathode. The gun will be driven by a third harmonic of a Ti:Sa laser with 100- μJ energy in a picosecond pulse. The photocathode will be made of CVD diamond film which has high QE, long lifetime and is robust with respect to the vacuum conditions.

RF GUN DESIGN

The gun has classical design based on bunch acceleration in 1.5-cell cavity fed by a KIU-111 klystron, built by Toriy, operating at 2.45 GHz [2-3]. The klystron radiation is synchronized with laser system based on third harmonics of Ti:Sa laser.

Klystron

The klystron, shown in Fig. 1, generates output power up to 5 MW over a pulse duration of 7 μs . It provides 10-40% efficiency and 50 dB power gain at a frequency band of 10 MHz. Its repetition rate can reach 1 kHz. In our RF gun the repetition rate is planned to be as high as only 10 Hz. The klystron requires a 55-kV power supply supporting 250 A of current. In order to deliver the necessary 100-200 W of input RF power to klystron, we are going to use a so-called preamplifier which has been already produced.

Laser

We carried out experiments to generate 10-ps, 0.1- μJ laser pulses (at third harmonics of 1030 nm wavelength) with cylindrical and 3D ellipsoidal distributions of the intensity [4]. The system setup is shown in Fig. 2. Two methods were exploited. In both methods, the fact was

used that for pulses with essential linear frequency modulation the spectra distribution follows for intensity distribution in time, and that control for spectrum shape corresponds to the control of the intensity distribution. The first method is based on using of pulse compressor with zero frequency dispersion and a programmed mirror SLM (Spatial Light Modulator). This method allowed to generate quasi-ellipsoidal laser pulses with 90° axial symmetry. The second method is based on a use on SLM matrix and the profiled volume Bragg grating. The Bragg grating was written inside ellipsoidal volume and is absent outside it at all. By means of SLM laser pulses were formed with cylindrical intensity distribution in a space and were guided to the Bragg grating. The reflected radiation also had the ellipsoidal intensity distribution in a space.

We have performed a project of an original system for synchronization of the klystron KIU-111 with the laser.



Figure 1: The klystron KIU-111.

*This work was supported by the Russian Scientific Foundation (grant #16-19-10448).

[†]sergeykuzikov@gmail.com

PULSE DURATION MEASUREMENT OF PICO-SECOND DUV PHOTO-CATHODE DRIVING LASER BY AUTOCORRELATION TECHNIQUE USING TWO-PHOTON ABSORPTION IN BULK MATERIAL*

H. Zen[†], T. Nakajima, T. Kii, K. Masuda, and H. Ohgaki, Institute of Advanced Energy, Kyoto University, Uji, Japan

Abstract

Photocathode RF guns have been used for generating high brightness electron beams. Measurement of the pulse duration of photocathode driving laser in deep-ultraviolet (DUV) wavelength is quite important to estimate the electron beam properties generated from the RF gun. The autocorrelation technique has been commonly used for pulse duration measurement of laser pulses. Two-photon absorption has been utilized as the nonlinear process in the autocorrelation measurement of ultrashort pulse laser beams in DUV region. In this study, DUV autocorrelator utilizing the two-photon absorption in a sapphire plate as the nonlinear process was developed. The developed autocorrelator was used to measure the pulse duration of ps-DUV laser pulses which has been used for driving photocathode RF guns in the free electron laser facility at Institute of Advanced Energy, Kyoto University. As the result, the pulse duration of deep-UV laser pulse was measured as 5.8 ± 0.2 ps-FWHM.

INTRODUCTION

Recently, photocathode RF guns are widely used for generation of high brightness electron beams. At the Institute of Advanced Energy, Kyoto University, a 4.5-cell RF gun with a LaB₆ thermionic cathode used for driving mid-infrared free electron laser (MIR-FEL) has been operated with laser induced photoelectron emission [1]. And the MIR-FEL performance, especially for the peak power, has been significantly increased with the photocathode operation. In parallel, a compact THz coherent undulator radiation source using a 1.6-cell photocathode RF gun has been developed [2]. For driving those RF guns, a multi-bunch picosecond-deep-ultraviolet (ps-DUV) photocathode driving laser system has been developed [3]. The pulse duration of DUV photocathode driving laser is so important parameter, which determines the initial electron pulse duration at the cathode. Therefore, measurement of its pulse duration is so important to estimate the available electron beam parameter. In many electron accelerator facilities, streak cameras have been used for measuring the pulse structure of DUV laser pulses. However, the streak camera is so expensive and not easy to use. As an alternative method, some facilities using photocathode RF guns have been developed cross correlator which uses femto-second near infrared (fs-NIR) laser as a probe to measure the cross correlation between the ps-DUV laser and the fs-NIR laser using difference frequency generation [4, 5].

The cross correlation method is only available in the facilities where the fs-NIR lasers are available.

In the ultrafast laser community, an autocorrelation technique utilizing a two-photon absorption (TPA) in a bulk material has been developed for measuring the pulse duration of ultrashort UV and DUV pulses [6, 7]. In this study, an autocorrelator using TPA in a sapphire crystal was developed and used for measuring the pulse duration of photocathode driving laser at the Institute of Advanced Energy, Kyoto University. The measurement principle, the developed autocorrelator, and measured results are reported in this paper.

MEASUREMENT PRINCIPLE

In general, intensity autocorrelation technique is used for measuring the pulse duration of short pulse lasers. The basic setup of the intensity autocorrelator is shown in Fig. 1. At first, the laser beam is divided into two pulses by a beam splitter. Those two beams are focused by a focusing optics on a nonlinear material. The arrival time difference of the two pulses is controlled by an optical delay inserted in one side of the optical beam path. The nonlinear signal generated at the nonlinear crystal as the function of the arrival time difference is recorded to obtain the information of overlap of those two pulses. Finally, by analyzing the recorded result, the pulse duration of injected laser beam is determined. In the visible and infrared region, second harmonic generation crystals are normally used as the nonlinear crystal and then the intensity of second harmonic light is measured by photodetectors.

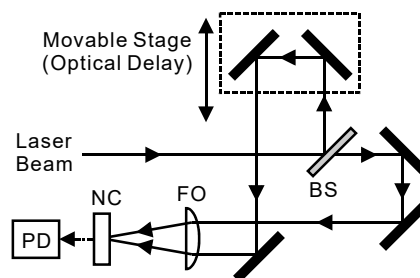


Figure 1: Schematic diagram of basic setup of the intensity autocorrelator used for laser pulse duration measurements. BS: Beam Splitter, FO: Focusing Optics, NC: Nonlinear Crystal, PD: Photodetector.

The laser pulses with the wavelength shorter than 300 nm were mainly used for photoelectron generation in photocathode RF guns. In our case, the laser wavelength is 266 nm and its second harmonic wavelength is 133 nm. The second harmonic wavelength (133 nm) is in the vac-

* Work supported by Collaboration Program of the Laboratory for Complex Energy Processes, Institute of Advanced Energy, Kyoto University
[†] e-mail address zen@iae.kyoto-u.ac.jp

CURRENT EXPERIMENTAL WORK WITH DIAMOND FIELD-EMITTER ARRAY CATHODES

H. L. Andrews[†], B. K. Choi, R. L. Fleming, J. L. Lewellen, K. Nichols, D. Yu. Shchegolkov,
E. I. Simakov, Los Alamos National Laboratory, Los Alamos, USA

Abstract

Diamond Field-Emitter Array (DFEA) cathodes are arrays of micron-scale diamond pyramids with nanometer-scale tips, thereby providing high emission currents with small emittance and energy spread. To date they have been demonstrated in a “close-diode” configuration, spaced only a few hundred microns from a solid anode, and have shown very promising results in terms of emittance, energy spread, and per-tip emission currents. We present recent results investigating DFEA performance in a large-gap configuration, such that the cathodes are a few millimeters from a solid anode, and show that performance is the same or better as the close-diode geometry previously studied. However, array performance is still limited by anode damage. We are redesigning our cathode test stand to overcome the inherent limitations of a solid anode, allow for transport of the emitted beam, and further explore real-world DFEA performance.

INTRODUCTION

Diamond Field-Emission Array (DFEA) cathodes are arrays of exquisitely sharp diamond pyramids [1]. They are a promising cathode option for a wide range of applications. DFEAs are particularly relevant to FELs because they can produce high-current, low emittance beams. LANL is currently investigating using DFEAs as the cathode for a dielectric laser accelerator (DLA), which can achieve acceleration gradients of GV/m in a structure where the transverse and longitudinal dimensions of the accelerating field are on the order of the laser wavelength [2]. The promise of DLAs is that they can be orders of magnitude more compact than conventional linacs driven by RF sources. We are currently working to characterize DFEA emission in order to understand how to gate, focus, and collimate beams from a single or few tips. The experimental work presented here is supported by a theoretical modelling effort [3].

DFEAs emit in high or low vacuum, can be transported in air, and have good thermal conductivity that allows for very high per tip current emission without failure. We fabricate DFEAs using standard silicon wafer fabrication processes, so that they can be fabricated in any array configuration. Individual pyramid base sizes range from 25 micrometers to 2 micrometers.

DFEAs were first fabricated at Vanderbilt University, but are now used at several institutions. Originally (see Fig. 1), the diamond was highly conductive and yielded

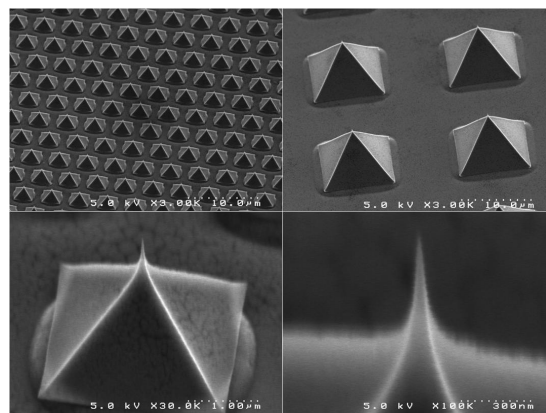


Figure 1: DFEA pyramids at four magnifications, showing the exquisitely sharp tip. (Vanderbilt University).

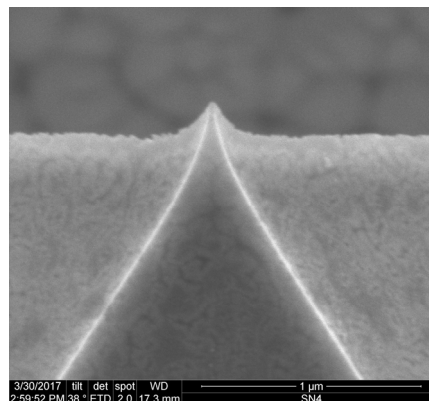


Figure 2: An SEM image of a recent DFEA tip. It has a diameter of around 50 nm.

exquisitely sharp tips, however more recent DFEAs consist of less conductive diamond and exhibit the blunter tips shown in Figure 2. The overall emission properties of the two types of diamond appear similar. We hope to investigate these differences more in the future.

EXPERIMENTAL SETUP

Our cathode characterization experiments are conducted in a vacuum test stand that is equipped with several diagnostics and shown in Figure 3. The test chamber has an ion gauge mounted adjacent to the cathode and anode. The chamber is also equipped with an RGA to analyse constituent gasses. The high-voltage is supplied by a negative 60-kV supply connected to the cathode mount. Experiments are typically conducted at 40 kV, allowing us

* Work supported by the LDRD program at LANL. LA-UR-17-27451.

[†] hlac@lanl.gov

MODELING OF DIAMOND FIELD-EMITTER ARRAYS FOR HIGH-BRIGHTNESS PHOTOCATHODE APPLICATIONS*

C.-K. Huang[†], H. L. Andrews, B. K. Choi, R. L. Fleming, T. J. T. Kwan, J. W. Lewellen, D. C. Nguyen, K. Nichols, V. Pavlenko, A. Piryatinski, D. Shchegolkov, E. I. Simakov, Los Alamos National Laboratory, Los Alamos, 87544, USA

Abstract

Dielectric Laser Accelerators (DLA) are capable of generating high output power for an X-ray free-electron laser (FEL), while having a size 1-2 orders of magnitude smaller than existing Radio-Frequency (RF) accelerators. A single Diamond Field-Emitter (DFE) or an array of such emitters (DFEA) can be employed as high-current ultra-low-emittance photocathodes for compact DLAs. We are developing a first principle semi-classical Monte-Carlo (MC) emission model for DFEAs that includes the effects of carriers' photoexcitation, their transport to the emitter surface, and the tunnelling through the surface. The electronic structure size quantization affecting the transport and tunnelling processes within the sharp diamond tips is also accounted for. These aspects of our model and their implementation and validation, as well as macroscopic electromagnetic beam simulation of DFE are discussed.

INTRODUCTION

DLAs can achieve acceleration gradients of GV/m in a structure that is orders of magnitude more compact than conventional metallic linacs driven by RF sources. To accelerate high current-density electron beams in DLAs, where the transverse and longitudinal dimensions of the accelerating field structure are on the order of the laser wavelength, new cathodes capable of producing small divergence, low emittance beams with dimensions matching the aperture of DLA need to be developed. DFEAs (Fig. 1), manufactured from the mold-transfer process and Microwave Plasma Chemical Vapor Deposition, are promising candidates for such a high-brightness cathode. These DFEAs consist of micron-scale diamond pyramids, together with nanometer-scale tips (Fig. 1) sharpened by an oxide layer in the mold process. DFEAs may produce tightly focused high-current bunched beams ideal for DLAs under suitable photo excitation. The effect and the required conditions of photoemission from a DFEA cathode are being studied at LANL [1].

DFEAs have already been demonstrated experimentally for the field emission [2]. Recently, DFEA field emission test is carried out at LANL with a variable anode-cathode (A-K) gap at a fixed voltage of 40 kV. The measured current is shown in Fig. 1 for the cases of most robust emission (A-K gap $d < 7.2$ mm, greater than ~60% emitters emit). Note the average current I per emitter may be fitted by $I \propto d^{-5.8}$, as compared to d^{-2} (d^{-m} , $m \sim 1.1-1.2$) for the space-charge limited emission from a flat (sharp) metallic surf-

ace. This result indicates that the material and complex geometry/features of the DFE, as well as possible space-charge effect may play important roles in emission.

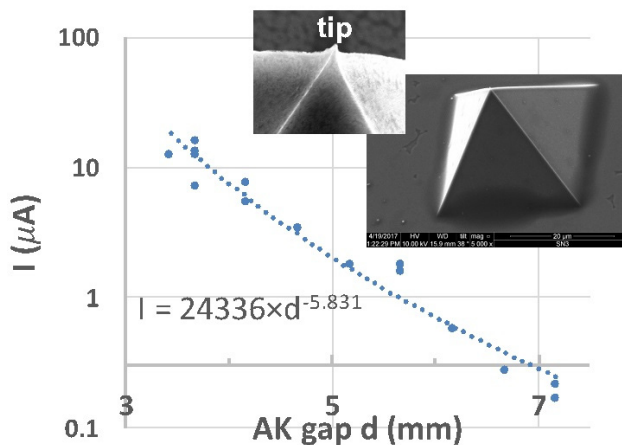


Figure 1: Averaged current (dots) per emitter as a function of A-K gap distance and their fit (dashed). The cathode has a 5×5 emitter array and each emitter has a 20 μ m×20 μ m base and is separated by 500 μ m. Insets show the pyramid base and the sharp tip of a DFE.

SIMULATION MODEL

Since diamond is a semiconductor material (with a band gap E_g approximately 5.5 eV), its field- and photo-emission properties will depend on the charge carrier excitation (mostly electrons in the absence of impact ionization process) and subsequent transport and tunnelling processes in the emitter. Furthermore, the dielectric property of the DFEA, the geometric field enhancement at the top of the emitter and its nm-scale tip can change the field distribution over the surface. Additionally, the electronic structure size quantization effect should modify the transport and emission at the tip. A simulation model, integrating (1) carrier transport within the diamond pyramid and the surface tunnelling, (2) the quantum-size effects in the tip, and (3) the space charge effects of the emitted electrons, is essential to understand DFEA electron emission, to predict conditions favouring efficient photoemission and for the production and transport of tightly focused electron beams to a DLA. We develop such a model by combining the semi-classical MC device simulations with the electromagnetic simulations. The model components along with some preliminary results are presented below.

* Work supported by the LDRD program at LANL.

[†] huangck@lanl.gov

Content from this work may be used under the terms of the CC BY 3.0 licence (© 2018). Any distribution of this work must maintain attribution to the author(s), title of the work, publisher, and DOI.

ELECTRON BEAM HEATING WITH THE EUROPEAN XFEL LASER HEATER*

M. Hamberg[†], Uppsala University, Uppsala, Sweden
 F. Brinker, M. Scholz, B. Manschwetus, S. Koehler, L. Winkelmann, I. Hartl,
 DESY, Hamburg, Germany

Abstract

The Laser Heater of the European XFEL is installed and is in commissioning phase. In this paper, results of heating in the injector section with an additional laser amplifier is discussed.

INTRODUCTION

The European X-ray Free Electron laser (EU-XFEL) will produce fs photon flashes in the interval of 0.05 to 4.7 nm. The setup is based on a 3.4-km long electron accelerator. Longitudinal micro bunch instabilities may occur in the electron beam and hamper the X-ray power level [1]. To overcome such problems a Laser Heater (LH) is installed as in LCLS and FERMI [2-3]. In the LH, a NIR laser is overlapping the electron bunches when they pass a 0.7-m magnetic undulator situated in a chicane section 23-m downstream of the electron gun. The undulator is tuned to resonance which cause a phase space modulation which subsequently is transferred into a net heating effect while leaving the chicane. This heating decreases the instability effects without hampering the FEL performance.

The EU-XFEL LH is a Swedish in-kind contribution which previously has been described [4-8]. Here we report results of injector section measurements after implementation of a NIR laser amplifier [9].

PRECONDITIONING

As described in ref. 6 and 7 overlap of the NIR laser over the electron beam was created in transverse direction in an iterative procedure by readout from Cromox screens. The temporal overlap was adjusted by a fine delay line made up by moving a retro reflector installed on a μm resolution 210 mm linear stage and simultaneously observing heating of the electron bunches as increase in beam width in the dispersive dump section at the injector with an Lyso screen. The accelerator optics was optimized for large dispersion and small beta function at the Lyso screen location to increase the resolution.

The undulator gap was tuned to 42.4 mm to fulfill the resonance condition at the electron energy of 130 MeV with a NIR laser wavelength of (λ_L) of 1030 nm and undulator period (λ_u) of 7.4 cm according to:

$$B_u = \frac{2\pi m_e c}{q_e \lambda_u} \cdot \sqrt{2 \left(\frac{\lambda_L}{\lambda_u} \cdot 2 \cdot \gamma^2 - 1 \right)}.$$

A NIR laser amplifier was installed [9], increasing the NIR laser energy from $\sim 4 \mu\text{J}$ to a maximum of $\sim 200 \mu\text{J}$ per pulse inside of the undulator. The standard deviation radius

of the electron and laser beams were both tuned to approximately $\sigma \approx 0.3 \text{ mm}$ whereas the temporal FWHM of the UV cathode laser and LH NIR laser was tuned to $\sim 12 \text{ ps}$ and $\sim 36 \text{ ps}$, respectively. Since they derive from the same oscillator they are inherently temporally locked.

HEATING

As in previous tests the temporal overlap was adjusted through scan of a linear stage made by a $\sim \mu\text{m}$ stepsize linear stage with an implemented retro reflector and simultaneous readout of the STD beam width on the downstream Lyso screen in the dispersive section. Such measurement is illustrated in Fig. 1 when using a NIR pulse energy of $\sim 35 \mu\text{J}$. The horizontal axis corresponds to temporal offset whereas the vertical axis indicates the STD beam width in mm increasing from $150 \mu\text{m}$ to $325 \mu\text{m}$ which corresponds to an energy spread increase from $\sim 11 \text{ keV}$ to $\sim 31 \text{ keV}$. This should be compared to previous results without amplifier (and therefore a limited NIR pulse energy of $\sim 4 \mu\text{J}$) of $\sim 14 \text{ keV}$ to $\sim 18 \text{ keV}$ [8].

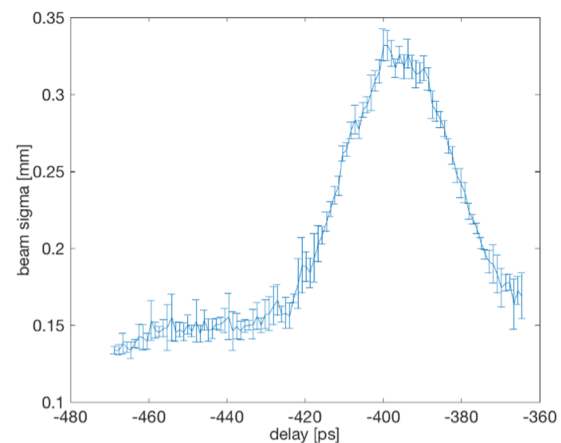


Figure 1: The fine delay scan illustrating the beam size standard deviation in mm versus temporal delay of the cathode laser relative to the beam.

Furthermore, the transverse deflecting structure (TDS) was used to illustrate the effect of the heating. The vertical direction corresponds to longitudinal direction of the electron bunch whereas the horizontal direction corresponds to the energy and therefore illustrate the energy spread at each part of the bunch. An example can be seen in Fig. 2 where the NIR laser is off (top) and partly overlapping (bottom) respectively. It is clear that the whole bunch is strongly heated. The upper part of the heated (bottom figure) bunch is more heated than the lower part.

Content from this work may be used under the terms of the CC BY 3.0 licence (© 2018). Any distribution of this work must maintain attribution to the author(s), title of the work, publisher, and DOI.

HIHG STABLE PULSE MODULATOR FOR PAL-XFEL*

Soung Soo Park[†], Heung-Sik Kang, Sang-Hee Kim, Heung-Soo Lee
 Pohang Accelerator Laboratory, Pohang City, Korea

Abstract

The construction of Pohang Accelerator Laboratory X-ray Free Electron Laser (PAL-XFEL) was completed by the end of 2015. The commissioning began in April 2016, and the lasing of the hard X-ray FEL was achieved on end of 2016. The PAL-XFEL needs a highly stable electron beam. The very stable beam voltage of a klystron-modulator is essential to provide the stable acceleration field for an electron beam. Thus, the modulator system for the XFEL requires less than 50 ppm beam voltage stability. To get this high stability on the modulator system, the inverter type HVPS is a pivot component. And the modulator needs lower noise and more smart system. We report the stability of the pulse voltage and the test results of the pulse modulator.

INTRODUCTION

PAL-XFEL is a 4th generation light source, a coherent X-ray free electron laser (XFEL). The RF stability is a key issue to get stable FEL output. The reasonably stable output requests the RF stability of 0.02% (rms) for both RF phase and amplitude. The modulator systems consist of 46 sets of 80 MW klystrons and 200 MW modulators to achieve 10 GeV energy for PAL XFEL. To get the RF phase stability of < 0.05 degree, the required beam voltage stability of the PAL XFEL will be < 50 ppm (rms). This requires that we need to use an ultra precision inverter power supply and a fine controller of feedback signal of the charging voltage in order to stabilize the PFN charging level. The proper conditioning of feedback signal with a thermally stable probe is necessary to realize an ultra stable charging performance [1]. And the modulator needs lower noise level and the heater power of the klystron and thyratron was trigger synchronised to the cluster part where the change was small.

PULSE MODULATOR SYSTEM

The pulse modulator system uses a constant current source such as an inverter power supply type.

High Power Klystron and Modulator

An inverter power supply is called capacitor charging power supply (CCPS) because it supplies constant current into the capacitors. In the CCPS, to turn off a thyratron switch in the modulator safely after every discharge, the next charging schedule, digitally safe system, is under short-circuit condition due to the current limit feature. With this CCPS, the modulator system will be naturally compact.

These features are well matched to the next generation modulator for PAL XFEL facility. The CCPS power rating is 120 kJ/s. Total charging time is about 14 ms. The specifications of the modulator are output power of 200 MW, beam voltage of 400 kV, beam current of 500 A, pulse width of 8 μ s and repetition rate of 60 Hz. To achieve those demands, we adopted the fine CCPS as well as the coarse CCPS. Table 1 summarizes the specification of the modulator. As a load s-band E37320 80 MW klystron will be matched to the modulator system. Fig. 1 shows the circuit diagram of a modulator using CCPS.

Table 1: PAL-XFEL Modulator Specifications

Discription	Unit	Value
Peak Power	MW max.	200
Repetition Rate	Hz (normal)	60
Pulse Voltage Stability	ppm	>50
Pulse Peak Voltage	kV	400
Pulse Peak Current	A	500
Pulse Width	μ s	7.5
PFN Impedance	Ω	2.63
Main CCPS Power	kJ/s	120

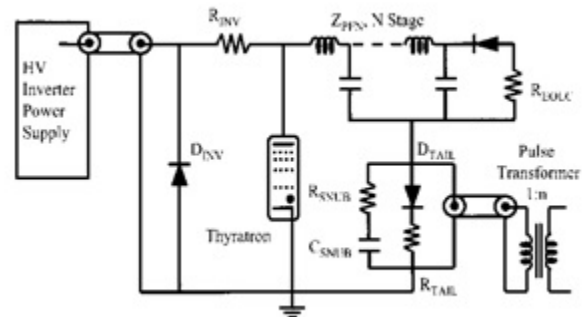


Figure 1: Circuit diagram of a modulator with a CCPS.

Inverter High Voltage Power Supply

To meet specifications of Table 1, two different types of current charging power supply (CCPS) are employed. One is a fine CCPS which is a high precision type (< 50 ppm) and the other is a coarse CCPS (< 1000 ppm). The coarse charging and fine charging is arranged to get the regulation with optimum power sharing. Figure 2 shows the charging schedule with parallel operation of inverters [2]. Total charging time T_c and charging voltage V_o are given by

$$\begin{aligned} (m+n) t_o &= T_c, m(D+d) + n d = V_o, \\ n d &= V_o - V = j D, \\ m+n &= a, m^2 - a m + (a+b)j = 0, \end{aligned}$$

* Work supported by Ministry of Science, ICT(Information/Communication Technology) and Future Planning.

[†] sspark@postech.ac.kr

PRELIMINARY RESULTS OF THE DARK CURRENT MODELLING FOR THE POLFEL SUPERCONDUCTING LEAD PHOTOCATHODE

Karol Szymczyk, Jerzy Andrzej Lorkiewicz, Robert Nietubyć, NCBJ, Świerk, Poland
Jacek Sekutowicz, DESY, Hamburg, Germany

Abstract

Preparation for the construction of the Polish Free Electron Laser (POLFEL) has been launched at NCBJ. POLFEL is a 4th generation light source driven by a continuous wave or long pulse operating superconducting electron accelerator. The concept includes all-superconducting injector, with a thin-film lead superconducting photocathode, dedicated for generation of low-current ($\sim 25 \mu\text{A}$), low-emittance beam.

One of the issues which emerges in connection with operation of high gradient electron guns furnished with dismountable photocathode plugs is the dark current (DC) emitted from the cathode plug edges and surface inhomogeneities, which degrade the accelerator performance.

The purpose of this paper is to present an approach to dark current investigation and the preliminary results obtained. Specific features of the geometric configuration like rounded plug edges, a gap between the plug and back wall as well as surface roughness have been taken into account for the electron emission and RF field calculations.

THz SOURCE

The POLFEL will consist of a linear accelerator that will deliver 30 MeV (100 MeV in the second step) electron beam, used to emit a THz-IR ranged electromagnetic radiation in plane, variable gap undulator.

The construction of the first Polish FEL is planned for 3 years. The POLFEL will be used in two parallel experimental end-stations that will foster major advances from materials studies such as diffraction imaging with spatial and temporal resolution, spectral investigations of photoionized plasmas by direct or multiphoton ionization of molecules.

DARK CURRENT

One of the main problems of a dismountable photocathode plug is dark current. Incoherently propagating electrons may collide with photocurrent beam, load the cryogenic system, may cause activation or damage of accelerator components and induce cavity quenches. Moreover, dark current caused by field emission limits lifetime of photocathodes.

The main dark current sources of the RF gun cavity are:

- the photocathode plug,
- the cavity backplane close to the cathode,
- the irises because of the strong surface field.

The dark current is preferably emitted from the rough fragments of arc deposited lead layer, and from the plug bends. The intensity of dark current depends on the cavity and photocathode surface finishing.

There are developed dark current reduction methods:

- Suppressing field emission by improved surface preparation.
- Lowering RF gradient at the cathode.
- Applying a collimator.

The main topic of this publication is modeling of surface roughness and its influence on the DC generation. Special attention was paid for RF field calculation, taking into account specific features of the geometric configuration like rounded plug edges, a gap between the plug and back wall as well as surface roughness.

At the FLASH [1] injector, the normal conducting RF gun operated at the nominal gradient of 40–44 MV/m, produces a steady DC electron flux of 200–300 μA as measured with a Faraday cup near the exit of the gun structure. The dark current rises exponentially, regards to the max RF field at the cathode (see Fig.1).

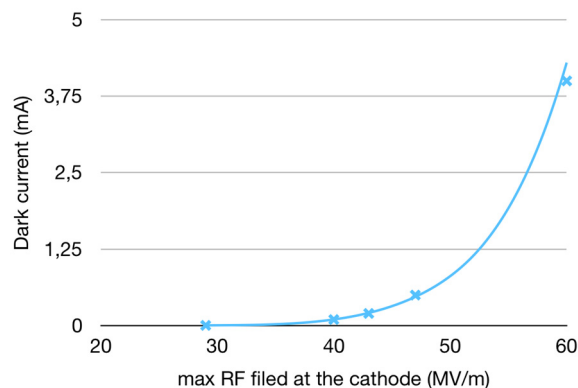


Figure 1: Relationship of dark current to RF field.

CALCULATION METHOD

The main part of calculation was performed using: Astra (A Space Charge Tracking Algorithm) [2] and FEM [3] codes. The FEM uses finite element approximation based on the mesh optimised to map curvilinear boundary of gun resonator. It was used to calculate the RF field in the cavities. For the particles tracking simulation, the Astra program was used.

RESULTS

Work was performed in following steps. Firstly, the RF field distribution with the FEM program, was calculated inside the gun cavities, with the flat back wall surface. Fig. 2 and 3. The programme calculates two-dimensional field distribution assuming cylindrical symmetry relative to the longitudinal z axis.

DESIGN AND RESEARCH OF A MICRO-PULSE ELECTRON GUN

D. Y. Yang, J. F. Zhao, B. T. Li, Y. J. Yang, K. Zhao, X. Y. Lu[†], Z. Q. Yang, W. W. Tan, L. Xiao
State Key Laboratory of Nuclear Physics and Technology at Peking University, Beijing, China

Abstract

Micro-pulse electron guns (MPG) are a novel electron source which can produce narrow-pulse, high-repetition rate electron current. Theoretical and experiment work have been done to study physical properties and steady operating conditions of MPG. Proof-of-principle work has been finished and the next work is to research the parameters of the MPG electron beam and understand the MPG properties. Thus, a high-voltage accelerating platform which can supply 100 kV direct voltage was designed. Furthermore, electromagnetic and mechanism designs were operated to adapt the high voltage platform and measure beam parameters.

INTRODUCTION

The multipactor, based on a secondary electron emission (SEE) [1], is often destructive to the microwave device such as waveguide, coupler, RF resonant cavity [2-3], and its avoidance has been a major task for sic-tech workers.

The underlying mechanism behind the multipactor has been studied deeply [4-7]. But before the publications of this theoretical work, the first electron gun based on multipacting was made by Gallagher in 1969 [8]. Among those publications, the beam self-bunching effect attracted the attention of Mako, who gave the concept of the micro-pulse electron gun (MPG) and obtained important conclusions about MPG [9-11]. After the initial work of Mako, many other research institutions have made their contributions to the development of MPG [12-14].

MPG could produce a narrow-pulse electron beam due to the self-bunching effect. In addition, simple structure and high tolerance to contamination make it a potential electron source for accelerators and microwave systems [15]. However, no records on the applications of MPG have been reported until now. One of the reasons to explain the limitation of the MPG applications may be the bad stability of MPG operation.

In our previous work, a prototype electron gun has been designed, tested and the steady operation of MPG has been obtained [15]. Yet several problems remained. For instance, the steady operation time cannot meet the demands of MPG applications as a novel electron source, the beam parameters such as energy spread, intrinsic emittance need to be detected and the former system doesn't have the ability to do this job. Our goal is to design and build a new MPG test system at the basis of previous work in addition to detect the beam parameters and study the principle of MPG steady operation.

This paper presents the electromagnetic design and test of a MPG which works for high voltage accelerator plat

form. In the second section, basic concepts of MPG are introduced and several types of gun shape are compared. The third section gives the fabrication of the new gun, and brief introduction of HV platform. Finally, primary experiment results are presented.

THE MPG MODEL

Working Principle of MPG

The MPG shown in Figure 1 consists of three parts in general: RF cavity which works at TM₀₁₀ mode, cathode with the secondary electron yield (S.E.Y) of δ_1 grid anode with the S.E.Y of δ_2 .

The initial electrons in the RF cavity which are caused by field emission move from cathode to grid anode by means of their interaction with electromagnetic fields, and they impact the anode after odd multiple of half period and generate secondary electrons. The triggered secondary electrons traverse back and forth between the electrons until saturation.

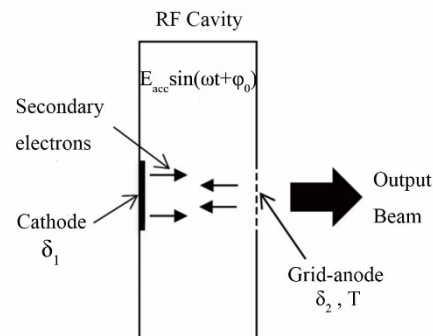


Figure 1: The schematic diagram of the MPG model.

The Choice of Cavity Shape

The general cavity type for TM₀₁₀ mode is pill-box cavity. Figure 2 shows the comparison of three pill-box like cavities. (a) is the general pill-box cavity, (b) is the concave cavity that equivalent to pill-box with a part cut inside, (c) is the convex cavity that shapes like a pill-box added two parts. Figure 3 demonstrates the electric field distribution of three different cavities. a1/a2 are three-dimensional diagrams and pseudo-color maps of general pill-box cavity. b1/b2, c1/c2 are have the same meaning for concave cavity and convex cavity separately. Concave cavity has the sharpest peak among these three cavities. What's more, there is a 'flat roof' in the centre electric field of concave cavity and it helps decrease the electron transverse energy difference.

Content from this work may be used under the terms of the CC BY 3.0 licence (© 2018). Any distribution of this work must maintain attribution to the author(s), title of the work, publisher, and DOI.

EMITTANCE MEASUREMENTS AND SIMULATIONS FROM SRF GUN IN CEC ACCELERATOR

Kentaro Mihara, Vladimir N. Litvinenko¹, Irina Petrushina

Center for Accelerator and Science and Education, Department of Physics and Astronomy,
 Stony Brook University, New York, USA

Igor Pinayev, Gang Wang, Yichao Jing

Collider-Accelerator Department, Brookhaven National Laboratory, New York, USA

¹also at Collider-Accelerator Department, Brookhaven National Laboratory, New York, USA

Content from this work may be used under the terms of the CC BY 3.0 licence (© 2018). Any distribution of this work must maintain attribution to the author(s), title of the work, publisher, and DOI.

Abstract

In this paper, we report on extremely good performance of 113 MHz SRF CW gun. This gun is a part of the system built to test coherent electron cooling concept and was aimed to generate trains of 78 kHz pulses with large 1 nC to 5 nC charge per bunch. While it was not built for attaining record low emittances, the machine can achieve very low normalized emittances ~ 0.3 mm mrad with 0.5 nC charge per bunch using CsK2Sb photocathode. In addition to excellent performance, this gun provides for very long lifetime of these high QE photocathodes, with a typical using time of 2 months.

INTRODUCTION

Coherent electron Cooling (CeC) is a novel technique promising high cooling rates for high energy hadron beams [1], BNL's future electron-ion collider, eRHIC especially concerns its feasibility [2]. We found CeC efficiency to outperform other cooling methods such as electron cooling or stochastic cooling by orders of magnitude. Since CeC is untested method, it will need to be tested by cooling a single bunch of gold ions circulating in RHIC [1]. The proof-of-principle experiment is conducted at BNL to demonstrate this technique. The dedicated accelerator, shown in Fig.1, comprising of 113 MHz SRF electron gun, two 500 MHz room-temperature bunching cavities and 704 MHz SRF linac built for this purpose has been commissioned and now is fully operational [3].

Since CeC SRF accelerator uses cryogenic system supplied by RHIC, it is able to operate only during RHIC runs. The SRF electron gun with CsK2Sb photo-cathode is operating for third season and generates electron beams with kinetic energy of 1.05-1.15 MeV and to 3.9 nC charge per

bunch. In this paper, we pre-sent selected simulation and experimental results focused on the transverse beam emittance.

SRF GUN AND PARMELA SIMULATIONS

The electrons in the SRF gun are generated from CsK2Sb photocathode by illumination from green 532 nm laser generating pulses with 0.25-nsec to 0.5-nsec duration. After accelerating to kinetic energy of 1.05 MeV (total energy 1.56 MeV), the beam propagates through the gun solenoid (located $z = 0.65$ m from the cathode, further in the text all distances are from the cathode surface), the bunching cavities (turned off for this measurements) and first transport solenoid (LEBT1, at $z = 3.65$ m) before it can be observed at YAG profile monitor ($z = 4.28$ m). The arrangement of this beamline is shown in Fig. 2. Being a low energy beam, its beam dynamics is strongly influenced by space charge starting from charge per bunch of few hundreds of pC. The particle tracking code PARMELA [4] has been used to simulate the beam dynamics.

We simulated the evolution of projected emittance and attempt to optimize strength of the gun and LEBT1 solenoids as well as the laser spot size on the cathode. Table 1 summarizes the parameters used in this optimization and result is summarized in Fig. 3. Cathode is located without recession in this simulation.

Table 1: Parameters Used for Optimization

Laser spot [mm]	Pulse length [ps]	Bunch charge [nC]	Energy gain [MeV]
1.25 ~ 2.5	300	0.1~0.5	1.05

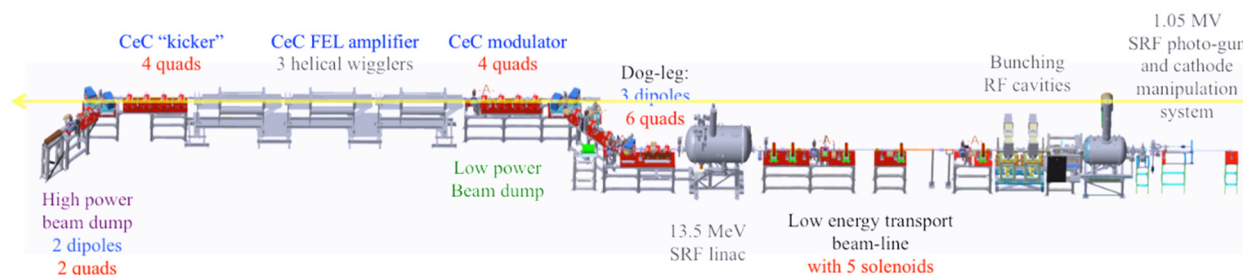


Figure 1: The layout of CeC experiment.

INDUCING MICROBUNCHING IN THE CLARA FEL TEST FACILITY

A. D. Brynes*

STFC Daresbury Laboratory & Cockcroft Institute, Warrington, UK

Abstract

We present simulation studies of the laser heater interaction in the CLARA FEL test facility using a non-uniform laser pulse. The microbunching instability, which manifests itself as correlated energy or density modulations in an electron bunch, can degrade the performance of an FEL. Most x-ray free electron lasers (FELs) utilise a so-called laser heater system to impose a small increase in the uncorrelated energy spread of the bunch at low energy to damp the instability – this technique involves imposing a laser pulse on the bunch while it is propagating through an undulator in a dispersive region. However, if the instability can be controlled, the electron bunch profile can be manipulated, yielding novel applications for the FEL, or for generation of THz radiation. Control of the microbunching instability can be achieved by modulating the intensity profile of the laser heater pulse to impose a non-uniform kick along the electron bunch. We have simulated this interaction for various laser intensity profiles and bunch compression factors.

INTRODUCTION

The quality of a photon beam produced by an FEL, in terms of spatial and temporal coherence, is strongly dependent on the electron bunch parameters. One important factor which can degrade the quality of an electron bunch in an FEL is the influence of collective effects, such as coherent synchrotron radiation (CSR) [1], or the microbunching instability [2]. This instability arises from density or energy variations in the bunch at low energies (due to factors such as shot noise [3], or longitudinal space charge [4]), and can become amplified due to CSR in dispersive regions, for example in bunch compressors [5]. Upon reaching the FEL undulator section, the electron beam can develop a correlated energy spread, which can limit the performance of x-ray FELs. The most commonly implemented solution to this is the laser heater [6].

Laser heater systems have proven to be crucial in improving the performance of x-ray FELs [7–9]. Recent results have also shown that, through modulating the temporal profile of the laser pulse used in the laser heater, it is possible to achieve a greater degree of control over the longitudinal profile of the electron bunch, yielding novel applications in the production of multi-colour FEL beams, or the production of THz radiation via a bunch with induced microbunching [10]. This technique is similar to the echo-enabled harmonic generation scheme [11], but it can achieve similar results in a shorter space, as it does not require multiple modulators before the FEL radiator section. In this paper we investigate the possibility of providing a tunable longitudinal profile of the

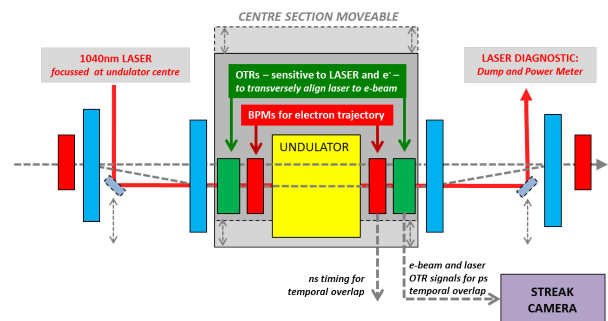


Figure 1: Schematic of laser heater system. Dipoles are shown in blue.

electron beam in the CLARA FEL test facility [12], which is currently under construction at Daresbury Laboratory.

THE CLARA LASER HEATER

In a typical laser heater system, an unmodulated Gaussian laser pulse is propagated with the bunch in the undulator, and any small-scale modulation is removed through the uncorrelated energy spread increase and the R_{52} parameter of the second half of the chicane. A schematic of the CLARA laser heater system is shown in Fig. 1, and the laser heater system parameters are given in Table 1; further details can be found in [13]. Simulations have shown that, while the microbunching instability is not expected to have a large impact on the nominal CLARA modes of operation, it would still be useful to install a laser heater in order to investigate potential methods of utilising the laser heater in novel configurations in order to achieve flexible control of the electron bunch properties. Current profiles and longitudinal distributions up to the exit of the CLARA accelerating section, at 240 MeV, have been simulated using the Elegant code [14] (with CSR and longitudinal space charge included) for the nominal laser heater operating mode, and with the laser heater off are shown in Fig. 2. In the nominal laser heating operating mode, sufficient power will be available to damp any small-scale structure in the electron bunch. Simulations have shown that a small increase in the RMS energy spread of 25 keV, or 0.1 % of the final beam energy, should be sufficient to heat the beam without greatly degrading the quality of the FEL – for this nominal operating mode of the laser heater, a pulse energy of around 48 μ J is required.

CHIRPED-PULSE BEATING

There are various ways of using modified laser pulses to modulate the longitudinal profile of an electron bunch. One method for achieving this is through chirped-pulse beating [15] of the laser heater pulse. The pulse is stretched

* alexander.brynes@stfc.ac.uk

NUMERICAL STUDY OF CHERENKOV RADIATION FROM THIN SILICA AEROGEL*

H. Hama[†], K. Nanbu, H. Saito, Y. Saito,

Research Center for Electron Photon Science, Tohoku University, Sendai, Japan

Abstract

Vavilov-Cherenkov radiation, usually just Cherenkov radiation (CR), is commonly used in high energy charged particle and cosmic rays detectors. We have studied CR emitted from very low refractive index material such as silica-aerogel and found it may be useful tool for electron beam diagnostics since the opening angle (Cherenkov angle) is small, then the CR can be transported onto a detector located far from the radiator. We have prepared a thin (1 mm thick) hydrophobic silica-aerogel having refractive index of 1.05 that has been developed at Chiba University. Since the intensity of CR is much stronger than that of optical transition radiation, the CR is a better light source for low intensity beam diagnostics. In order to apply the CR to measurement of bunch length of electron beams, we have investigated properties of CR by numerical simulation study based on the Liénard-Wiechert potentials. In addition, possibility of intense THz source is also discussed.

CHERENKOV RADIATION

Frank-Tamm theory [1] explaining properties of the Vavilov-Cherenkov radiation [2,3] without charged particle (de-)acceleration is based on the assertion that a charge moving uniformly in a dielectric medium with the velocity faster than the velocity of light in the medium radiates spherical electromagnetic waves from each point of its trajectory, it is the so-called “Cherenkov ring”. Although the CR property seemed to be mostly understood because Tamm’s first consideration was in 1939, it is however very interesting that we can find some theoretical works regarding “Tamm Problem” arising from an instantaneous acceleration and deceleration of a charge at the beginning and termination of its motion [4,5].

The opening angle, Cherenkov angle θ_C , is in general characterized by the refractive index n and the particle velocity β as

$$\cos\theta_C = 1/(n\beta). \quad (1)$$

Therefore, the radiation does not occur when $n\beta < 1$. Photon numbers of CR between the wavelengths λ_1 and λ_2 is given as [1]

$$N_{\text{photon}} = 2\pi\alpha z \left| \frac{1}{\lambda_1} - \frac{1}{\lambda_2} \right| \sin^2\theta_C, \quad (2)$$

*This work supported by JSPS KAKENHI: Grant numbers JP15K13394 and JP17H01070.

[†]hama@lms.tohoku.ac.jp

where α and z are the fine structure constant and the radiator thickness, respectively. Although common e-beam diagnostics, transition radiation is often employed, the photon number of it is poorly small. Since CR is a significant effect, the study has probed the potential ability of CR for beam diagnostics. For example, yield of 500-nm photons with 1% bandwidth from relativistic electron is ~ 0.5 per electron for a 1-mm thick radiator having $n = 1.5$.

NUMERICAL EVALUATION

We start our analysis with the well-established Liénard-Wiechert potential [6]

$$\frac{dI}{d\omega d\Omega} = \frac{1}{4\pi\epsilon_0} \frac{e^2}{4\pi^2 c(\omega)} \omega^2 \times \left| \int \mathbf{n} \times (\mathbf{n} \times \boldsymbol{\beta}(\omega)) e^{i\omega \left(t' - \frac{\mathbf{n} \cdot \mathbf{r}(t')}{c(\omega)} \right)} dt' \right|^2 \quad (3)$$

where $c(\omega)$ is the speed of light in the medium and $\boldsymbol{\beta}(\omega)$ is a particle speed with respect to $c(\omega)$. A vector \mathbf{n} denotes a unit vector to the observing point from the particle located at $\mathbf{r}(t')$. Assuming a charge travelling in a straight line at a velocity and the velocity of light in the medium is

$$c(\omega) = 1 / \sqrt{\epsilon(\omega)\mu_0}, \quad (4)$$

then eq. (3) becomes

$$\frac{dI}{d\omega d\Omega} = \frac{\mu_0}{4\pi} \frac{e^2}{4\pi^2 c(\omega)} \omega^2 v^2 \sin^2\theta \left| \int e^{i\omega(1-\boldsymbol{\beta}(\omega)\cos\theta)} dt' \right|^2. \quad (5)$$

After some mathematical treatment, it can be shown that

$$\int e^{i\omega(1-\boldsymbol{\beta}(\omega)\cos\theta)} dt' = 2\pi\delta[\omega(1-\boldsymbol{\beta}(\omega)\theta)]. \quad (6)$$

Thus, we obtain

$$\frac{dI}{d\omega d\Omega} = \frac{\mu_0}{4\pi} \frac{e^2 \omega^2}{4\pi^2 c(\omega)} \sin^2\theta \left(\frac{\sin\alpha}{\alpha} \right)^2 (dz)^2, \quad (7)$$

where

$$\alpha = \frac{1}{2} [1 - \boldsymbol{\beta}(\omega)\cos\theta] \omega \Delta t, \quad (8)$$

and Δt denotes the time passing through the medium.

RECENT EXPERIMENTAL RESULTS ON HIGH-PEAK-CURRENT ELECTRON BUNCH AND BUNCH TRAINS INTERACTING WITH A THz UNDULATOR*

Xiaolu Su, Lixin Yan[†], Dan Wang, Yifan Liang, Lujia Niu, Qili Tian,
 Dong Wang, Yingchao Du, Wenhui Huang, Chuanxiang Tang,
 Department of Engineering Physics, Tsinghua University, Beijing, China

Abstract

In this paper, experimental results based on THz undulator with widely tunable gap installed at Tsinghua Thomson scattering X-ray (TTX) beamline are introduced. This is a planar permanent magnetic device with 8 regular periods, each 10-cm long. The undulator parameter varies from 9.24–1.39 by changing the magnetic gap from 23 mm to 75 mm. The coherent undulator radiation can be used as a narrow-band THz source with central frequency ranging from 0.4 THz to 10 THz. The bunch length was determined from the radiation intensity at different undulator gaps, agreeing well with simulations. Furthermore, slice energy modulation was directly observed when high-peak-current bunch trains based on nonlinear longitudinal space charge oscillation passed through the undulator. The demonstrated experiment in the THz regime provides a significant scaled tool for FEL mechanism exploration owing to the simplicity of bunch modulation and diagnostics in this range.

INTRODUCTION

High-peak-current electron bunch and bunch trains have many important applications in accelerator research. Ultrashort bunches are widely used in high-gain free electron lasers (FEL) [1], wake-field acceleration [2], ultrafast electron diffraction (UED) [3] and high-power coherent radiation in the terahertz (THz) spectral range [4]. The resonant excitation of wakefield accelerators [5] and production of narrow-band terahertz radiation [6] rely on the development of bunch trains with a large number of equally spaced electron micro bunches. The measurement of ultrashort bunch length and bunch train distribution is of vital importance for these frontier applications.

the electron-bunch form factor, defined as:

$$F(\omega) = \left| \int_{-\infty}^{\infty} e^{i\omega z/c} S(z) dz \right|^2 \quad (1)$$

is derived from the Fourier transform of the longitudinal electron density in the bunch, where $S(z)$ is the distribution function for particles in the bunch, measured relative

to the bunch centre, c is light velocity in vacuum. Form factor is closely related to the bunch longitudinal distribution, both for ultrashort bunch and bunch trains. There have been several methods for bunch form factor or longitudinal distribution measurement. Deflecting cavity is one of the most useful tool for beam diagnostics, converting the longitudinal distribution into transverse coordinate [7]. Electro-optic method can measure bunch length with temporal resolution limited to sub-ps level [8]. Moreover, spectrum and intensity of coherent radiation are used for bunch longitudinal distribution diagnose or monitoring, including coherent diffraction radiation (CDR), coherent transition radiation (CTR) [9], and coherent Smith-Purcell radiation [10]. In this paper, ultrashort bunch length and bunch train distribution are derived from THz radiation energy of a tunable-gap undulator.

Moreover, radiation spectrum and energy from the tunable-gap undulator were measured, which is an intense narrow-band THz source. Terahertz sources have many potential applications in biophysics, medical, industrial imaging, nanostructures, and metal science [11]. Intense THz radiation has been utilized as probes of low-frequency excitations, which is a powerful tool to improve the fundamental understanding of matter. THz sources based on relativistic electrons are usually with high power and have various properties based on emission mechanisms. Coherent undulator radiation is naturally narrow-band, which is of great advantage for scientific research. The resonant frequency is defined as:

$$f = \frac{2\gamma^2 c}{(1 + K^2/2)\lambda_u}, \quad (2)$$

where γ is the Lorentz factor, K is the undulator parameter, and λ_u is the period.

When electron bunch train with the same period passes through undulator, the radiation from bunch tail slips ahead the bunch and interact with the electron ahead. Furthermore, if the resonant wavelength is the same with bunch train period, the radiation from micro bunches add coherently and interact with electron bunch. Bunch energy modulation was observed at Terahertz spectrum during the experiment. The beamline and experimental results are introduced in the following sections.

*Work supported by the National Natural Science Foundation of China (NSFC Grants No. 11475097) and the National Key Scientific Instrument and Equipment Development Project of China (Grants No. 2013YQ12034504).

[†]yanlx@mail.tsinghua.edu.cn

LARGE-SCALE TURNKEY TIMING DISTRIBUTION SYSTEM FOR NEW GENERATION PHOTON SCIENCE FACILITIES

K. Şafak[†], H. P. H. Cheng, J. Derksen, A. Berlin, E. Cano, A. Dai, D. Forouher, W. Nasimzada, M. Neuhaus, P. Schiepel, E. Seibel, Cycle GmbH, Hamburg, Germany
 A. Kalaydzhyan, J. Meier, D. Schimpf, A. Berg, T. Tilp, F. X. Kärtner¹, CFEL, Hamburg, Germany
¹also at RLE, MIT, Cambridge, Massachusetts, USA

Abstract

We report a large-scale turnkey timing distribution system able to satisfy the most stringent synchronization requirements demanded by new generation light sources such as X-ray free-electron lasers and attoscience centers. Based on the pulsed-optical timing synchronization scheme, the system can serve 15 remote optical and microwave sources in parallel via timing stabilized fiber links. Relative timing jitter between two link outputs is less than 1 fs RMS integrated over an extended measurement time from 1 μ s to 2.5 days. The current system is also able to generate stabilized microwaves at the link outputs with 25-fs RMS precision over 10 h, which can be easily improved to few-femtosecond regime with higher quality VCOs.

INTRODUCTION

Low-noise transfer of time and frequency standards over large distances provides high temporal resolution for ambitious scientific explorations such as sensitive imaging of astronomical objects using multi-telescope arrays [1], comparison of distant optical clocks [2] or gravitational-wave detection using large laser interferometers [3]. In particular, rapidly-emerging new generation light sources such as X-ray free-electron lasers (FELs) [4] and attoscience centers [5] have the most challenging synchronization requirements on the order of few femtoseconds or below to generate ultrashort X-ray pulses for the benefit of creating super-microscopes with sub-atomic spatiotemporal resolution. The critical task in these facilities is to synchronize various pulsed lasers and microwave sources across multi-kilometer distances as required for seeded FELs and attosecond pump-probe experiments.

Recently, it has been shown that the pulsed-optical timing synchronization scheme based on balanced optical cross-correlators (BOCs) and balanced optical-microwave phase detectors (BOMPDs) can deliver sub-femtosecond precision between remotely synchronized lasers and microwave sources in laboratory environment [6,7]. Here, we transform this experimental system into a large-scale turnkey timing distribution system (TDS) that is able to serve 15 remote optical and microwave sources via timing stabilized fiber links. The system exhibits less than 1-fs RMS timing jitter at the outputs of the fiber links over 2.5 days of operation. The current system is able to serve remote microwave devices with 25-fs RMS precision over 10 h which can be easily improved to few femtoseconds with higher quality VCOs.

In this paper, we describe the layout of the TDS together with its dedicated control system. We also discuss the characterization measurements of the timing stabilized fiber links and the remote microwave synchronization.

SYSTEM LAYOUT AND ARCHITECTURE

Figure 1 shows the layout of the TDS capable of serving 15 remote clients. The optical master oscillator (OMO) is a low-noise mode-locked laser operating at 1550-nm center wavelength with a free-running timing jitter of 0.4 fs RMS integrated between 1 kHz and 1 MHz [8]. A BOMPD (i.e., BOMPD-OMO in Fig. 1) is employed to lock the OMO to an external RF master oscillator in order to ensure the TDS operates synchronously with the facility's RF reference (e.g., low-level RF system). Then the output of the OMO is split into 15 separate polarization maintaining (PM) fiber links. In order to preserve the low noise properties of the OMO during the delivery to remote locations, fiber link stabilizers (FLS) are developed. Each FLS contains a BOC to detect the time-of-flight fluctuations of the optical pulses during fiber-link transmission with attosecond precision. Then, the integral control elements of the FLS (i.e., a fiber stretcher and a motorized delay line) are activated to stabilize the arrival time of the delivered optical pulses at the fiber link output. Once the fiber links are stabilized, two-color BOCs (TCBOCs) and BOMPDs are activated to synchronize ultrafast lasers and microwave sources to the link outputs at remote locations. The TCBOC detects the timing error between the two optical pulse trains, emanating from the fiber link output and the remote slave laser. The voltage response of the TCBOC is then used as a feedback signal to control the frequency of the remote slave laser via its

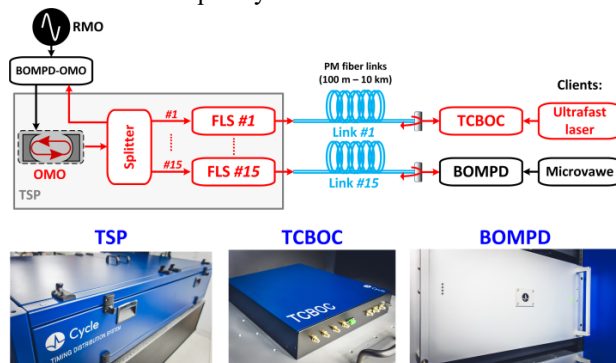


Figure 1: Layout of the timing distribution system (top sketch) and its individual modules as built in the lab (bottom pictures). RMO: RF master oscillator; OMO: optical master oscillator; TSP: temperature-stabilized platform; FLS: fiber link stabilizer; TCBOC: two-color balanced optical cross-correlator; BOMPD: balanced optical-microwave phase detector.

[†] kemal.shafak@cyclelasers.com

DIAGNOSTICS UPGRADES FOR INVESTIGATIONS OF HOM EFFECTS IN TESLA-TYPE SCRF CAVITIES*

A.H. Lumpkin[#], D. Edstrom Jr., J. Ruan, R. Thurman-Keup Y. Shin, P. Prieto, N. Eddy
Fermilab Accelerator Laboratory, Batavia, IL 60510 USA

B.E. Carlsten^{**}, Los Alamos National Laboratory, Los Alamos, NM 87545 USA

Abstract

We describe the upgrades to diagnostic capabilities on the Fermilab Accelerator Science and Technology (FAST) electron linear accelerator that will allow investigations of the effects of high-order modes (HOMs) in SCRF cavities on macropulse-average beam quality. We examine the dipole modes in the first pass-band generally observed in the 1.6-1.9 GHz regime for TESLA-type SCRF cavities due to uniform transverse beam offsets of the electron beam. Such cavities are the basis of the accelerators such as the European XFEL and the proposed MaRIE XFEL facility. Preliminary HOM detector data, prototype BPM test data, and first framing camera OTR data with ~20-micron spatial resolution at 250 pC per bunch will be presented.

INTRODUCTION

There are current Free-Electron Laser (FEL) initiatives that will be enabled by the use of the TESLA-type SCRF cavities in Europe (the European XFEL) and proposed in the USA (the MaRIE facility). One of the challenges is the control of the high-order modes (HOMs) that develop in these cavities due to transverse beam offsets. Diagnostic capabilities are being upgraded on the Fermilab Accelerator Science and Technology (FAST) facility [1] that will allow investigations of the effects of high-order modes (HOMs) in SCRF cavities on macropulse-average beam quality. We focus on the dipole modes in the first pass-band generally observed in the 1.6-1.9 GHz regime in TESLA-type SCRF cavities due to beam offsets. Such cavities are the basis of the accelerators for the European XFEL and the proposed MaRIE XFEL facility. Raw HOM data indicate that the mode amplitudes oscillate for ~10 μ s after the micropulse enters the cavity. With a 3-MHz pulse train, we expect transverse centroid shifts will then occur during the macropulse resulting in a blurring of the beam-size image averaged over the macropulse.

To evaluate these effects, upstream corrector magnets were tuned to steer the beam off axis upon entering the first of the two cavities. From there, several parameters were tracked, including the two HOM detector signal strengths for each cavity, the average transverse beam positions from rf beam position monitors (BPMs), and the

average beam size using intercepting screens and imaging. Preliminary efforts demonstrated reduction of the HOM signals by beam steering. Our initial data from an optical transition radiation (OTR) source indicated a framing camera mode can provide ~20-micron spatial resolution at ~250 pC per bunch while the prototype rf BPM required higher charge to approach this resolution for single-bunch beam position. The preliminary HOM detector data, prototype BPM test data, and framing camera data will be presented later in this paper.

EXPERIMENTAL ASPECTS

The FAST Linac

The FAST linac is based on the L-band rf photocathode (PC) gun which injects beam into two superconducting rf (SCRF) capture cavities denoted CC1 and CC2, followed by transport to a low energy electron spectrometer. A Cs₂Te photocathode is irradiated by the UV component of the drive laser system described elsewhere [2]. The basic diagnostics for the HOMs studies include the rf BPMs located before, between, and after the two cavities as shown in Fig. 1. These are supplemented by the imaging screens at X107, X108, X121, and X124. The HOM couplers are located at the upstream and downstream ends of each SCRF cavity, and these signals are processed by the HOM detector circuits with the output provided online through ACNET, the Fermilab accelerator controls network. The upgrades will include optimizing the HOM detectors' bandpass filters, reducing the 1.3 GHz fundamental with a notch filter, converting the rf BPMs electronics to bunch-by-bunch capability with reduced noise, and using the C5680 streak camera in a rarely-used framing mode for bunch-by-bunch spatial information.

The Streak Camera System

In an initial framing camera study [3] we observed the green component remaining from UV-conversion at 3 and 9 MHz micropulse frequencies with the laser lab streak camera. We have also recently applied the principle to optical transition radiation (OTR) from an Al-coated Si substrate with subsequent transport to a beamline streak camera that views OTR from the X121 screen location. Commissioning of the streak camera system was facilitated through a suite of controls centered around ACNET. This suite includes operational drivers to control and monitor the streak camera as well as Synoptic displays to facilitate interface with the driver. Images are

* Work supported under Contract No. DE-AC02-07CH11359 with the United States Department of Energy.

** Work at LANL supported by US Department of Energy through the LANL/LDRD Program.

lumpkin@fnal.gov

ADAPTIVE FEEDBACK FOR AUTOMATIC PHASE-SPACE TUNING OF ELECTRON BEAMS IN ADVANCED XFELS

A. Scheinker*, Los Alamos National Laboratory, Los Alamos, USA
D. Bohler†, SLAC National Accelerator Laboratory, Menlo Park, USA

Abstract

Particle accelerators are extremely complex devices having thousands of coupled, nonlinear components which include magnets, laser sources, and radio frequency (RF) accelerating cavities. Many of these components are time-varying. One example is the RF systems which experience unpredictable temperature-based perturbations resulting in frequency and phase shifts. In order to provide users with their desired beam and thereby light properties, LCLS sometimes requires up to 6 hours of manual, experience-based hand tuning of parameters by operators and beam physicists, during a total of 12 hours of beam time provided for the user. Even standard operational changes can require hours to switch between user setups. The main goal of this work is to study model-independent feedback control approaches which can work together with physics-based controls to make overall machine performance more robust, enable faster tuning (seconds to minutes instead of hours), and optimize performance in real time in response to un-modeled time variation and disturbances.

INTRODUCTION

While existing and planned free electron lasers (FEL) have automatic digital control systems, they are not controlled precisely enough to quickly switch between different operating conditions. Existing controls maintain components at fixed set points, which are set based on desired beam and light properties, such as, for example, the current settings in a bunch compressor's magnets. Analytic studies and simulations initially provide these set points. However, models are not perfect and component characteristics drift in noisy and time-varying environments; setting a magnet power supply to a certain current today does not necessarily result in the same magnetic field as it would have 3 weeks ago. Also, the sensors are themselves noisy, limited in resolution, and introduce delays. Therefore, even when local controllers maintain desired set points exactly, performance drifts. The result is that operators continuously tweak parameters to maintain steady state operation and spend hours tuning when large changes are required, such as switching between experiments with significantly different current, beam profile (2 color, double bunch setups), or wavelength requirements. Similarly, traditional feed-forward RF beam loading compensation control systems are limited by model-based beam-RF interactions, which work extremely well for perfectly known RF and beam properties, but in practice are limited by effects which include un-modeled drifts and fluc-

tuations and higher order modes excited by extremely short pulses. These limitations have created an interest in iterative (beam-based feedback), machine learning, and adaptive techniques.

The focus of this work is on minimizing the lengthy (1-10 hours) suboptimal manual tuning is required when beam parameters are changed between experiments, especially when settings of the low energy beam sections (<500 MeV) are changed. The sources of tuning difficulty include complex effects such as: space charge and coherent synchrotron radiation, which depend on many machine settings simultaneously, unobservable parameters, which are not well controlled, and time varying, drifting components. Such difficulties will only increase as existing and future light are exploring new and exotic schemes such as two-color operation (LCLS, LCLS-II) and next generation light sources seek to provide brighter, shorter wavelength (0.1nm at PAL, 0.05 nm at EuXFEL, and 0.01 nm at MaRIE), more coherent light [1]. To achieve their performance goals, new machines face unique challenges, such as requiring extremely low electron beam emittance and energy spread. LCLS-II requires <0.01% rms energy stability, which is >10x more than the existing LCLS linac [2]. EuXFEL requires < 0.001 %/deg rms RF amplitude and phase errors, respectively (current state of the art is 0.01) [3]. Existing and future accelerators will benefit from an ability to quickly tune between experiments and to compensate for extremely closely spaced electron bunches, such as might be required for MaRIE, requiring advanced controls and approaches such as droop correctors [4, 5].

The type of tuning problems that we are interested in have recently been approached with powerful machine learning methods [6, 7], which are showing very promising results. Our approach to this problem is complementary to other machine learning methods in that instead of learning over long periods of time, we attempt to respond quickly in real time, based on very limited measurements. One possible limitation of our approach is that being a real time, local feedback, it may become trapped in a local minimum. Future plans exist for combining the work discussed here with machine learning. We utilize a novel model-independent extremum seeking (ES) based feedback scheme, which operates based only on noisy measurements without dependence on accurate system models [8, 9] and is closely related to vibrational control [10]. The advantages of this approach are:

* ascheink@lanl.gov

† dbohler@slac.stanford.edu

SUB-FEMTOSECOND TIME-RESOLVED MEASUREMENTS BASED ON A VARIABLE POLARIZATION X-BAND TRANSVERSE DEFLECTION STRUCTURE FOR SwissFEL

P. Craievich*, M. Bopp, H.-H. Braun, R. Ganter, M. Pedrozzi, E. Prat,
 S. Reiche, R. Zennaro, Paul Scherrer Institut, Villigen-PSI, Switzerland
 A. Grudiev, N. Catalan Lasheras, G. Mcmonagle, W. Wuensch, CERN, Geneva, Switzerland
 B. Marchetti, R. Assmann, F. Christie, R. D'Arcy, D. Marx, DESY, Germany

Abstract

The SwissFEL project, under commissioning at the Paul Scherrer Institut (PSI), will produce FEL radiation for soft and hard X-rays with pulse durations ranging from a few to several tens of femtoseconds. A collaboration between DESY, PSI and CERN has been established with the aim of developing and building an advanced X-Band transverse deflection structure (TDS) with the new feature of providing variable polarization of the deflecting force. As this innovative CERN design requires very high manufacturing precision to guarantee highest azimuthal symmetry of the structure to avoid the deterioration of the polarization of the streaking field, the high-precision tuning-free assembly procedures developed at PSI for the SwissFEL C-band accelerating structures will be used for the manufacturing. Such a TDS will be installed downstream of the undulators of the soft X-ray beamline of SwissFEL and thanks to the variable polarization of the TDS it will be possible to perform a complete characterization of the 6D phase space. We summarize in this work the status of the project and its main technical parameters.

INTRODUCTION

The SwissFEL project at PSI consists out of a 6 GeV accelerator complex and two undulator beam lines. The Aramis beam line, presently under commissioning, covers the energy photon ranges from 12.4 to 1.8 keV [1], while the Athos beam line the range from 1.9 to 0.25 keV [2]. The Athos line will operate in parallel to the Aramis line and, actually consists of a fast-kicker magnet, a dog-leg transfer line, a small linac and 16 APPLE undulators. It is designed to operate in advanced modes of operation slightly different to standard SASE operation and will produce soft X-rays FEL radiation with pulse durations ranging from a few to several tens of femtoseconds [3]. Electron beam diagnostic based on a transverse deflection structure (TDS) placed downstream of the undulators (post-undulator TDS) in conjunction with an electron beam energy spectrometer can indirectly measure the pulse length of these ultra-short photon beam analysing the induced energy spread on the electron bunch due to the FEL process [4, 5]. Furthermore, a complete characterization of the electron beam 6D phase space by means of measurements of the bunch length, energy and of the transverse slice emittances (vertical and horizontal) are important tasks for

commissioning and optimization of FEL process [6–9]. In this context, the design of an innovative X-band TDS structure, including a novel variable polarisation feature, has been proposed by CERN [10, 11]. In order to avoid the rotation of the polarization of the dipole fields along the structure, a high-precision tuning-free assembly procedure developed for the C-band linac at PSI will be used for the fabrication of the TDSs [12]. This procedure has been used to fabricate 120 cavities for the SwissFEL linac and it is currently being used for the fabrication of the tuning free X-band structure prototypes for CLIC [13]. Several experiments at DESY (FLASH2, FLASHForward, SINBAD) and PSI (Athos) are interested in the utilization of high gradient X-band TDS systems for high resolution longitudinal diagnostics. In this context a collaboration between DESY, PSI and CERN has been established with the aim of developing and building an advanced X-Band transverse deflection structure (TDS) with the new feature of providing variable polarization of the deflecting field [14]. In this paper we summarize the specifications of the TDS system for the Athos line and we also introduce some details of the mechanical design of the first prototype that will be compatible with the requests from DESY and PSI [14].

TDS DIAGNOSTIC LINE

Table 1 contains the electron beam parameters at Athos post-undulator diagnostic section that have been used for the following calculations. Layout and more details on the Athos line are in [2].

Table 1: Beam and optical parameters involved in the streaking process at ATHOS post-undulator diagnostic section.

Parameter	Sy.	Value	Unit
Beam energy	E	2.9-3.4	GeV
Charge	Q	10-200	pC
Bunch length	σ_t	2-30	fs
β @TDS	$\beta_x = \beta_y$	50	m
Emittance	$\gamma\epsilon_x = \gamma\epsilon_y$	0.1-0.3	μm
Rep. rate		100	Hz

Figure 1 shows a schematic layout of the post-undulator diagnostic section. Beam slice emittance in both transverse planes will be investigated by a multi-quadrupole scan technique combined with the TDS. By means of the TDS, the

* paolo.craievich@psi.ch

HLS TO MEASURE CHANGES IN REAL TIME IN THE GROUND AND BUILDING FLOOR OF PAL-XFEL, LARGE-SCALE SCIENTIFIC EQUIPMENT*

Hyojin Choi[†], Sangbong Lee, Hong-Gi Lee, Jang Hui Han, Seung Hwan Kim, Heung-Sik Kang
 Department of Accelerator, PAL-XFEL, Pohang, Korea

Abstract

A variety of parts that comprise large-scale scientific equipment should be installed and operated at accurate three-dimensional location coordinates X, Y, and Z through survey and alignment in order to ensure optimal performance. However, uplift or subsidence of the ground occurs over time and consequently this causes the deformation of building floors. The deformation of the ground and buildings cause changes in the location of installed parts, and eventually that leads to alignment errors (ΔX , ΔY , and ΔZ) of components. As a result, the parameters of the system change and the performance of large-scale scientific equipment is degraded.

Alignment errors that result from changes in building floor height can be predicted by real-time measurement of changes in building floors. This produces the advantage of reducing survey and alignment time by selecting the region where great changes in building floor height are shown and re-aligning components in the region in a short time. To do so, HLS (hydrostatic levelling sensor) with a resolution of $0.2 \mu\text{m}$ and a waterpipe of 1000 meters are installed and operated at the PAL-XFEL building. WPS (wire position sensor) with a resolution of $0.1 \mu\text{m}$ is installed at undulator section where the changes in the location of equipment should be measured with two-dimensional coordinates (vertical Y and horizontal X). This paper introduces the installation and operation status of HLS.

INTRODUCTION

As shown in Figure 1, if the ground and the floor of a building changes, the location of equipment changes accordingly and the performance of the PAL-XFEL is degraded [1]. To measure the displacement of building floors in a real time, an ultrasonic-type HLS, which was manufactured by Budker Institute of Nuclear Physics (BINP) of Russia, was installed as shown in Figure 2 [2-3].

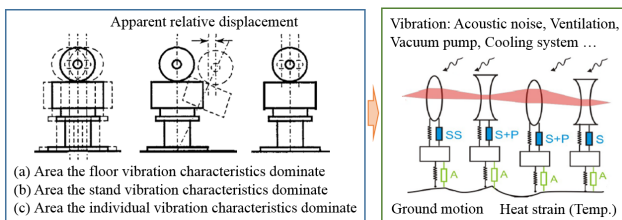


Figure 1: Three vibration patterns which generate relative displacement [1].

*Work supported by Ministry of the Science, ICT and Future Planning
[†]choihyo@postech.ac.kr

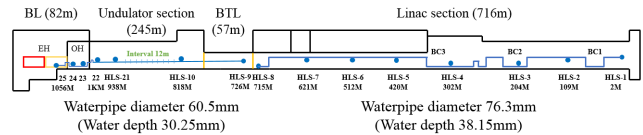


Figure 2: Locations where HLS of PAL-XFEL is installed.

SOURCES OF GROUND VIBRATION

In the section ‘Between model and reality, Part I’ (pp. 237-244) of the Beam Diagnostic textbook published by CERN Accelerator School [4], beam-orbit instability-inducing elements were classified in categories depending on the time scale as shown in Table 1. In addition to geological changes, various vibrations generating inside and outside the buildings affect the equipment and cause beam orbit instability. The CAS textbook describes the elements and countermeasure of beam orbit instability in detail [4].

Table 1: Instability Classified by Time Scale

Instability	Time Scale
Long term	Weeks to years - sun and moon motion - ground settlement - seasonal ground motion
Medium term	Minutes to days - weather (rain, hot, dry, cold, etc.) - diurnal temperature - thermal drift
Short term	Milliseconds to seconds - ground vibration - cooling water flow vibration - machinery vibration (chillers, air conditioners, vacuum pumps, etc.)
Very short term	Higher frequency or shorter periods

Some instability elements described in the CAS textbook are observed on HLS data as shown in Figure 3. Temperature variation is included in the instability elements. The temperature on the HLS was measured to correct the thermal deformation of instruments according to temperature variation.

TUNE-UP SIMULATIONS FOR LCLS-II

M. W. Guetg*, P. J. Emma

SLAC National Accelerator Laboratory, Menlo Park, CA 94025, USA

Abstract

The planned superconducting LCLS-II linac poses new operational constraints with respect to the existing copper linac currently operated for LCLS. We present the results of exhaustive accelerator simulations, including realistic machine errors and exploring beam tune-up strategies. Specifically, these simulations concentrate on longitudinal and transverse beam matching as well as orbit and dispersion control through the new linac and up to the hard x-ray FEL. Dispersion control is achieved by a novel method presented within this paper. The results confirm that the beam diagnostics in the current scheme are sufficient for tune-up, yet identify the importance of dispersion control leading to minor changes in the lattice to further improve performance.

INTRODUCTION

The planned FEL upgrade LCLS-II includes a variety of new subsystems. The complex interplay of all the systems requires good electron beam diagnostics to guarantee beam quality and thus FEL performance. This proceeding outlines three key aspects to evaluate tune-up performance through simulations:

- ▶ Identify redundancy and lack of diagnostics
- ▶ Assess tolerances
- ▶ Test tune-up algorithms

All simulations were done using Elegant 29.0 [1]. The simulations start off with machine settings as present after preliminary phasing of the cavities and initial steering to establish partial transmission and simulate tune-up using readouts as available from LCLS-II diagnostics (Figure 1)

only. Low probability corner cases were covered by repetitions of the simulation using newly generated machine and beam imperfections for each run. Simulated machine imperfections include misalignments of magnets, cavities and beam position monitors (BPMs) as well as strength errors of magnets and cavities. Non-static imperfections like shot-to-shot fluctuations and machine drifts are expected to be small and were neglected. The beam was simulated with a standard setup of 750 A final peak current, 100 pC bunch charge and 4 GeV final beam energy, but initially off momentum and displaced in space for all 3 dimensions, optics and charge. All initial values but the beam optics parameters were randomly drawn from normal distributions with standard deviations as summarized in Table 1. The beam optics error is expressed by the mismatch parameter [2], which was simulated with constant magnitude but random phase drawn independently for both transverse planes. To ensure validity of these studies, the assumed errors are larger than what is expected after initial RF machine phasing and beam based alignment.

The main components of beam misalignment are orbit offsets, dispersion and transverse and longitudinal mismatches. Orbit offsets may arise from various effects. With increasing offset the following effects manifest: Quadrupole magnets will kick the beam and thereby generate dispersion, small apertures (RF cavities, etc) excite transverse wakefields and the beam halo will be lost along the machine. Core beam losses are not assumed for the simulation as the collimation and machine protection system would prevent prolonged operation in this condition [3] and initial phasing and steering is expected to establish transmission.

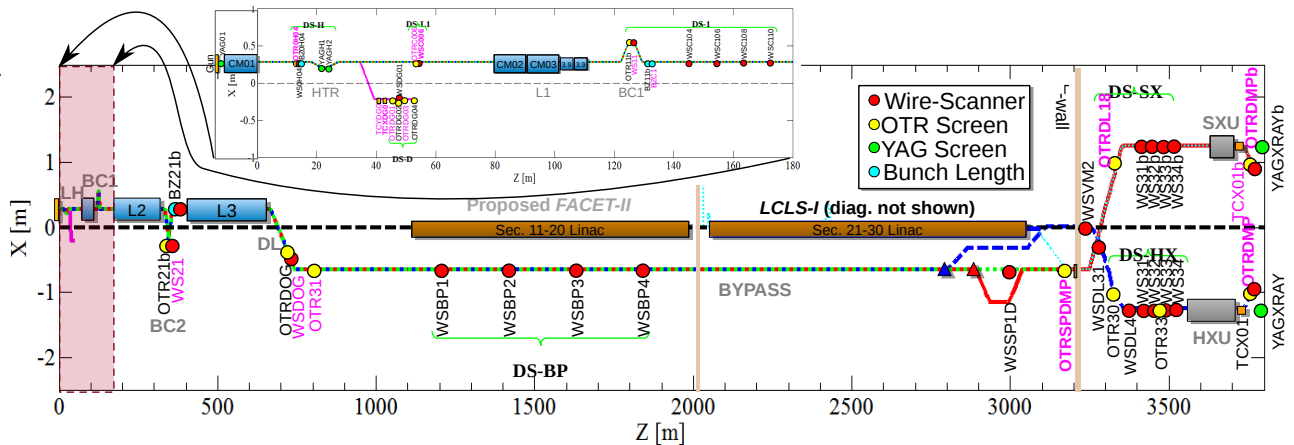


Figure 1: Schematic setup of LCLS-II highlighting locations where the bunch profile can be measured. Not shown on the scheme are BPMs and bunch length monitors

* marcg@slac.stanford.edu

BEAM LOSS MONITOR FOR UNDULATORS IN PAL-XFEL*

H. Yang[†] and D. C. Shin

Pohang Accelerator Laboratory, Pohang 790-784, Korea

Abstract

PAL-XFEL consists of a hard x-ray line, based on a 4-10-GeV electron beam, and a soft x-ray line, based on a 3-3.5 GeV electron beam. The HX line consists of 20 undulators and the SX line consists of 7 undulators. The permanent magnets in an undulator should be protected from the radiation-induced demagnetization. We develop a beam loss monitor (BLM) for undulators in PAL-XFEL. It consists of a detector part (head) and an ADC part. The BLM head consists of two fused quartz rods, two photo-multiplier tube (PMT) modules, and an LED bulb. It is based on the Cherenkov radiator: two fused quartz rods are used for radiators. Two sets of the radiator and PMT module are installed up and down the beam tube. An LED bulb is between the radiators for the heartbeat signal. The ADC part digitizes the output signal of the PMT module. It measures and calculates the beam loss, background, and heartbeat. One ADC processes the signal from 6-8 heads. The BLM system generates interlock to the machine interlock system for over-threshold beam loss. The 28 BLM heads are installed downstream of each undulator. Those are calibrated by the heartbeat signal and operated in the electron beam transmission with 150 pC.

INTRODUCTION

PAL-XFEL produces 0.1 – 1 nm FEL with 4 – 10 GeV electron beam in the hard x-ray (HX) line and 1–10 nm FEL with 3 – 3.5 GeV electron beam in soft x-ray (SX) line. 20 and 7 undulators are installed respectively in the HX line and the SX line. Undulators made with permanent magnets are used for the FEL generation in the XFEL machines [1-3]. Since there is the radiation-induced demagnetization for the permanent magnet, it is important to prevent the electron beam irradiation in the undulator [4]. This irradiation is occurred unintentionally by the electron beam loss in the undulator region caused by abnormal beam orbit and beam size. The beam operation should be blocked until the system is recovered in the normal condition.

We develop the SLAC type Beam Loss Monitor (BLM) system for interlock of the undulator region [5]. The system consists of the BLM head (detector part) and the ADC part. The BLM heads are based on Cherenkov radiators. They are installed after each undulator and measure the beam loss occurred at the drift in each undulator. The beam loss signal is digitized in the ADC system. It calculates the beam loss and generates interlock signal for over threshold beam loss. In this paper, we present the design of the BLM head and ADC system. Also, we present the details of the installation, calibration, and operation of this system.

* work supported by MSIP, Korea.

[†] highlong@postech.ac.kr

BLM HEAD

The BLM head converts Cherenkov radiation by the electron loss into electric signal. It is located in the 1-m long intersection of the undulator region (Fig. 1(a)). It consists of radiators, PMT modules, an LED bulb, and a case (Fig. 2). The radiators are located at up and down of the beam tube (Fig. 1(b)) and the PMT should receive photons from two radiators. Since the width of the BLM head should be minimized for installation of other components in the intersection, we used two PMT modules with small size for each radiator.

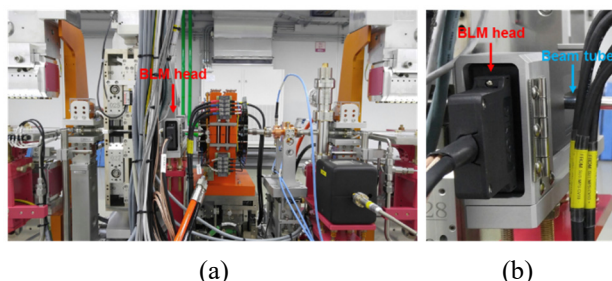


Figure 1: (a) Location of the BLM head at the intersection in the undulator region. (b) Location of the BLM head and the beam tube.

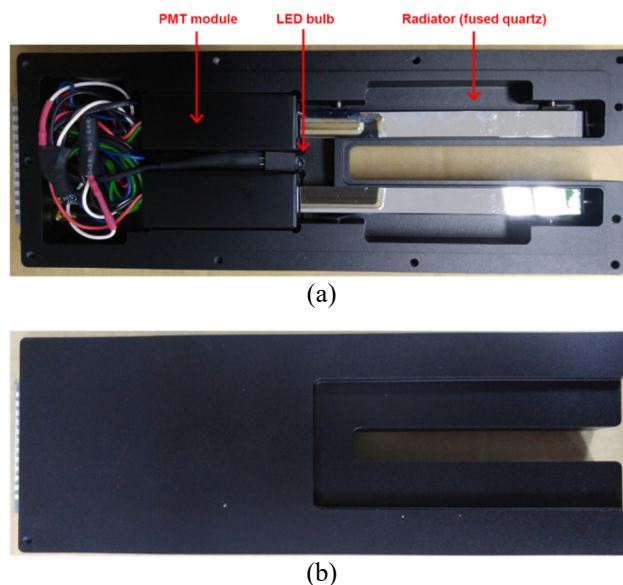


Figure 2: Structure of (a) the inside and (b) the back of the BLM head.

COHERENT UNDULATOR RADIATION FROM A KICKED ELECTRON BEAM

J. P. MacArthur*, A. A. Lutman, J. Krzywinski, Z. Huang,
SLAC National Accelerator Laboratory, Menlo Park, USA

Abstract

The properties of off-axis radiation from an electron beam that has been kicked off axis are relevant to recent Delta undulator experiments at LCLS. We calculate the coherent emission from a microbunched beam in the far-field, and compare with simulation. We also present a mechanism for microbunches to tilt toward a new direction of propagation.

INTRODUCTION

During the commissioning of the Delta undulator at LCLS, a highly circularly polarized beam was produced by kicking the electron beam prior to the Delta undulator [1]. This situation is depicted in Figure 1. With the right detune in the Delta undulator parameter K , a large angular separation between linear light produced prior to the Delta and circular light produced in the Delta was observed. This result is non-intuitive because, as seen in Figure 1, the microbunches don't realign themselves in the direction of propagation.

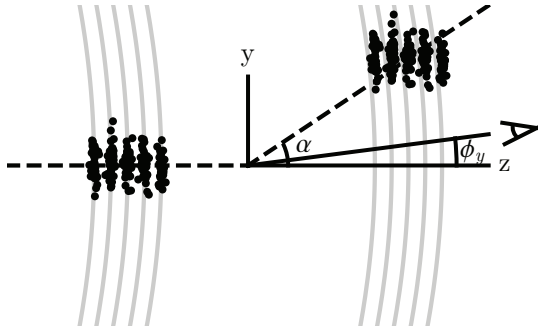


Figure 1: Microbunched electrons traveling left to right (black) are kicked by an angle $\alpha \ll 1$ in the y direction. The microbunches drift relative to the extant electric field (gray). An observer examines the far-field power at an angle ϕ_y .

Here the coherent radiation from a kicked beam is analyzed from a classical synchrotron radiation perspective. The motion of an electron in a diffracting electric field is also investigated.

COHERENT EMISSION FROM ANGLED MICROBUNCHES

The electric field in the paraxial approximation from a single electron traveling on axis and with no transverse velocity in an undulator of length L_u is [2]

$$\mathcal{E}_{\nu,j}^0(\phi, z = L_u) \propto e^{i\omega t_j} \int_0^{L_u} e^{ikz'\phi^2/2} e^{i(\nu-1)k_u z'} dz', \quad (1)$$

* jmacart@slac.stanford.edu

where $\mathcal{E}_{\nu}^0(\phi, z)$ is the field at an angle ϕ and wavenumber $k = \omega/c = \nu k_1$, t_j is the electron arrival time at $z = 0$, and k_1 is the wavenumber resonant to an undulator of period $\lambda_u = 2\pi/k_u$. The frequency of interest is detuned by an amount $\Delta\nu = \nu - 1 = (k - k_1)/k_1$ from the undulator resonant frequency.

The electric field from an electron with position \mathbf{x}_j , transverse velocity $d\mathbf{x}_j/dz = \mathbf{x}'_j$, and energy deviation from resonance $\eta_j = (\gamma - \gamma_r)/\gamma_r$ is [2]

$$\mathcal{E}_{\nu,j}(\phi, L_u) = e^{-ik\phi \cdot \mathbf{x}_j} \mathcal{E}_{\nu-2\eta_j,j}^0(\phi - \mathbf{x}'_j, L_u). \quad (2)$$

In order to calculate the power from the kicked beam shown in Figure 1, we sum and square the contributions from all N_e electrons,

$$P(\phi, L_u) = \sum_j^{N_e} |\mathcal{E}_{\nu,j}|^2 + \sum_j^{N_e} \sum_{k \neq j}^{N_e} \mathcal{E}_{\nu,j} \mathcal{E}_{\nu,k}^*. \quad (3)$$

The first sum is inconsequential for a bunched beam, while the double sum is typically converted into a double integral over the electron probability distribution, $f(\mathbf{x}_j, \mathbf{x}'_j, \eta_j, t_j)$.

For simplicity we assume that all variables are independent and therefore f is separable. The expression for the power takes a simple form when the beam has no spread in energy ($\eta_j = 0$), and no spread in angle ($\mathbf{x}'_j = 0$). These assumptions eliminate the emittance effects discussed in Ref [3], but other effects become more apparent. To match Figure 1, we set $\mathbf{x}'_j = (0, \alpha)$. The explicit form of the longitudinal distribution $f(t_j)$ is not important for this calculation, so we set

$$\int e^{i\omega t} f(t) dt = b. \quad (4)$$

After integrating over \mathbf{x} and t , the power is seen to be

$$P(\phi_x, \phi_y) \propto |b|^2 |\tilde{f}(\phi_x, \phi_y)|^2 \times \text{sinc}^2 \left[\pi N_u \left(\Delta\nu + \gamma_z^2 \phi_x^2 + \gamma_z^2 (\phi_y - \alpha)^2 \right) \right], \quad (5)$$

where

$$\tilde{f}(\phi_x, \phi_y) = \int d\mathbf{x} f(x, y) e^{ik\phi \cdot \mathbf{x}} \quad (6)$$

is the spatial transform of the transverse distribution, $N_u = L_u/\lambda_u$ is the number of oscillations in the wiggler, and $\gamma_z^2 = \gamma^2/(1 + K^2)$. Expressions similar to Equation 5 are derived elsewhere [3–5]. If \mathbf{x} is normally distributed around zero with rms spread σ ,

$$P(\phi_x, \phi_y) \propto |b|^2 e^{-k^2 \sigma^2 (\phi_x^2 + \phi_y^2)} \times \text{sinc}^2 \left[\pi N_u \left(\Delta\nu + \gamma_z^2 \phi_x^2 + \gamma_z^2 (\phi_y - \alpha)^2 \right) \right], \quad (7)$$

HELICAL UNDULATORS FOR COHERENT ELECTRON COOLING SYSTEM*

P. Pinayev[†], Y. Jing, R. Kellerman, V.L. Litvinenko, J. Skaritka, G. Wang,
 BNL, Upton, NY 11973, U.S.A.
 I. Ilyin, Yu. Kolokolnikov, S. Shadrin, V. Shadrin, P. Vobly, V. Zuev,
 Budker INP, Novosibirsk, Russia

Abstract

In this paper, we present the description and results of the magnetic measurements and tuning of helical undulators for the Coherent electron Cooling system (CeC). The FEL section of the CeC comprises three 2.5-m long undulators separated by 40-cm drift sections, where BPMs and phase-adjusting 3-pole wigglers are located. We present design, tuning techniques and achieved parameters of this system.

INTRODUCTION

Coherent electron cooling proof-of-principle (CeC PoP) experiment is conducted at relativistic hadron collider (RHIC) in the Brookhaven National Laboratory (USA) to test the basic physical principles underlying coherent electronic cooling [1]. The coherent electron cooling is based on the electrostatic interaction between electrons and hadrons, when density modulation of the electron bunch induced by the hadrons is amplified by a high-gain single pass free-electron laser (FEL) structure and is subsequently used to reduce the energy spread of the hadron beam [2].

The requirements on the wiggler parameters shown Table 1 are defined by the CeC PoP physics and are set to obtain high gain in the FEL. The high gain requirement contributed to the choice of the helical undulator as well. The undulator have fixed gap which simplifies design, manufacturing and tuning.

The undulator gap is rather large to accommodate hadron beams circulating in RHIC. The hadron beams have vertical separation of 10 mm at the location of the FEL to prevent their collision. Therefore, we decided to make undulator vacuum chamber square and rotated by 45°. Although gap is fixed the undulator design should provide capability for opening for insertion the vacuum chambers.

Table 1: Undulator Specifications

Parameter	Value
Wiggler parameter, a_w	0.5 +0.05/-0.1
Undulator gap	32 mm
Period	40±1 mm
RMS Phase Error	< 1° (3° peak-to-peak)
1 st field integral	< 30 Gs·cm
2 nd field integral	< 300 Gs·cm ²

* Work supported by the US Department of Energy under contract No. DE-SC0012704.

[†] pinayev@bnl.gov

DESIGN AND MANUFACTURING

The undulator body was made from the aluminum alloy, which has sufficient stiffness and no magnetic properties. Its magnetic structure is pure permanent magnet [3]. A design allows for the correction of the magnetic field at any point of the undulator.

The magnetic structure of the undulator comprises of two types of magnets. The first one has longitudinal magnetization, and the second type has transverse magnetization. Since a magnet with longitudinal magnetization has zero first integral, the error correction can be performed only by a magnet with transverse magnetization. The size and configuration of magnets with transverse magnetization is chosen such that a magnetic force of 10 kg pushes them out of the groove and presses the magnet to adjusting screws, and magnets with longitudinal magnetization are pushed back against the cassette slot with a force of 6 kg (see Fig. 1).

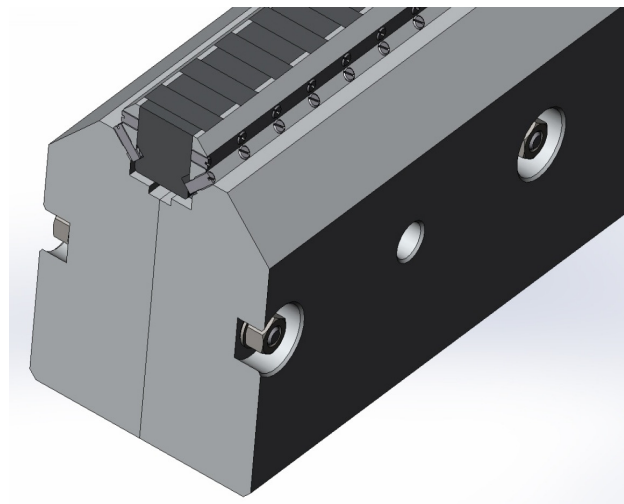


Figure 1: Cassette design. Cassette comprises two precisely machined halves bolted together. The magnets are inserted after cassette assembly and are hold in place with adjusting and fixing screws made of the stainless steel.

At the entrance to the undulator has such a distribution of the magnetic field that the electron beam, when entering the regular structure of the undulator, begins to perform symmetrical oscillations with respect to the longitudinal axis of the undulator. Figure 2 schematically shows the arrangement of magnets that satisfies this requirement as well as magnetic field and its integrals.

THE MAGNETIC FIELD INTEGRAL HYSTERESIS ON THE EUROPEAN XFEL GAP MOVABLE UNDULATOR SYSTEMS

F. Wolff-Fabris[†], Y. Li, J. Pflüger, European XFEL GmbH, 22869 Schenefeld, Germany

Abstract

Magnetic field hysteresis effects between opening and closing the gap of an undulator or phase shifter of the Undulator System of the European X-ray FEL may have an impact on the radiation properties. Using the moving wire technique the hysteresis between opening and closing the magnetic gap has been measured with high accuracy. Within the measurement accuracy undulator segments show negligible magnetic hysteresis between opening and closing the gap so that no effect on beam operation is to be expected. In contrast, about 2/3 of the phase shifters show a small hysteresis of the first field integrals of a few G.cm. In one direction of the gap movement they exceed field integral specifications. However the hysteresis is very reproducible. All phase shifters are magnetically tuned so that they fully satisfy magnetic specifications for beam operation when the gap is opened.

INTRODUCTION

The European XFEL (XFEL.EU) is designed to use three gap movable SASE Undulator Systems to produce FEL radiation tunable from 0.05 to 5.2 nm and pulse lengths of less than 100 fs [1,2]. The radiation wavelength can be tuned while selecting the e-beam energy between 8.5 to 17.5 GeV and / or changing the gap of the undulator systems. A total of 91 so called undulator cells are built and each is composed of a 5-metre long undulator segment equipped with two horizontal/vertical air coil correctors on both ends and a 1.1-metre long intersection unit containing a phase shifter (PS), a quadrupole mover with quadrupole magnet, the vacuum system and the beam position monitor. All undulator segments and phase shifters [3] for the XFEL.EU are built using NdFeB hard magnets. All devices were magnetically tuned to tight specifications in order to optimize the SASE effect (see Table 1).

The quality of the produced SASE radiation is essentially influenced by the global electron trajectory while traveling through the whole SASE System. At either end of an undulator segment there might occur entrance and exit kicks, which are related to imperfections in the magnetic structures. They are compensated by using the air coils correctors. Similarly, small field integrals in the phase shifters [4] are required to guarantee minimum FEL power loss and no beam wander in between undulator segments. While tuning the wavelength and changing the gaps of the permanent magnet undulator systems, the presence of hysteresis effects on the magnetic field integrals while opening or closing the gaps may result in

uncorrected compensation for the end kicks or mismatch of the e-beam phase between undulator cells. As a consequence the global trajectory of the electron beam and the quality of the produced SASE radiation is deteriorated. These considerations gave the motivation to investigate and monitor the presence of hysteresis of magnetic field integrals on undulators and phase shifters during the serial production.

Table 1: XFEL.EU Magnetic Specifications

Undulators	SASE1-2	SASE3
# of Segments	35	21
K-parameter @10mm	≥ 3.9	≥ 8.0
End kicks B_y and B_z (T.mm)	$ \leq 0.15 $	$ \leq 0.15 $
RMS Phase jitter (degrees)	≤ 8	≤ 8
Phase shifters		
# of Phase Shifters		95
Magnetic Field at gap = 10.5 mm		≥ 1.26 T
Phase Integral at gap = 10.5 mm		≥ 25000 T ² m ³
First Field Integrals (T.mm or 10 ³ G.cm)	Gap (mm)	\pm Tolerance
	16	± 0.004
	15	± 0.007
	14	± 0.009
	13	± 0.012
	12	± 0.014
	11	± 0.017
	10.5	± 0.018

EXPERIMENTAL METHODS AND FIELD INTEGRAL PROPERTIES

Direct field integral measurement techniques provide much higher accuracy [5–7] than Hall sensor measurements for the evaluation of total first and second field integral properties. The stretched wire (SW) method [5] was chosen and two dedicated moving wire (MW) systems [8] were built. The first, so-called “short MW”, is designed to measure first field integrals in short devices such as phase shifters or air coils with sub-G.cm accuracy. The “long MW” system is focused to measure both first and second field integrals of the 5-metre long undulator segments and to determine the end kicks and their respective compensations. In both systems the first and second

[†] f.wolff-fabris@xfel.eu

TAPERED FLYING RADIOFREQUENCY UNDULATOR*

S. V. Kuzikov^{†,2}, A. V. Saviolov, A. A. Vikharev

Institute of Applied Physics, Russian Academy of Sciences, Nizhny Novgorod, Russia

S. Antipov, A. Liu, Euclid Techlabs LLC, Bolingbrook, IL, USA

²Euclid Techlabs LLC, Bolingbrook, IL, USA

Abstract

We propose an efficient XFEL consisting of sequential RF undulator sections using: 1) tapered flying RF undulators, 2) short pulse, high peak-power RF and 3) driving undulator sections by spent electron beam. In a flying RF undulator, an electron bunch propagates through a high-power, nanosecond, co-propagating RF pulse. Helical waveguide corrugation supports a space harmonic with a negative propagation constant, providing a large Doppler up-shift. The undulator tapering technique improves FEL efficiency by 1-2 orders of magnitude in comparison with other facilities by decreasing the undulator period so that particles are trapped in the combined field of the incident x-ray and undulator field. We develop a so-called non-resonant trapping regime not requiring phase locking for feeding RF sources. Simulations show that by decreasing the corrugation periodicity one can vary an equivalent undulator period by 15%. The spent electron beam can be used to produce wakefields that will drive the RF undulator sections for interaction with the following beam. We have already manufactured and tested the 30-GHz simplified version of the 50-cm long undulator section for cold measurements and currently start low-power test of the tapered prototype.

FLYING-RF UNDULATOR

The RF undulator based on a travelling wave benefits from a Doppler up-shift when the electron beam interacts with oncoming microwaves. In [1] an RF pulse co-propagating (with the electron beam) was proposed where a benefit of the Doppler up-shift of Compton scattering is not lost due to the mode having strong -1st spatial harmonic transverse fields at axis of a helical corrugated waveguide (Figure 1). In this “flying” undulator the effective interaction length L_{eff} of a pulse with length τ and group velocity v_{gr} is proportional to $(1-v_{\text{gr}}/c)^{-1}$. For a large group velocity L_{eff} can be much larger than the pulse length.

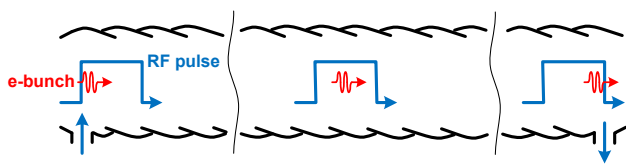


Figure 1: Flying RF undulator geometry (helical corrugation) and interaction timing structure.

*This work was supported by DoE Small Business Innovative Research Phase I Grant #DE-SC0017145.

[†]sergeykuzikov@gmail.com

In [1-2], a 30 GHz, 10 ns, 1 GW relativistic backward wave oscillator powers a 10-m long RF undulator with effective undulator strength $K = 0.3$ and undulator period $\lambda_u \approx 5$ mm. There are high power Ka-band BWO's which are good candidates for powering of the proposed flying undulator [3-4].

Figure 2 shows the dispersion characteristic of the operating mode of the TE_{11} - TM_{01} - TM_{11} RF undulator for the following geometrical parameters: $R_0 = 6.1$ mm, periodicity $D = 6$ mm and corrugation depth $a = 0.3$ mm (red solid curve). The dashed curve is the dispersion characteristic of the same mode in the waveguide with smaller corrugation period, 5.4 mm. Therefore, a tapered undulator can be built near 34 GHz using adiabatic variation of corrugation period so that the effective undulator period change is as high as 10%.

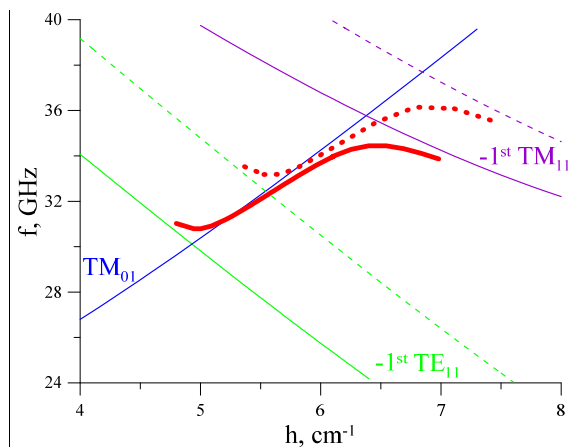


Figure 2: Dispersion of the operating mode (red solid curve) of the helical undulator with period of corrugation 6 mm and dispersion of this mode (red dashed curve) of the undulator with period of corrugation 5.4 mm.

HIGH-EFFICIENCY, TAPERED FLYING-RF UNDULATOR

For a high efficiency free electron laser we consider a string of tapered flying undulators (Figure 3). Each RF undulator section is assumed to be a helical corrugated structure with periodicity and corrugation depth changing as a function of z (coordinate along electron beam propagation).

EFFECT OF BEAM TRANSVERSE ANGLE DEFLECTION IN TGU ON FEL POWER

G. Zhou^{1,2,3†}, J. Wu^{1‡}, J. Yi², J. Wang²,

¹SLAC National Accelerator Laboratory, Menlo Park, California, U.S.A

²Institute of High Energy Physics, Chinese Academy of Science, Beijing, China

³University of Chinese Academy of Science, Beijing, China

Abstract

Recent study shows that electron beams with constant dispersion together with the transverse-gradient undulator (TGU) can reduce the sensitivity to energy spread for free-electron laser (FEL). By inducing dispersion function, electrons with different energy are placed at different positions corresponding to proper magnetic fields. Thus, FEL resonant condition can be kept for electrons with different energy. In this paper, we mainly studied: 1. The effects of electron beam angle deflection at the entrance of the TGU on the radiation power. 2. The utility of a kicker to introduce an angle deflection of electron beam to improve the FEL radiation power.

INTRODUCTION

Free-electron lasers (FELs) greatly benefit fundamental research in physics, chemistry, materials science, biology, and medicine by producing intense tunable radiation ranging from the infrared to hard x-ray region [1]. However, the FEL facilities are usually large and costly. Efforts have been made to develop compact FELs with similar radiation properties but smaller size. One optional way is to use laser-plasma accelerators (LPAs) to drive a high-gain FEL instead of conventional linear accelerator (LINAC) [2].

Compared to traditional LINAC, LPAs have much higher accelerating field gradient, smaller size and less cost but larger electron beam energy spread. At present, LPA can produce high energy (~ 1 GeV), high peak current (~ 10 kA), and low emittance ($\sim 0.1 \mu\text{m}$) electron beam with a relatively large energy spread about 1% experimentally [3, 4]. Such a relatively large energy spread, compared to conventional LINAC, terribly interferes the FEL gain process, which hinders LPAs from driving a high-gain FEL, which can be understood from the FEL resonance condition,

$$\lambda_r = \frac{1 + K_0^2 / 2}{2\gamma^2} \lambda_u, \quad (1)$$

where $K_0=0.934\lambda_u[\text{cm}]B[\text{T}]$, λ_u is the undulator period, B is the peak field of the undulator, γ is the electron beam energy in unit of the rest energy. Energy spread would lead to a spread of the above equation, leading to a weak

radiation power adverse to diffraction imaging experiments [5]. To overcome the impediment caused by electron beam energy spread in the FEL gain process, approaches, such as transverse gradient undulator (TGU) [6] and decompression [7], have been proposed and studied in detail. Recent study on TGU for high-gain FEL driven by LPAs points out that electron beam with a proper dispersion cooperating with TGU would increase the output radiation power significantly, about two orders, more effective than decompression [2].

TGU was proposed to reduce the sensitivity to the electron beam energy spread [2, 6]. By canting the magnetic poles, a linear transverse dependence of undulator field can be generated, like

$$\frac{\Delta K}{K} = \alpha x, \quad (2)$$

where α is the transverse gradient of the undulator. For an electron beam dispersed horizontally according to its energy, we get $x=\eta_0\delta$, where η_0 is the electron beam dispersion. Properly choosing the dispersion

$$\eta_0 = \frac{2 + K_0^2}{\alpha K_0^2}, \quad (3)$$

and keeping it constant along the TGU, the spread in electron beam's energy would be compensated. Note that, in this paper, we only consider the electron beam dispersed in x direction.

In this paper, we study the effect of beam transverse angle deflection on radiation power. We first analyse the case that the electron beam has an angle deflection at the entrance of TGU. Numerical simulation scan has been done to further quantitatively study the power decrease caused by angle deflection. Then, we study the case that the angle deflection induced at proper position in TGU. By comparing this case with linear tapered undulator, we find that it is possible to make use of angle deflection to improve the radiation power simply with an additional kicker. Multi-dimension optimization has been done and we find that the radiation power improves significantly. Simulations are done based on GENESIS, a 3D FEL simulation software, presenting reliable FEL process, proved by experiments [8].

* The work was supported by the US Department of Energy (DOE) under contract DE-AC02-76SF00515 and the US DOE Office of Science Early career Research Program grant FWP-2013-SLAC-100164

†gzhou@SLAC.Stanford.EDU

‡jhwu@SLAC.Stanford.EDU

DESIGN OF A COMPACT HYBRID UNDULATOR FOR THE THz RADIATION FACILITY OF DELHI LIGHT SOURCE (DLS)

S. Tripathi[†], S. Ghosh, R. K. Bhandari, D. Kanjilal,
 Inter-University Accelerator Centre (IUAC), New Delhi, India
 M. Tischer, Deutsches Elektronen-Synchrotron (DESY), Hamburg, Germany
 U. Lehnert, Helmholtz Zentrum Dresden Rossendorf (HZDR), Dresden, Germany

Abstract

A compact Free Electron Laser (FEL) facility to produce coherent THz radiation is in the development stage at Inter-University Accelerator Centre (IUAC), New Delhi, India [1-3]. The facility is named the Delhi Light Source (DLS). It is planned to produce an 8-MeV electron beam from a photo-cathode RF gun, and the electron beam will be injected into a compact undulator to generate the radiation. To produce THz radiation in the range of 0.15 to 3.0 THz, the electron beam energy and the undulator gap will be varied from 4 to 8 MeV and 20 to 45 mm, respectively. The variable-gap undulator of 1.5-m length will consist of NdFeB magnets with vanadium permendur poles. The magnet design and dimensions are optimised by using code 3D RADIA [4]. The detailed design of the compact hybrid undulator is presented in this paper.

INTRODUCTION

The compact light source project at IUAC named as Delhi Light Source (DLS) is in the developmental stage [2]. In the first phase (Phase I) of the DLS, a normal conducting (NC) photocathode electron gun will be used to generate the pre-bunched electron beam which will be injected in to a compact undulator magnet to produce THz radiation. The layout of the facility is shown in Figure 1. Permanent magnet technology, both pure permanent magnet and hybrid design, is most common for undulators of several-cm period length, while electromagnetic devices are usually built for longer period length. For DLS, we decided to go for a hybrid permanent magnet design as it will provide the biggest magnetic field. It is, however, a little more demanding in terms of field tuning than a pure permanent magnet structure due to the nonlinear behaviour of the iron poles.

THE 50 MM HYBRID UNDULATOR

An undulator is a spatially periodic magnetic structure and can be explained as pack of dipole magnets making alternating direction of magnetic fields. The magnetic field in a planar undulator is of the form $B_0 \sin(2\pi y/\lambda_u)$, where λ_u is the period length of the undulator.

When an electron passes through such magnetic fields, it will undergo a sinusoidal path with a certain period length and release synchrotron radiation as the electron

changes its direction. This radiation has high intensity and the radiation concentrates into a narrow band spectrum at the fundamental wavelength of

$$\lambda = \frac{\lambda_u}{2\gamma^2} \left(1 + \frac{K^2}{2} + \gamma^2 \theta^2 \right),$$

where λ_u is the period length of the undulator, γ is the Lorentz factor, and θ is the observation angle. The undulator parameter K , representing the undulator strength, can be written as $K = 0.934 \times B_0 [T] \times \lambda_u [cm]$, where B_0 is magnetic field at the undulator mid-plane.

The undulator for the Delhi Light Source (U50-DLS) has a period length of 50 mm in an antisymmetric configuration and optimised using the code RADIA. The undulator has magnet block of 80 mm wide, 55-mm high and 19-mm thick with 5 mm \times 5 mm square cuts at the corners for clamping the block with the holders. The vanadium permendur poles are 60-mm wide, 45-mm high and 6-mm thick. The end sections are designed and optimised with the configuration of 1/4 : 3/4 : 1 in terms of end pole strength [5].

A full five-period model undulator is shown in Figure 2. The end section consists of two magnet blocks and two end poles separated by air spaces. The inner 2nd last end magnet block has the same shape as the full-size blocks but the thickness is reduced to 75% of the thickness of the full-size blocks while the last end magnet has 25% of thickness as compared to regular magnet block. There is an air space between the second last magnet block and the second last end pole as well as between last magnet & last pole. The shape of both end poles is the same as for the full-size poles. In Table 1, the specifications of U50-DLS are summarised.

Table 1: Specification of U50-DLS Undulator

Technology	Hybrid planar, anti-symmetric
Magnet	Permanent NdFeB magnet ($B_r = 1.21T$)
Pole	Vanadium permendur
Magnetic gap	20 - 45 (mm)
Period length	50 mm
No of Periods	28 (full)
Magnetic field	0.62 - 0.11 (T)
Undulator parameter (K)	2.89 - 0.61
Device length	~1.5 m

[†] stri_29sep@yahoo.co.in

CHARACTERIZING SUB-FEMTOSECOND X-RAY PULSES FROM THE LINAC COHERENT LIGHT SOURCE

S. Li*, R. Coffee, K. Hegazy, Z. Huang, A. Natan¹, T. Osipov, D. Ray, J. Cryan¹, and A. Marinelli,
 SLAC National Laboratory, Menlo Park, United States

¹also at Stanford PULSE Institute, Menlo Park, United States

Z. Guo, Stanford University, Stanford, United States

Abstract

The development of sub-femtosecond x-ray capabilities at the Linac Coherent Light Source requires the implementation of time-domain diagnostics with attosecond (as) time resolution. Photoelectrons created by attosecond duration x-ray pulses in the presence of a strong-laser field are known to suffer an energy spread which depends on the relative phase of the strong-laser field at the time of ionization. This phenomenon can be exploited to measure the duration of these ultrashort x-ray pulses. We present an implementation which employs a circularly polarized infrared laser pulse and novel velocity map imaging design which maps the phase dependent momentum of the photoelectron onto a 2-D detector. In this paper, we present the novel co-linear VMI design, simulation of the photoelectron momentum distribution, and the reconstruction algorithm.

INTRODUCTION

Electron motion in atoms and molecules is the essential key to understanding the earliest processes involved in chemical changes. Electrons move across a molecular bond in 0.1 to 1 femtosecond (fs), a time scale of which direct measurement was impossible until recently when high harmonic generation [1, 2] became a widely used tool to synthesize light pulse in the extreme ultra-violet regime with sub-femtosecond duration. Extending the photon wavelength to the soft x-ray regime, the enhanced self-amplified spontaneous emission (eSASE) from x-ray free electron lasers enables the production of high intensity attosecond pulses [3]. The method of eSASE is currently being implemented experimentally at the linac coherent light source (LCLS) [4]. The electron bunch goes through an emittance spoiler which destroys the bunch except for a femtosecond duration beam core. The unspoiled core then interacts with an optical laser which imprints energy modulation on to the beam. Going through a dispersive section, the energy modulation turns into a single current spike with sub-femtosecond duration. The current spike goes through the undulator which emits coherent attosecond x-ray pulses.

Therefore, in order to measure the temporal profiles of sub-femtosecond x-ray pulses we employ a variant of the well known “attosecond streak camera” technique [5]. Our variation, which is closely related to the “atto-clock” technique [6], exploits the correlation between optical-cycle phase and streaking direction in a circularly polarized laser pulse. The

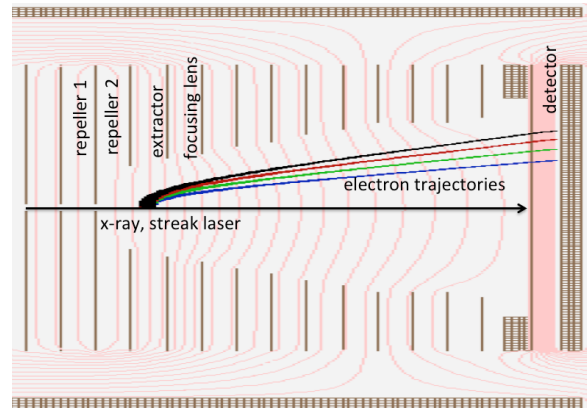


Figure 1: Side view of the cVMI design, with the linearly polarized x-ray pulse and circularly polarized streaking laser pulse propagating co-linearly. Picture taken in SIMION-8.0.

photoelectrons generated by the attosecond x-ray pulse interacting with gas molecules in the presence of a strong laser field experience an energy spread which depends on the duration of these ultrashort x-ray pulses. With a circularly polarized streaking laser, we provide a kick to the photoelectrons momentum distribution, and the angle and the strength of the momentum shift contains timing information of the x-ray pulse. Similar work has been done with longer x-ray pulses and a detector that measures a slice of the photoelectron momentum distribution [7]. With our novel co-linear velocity map imaging (cVMI), we will measure a 2-D projection of the 3-D momentum distribution of electrons generated by the linearly polarized attosecond x-ray pulse and the circularly polarized IR streaking pulse.

We develop an algorithm to reconstruct the x-ray pulse from the 2-D photoelectron momentum distribution. We use the von Neumann representation [8] to decompose the x-ray pulse into a set of basis functions. The fitting algorithm searches for the complex coefficients related to the basis functions by minimizing the difference between the measurement image and the fitted image. We demonstrate that we can successfully reconstruct attosecond x-ray pulses generated from free electron laser simulations.

VMI DESIGN

A VMI spectrometer has the advantages of high collection efficiency and high angular resolution. The critical requirement for a VMI to work is to image the charged particles with the same momentum onto the same position on the

* siqili@slac.stanford.edu

THERMAL STRESS ANALYSIS OF A THIN DIAMOND CRYSTAL UNDER REPEATED FREE ELECTRON LASER HEAT LOAD*

Bo Yang[†], Department of Mechanical and Aerospace Engineering,
 University of Texas at Arlington, Arlington, TX 76019, USA

Juhao Wu[‡], SLAC National Accelerator Laboratory, Menlo Park, California, 94025, USA

Abstract

Thin crystals are used as many important optical elements in XFELs, such as monochromators and spectrometers. To function properly, they must survive the ever-increasing heat load under repeated pulses. Here, we conduct a thermal stress analysis to examine the crystal lattice distortion due to the thermal load under various rep rates from 0.1 to 1 MHz. The thermal field is obtained by solving the transient heat transfer equations. The temperature-dependent material properties are used. It is shown that for pulse adsorption energy around tens of μJ over a spot size of $10\ \mu\text{m}$, the thermal response of diamond is sensitive to rep rate. The thermal strain components are very different in the in- and out-of-plane directions, due to different constraint conditions. It suggests complicated strain effects in the Bragg and Laue diffraction cases.

INTRODUCTION

XFELs generate high peak-power pulses with atomic and femtosecond scale resolution, impacting high-frontier scientific research [1,2]. Thin crystals are used in several important elements, such as monochromators [3,4], single-shot spectrometers [5–7], and other applications [8]. In pursuit of high-brightness XFELs, the power has been increased by orders of magnitude, so the thin crystals will experience much increased heat load. Thus, it is important to understand their photo-thermo-mechanical behaviours at higher temperature. Here, we perform a thermal stress analysis to elucidate the deformation field in a thin diamond crystal subjected to repeated heat load of XFEL pulses. The stress/strain field is obtained with a thermal field as a loading source by solving the static equilibrium equation. The thermal field is modelled by solving transient heat transfer equations and material properties, such as the thermal expansion, heat capacity [9] and thermal conductivity [10] valid up to temperatures $\sim 3000\ \text{K}$. The problem is solved with a finite volume method [11,12]. The case of a $40\text{-}\mu\text{m}$ thick plate with a Gaussian beam of FWHM of $20\ \mu\text{m}$ is studied with rep rates from 0.1 to 1 MHz. For a pulse depositing tens of μJ energy, the temperature that a next pulse sees ratchets up slowly at 0.1-0.2 MHz, but upsurges at higher rep rates. At 1 MHz, a runaway increase of temperature is found after a few pulses. It is because the heat relaxation rate through con-

duction decreases with temperature due to decreasing heat conductivity. The thermal stress/strain fields are analysed with a residual thermal field as a loading source. The strain components are different, implying complicated strain effects in Bragg and Laue diffractions.

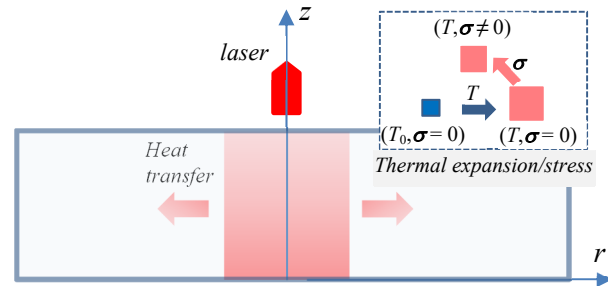


Figure 1: Schematics of instantaneous heating and subsequent heat transfer upon laser energy deposition in a thin crystal. The inset on the upper-right shows the thermal expansion and the stress to be built up due to constraint. The cylindrical coordinate with axisymmetry is used.

PROBLEM FORMULATION

Governing Equations

An XFEL impinging on a crystal would interact with the electrons and deposit a part of energy first onto the electrons [13]. Later the energy is transferred to the lattice raising the temperature. This process occurs at the pico-to-nano second scale. Then, the thermalized lattice expands emitting stress waves at the nano-to-tens-of-nano second scale at the sound speed [14]. The thermal diffusion will start, but not become effective until hundreds of nanoseconds. During this time, the stress waves would have bounced back and forth between boundaries for tens of times. If passive damping is instated, the inertia effect will soon become trivial. Thus, we assume that the specimen is in the mechanical equilibrium despite the transient heat transfer. The thermal field will significantly affect the deformation field, but the effect of deformation on thermal field is trivial. We analyse the processes of transient heat transfer and resulting thermal stress field. A cylindrical coordinate system (r, θ, z) is used with z -axis normal to the crystal surface as in Fig. 1. Only a pulse perpendicular to the crystal surface is studied.

The equilibrium equation without body forces is:

$$\nabla \cdot \boldsymbol{\sigma} = 0, \quad (1)$$

where $\boldsymbol{\sigma}$ is the stress tensor. Assuming the isotropic thermoelasticity, the constitutive law is given by [15]:

*Work supported by the US Department of Energy (DOE) under contract DE-AC02-76SF00515 and the US DOE Office of Science Early Career Research Program grant FWP-2013-SLAC-100164.

[†]boyang@uta.edu

[‡]jhwu@slac.stanford.edu

OPTICAL BEAM QUALITY ANALYSIS OF THE CLARA TEST FACILITY USING SECOND MOMENT ANALYSIS

H. M. Castañeda Cortés*, D. J. Dunning, M. D. Roper and N. L. Thompson
 ASTeC, Cockcroft Institute, STFC, Daresbury Laboratory, Warrington, United Kingdom

Abstract

We studied and characterised the FEL optical radiation in simulations of the CLARA FEL test facility under development at Daresbury Laboratory in the UK. In particular, we determined the optical beam quality coefficient, waist position and other source properties corresponding to different potential FEL operating modes via wavefront propagation in free space using OPC (Optical Propagation Code) and second moment analysis. We were able to find the operation mode and undulator design for which the optical beam has the optimum quality at highest brightness. Furthermore, we studied the way that different properties of the electron bunches (emittance, peak current, bunch length) affect the optical beam. We are now able to understand how the optical beam will propagate from the end of the undulator and through the photon transport system to the experimental stations. This knowledge is necessary for the correct design of the photon transport and diagnostic systems.

INTRODUCTION

The CLARA FEL test facility, currently under construction at Daresbury Laboratory [1], will have different operation modes in order to probe and test several advanced FEL concepts, such as high brightness SASE, mode-locking and afterburner schemes [2]. An aspect of fundamental interest in the design of CLARA is the assessment of the radiation properties obtained at the end of the FEL process. It is extremely important to optimise the design of the facility so that the optical beam quality does not degrade as the beam is transported through the optical beamline. This paper summarises the studies of optical beam quality carried out for the long bunch operation mode, assessing the different design parameters which could degrade or enhance it. The spatial source properties are calculated by using second moment analysis.

SECOND MOMENT ANALYSIS

The M^2 analysis states that the second moment of the optical beam profile follows a quadratic free-space propagation rule in terms of the propagating distance z as [3]

$$\sigma_i^2 = \sigma_{i0}^2 + \left(\frac{M_i^2 \lambda}{4\pi\sigma_{i0}} \right)^2 (z - z_0)^2, \quad \text{where } i = x, y. \quad (1)$$

The M^2 parameter compares the beam quality of the propagated beam to the free-space propagation of a TEM₀₀ Gaussian beam ($M_i^2 = 1$). The rms size at the beam waist is σ_{i0} and z_0 the waist position. M_i^2 , σ_{i0} and z_0 can be calculated

from fitting the evolution of the optical beam profile (defined as $\sigma_i^2(z) = C_2 z^2 + C_1 z + C_0$) to the measured values of second moments, [4],

$$M_i^2 = \frac{2\pi}{\lambda} \sqrt{4C_0 C_2 - C_1^2}, \quad (2)$$

$$z_0 = -\frac{C_1}{2C_2}, \quad \text{and} \quad (3)$$

$$\sigma_{i0} = \sqrt{C_0 - \frac{C_1^2}{4C_2}}. \quad (4)$$

The optical code OPC [5, 6] was used to perform the free-space propagation of the calculated radiation at the end of the undulator. Time-dependent FEL simulations were carried out in GENESIS 1.3 [7] to obtain the radiation field.

PRELIMINARY STUDY

The long bunch operation mode in CLARA is designed to demonstrate FEL schemes generating radiation pulses significantly shorter than the electron bunch length. It will have between 150 and 250 MeV beam energy, 250 pC bunch charge, $\sigma_t = 800$ fs, peak current of 125 A, 0.5 mm-mrad normalised emittance and 25 keV energy spread. Planar variable gap undulators will have a 2.5 cm period and maximum rms of the undulator parameter of 1.4, allowing resonant wavelengths between 100 and 400 nm. A comparison of steady state and time-dependent simulations in GENESIS 1.3 was done to have a rough estimate of the source properties and demonstrate the validity of time-dependent approach for beam quality calculations. Previous CLARA undulator values were used, as given in Table 2. The radiation wavelength defined for the simulations is set to be 266 nm (the shortest wavelength for single-shot temporal diagnostics).

Table 1: Comparison Between Optical Beam Parameters Obtained from Steady State and Time-Dependent Simulations.

Parameter	Steady State		Time-Dependent	
	x	y	x	y
M^2	3.8	3.6	3.6	3.5
z_0 (m)	-1.85	-1.93	-1.27	-1.27
σ_{z_0} (μm)	283	273	274	278

Second moment analysis was performed via the wavefront propagation code FOCUS (for steady state simulations) [8] and OPC (for time-dependent simulations). The obtained source properties for both scenarios (following Eqs. (2), (3), and (4)) are shown in Table 1. The M^2 parameters obtained

* hector.castaneda@stfc.ac.uk

A TWO-IN-ONE TYPE UNDULATOR*

D. Wang[†], H. Deng, Z. Jiang, Shanghai Institute of Applied Physics,
 Chinese Academy of Sciences, 239 Zhangheng Road, Shanghai 201204, China

Abstract

The high repetition-rate X-ray Free Electron Lasers based on superconducting radiofrequency technologies [1,2] have tremendous advantages in many aspects. Such a facility is able to serve many FEL photon beamlines simultaneously with each of which have large flexibilities in selecting wavelength, intensity, polarization, coherence and other properties through independent tuning of the undulator magnets. In reality a lot of spaces needed to accommodate many undulator lines could be a limiting factor of user capacity, especially for the high rep rate XFELs that tend to utilize the underground tunnel to host long superconducting accelerator machine with the relatively low acceleration gradient and for radiation safety considerations. In this paper we present a design of two-in-one type undulator for more efficiently using precious spaces in tunnels or similar buildings and open the possibilities for easier convene of different photon beams.

INTRODUCTION

The Shanghai Coherent Light Facility (SCLF) is a high repetition rate X-ray Free Electron Lasers based on superconducting radiofrequency technologies [3]. The superconducting electron accelerator and undulators as well as photon beamlines/endstations are all installed in underground tunnels with an overall length of more than 3 km. The electron beams are distributed in the switchyard shaft to different undulator lines. The current design assumes single tunnel for main accelerator and three tunnels for undulators and beamlines, all with an inner diameter of 5.9 m, as shown in Figure 1.

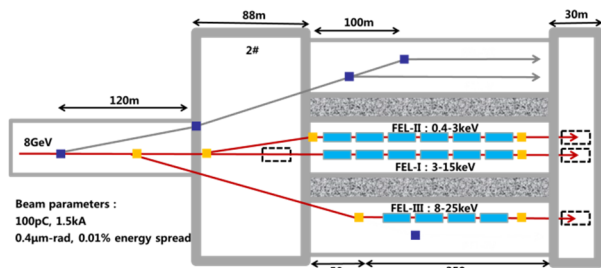


Figure 1: General layout of undulator lines of SCLF.

The dimension of cross section of tunnels is chosen to accommodate two conventional undulator lines and enough spaces for installations, illustrated in Figure 2.

The maximum number of FEL lines is mainly limited by the spaces of undulator tunnels. In the first phase of the project there are three undulator lines planned for

producing bright FEL beams in hard and soft X-ray regimes. The FEL-I and FEL-II will be located at the central tunnel in parallel using conventional out-vacuum undulator technology. The FEL-III is going to adopt the superconducting undulator concept for achieving stronger magnetic field strength with small undulator period hence the higher photon energies with relatively moderate electron beam energy. Currently SCLF is designed to cover the wide range of photon energy from soft to hard x-ray with 8-GeV electron beam and three undulator lines. In future it is crucial for this kind of facility to maximize its ultimate capabilities of providing photon beamlines for scientific users.

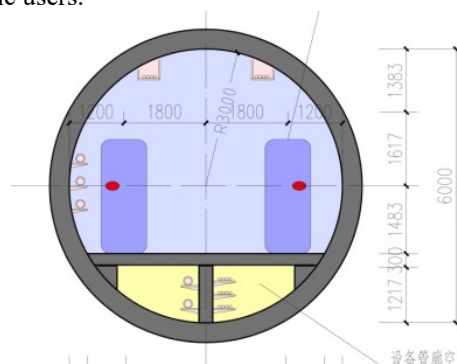


Figure 2: Cross section of undulator tunnel accommodating FEL-I and FEL-II lines.

TWO-IN-ONE UNDULATOR

A simple concept of two-in-one type of undulator was proposed in order to save the precious space in tunnels. Figures 3 and 4 illustrate the overall undulator layout.

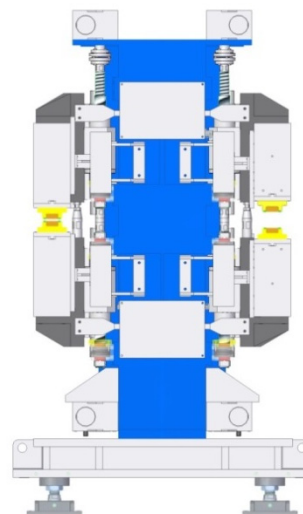


Figure 3: Concept of a two-in-one type of undulator.

[†]wangd@sinap.ac.cn

TUNABLE HIGH-GRADIENT QUADRUPOLES FOR A LASER-PLASMA ACCELERATION-BASED FEL*

A. Ghaith[†], F. Marteau, P. N'gotta, M. Valléau, J. Veteran, F. Blache, C. Kitegi, M. E. Couprie, Synchrotron SOLEIL, Gif-sur-Yvette, France
 C. Benabderrahmane, ESRF, Grenoble, France
 O. Cosson, F. Forest, P. Jivkov, J. L. Lancelot, SigmaPhi, Rue des Freres Montgolfier, Vannes, France

Abstract

The magnetic design and characterization of tunable high gradient permanent magnet based quadrupole, or so-called QUAPEVAs, are presented. To achieve a high gradient field with a compact structure, permanent magnets are chosen rather than usual electro-magnets due to their small aperture. The quadrupole structure consists of two superimposed quadrupoles capable of generating a gradient of 210 T/m. The first quadrupole is composed of permanent magnets in a Halbach configuration shaped as a ring which attains a constant gradient of 160 T/m, and the second is composed of four permanent magnet cylinders surrounding the ring and capable of rotating around their axis in order to achieve a gradient tunability of ± 50 T/m. Each tuning magnet is connected to a motor and is controlled independently, enabling the gradient to be tuned with a rather good magnetic center stability (20 μm and without any field asymmetry). Seven quadrupoles have been built with different magnetic lengths in order to fulfill the integrated gradient required. A set of QUAPEVA triplet are now in use, to focus a high divergent electron beam with large energy spread generated by a laser plasma acceleration source for a free electron laser application [1].

INTRODUCTION

Accelerator physics and technology have recently seen tremendous developments especially in the synchrotron radiation domain, which is actively investigating low emittance storage rings with multibend achromat optics for getting closer to the diffraction limit and providing a high degree of transverse coherence [2]. In addition, Laser Plasma Acceleration (LPA) can now generate a GeV beam within a very short accelerating distance, with high peak current of ~ 10 kA, but the high divergence (on the order of a few mrad) and large energy spread (a few percent) can present problems.

All these recent developments require high gradient quadrupoles that can not be provided by usual room temperature electro-magnet technology. To achieve a high gradient, one is more likely to choose either superconducting or permanent magnet [3] technologies. Permanent Magnets (PMs)

can be arranged in the so-called Halbach configuration [4], to provide a quadrupolar field. Interest in permanent magnet quadrupoles has been recently renewed because of their compactness and their capability of reaching high field gradient, alongside the absence of power supplies, letting them to be a solution for future sustainable green society.

DESIGN

The QUAPEVA is composed of two superimposed quadrupoles, one placed at the center following a Halbach configuration, surrounded by another that consists of four rotating cylindrical magnets to provide the gradient variability, illustrated in Fig. 1). Figure 1 also shows three particular configurations of the tuning magnets; (a) maximum gradient: tuning magnets easy axis towards the central magnetic poles, (b) intermediate gradient: the tuning magnets are in the reference position, *i.e.* their easy axis is perpendicular to the central magnetic poles, (c) minimum gradient: tuning magnets easy axis is away from the central magnetic poles. Table 1 shows the QUAPEVA parameters alongside the characteristics of the magnets and poles.

Table 1: QUAPEVA Parameters.

Parameters	Value	Unit
Gradient (G)	110 - 210	T/m
Remanent Field (B_r)	1.26	T
Coercivity (H_{cj})	1830	kA/m
Good-Field Region	4	mm
$\Delta G/G$	< 0.01	at 4 mm

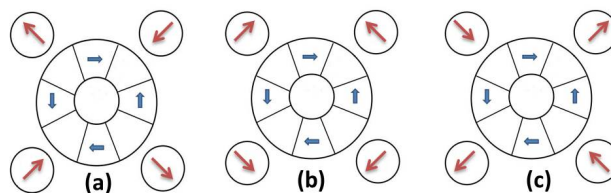


Figure 1: (a) maximum gradient, (b) intermediate gradient, (c) minimum gradient.

* Synchrotron SOLEIL

[†] amin.ghaith@synchrotron-soleil.fr

CRYOGENIC PERMANENT MAGNET UNDULATOR FOR AN FEL APPLICATION*

A. Ghaith[†], M. Valléau, F. Briquez, F. Marteau, M. E. Couprie, P. Bertheaud, O. Marcouillé,
 T. Andre, I. Andriyash, M. Labat, E. Roussel, M. Tilmont, K. Tavakoli, N. Bechu,
 C. Herbeaux, M. Sebdaoui, Synchrotron SOLEIL, Gif-sur-Yvette, France

Abstract

Cryogenic Permanent Magnet Undulator (CMPU) is capable of achieving high brightness radiation at short wavelengths, by taking advantage of the permanent magnet's enhanced performance at low temperature. A CPMU of period 18 mm (U18) that has been built at Synchrotron SOLEIL is used for the COXINEL project to demonstrate Free Electron Laser (FEL) at 200 nm using a laser plasma acceleration source. Another undulator of period 15 mm (U15) is currently being built to replace U18 undulator for FEL demonstration at 40 nm. A new method is also introduced, using SRWE code, to compute the spectra of the large energy spread beam (few percent) taking into account the variation of the Twiss parameters for each energy slice. The construction of U18 undulator and the magnetic measurements needed for optimization, as well as the mechanical design of U15, are presented.

INTRODUCTION

Third generation synchrotron radiation has been used widely in different applications, due to the intense brightness produced ranging from infrared to x-rays. This intensity is generated by the use of a low emittance beam and an insertion device most commonly known as undulator. An undulator consists of periodic arrangements of dipole magnets generating a periodic sinusoidal magnetic field, and is capable of producing an intense and concentrated radiation in narrow energy bands as relativistic electrons are traversing it. The emitted radiation wavelength observed is expressed as $\lambda_R = (\lambda_u/2\gamma^2)[1 + K^2/2]$, where λ_u is the magnetic period, $K = 93.4\lambda_u[m]B[T]$ the deflection parameter, and B the peak field. Fourth generation sources, such as Free Electron Laser (FEL) based experiments, exceed the performance of previous sources by one or more orders of magnitude in important parameters such as brightness, coherence, and shortness of pulse duration. The future FEL based projects relies on the compactness of the machine. Hence, compact undulators are needed for such developments.

Permanent magnet undulators are able to function at room temperature and attain a fair magnetic field depending on the magnet material. Most pure permanent magnet undulators use the Halbach geometric design [1], and by replacing poles with the vertically magnetized magnets making it a hybrid type [2] and enhances its magnetic peak field. In order to achieve a more compact undulator with sufficient field, one has to decrease the size of magnets which will reduce

the peak field. So the idea was proposed at SPring-8 [3] to cool down the undulator to cryogenic temperature and enhancing the performance of the permanent magnets. The Cryogenic Permanent Magnet Undulator (CPMU) design is easily adapted to the in-vacuum undulator, achieving a high peak field with a shorter period length making it suitable for compact FEL based applications.

MAGNETIC AND MECHANICAL DESIGN

The prototypes design has been done using RADIA [4] as shown in Fig. 1. The magnets used are $Pr_2Fe_{14}B$ [5] and Vanadium Permendur poles, and their characteristics are presented in Table 1 for both CPMUs, period 18 mm (U18) and period 15 mm (U15).

Figure 2 shows the field computed for the two cryogenic undulators at both room and cryo temperature. The field is increased by ~12% from room temperature to cryo temperature. The minimum gaps reached by U15 and U18 are 3 mm and 5 mm respectively.

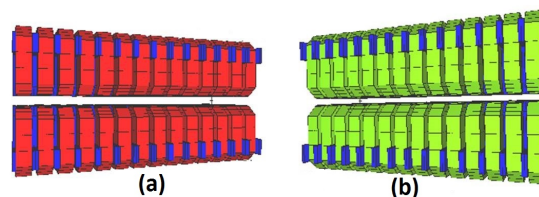


Figure 1: (a) prototype design of the undulator U18 and (b) of U15 with 7 periods, using RADIA code with IGOR Pro as front end.

Table 1: U18 prototype characteristics.

Parameters	Value	Unit
Magnet dimension (U18)	50 x 30 x 6.5	mm ³
Magnet dimension (U15)	50 x 30 x 5.5	mm ³
Pole dimension (U18)	33 x 26 x 2.5	mm ³
Pole dimension (U15)	33 x 26 x 2	mm ³
B_r @ RT	1.32	T
B_r @ CT	1.57	T

The mechanical design consists of a carriage with a metallic base where the frame is welded, two out-vacuum (external) girders fixed on the frame that can move vertically thanks to two series of sliders. The magnetic system components are fixed on two in-vacuum girders connected to the

* Synchrotron SOLEIL

[†] amin.ghaith@synchrotron-soleil.fr

LIE MAP FORMALISM FOR FEL SIMULATION*

Kilean Hwang[†], Ji Qiang, Lawrence Berkeley National Laboratory, Berkeley, USA

Abstract

Undulator averaging and non-averaging are in compromise between computational speed and reliability. It is hard to catch the advantages of the both methods simultaneously. In this report, we present a method that compromises the between the averaging and non-averaging methods through Lie map formalism.

INTRODUCTION

In a more general sense, the method of averaging can be viewed by an instance of the re-formulation of the equations of particle and field motion to a numerically or analytically simpler form. Performance of such methods are based on analytic capability of producing accurate but simple enough equations and corresponding solutions that can alternatively describe the original system. A simple averaging can overlook the coupling between the betatron and wiggling motion, nonlinear and high order field strength. This coupling can be important when the undulator fringe field at entrance is not well tapered so that the averaged closed orbit is offset by half of the undulator oscillation amplitude. On the other hand, if one can obtain re-formulated equations that can describe the original system to a good accuracy, then it can have both advantages of averaging and non-averaging method. Such a robust set of equations can be derived using perturbative Lie map. Since the map over undulator period integrate out the fast undulator oscillation, the numerical performance can be as good as the method of averaging.

OVERVIEW

To start with, we briefly review the perturbative Lie map method.

Lie Map Perturbation

Let the Hamiltonian be decomposed with slow S , fast F and radiation field potential V , i.e. $H(z) = S(z) + F(z) + V(z)$ where z is the longitudinal coordinate used as a time variable. Then, the map of the Hamiltonian system can be written by [1]

$$\mathcal{H}(z|z_0) = \mathcal{V}(z|z_0)\mathcal{F}(z|z_0)\mathcal{S}(z|z_0), \quad (1)$$

where z_0 is the starting location of the integrator, $\mathcal{S} \equiv e^{\mathcal{G}_S}$, $\mathcal{F} \equiv e^{\mathcal{G}_F}$, $\mathcal{V} \equiv e^{\mathcal{G}_V}$ are slow, fast, field map respectively,

and the generators of each map are

$$\begin{aligned} \mathcal{G}_S &= -\int_{z_0}^z dz : S : + \frac{1}{2} \int_{z_0}^z dz_1 \int_{z_0}^{z_1} dz_2 :: S_2 : S_1 : + \dots \\ \mathcal{G}_F &= -\int_{z_0}^z dz : F^{\text{int}} : + \frac{1}{2} \int_{z_0}^z dz_1 \int_{z_0}^{z_1} dz_2 :: F_2^{\text{int}} : F_1^{\text{int}} : + \dots \\ \mathcal{G}_V &= -\int_{z_0}^z dz : V^{\text{int}} : + \frac{1}{2} \int_{z_0}^z dz_1 \int_{z_0}^{z_1} dz_2 :: V_2^{\text{int}} : V_1^{\text{int}} : + \dots, \end{aligned} \quad (2)$$

where the interaction picture potentials are

$$\begin{aligned} F_i^{\text{int}} &\equiv \mathcal{S}(z_i|z_0)F(z_i) \\ V_i^{\text{int}} &\equiv \mathcal{F}(z_i|z_0)\mathcal{S}(z_i|z_0)V(z_i). \end{aligned} \quad (3)$$

Field Model

In order to calculate the field map \mathcal{G}_V for particle motion, one need to know the force field priori. Therefore, the method we are presenting involves field modeling and requires the field solver to solve for the model field. This is a generalization of the spectral method. Since, we expect narrow-band and slowly varying envelope radiation, we model the radiation vector potential normalized by e/mc as

$$a_r \equiv \Re \sum_{h=1}^5 [\mathbb{K}_h + (z - z_0) \partial_z \mathbb{K}_h] e^{ih(\theta - k_u z)}, \quad (4)$$

where $\theta = k_s(z - ct) + k_u z$ is the ponderomotive phase of radiation k_s and undulator k_u wave numbers. $\mathbb{K}_h(x, y, \theta)$ is the model field envelope at each integration step. Note that dependence of field amplitude on z is removed while the longitudinal gradient $\partial_z \mathbb{K}_h$ is included based on slowly varying envelope approximation. The gradient term and can be important for fast growth mode when the pre-unched beam is seeded [3], and thus can be beneficial for both averaging and non-averaging method. The order of magnitude of the normalized field strength is roughly about $\mathbb{K}_1 \sim 10^{-6}$ at saturation estimated using $P_{\text{rad}} \sim 1.6\rho P_{\text{beam}}$ and LCLS parameters [2].

Effective Hamiltonian

In general, the solution of the perturbed map \mathcal{V} is not available, so it is hard to build a high order map out of the perturbed Lie map. On the other hand, an effective Hamiltonian can be obtained using Baker-Campbell-Hausdorff (BCH) formula.

$$\begin{aligned} H_{\text{eff}} &= -\frac{1}{L} (\mathcal{G}_S + \mathcal{G}_F + \mathcal{G}_V) \\ &\quad -\frac{1}{2L} (: \mathcal{G}_S : \mathcal{G}_F + : \mathcal{G}_S : \mathcal{G}_V + : \mathcal{G}_F : \mathcal{G}_V) + \dots \end{aligned} \quad (5)$$

Since the fast oscillating motion is already integrated out, re-concatenation of the perturbed Lie map through BCH formula can be well truncated within few orders.

* Work supported by the Director of the Office of Science of the US Department of Energy under Contract no. DEAC02-05CH11231

[†] kilean@lbl.gov

SIMULATIONS OF THE DEPENDENCE OF HARMONIC RADIATION ON UNDULATOR PARAMETERS*

G. Penn[†], LBNL, Berkeley, CA 94720, USA

Abstract

The flux and bandwidth of radiation produced at harmonics of the fundamental are very sensitive to the undulator parameter, and thus the beam energy or undulator period. We look at high-energy XFELs with parameters relevant to the MaRIE FEL design. Both SASE and seeded FELs are considered.

INTRODUCTION

One method to extend the photon energy reach of free electron lasers (FELs) is to radiate at harmonics of the resonant wavelength. There are two main versions of this technique. Nonlinear harmonic gain [1, 2] occurs as the fundamental radiation enters saturation; the microbunching becomes sufficiently strong to include a significant component at harmonics of the fundamental. This is most prominent for planar FELs, which can couple to the microbunching at odd harmonics to produce strong, forward-directed radiation. There is also linear harmonic gain, where radiation at wavelengths shorter than resonance self-amplifies. In this case the amplification process almost requires a planar undulator and use of an odd harmonic. Strong radiation at the fundamental wavelength tends to interfere with linear harmonic gain, but there are methods to overcome this [3] and, for an FEL seeded at a harmonic, that harmonic can reach saturation well before the fundamental.

Linear harmonic gain can reach much higher power than nonlinear harmonic gain. However, it imposes greater demands on the electron beam and other systems. This paper will mostly focus on nonlinear harmonics.

IMPORTANCE OF THE UNDULATOR PARAMETER

For nonlinear harmonic generation in a planar undulator, ignoring transverse effects such as the angular and energy spread of the electrons, the ratio of the third harmonic radiation to the fundamental near saturation has been calculated as [2]:

$$\frac{P_3}{P_1} \approx 0.094 \frac{J_1(3\xi) - J_2(3\xi)}{J_0(\xi) - J_1(\xi)}, \quad (1)$$

where the J_i are Bessel functions, $\xi \equiv 0.5 a_u^2 / (1 + a_u^2)$, and a_u is the rms undulator parameter. For undulator parameters close to unity, there is a strong improvement in this ratio as a_u is increased. As the undulator parameters becomes $\gg 1$, the ideal ratio saturates close to 2.1%. The power of the fundamental also improves with the undulator parameter,

* This work was supported by the Director, Office of Science, Office of Basic Energy Sciences, U.S. Department of Energy under Contract No. DE-AC02-05CH11231.

[†] gepenn@lbl.gov

but the term defined above varies more rapidly. The scaling with undulator parameter is shown in Fig. 1.

This effect is multiplied by the “3D” effects corresponding to beam emittance and energy spread. The third harmonic can only tolerate roughly 1/3rd of the energy spread or emittance, and so it can be strongly suppressed by changes which only slightly affect the fundamental.

For undulators tuned to a fundamental photon energy of 14 keV, the undulator parameter $a_u \geq 2$, and the harmonic is not sensitive to small changes in the undulator parameter.

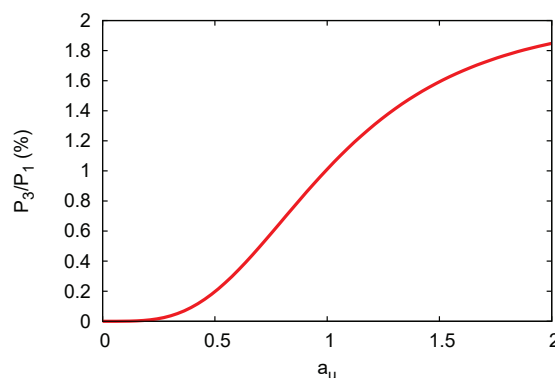


Figure 1: Scaling of the ratio of nonlinear third harmonic to fundamental radiation near saturation, for ideal beams.

BEAM PARAMETERS AND CONFIGURATION

The beamline parameters are modeled loosely after those of the MaRIE X-FEL [4] as summarized in Table 1. A self-seeding stage uses undulators tuned to 14 keV to produce not only strong SASE radiation at the fundamental but also a significant 3rd harmonic component. This harmonic component is then put through a monochromator. At this point, there can be a fresh-slice [5] or multi-bunch stage to allow for unperturbed electrons to interact with the narrow-bandwidth 40-keV radiation. This radiation is then amplified and can be used to produce third harmonic radiation in turn.

The undulator sections used for the final stage are taken to each be 3.6 m in length. Breaks in between sections are either 0.9 m or 1.26 m in length. Undulator periods in the range of 15 mm to 20 mm have been considered, corresponding to undulator parameters of 1.10 to 0.81. The corresponding ideal ratio P_3/P_1 ranges from 1.16% to 0.69%. Superconducting undulators with a 15-mm period are consistent with a beam pipe diameter of roughly 9 mm, if a large tuning range is not required. PPM undulators with an 18-mm period are consistent with a beam pipe diameter of roughly 5 mm. Advanced designs such as superconducting

PERIOD-AVERAGED SYMPLECTIC MAPS FOR THE FEL HAMILTONIAN*

S. D. Webb[†], RadiaSoft, LLC, Boulder, USA

Abstract

Conventional treatments of synchrotron radiation in electron beams treat the radiation as a non-Hamiltonian aspect to the beam dynamics. However, the radiation can be modeled with an electromagnetic Hamiltonian. We present a period-averaged treatment of the FEL problem which includes the Hamiltonian aspects of the coupled electron-radiation dynamics. This approach is then applied to two problems: a 3D split-operator symplectic integrator, and a 1D single-mode FEL treated using Hamiltonian perturbation theory.

SYMPLECTIC MAP TREATMENT

Symplectic maps are useful for computing invariants in Hamiltonian systems and deriving symplectic integration schemes (among others) in single- or few-particle systems. Recent work has highlighted their use for studying many-body systems and self-consistent electromagnetic algorithms. Maps can also be applied to the period-averaged free-electron laser problem, using the factored map formalism and a first order Magnus expansion.

We begin with the Lagrangian for a system of relativistic electrons in a mix of external and self-consistent electromagnetic fields [1–3]:

$$\mathcal{L} = \sum_j -mc^2 \sqrt{1 - \left(\frac{\dot{\mathbf{x}}_j}{c}\right)^2} - e\phi(\mathbf{x}_j) + \frac{e}{c} \dot{\mathbf{x}}_j \cdot \mathbf{A}(\mathbf{x}_j) + \frac{1}{8\pi} \int d\mathbf{x} \left(\frac{1}{c} \frac{\partial \mathbf{A}}{\partial t} - \nabla \phi \right)^2 - (\nabla \times \mathbf{A})^2. \quad (1)$$

It is convenient to use s , the longitudinal variable, as the independent variable. We can do this by noting that the action integral $\mathcal{A} = \int dt \mathcal{L}$, and that $dt = (dt/ds)ds$ is a valid transformation of the integral as long as $ds/dt \neq 0$. This allows us to change the independent variable to the s -dependent Lagrangian \mathcal{S} as

$$\mathcal{S} = \sum_j -mc^2 \sqrt{\left(\frac{1}{c} \frac{d\tau_j}{ds}\right)^2 - \left(\frac{(\mathbf{x}_\perp)_j'}{c}\right)^2} + \frac{e}{c} \tau_j' \phi(\mathbf{x}_j) + \frac{e}{c} (\mathbf{x}_j')_\perp \cdot \mathbf{A}_\perp(\mathbf{x}_j) + \frac{e}{c} A_s(\mathbf{x}_j) - \frac{1}{8\pi} \frac{1}{c} \int d\mathbf{x}_\perp d\tau \left(\frac{\partial \mathbf{A}}{\partial \tau} + \nabla \phi \right)^2 - (\nabla \times \mathbf{A})^2 \quad (2)$$

* Work supported by the United State Department of Energy, Office of Scientific Research, under SBIR contract number DE-SC0017161.

[†] swebb@radiasoft.net

where the prime denotes total differentiation with respect to s and we have defined $\tau = -ct$ for dimensional convenience, so all the generalized coordinates have the same units. The action integral remains unchanged.

The scalar potential comes purely from self-consistent source terms – there are no electrostatic elements in our beamline – and \mathbf{A} can be broken into external and self-consistent components. We need not worry about the dynamics of the external vector potentials. For simplicity, we can make the choice that $A_s^{(sc)} = 0$ (equivalent to the Weyl gauge $\phi = 0$ when we use t as the independent variable) and assume that $\phi = 0$ which neglects space charge effects. This leaves $\mathbf{A}_\perp = \mathbf{A}_\perp^{(ext.)} + \mathbf{A}_r$ and $A_s = A_s^{(ext.)}$, which captures the undulator fields and any external focusing elements like quadrupoles or dipoles, as well as the self-consistent radiation field.

We write the radiation field as

$$\mathbf{A}_r = \frac{mc}{e} \mathbf{e}_p \sum_\sigma u_\sigma e^{ik_\perp^{(\sigma)} \cdot \mathbf{x}_\perp + ik_0^{(\sigma)} \tau} + c.c. \quad (3)$$

for a fixed, generally complex, polarization vector $\mathbf{e}_p = p_x \hat{\mathbf{x}} + p_y \hat{\mathbf{y}}$ with unit norm $|p_x|^2 + |p_y|^2 = 1$, and a range of perpendicular k -vectors and τ -components. The individual $u_\sigma(s)$ give the complex amplitude of a given radiation mode as a function of s . This gives the Lagrangian in terms of the individual mode amplitudes for the radiation, the external fields, and the particles to be:

$$\mathcal{S} = \sum_j -mc \sqrt{(\tau_j')^2 - ((\mathbf{x}'_\perp)_j)^2} + \frac{e}{c} (\mathbf{x}'_\perp)_j \cdot (\mathbf{A}_\perp^{(ext.)}(\mathbf{x}_j) + \mathbf{A}_r) + \frac{e}{c} A_s(\mathbf{x}_j) - \frac{1}{8\pi} \frac{1}{c} \left(\frac{mc}{e}\right)^2 \sum_\sigma \left((k_0^{(\sigma)})^2 - |p_y k_x^{(\sigma)} - p_x k_y^{(\sigma)}|^2 \right) |u_\sigma|^2 - |u_\sigma'|^2 \quad (4)$$

which then gives the canonical momenta for the electrons as well as for the individual modes as:

$$p_\tau = \frac{mc\tau'}{\sqrt{\tau'^2 - 1 - (\mathbf{x}'_\perp)^2}}, \quad (5)$$

$$\mathbf{p}_\perp = \frac{mc\mathbf{x}'_\perp}{\sqrt{\tau'^2 - 1 - (\mathbf{x}'_\perp)^2}} - \frac{e}{c} (\mathbf{A}_\perp^{(ext.)}(\mathbf{x}_j) + \mathbf{A}_r)$$

and

$$\mathcal{P}_\sigma = -\frac{1}{4\pi c} \left(\frac{mc}{e}\right)^2 u_\sigma'^* \quad (6)$$

NON-STANDARD USE OF LASER HEATER FOR FEL CONTROL AND THZ GENERATION

E. Allaria[†], M. B. Danailov, S. Di Mitri, D. Gauthier, L. Giannessi, G. Penco, M. Veronese, P. Sigalotti, L. Badano, M. Trovo', S. Spampinati, A. Demidovich, E. Roussel¹, Elettra Sincrotrone Trieste S.C.p.A., 34149 Basovizza, Italy
¹now at SOLEIL, Paris, France

Abstract

The laser heater system is currently used at various FEL facilities for an accurate control of the electron beam energy spread in order to suppress the micro-bunching instabilities that can develop in high brightness electron beams. More recently, studies and experiments have shown that laser-electron interaction developing in the laser heater can open new possibilities for tailoring the electron beam properties to meet special requirements. A suitable time-shaping of the laser heater pulse opened the door to the generation of (tens of) femtosecond-long FEL pulses.

Using standard laser techniques it is also possible to imprint onto the electron bunch, energy and density modulations in the THz frequency range that, properly sustained through the accelerator, can be exploited for generation of coherent THz radiation at GeV beam energies.

In this report, recent results at the FERMI FEL are presented together with near future plans.

INTRODUCTION

Modern linear accelerators that opened the era of X-ray Free Electron Lasers (X-FELs) [1–5] are required to generate very high peak current and high-quality electron beams in order for them to sustain the FEL process. The high peak current is generally achieved with the compression of the electron bunch in magnetic chicanes. Due to the very high density that electrons reach in the 6-D phase space, the beam develops collective effects, such as the microbunch instability, that can deteriorate the electron beam properties [7]. This instability can be driven by longitudinal space charge (LSC) [8] and coherent synchrotron radiation (CSR) [9]. These instabilities can introduce into the electron beam very strong energy modulations [10] that are a limitation for the operation of X-FELs at short wavelengths and in particular for seeded FELs because they produce a reduction of the longitudinal coherence [11, 12].

In order to fight the development of the microbunch instability, the so-called laser heater (LH) has been proposed [7] and is currently used in most FELs [13,14]. By using a resonant interaction between the electron beam and an external laser, the LH introduces a controlled spread in energy of the uncompressed beam and at low energy. This process can be optimized to suppress the microbunch instability [7]. As a result of the LH, the

FEL intensity can be increased significantly [13,14]. In addition, specifically for seeded FELs, it has been shown that the LH is essential to produce narrow-bandwidth FEL radiation [11,12].

NON-GAUSSIAN ENERGY DISTRIBUTION

The optical energy modulation introduced to the beam by the interaction with the laser is removed by the LH chicane who is designed to smear out short wavelength modulations. This lead to an uncorrelated energy spread on the beam. It has been shown that the shape of distribution of the energy spread can be controlled acting on the relative transverse size of the laser and electron beam in the interaction region [13]. In particular the use of a laser with a transverse mode significantly larger than the electron beam can lead to distributions that differ significantly from a Gaussian and can become a double horn distribution [15].

Having the possibility to control the shape of the electron energy distribution is important in the case of seeded FELs. Indeed, the use of non-Gaussian distributions can lead to a more efficient bunching process at higher harmonics.

Figure 1 reports the results of numerical simulations showing the advantage of using a non-Gaussian distribution for wavelengths shorter than 16 nm. For details about the parameters in the simulations refer to [16].

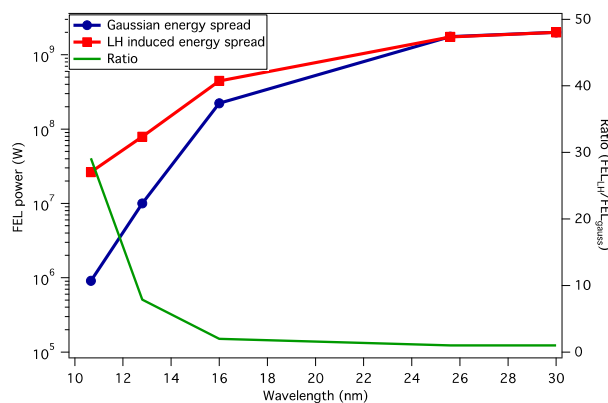


Figure 1: Simulations results of FEL power vs wavelength for standard Gaussian energy spread and LH induced non-Gaussian energy spread [16].

Content from this work may be used under the terms of the CC BY 3.0 licence (© 2018). Any distribution of this work must maintain attribution to the author(s), title of the work, publisher, and DOI.

[†]enrico.allaria@elettra.eu

TIME-DOMAIN ANALYSIS OF ATTOSECOND PULSE GENERATION IN AN X-RAY FREE-ELECTRON LASER

P. Baxevanis, Z. Huang and A. Marinelli,
 SLAC National Accelerator Laboratory, Menlo Park, CA 94025, USA

Abstract

The method of enhanced self-amplified spontaneous emission (eSASE) is one of the strongest candidates for the generation of sub-femtosecond X-ray pulses in a free-electron laser. The optimization of an eSASE experiment involves many independent parameters, which makes the exploration of the parameter space with 3-D simulations computationally intensive. Therefore, a robust theoretical analysis of this problem is extremely desirable. We provide a self-consistent, analytical treatment of such a configuration using a one-dimensional, time-dependent FEL model that includes the key effects of linear e-beam chirp and linear undulator taper. Verified via comparison with numerical simulation, our formalism is also utilized in parameter studies that seek to determine the optimum setup of the FEL.

INTRODUCTION

Because of their attractiveness to users, the generation of ultrashort X-ray pulses is one of the main objectives of research into advanced operation modes in a modern FEL facility. One of the more prominent schemes for generating sub-fs X-rays in an FEL is eSASE [1] (enhanced Self-Amplified Spontaneous Emission). This technique involves the interaction of an electron beam with an optical laser pulse in the presence of a short wiggler, prior to the beam being sent into a conventional undulator. This process relies on some intense manipulation of the longitudinal phase space of the e-beam, after which the strongly chirped beam typically has to travel through a tapered undulator in order to achieve lasing with the required properties. Apart from a significant improvement in the performance of the FEL, this method provides an attractive scheme for generating X-ray pulses in the attosecond range.

In this paper, we provide a self-consistent, analytical treatment of such a configuration using a simple, one-dimensional (1D) FEL model that includes the effects of startup from noise (SASE), slippage, electron beam chirp (linear and nonlinear) and undulator taper. 3D effects such as radiation diffraction, emittance and focusing are excluded. This allows us to calculate various key properties of the FEL radiation in the latter stage of the exponential gain regime. After verifying its validity through comparison with the output of a 1D FEL simulation code, our analysis is also utilized in parameter studies that seek to determine the optimum setup of the FEL. This enables us to obtain a more thorough understanding of the physics behind the experimental method.

1D FEL ANALYSIS

In this section, we outline the main results of our theoretical analysis, leaving the details of the derivation for another publication. In the context of our model, the main properties of the radiation can be extracted from a slowly-varying complex amplitude $a(\theta, z)$, which can be related to the actual electric field through the relation $E_{\text{rad}} = a(\theta, z)e^{ik_r(z-ct)}/2 + \text{c.c.}$. Here, $k_r = 2\pi/\lambda_r$ is the radiation wave number and $\theta = k_u z + k_r(z - ct)$ is the ponderomotive phase ($k_u = 2\pi/\lambda_u$, where λ_u is the undulator period). The θ variable also satisfies the relation $\theta = k_r s$, where s is an internal bunch coordinate. The main FEL parameters satisfy the resonance condition $\lambda_r = \lambda_u(1 + K_0^2/2)/(2\gamma_0^2)$, where λ_r is the radiation wavelength, K_0 is the (initial) undulator parameter and γ_0 is the average relativistic factor of the beam. The longitudinal phase space coordinates are (θ, η) , where $\eta = \gamma/\gamma_0 - 1$ is the energy deviation variable.

As far as the key properties of the e-beam are concerned, we assume that the current is given by $I(\theta) = I_0\chi(\theta)$, where $0 \leq \chi(\theta) \leq 1$ is a scaled profile and I_0 is the peak current, while the correlated energy (chirp) profile is $\eta = -\mu(\theta - \theta_m) - \Upsilon(\theta)$. Here, $\theta_m = \theta_b/2$ is the phase corresponding to the middle of the bunch (we have $\chi(0) = \chi(\theta_b) = 0$), μ is a constant linear chirp coefficient and the Υ function represents a nonlinear chirp component (we assume zero uncorrelated energy spread). For our purposes, we select a parabolic current profile of the form $\chi(\theta) = 1 - (\theta - \theta_m)^2/\theta_m^2$ and a nonlinear chirp profile given by $\Upsilon(\theta) = \mu_3(\theta - \theta_m)^3$, though the formalism can also accommodate the general case. The logic of this particular selection will be justified later on. Finally, we also assume a linear taper profile of the form $K = K_0(1 + \epsilon z)$.

We follow the self-consistent analysis of Ref. [2]. In the linear regime of the interaction, we can show that the complex radiation amplitude can be expressed as

$$a(\theta, z) \propto \sum_j e^{-i\theta_j} G(\theta, \theta_j, z), \quad (1)$$

where θ_j are the random initial electron phases (at $z = 0$) and $G(\theta, \theta_j, z)$ is a Green's function. The latter is non-zero only when $0 < \theta - \theta_j < k_u z$, in which case it is given in contour integral form (up to a phase term) by

$$G = -\frac{1}{2\pi i} \int_{-\infty+iy}^{+\infty+iy} \frac{d\hat{\lambda}}{\hat{\lambda}} \exp(-i\hat{\lambda}[\bar{z} - (\hat{\theta} - \hat{\theta}_j)] - i \int_{\hat{\theta}_j}^{\tau(\hat{\theta})} dt \times \hat{\chi}(t)[\hat{\lambda} + \hat{\Delta}_0(t - \hat{\theta}_j) + \hat{\mu}_3\{(t - \hat{\theta}_m)^3 - (\hat{\theta}_j - \hat{\theta}_m)^3\}]^{-2}). \quad (2)$$

DYNAMICS OF SUPERRADIANT EMISSION BY A PREBUNCHED E-BEAM AND ITS SPONTANEOUS EMISSION SELF-INTERACTION*

R. Iancu†, Shenkar College, Ramat Gan, Israel and University of Tel-Aviv, Tel-Aviv
 A. Gover, University of Tel-Aviv, Tel-Aviv, Israel
 A. Friedman, Ariel University, Ariel
 C. Emma, P. Musumeci, UCLA, Los Angeles

Abstract

In the context of radiation emission from an electron beam, Dicke's superradiance (SR) is the enhanced "coherent" spontaneous radiation emission from a pre-bunched beam, and Stimulated-Superradiance (ST-SR) is the further enhanced emission of the bunched beam in the presence of a phase-matched radiation wave. These processes are analyzed for Undulator radiation in the framework of radiation field mode-excitation theory. In the nonlinear saturation regime the synchronism of the bunched beam and an injected radiation wave may be sustained by wiggler tapering: Tapering-Enhanced Superradiance (TES) and Tapering-Enhanced Stimulated Superradiance Amplification (TESSA). Identifying these processes is useful for understanding the enhancement of radiative emission in the tapered wiggler section of seeded FELs. The nonlinear formulation of the energy transfer dynamics between the radiation wave and the bunched beam fully conserves energy. This includes conservation of energy without radiation reaction terms in the interesting case of spontaneous self-interaction (no input radiation).

INTRODUCTION

In the context of radiation emission from an electron beam, Dicke's superradiance (SR) [1] is the enhanced "coherent" spontaneous radiation emission from a pre-bunched beam, and Stimulated-Superradiance (ST-SR) is the further enhanced emission of the bunched beam in the presence of a phase-matched radiation wave [2]. These processes are analyzed for Undulator radiation in the framework of radiation field mode-excitation theory. In the nonlinear saturation regime the synchronism of the bunched beam and an injected radiation wave may be sustained by wiggler tapering: Tapering-Enhanced Superradiance (TES) and Tapering-Enhanced Stimulated Superradiance Amplification (TESSA) [3]. In section II we present the radiation modes expansion formulation (in the spectral Fourier frequency formulation) [2] and explain the radiation cases. In section III we derive the radiation from a single bunch and from a finite train of bunches in the spectral Fourier frequency formulations. In section IV we present the single frequency formulation of the radiation field mode-excitation, and calculate the power radiated by an infinite train of bunches, and in section V we derive an energy-conserving non linear model which results in a couple of differential equations and

present numerical results of those equations for some cases of interest.

SUPERRADIANCE AND STIMULATED SUPERRADIANCE IN SPECTRAL FORMULATIONS

As a starting point we review the theory of superradiant (SR) and stimulated superradiant (ST-SR) emission from free electrons in a general radiative emission process. In this section we use a spectral formulation, namely, all fields are given in the frequency domain as Fourier transforms of the real time-dependent fields. We use the radiation modes expansion formulation of [2], where the radiation field is expanded in terms of an orthogonal set of eigenmodes in a waveguide structure or in free space (eg. Hermite-Gaussian modes):

$$\{\tilde{\mathbf{E}}_q(\mathbf{r}), \tilde{\mathbf{H}}_q(\mathbf{r})\} = \{\tilde{\mathbf{E}}_q(\mathbf{r}_\perp), \tilde{\mathbf{H}}_q(\mathbf{r}_\perp)\} e^{ik_q z}$$

$$\check{\mathbf{E}}(\mathbf{r}, \omega) = \sum_{\pm q} \check{C}_q(z, \omega) \tilde{\mathbf{E}}_q(\mathbf{r})$$

$$\check{\mathbf{H}}(\mathbf{r}, \omega) = \sum_{\pm q} \check{C}_q(z, \omega) \tilde{\mathbf{H}}_q(\mathbf{r})$$

The amplitude coefficients \check{C}_q have dimensions of time, are in units of sec V/m and sec A/m.

The excitation equations of the mode amplitudes is:

$$\frac{d\check{C}_q(z, \omega)}{dz} = \frac{-1}{4\mathcal{P}_q} \int \check{\mathbf{J}}(\mathbf{r}, \omega) \cdot \tilde{\mathbf{E}}_q^*(\mathbf{r}) d^2\mathbf{r}_\perp. \quad (1)$$

where the current density $\check{\mathbf{J}}(\mathbf{r}, \omega)$ is the Fourier transform of $\mathbf{J}(\mathbf{r}, t)$.

The above is formally integrated and given in terms of the initial mode excitation amplitude and the currents:

$$\check{C}_q(z, \omega) - \check{C}_q(0, \omega) = -\frac{1}{4\mathcal{P}_q} \int \check{\mathbf{J}}(\mathbf{r}, \omega) \cdot \tilde{\mathbf{E}}_q^*(\mathbf{r}) dV,$$

where

$$\mathcal{P}_q = \frac{1}{2} Re \iint (\tilde{\mathbf{E}}_q \times \tilde{\mathbf{H}}_q) \cdot \hat{e}_z d^2\mathbf{r}_\perp = \frac{|\tilde{\mathbf{E}}_q(\mathbf{r}_\perp = 0)|^2}{2Z_q} A_{emq} \quad (2)$$

and Z_q is the mode impedance ($\sqrt{\mu_0/\epsilon_0}$ in free space). In the case of a narrow beam passing on axis near $\mathbf{r}_\perp = 0$, Eq. (2) defines the mode effective area A_{emq} in terms of the field of the mode on axis $\tilde{\mathbf{E}}_q(\mathbf{r}_\perp = 0)$.

* Partial support by US-Israel Binational Science Foundation (BSF) and by Deutsche-Israelische Projektkooperation (DIP).

† riancon@gmail.com

CANONICAL FORMULATION OF 1D FEL THEORY REVISITED, QUANTIZED AND APPLIED TO ELECTRON EVOLUTION*

Petr M. Anisimov[†], Los Alamos National Laboratory, Los Alamos, USA

Abstract

An original free-electron laser (FEL) paper relied on quantum analysis of photon generation by relativistic electrons in alternating magnetic field [1]. In most cases, however, the system of pendulum equations for non-canonical variables and the theory of classical electromagnetism proved to be adequate. As x-ray FELs advance to higher energy photons, quantum effects of electron recoil and shot noise has to be considered. This work presents quantization procedure based on the Hamiltonian formulation of an x-ray FEL interaction in 1D case. The procedure relates the conventional variables to canonical coordinates and momenta and does not require the transformation to the Bambini-Renieri frame [2]. The relation of a field operator to a photon annihilation operator reveals the meaning of the quantum FEL parameter, introduced by Bonifacio, as a number of photons emitted by a single electron before the saturation takes place [3]. The quantum description is then applied to study how quantum nature of electrons affects the startup of x-ray FEL and how quantum electrons become indistinguishable from a classical ensemble of electrons due to their interaction with a ponderomotive potential of an x-ray FEL.

INTRODUCTION

A one dimensional free-electron laser (FEL) theory has played a dominate role in understanding how FELs generate electromagnetic radiation in an undulator with a strength parameter $K = eB_0/k_u m_0 c^2$, which is given in CGS units here, and period λ_u . This theory allows for an universal scaling that only depends on the FEL parameter $\rho = (1/\gamma)(K\Omega_P/4ck_u)^{2/3}$ [4] and predicts that in a helical undulator, electrons with energy γ in $m_0 c^2$ units generate radiation at a wavelength $\lambda = \lambda_u/2\gamma^2(1+K^2)$. This generation is driven by electron bunching and is governed by the first order equation deduced from Maxwell's equations:

$$\frac{dA}{dz} = \frac{1}{N} \sum_{\alpha=1}^N e^{-i\theta_\alpha}, \quad (1)$$

where the field amplitude A is measured in terms of the saturation value $E_s = (m_0 c/e)\Omega_P \sqrt{\rho\gamma}$, time is replaced by the distance along the undulator $z = ct/L_{g0}$ measured in the units of the gain length $L_{g0} = (2k_u \rho)^{-1}$, and $\theta_\alpha = (k + k_u)z_\alpha - \omega t$ is a ponderomotive phase of the α^{th} electron out of N with respect to the radiation. The electron bunching by the generated radiation is described by the pendulum equations [5, 6] derived most often from the Lorentz force

equation:

$$\frac{d\theta_\alpha}{dz} = \eta_\alpha \quad (2a)$$

$$\frac{d\eta_\alpha}{dz} = -2\text{Re} \left(E e^{i\theta_\alpha} \right), \quad (2b)$$

where $\eta_\alpha = (\gamma - \gamma_r) / \rho\gamma_r$ is the relative energy detuning.

Future x-ray FEL designs, that reduce energy of electrons for a given energy of x-ray photons by reducing the undulator period, will require the quantum theory of FEL operation [7]. The equations above are not suitable for a quantum description since they assume that one can specify the exact ponderomotive phase, energy detuning and the field amplitude simultaneously at any point in time. Yet, the principle of stationary action S , which is an attribute of the dynamics of a physical system, from which the equations of motion of the system can be derived is better suited for generalizations. Moreover, it is best understood within quantum mechanics, where a system does not follow a single path but its behavior depends on all imaginable paths.

The principle of stationary action is a variational principle $\delta S = 0$ that was best formulated by W. R. Hamiltonian in 1834. It has been used on an occasion to describe electrons in a helical undulator [8] but not the generated radiation, which was described by Maxwell's equations. R. Feynman has demonstrated how this principle can be used in quantum calculations by introducing path integrals [9]. We however will use this principle for an FEL system consisting of relativistic electrons and generated radiation in order to derive a non-relativistic Hamiltonian without the Bambini-Renieri frame [2]. We will then generalize the Hamiltonian principle to quantum mechanics through Poisson brackets for canonical variables. We will finally apply this result to the study of quantum evolution of electrons in an FEL in order to determine if quantum uncertainty of an electron's position can reduce the electron bunching and degrade FEL performance.

HAMILTONIAN PRINCIPLE

The Hamiltonian principle is W. R. Hamilton formulation of the principle of stationary (least) action. It states that the dynamics of a physical system is determined by a variational problem for a functional based on a single function, the Lagrangian:

$$\delta S[\mathbf{q}(t)] = \delta \int_{t_1}^{t_2} L(\mathbf{q}(t), \dot{\mathbf{q}}(t), t) dt = 0. \quad (3)$$

One can use it to obtain equations of motion when applied to the action of a mechanical system such as electrons in an FEL but can be also used to derive Maxwell's equations.

* Work supported by LDRD-ER

[†] petr@lanl.gov

WIDE BANDWIDTH, FREQUENCY MODULATED FREE ELECTRON LASER

L.T. Campbell^{1,2}, B.W.J. McNeil¹

¹SUPA, Department of Physics, University of Strathclyde, Glasgow, G4 0NG and
 Cockcroft Institute, Warrington, WA4 4AD, UK

²ASTeC, STFC Daresbury Laboratory, Warrington, WA4 4AD, UK

Abstract

It is shown via theory and simulation that the resonant frequency of a Free Electron Laser (FEL) may be modulated to obtain an FEL interaction with a frequency bandwidth which is at least an order of magnitude greater than normal FEL operation. The system is described in the linear regime by a summation over exponential gain modes, allowing the amplification of multiple light frequencies simultaneously. Simulation in 3D demonstrates the process for parameters of the UK's CLARA FEL test facility currently under construction. This new mode of FEL operation has close analogies to Frequency Modulation in a conventional cavity laser. This new, wide bandwidth mode of FEL operation scales well for X-ray generation and offers users a new form of high-power FEL output.

The Free Electron Laser (FEL) is currently the world's brightest source of X-rays by many orders of magnitude [1–3]. The FEL consists of a relativistic electron beam injected through a magnetic undulator with a co-propagating resonant radiation field. Initially, co-propagating radiation will occur due to incoherent spontaneous noise emission from the electron beam and may be supplemented by an injected seed laser. The electrons can interact cooperatively with the radiation they emit and become density modulated at the resonant radiation wavelength. This coherently modulated oscillating electron beam exponentially amplifies the co-propagating radiation field in a positive feedback loop. In the single-pass high-gain mode, the energy of the initial incoherent, spontaneous X-rays may be amplified by around ten orders of magnitude. With such an increase in brightness over other laboratory sources, the X-ray FEL has unique applications across a wide range of the natural sciences. FEL science is, however, still under development, and the creation of novel and improved output from the FEL is still an active topic of research.

For example, it has been shown via simulations that equally spaced frequency modes may be generated in a single-pass FEL amplifier [4,5] by introducing a series of delays to the electron beam with respect to the co-propagating radiation field (e.g. by using magnetic chicanes placed between undulator modules). These radiation modes are formally identical to those created in an oscillator cavity. Analogously with a mode-locked conventional laser oscillator, a modulation of the electron beam energy [4,5] or current [6] at the mode spacing can phase-lock the modes and amplify them to generate a train of short, high power pulses.

Multiple colours may also be excited by directly tuning each undulator module to switch between 2 (or more) dis-

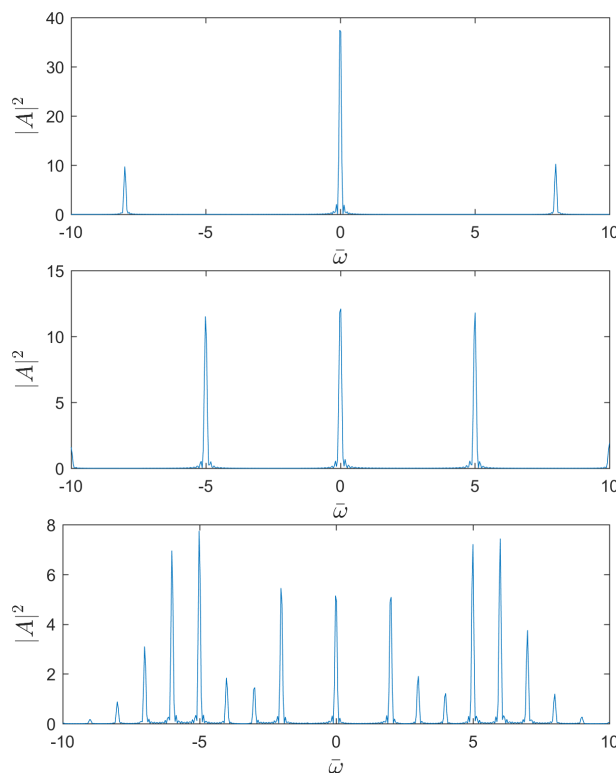


Figure 1: Result of analytic solution in equation (5) using the sinusoidal frequency modulation. The plots show the 1D scaled power spectrum (in arbitrary units) of a single electron radiating in a modulated wiggler with parameters $\rho = 0.001$ and modulation amplitude $\kappa = 0.014$, for 3 different values of modulation frequency \bar{k}_M . Values are, from top to bottom, $\bar{k}_M = 8$; $\bar{k}_M = 5$; and $\bar{k}_M = 1$, corresponding to modulation index $\mu = 0.875, 1.4$ and 7 respectively. Note how, as the modulation frequency is reduced, more modes are within the bandwidth described by the frequency modulation amplitude.

ting colours [7]. This colour switching may also excite and amplify modes via a resulting gain modulation [8].

In what follows, the resonant frequency of the FEL is continuously modulated by varying the magnetic undulator field, as opposed to either a continual temporal modulation of e.g. the beam energy, or a spatial variation between two distinct colours.

Control of the resonant frequency of the FEL ω_r , may be achieved by varying the electron beam energy γ_0 , the undulator wavenumber k_u , or undulator magnetic field strength B_u ,